Mathematical Modelling of Sediment Transport and Bed Transients in Multi-Channel River Networks under Conditions of Unsteady Flow

Thesis Submitted in Partial Fulfillment of a Doctorate of Philosophy in Civil Engineering

Brian Morse

University of Ottawa

January, 1991

ISBN 0-315-68046-6

UNIVERSITÉ D'OTTAWA
UNIVERSITY OF OTTAWA

Abstract

The fixed-bed, hydrodynamic and water quality model ONE-D has been successfully applied to virtually every major river system in Canada. In 1984 one of the supporting agencies, Environment Canada, expressed the desire to extend ONE-D for the simulation of sediment transport processes and river-bed dynamics. After performing a literature review it was found that currently available mobile-bed river models did not have the features that the basic ONE-D model had, particularly those required to model channel networks. Because of these numerical modelling limitations it was decided to proceed with this research effort. Sediment transport and bed dynamic routines were written in modular form and the resulting model (ONE-D-SED) became the mobile-bed version of ONE-D.

ONE-D-SED was initially validated for hypothetical test cases. This initial application showed that the model reproduced analytical solutions for the 'linear' cases examined. In addition, these simulations provided documentation of the numerical properties of ONE-D-SED's finite difference schemes. Following these preliminary tests correction coefficients were generated for analytical solutions of bed transients of finite height.

The subsequent application of ONE-D-SED to the Lower Fraser River was partly in response to the need expressed by Public Works Canada for accurate sediment budgets for certain reaches of this major river system. More importantly, part of this system is tidal, multi-channel network and hence is ideally suited for model validation purposes. Finally, superior sediment data were available for the study reach identified in this research. After analysis of Lower Fraser River sediment data, and calibration of the Ackers-White (A-W) sediment transport equation, ONE-D-SED was applied to the study reach at a "screening-level". Since the results of this application were encouraging, ONE-D-SED was then applied at a detailed level and simulated changes in bed elevation were compared to those observed.

In addition to the work directly related to model development, application and validation work was also undertaken to address the issue of representing suspended sediment 'fractions' consisting of a range of grain sizes. This work was motivated by the findings of analyses of the suspended sediment load in the Lower Fraser River and by the necessity of characterizing the representative grain size for natural rivers where there is a large gradation in the bed material composition. This study revealed that the representative grain size of a fraction depends on certain local hydraulic conditions. In addition, correction factors for modelling suspended sediment concentrations were obtained when the geometric grain size of the fraction is used in lieu of the mathematically accurate representative size.

Acknowledgements

I'd like to express my sincere gratitude to my thesis supervisor Dr. R. D. Townsend. To the staff of Environment Canada, particularly Maurice Sydor, Ted Yuzyk, Terry Day and Bruno Tassone, their efforts greatly facilitated the work. Many thanks to my parents Al and Lettie for all their help. To my wife Libo, for her work and support, my enduring love. I dedicate this essay to my sister Diane.

Contents

List of Figures

List of Tables

Nomenclature

a	=	relative reference depth (-);
A	=	channel cross-sectional area (m^2);
$\mathcal{A}$	=	reference depth (m);
A_h	=	channel cross-sectional area (m^2) evaluted at h constant as a function of x;
A-W	=	Ackers-White (equation for bml);
b	=	a constant (dimensions depend on value of m);
bml	=	bed material load (m^3/s);
B	=	constant of proportionality in the Rouse Number (-);
B_i	=	bias in concentration of d_i, applied to DI samples (-);
c	=	velocity of bed wave (m/s);
c_e	=	effective bed velocity (m/s);
c_n	=	numerically simulated bed velocity (m/s);
C	=	sediment concentration (-);
C_d	=	drag coefficient (-);
C_c	=	convergence coefficient for bed velocity (-);
C_d	=	convergence coefficient for bed attenuation (-);
C_h	=	Chezy coefficient ($m^{1/2}/s$);
C_F	=	mean concentration in the full water column (-);
C_M	=	mean concentration in the measurable portion of the water column (-);
C_0	=	an arbitrary concentration (-);
$\bar{C}$	=	mean concentration of a grain fraction (-);
$\bar{C}_1$	=	mean concentration of a grain fraction based on $\bar{\gamma} = 1.0$ (-);
d_1, d_2	=	lower and upper grain diameters of grain fraction I_{1-2};
d_x	=	sediment grain-size corresponding to x% passing; (mm)
d_{10}	=	sediment grain-size corresponding to 10% passing (mm);
d_{35}	=	sediment grain-size corresponding to 35% passing (mm);
d_{50}	=	sediment grain-size corresponding to 50% passing (mm);
d_{84}	=	sediment grain-size corresponding to 84% passing; (mm)
d_r	=	representative bed material size (mm);
d_g	=	geometric mean size of a grain fraction, $= \sqrt{d_1 \cdot d_2}$ (mm);
$\bar{D}$	=	average value of the measured depths at Mission (ft);
D_{gr}	=	dimensionless grain size used in A-W equation (-);
DI	=	Depth Integrated (suspended sediment sample);
E	=	eddy viscosity (m^2/s);

E_c	=	eddy viscosity in the constant eddy viscosity model (m^2/s);
EC	=	Environment Canada;
E_{s2}	=	sediment diffusion/dispersion coefficient (m^2/s);
f	=	friction factor -total resistance to flow (-);
f'	=	friction factor -grain resistance (-);
f''	=	friction factor -form resistance (-);
F	=	Froude Number (-);
F_{1-2}	=	area under the normal distribution curve between $\zeta(d_1)$ and $\zeta(d_2)$ (-);
g	=	acceleration due to gravity (m/s^2);
h	=	water surface elevation from a fixed horizontal datum (m or ft);
HD	=	hydraulic mean depth (=A/T) (-);
HR	=	hydraulic radius (m or ft);
I_{1-2}	=	grain fraction width, = d_2/d_1 (-);
k	=	wave number (= $2pi/l$) (m^{-1});
K	=	von Karman constant;
K_e	=	effective diffusion coefficient (m^2/s);
"K"	=	DI data taken at Daily vertical (-);
l	=	wavelength of full (sinusoidal) cycle (m);
L	=	half-wave length (=l/2) (m);
m	=	exponent in a simple sediment transport equation (-);
M	=	distance from channel bed where DI sample begins (ft);
n	=	Manning's coefficient ($m^{1/6}$);
n	=	can also specify a Natural number (-);
N_x	=	grid density (=$L/\Delta x$) (-);
p	=	sediment porisity (-);
P	=	Péclet number (= cl/K) (-);
P_e	=	Péclet number (= cL/K) (-);
P_E	=	Einstein's transport parameter (-);
PI	=	Point Integrated (suspended sediment sample);
PWC	=	Public Works Canada;
q	=	unit discharge ($m^3/s/m$);
q_l	=	lateral inflow ($m^3/s/m$);
q	=	unit discharge between A and surface ($m^3/s/m$);
Q	=	discharge (m^3/s or ft^3/s);
r	=	frequency (s^{-1});
$r(\Phi)$	=	statistical correlation coefficient (-);
R	=	hydraulic radius (m);
R_c	=	velocity coefficient (=$\frac{c_n}{c_e}$) (-);
R_d	=	attenuation coefficient (=$\frac{z_n}{z_L}$) (-);
"R"	=	DI data taken at all cross-section verticals (-);
s	=	unit sediment transport rate ($m^3/s/m$);
sbml	=	suspended bed material load (m^3/s);
s_l	=	lateral sediment inflow ($m^3/s/m$);

S	=	volumetric sediment transport rate (m^3/s);
S_0	=	bed slope (-);
S_f	=	friction slope (-);
S_F	=	sediment load in the entire water column ($m^3/s/m$);
S_M	=	suspended sediment load in the measurable portion of the water column
t	=	time (s);
t_0	=	boundary shear stresses (Pa);
t_y	=	local shear stress (Pa);
T	=	channel top-width (m or ft);
T_a	=	active river-bed width (m);
u	=	local water velocity (m/s);
$\bar{u}$	=	mean velocity (m/s or ft/s);
U	=	a complex amplitude function of k (m);
U_m	=	maximum velocity at $Y = Y_0$ (m/s or ft/s);
U_*	=	shear velocity (m/s);
U_*'	=	grain shear velocity (m/s);
wl	=	wash load (m^3/s);
$W(d)$	=	settling velocity of of grains size d (m/s);
W_g	=	setlling velocity of d_g (m/s);
W_r	=	the representative settling velocity of a sediment fraction (m/s);
WP	=	wetted perimeter (m or ft);
WPM	=	Water Planning and Management (branch of EC);
WSC	=	Water Survery Canada (branch of EC);
x	=	coordinate axis along the length of a river (m);
Y	=	local depth (m);
Y_0	=	full water depth (m or ft);
z	=	change in river bed elevation (m);
z_j^n	=	$z(j\Delta x, n\Delta t)$ (m);
z_L	=	$z(L, L/c_e)$ (m);
z_n	=	numerically simulated height of bed wave at $x = L$ (m);
z_0	=	initial height of bed wave (at $z(0,0)$) (m);
z_*	=	bed wave amplitude ($=z_0/Y_0$) (-);
Z	=	change of cross-sectional area of the river's mobile-bed perimeter (m^2);
$\mathcal{Z}$	=	Rouse Number (-);
$\mathcal{Z}_{i/j}$	=	ratio of Rouse numbers of grain size i and j (-);
α	=	a coefficient used in modified-Lax equations (-);
β	=	dimensionless pseudo-viscosity coefficient (-);
β_*	=	optimal value of β (-);
γ	=	fall velocity coefficient (-);
$\bar{\gamma}$	=	depth-averaged fall velocity coefficient (-);

Δt	=	time step (s);
Δx	=	distance between computational cross-sections (m);
ζ	=	normal variate (=$\ln \frac{d}{d_{50}} / \ln \sigma_g$) (-);
η	=	constant of proportionality (-);
Θ	=	q_m/q;
κ	=	diffusion coefficient (m^2/s);
ν	=	a function of C and F (-);
φ	=	cross-stream distribution factor (-);
ρ	=	fluid density (N/m^3);
σ	=	Courant number (=$c\Delta t/\Delta x$) (-);
σ_g	=	geometric standard deviation of a distribution (= d_{84}/d_{50}) (-);
ϕ	=	ratio of diffusion coefficient in fluid-sediment mixture and clear fluid (-);
Φ	=	ratio of relative concentrations (-);
ψ	=	a constant (-).

Chapter 1

Introduction

1.1 Motivation for the Study

This research was initiated following a meeting in September, 1984 between the writer, his supervisor, a representative of the Sediment Section of Water Survey of Canada (WSC) and the head of the Systems Section of the Water Planning and Management (WPM) Branch of Environment Canada. At this meeting, a review of existing morphological models showed that no tested public domain one-dimensional (1-D) mobile-bed model could simulate sediment processes in multi-channel networks under unsteady flow conditions. It was decided, therefore, that a research effort be initiated to extend a fixed-bed model known as "ONE-D" to include "morphological" simulations. Furthermore, it was agreed that a 45 km-long reach of the Lower Fraser River in British Columbia would be a test case for validating the new model.

From a model validation viewpoint, due to the multi-channel nature of the study area and the field character of the flow regime, the Lower Fraser provided an ideal model validation test case. In addition, there were specific reasons for choosing the Lower Fraser River as the first major case study. In 1964, Public Works Canada (PWC), the responsible agency for development and maintenance of navigation on the Lower Fraser, because of planning needs relating to a variety of hydraulic works and activities on the river, expressed the need for reliable hydrometric and sediment data. This data would be used in connection with maintenance and improvement of the navigational channel, (i.e., the data could assist in determining whether the problem could best be resolved by dredging, river training works or a combination thereof). The following is an excerpt from a letter written in 1964 by PWC to WSC:

> "... it is emphasized that for this Department the primary object is to determine the total sediment discharge at Port Mann, and also the ratio of bed load to suspended load and the particle size distribution at that point. It is understood that sampling stations between Hope and Port Mann are necessary to determine the situation at the latter place, and while valuable information will undoubtedly be obtained on the conditions above Port Mann, it is the river below as influenced by conditions at Port Mann which is the main concern of the Department at this time."

To answer this need, WSC set up survey stations along the Fraser River and its tributaries. To obtain the sediment discharge at Port Mann, ONE-D was used to model the hydraulics of the Mission to Port Mann reach (Sydor 1980). The computed discharge at Port Mann was used in conjunction with sediment samples obtained there to produce a sediment discharge for the site (Morasse 1985 and Zyrmiak 1987). Sediment data analyzed in this research came from WSC.

The motivations for applying ONE-D-SED to the same reach were threefold.

First, sediment measurements at Port Mann had been discontinued due to problems associated with the tidal nature of the station, hence an alternate means of obtaining the sediment load at Port Mann became necessary. ONE-D-SED offered a means of routing sediment measured at the Mission site through to Port Mann. Second, since there were some morphological concerns expressed about the river upstream of Port Mann (Kellerhals 1984), the application of ONE-D-SED to the study reach would provide insights into bed changes within the reach itself. Finally, if the application of ONE-D-SED to the Mission-Port Mann study reach was successful, it would lead the way to morphological modelling of the river downstream of the study reach.

1.2 Study Objectives

The primary objective of this research was to extend the capabilities of the fixed-bed, one-dimensional, in-channel mathematical model: "ONE-D" (Gunaratnam and Perkins 1970) such that the new mobile-bed version "ONE-D-SED" could, in addition to modelling unsteady fluid flows, model sediment transport processes in multi-channel river networks.

The study had the following secondary objectives:

(i) to use ONE-D-SED to define the limits for which analytical solutions for hypothetical tests cases were valid;

(ii) to define the representative fall velocity for modelling the transport of mixed suspended sediments; and,

(iii) to apply ONE-D-SED to examine sediment transport processes and channel bed dynamics in a 45 km-long study reach of the Lower Fraser River in British Columbia.

1.3 Development of the Research Project

In chapter 2 the place of mathematical modelling in the solution to river engineering problems is discussed. Chapter 3 presents a literature review of existing morphological river models and discusses important considerations with regards to the mathematical modelling of river processes. In chapter 4 river-bed transients are presented from a theoretical point of view. In chapter 5 ONE-D-SED is described and the model is applied to hypothetical test cases of bed transient motion. After confirming that simulated results correspond to analytical solutions for linear cases, coefficients are developed for bed transients of finite height.

In chapter 6 sediment dynamics particular to the Lower Fraser River are presented and the Ackers-White (1973) sediment transport equation is calibrated. In chapter 7 the application of standard vertical sediment dispersion-diffusion models to Lower Fraser River field data is explored. In chapter 8 the representative fall velocity of sediment classes of mixed grain sizes is characterized. The application of ONE-D-SED at a screen level to the Lower Fraser River study reach is presented in Chapter 9 and its application at a detailed level in chapter 10. Finally, results, conclusions and recommendations of the research are summarized in chapter 11.

Chapter 2

Mathematical Models in the Context of River Engineering

River engineering works include the construction of dams, bridges, ports, dykes, diversions, control structures, river training works, and dredging of navigational channels. Rivers are very effective instruments in the hydrological, sedimentological and geomorphic cycles. They adjust their depth, width, resistance, bed material size, planform geometry and slope in order to carry the imposed water and sediment load. As land use and climatic conditions change, there are often significant variations in both quantity and quality of runoff and sediment yield from a river basin. Because a river will adjust to engineering works and changes in runoff characteristics, the main task facing the river engineer is to quantify the river's response to imposed changes.

Since there are more parameters involved in the various river processes than there are equations which inter-relate them, this is a difficult task. The basic river engineering problem is indeterminate. As a result, researchers have searched for a supplemental equation to relate the river's width to various independent parameters. Empirical relationships and regime equations have been quantified. More recently, theoretically-based underlying principles (using extremal hypotheses) have been proposed (Shiqiang et al. 1986). Nevertheless, deterministic solutions for predicting the river's width and planform geometry remain elusive.

To compound the difficulty of the task, it is often difficult to distinguish between dependent and independent parameters. For example, over the long term sediment load is an independent parameter in that the river will adjust itself in order to transport whatever sediment load is imposed. On the other hand, the sediment load transported will depend on local hydraulic conditions. Also, in the short term, the bed slope of a river is fixed when the river's bed consists of bedrock whereas in an alluvial river, the river is free to adjust the composition and slope of its bed in response to imposed constraints. Moreover, the river's most dependent parameter (water depth or surface elevation) is in some situations an independent parameter, as is the case at the junction of the river and a lake or ocean.

The indeterminacy of river systems has meant that the discipline of river engineering remains partly science and partly art. With respect to the latter, the findings of the Workshop on "Downstream River Channel Changes Resulting from Diversions or Reservoir Construction" (Schumm 1980 and Theurer 1980) are revealing. The purpose of the workshops was to assemble the world's experts in river engineering to see how they practiced the subject. Experts were asked to give their opinion regarding two hypothetical case studies involving river works. Predictions of the rivers' responses to upstream regulation varied substantially from one expert to another. Whereas some predicted increases in bed material grain size, bed slope, channel width, and bank stability, others predicted decreases. The workshop concluded that the application of models would have helped the experts in forming their predictions but also, that river engineering remains a difficult discipline.

In his keynote address at the Third International Symposium on River Sedimentation (1986), Kennedy coined the phrase: "rivers, God's gift to mankind". In this talk, designed to address the frustration of the engineer in the face of his task, Kennedy expounded on two laws he introduced more formally in 1983. The first is that "every beneficent feature of a physical system increases the complexity of its mathematical modelling in direct proportion to the value of the attendant benefits". Commenting on this dilemma, Kennedy put forward his second law: "that for anguish and joy, the agony of the river researcher/engineer over the status of his subject is offset by the ecstasy of knowing how much remains to be elucidated and reliably formulated".

Reflecting on river research, he went on to state that though the "river problem" will never be "solved", "... the tripod on which the progress likely will rest will comprise of first, the generally adequate understanding of river-flow processes ..., second, modern computers (which) now make it possible... for numerical simulation..., and finally, modern electronic and optical instrumentation for experiments of unsteady flow conditions..." (Kennedy 1983).

Kennedy is not alone in his judgment that progress will depend, in part, on computer models. An almost unanimous recommendation coming out of the Workshop on Downstream Changes was that, in order to obtain more definitive predictions of a river's responses to hypothetical changes, mathematical modelling of the affected reaches would be required. These conclusions represent the hope that is placed in mathematically-modelled morphological computations -despite all their limitations.

In the following literature review, recent advances in research into river transport processes and related numerical models are presented. The objectives, characteristics and levels of sophistication of mathematical models are addressed in light of the complexity of river dynamics.

Chapter 3

Literature Review

Many concepts which form the body of knowledge concerning river processes are included in morphological models. It is self-evident that a model is only as good as the relationships on which it is based. Therefore a literature review should incorporate a brief review of the progress made in understanding these specific processes as well as a review of existing mathematical models.

3.1 River Processes

3.1.1 Flow Resistance

The key parameter with respect to movement of water is the resistance to flow (characterized by f). In the context of morphological modelling, because of the changing bed forms, bed material size, unsteady and non-uniform flow effects, the difficulty in predicting f has been a significant obstacle to model validation. Key contributions in this area have been made by Einstein (1950), Engelund and Hansen

(1967). White, Paris and Bettess (1980), and Karim (1981). While the first three contributions have related f to grain size and hydraulic parameters, Karim's main contribution is that sediment load is made an implicit parameter in the evaluation of f. This is the first time that flow resistance and sediment transport have been treated in an inter-dependent way. Bray (1987) has quantified resistance to flow in gravel-bed rivers. However, since certain processes involved in gravel-bed rivers are somewhat different to those in sand bed rivers, the present discussions are confined to the latter category.

In the case of unsteady flows, the common practice is to assume that the flow is "quasi-steady" and hence the friction slope calculation is simply a function of the local velocity (Biswas and Chakrabarti, 1974). From the point of view of morphological simulations, two additional problems arise in the evaluation of f. When the channel bed is degrading, the grain resistance f' is increasing due to an increase in mean bed material size, while at the same time changes in bedform may cause the form resistance f'' to decrease. The net result may be a change in f in the order of 30% (Newton 1951; Soni and Sarda 1982; and Torres and Subhash 1984).

de Vries (1982) presented a sensitivity analysis of morphological modelling with respect to estimated parameters. He notes that resistance to flow does significantly affect predictions. He further states that since field measurements of f are fairly easily obtained and are vastly superior to those estimated using uncalibrated equations, they should always be obtained prior to morphological simulations. Though his argument is definitive, nevertheless it is still recognized that the changing value of f during the simulation of morphological transients remains problematic.

3.1.2 Bed Load

Van Rijn (1986) and de Vries (1982) have shown that, more than any other parameter, the characterization of transients relies on a good estimation of the sediment discharge. In addition to classical bed load equations, more recent contributions by Karim (1981) and van Rijn (1984a) represent significant progress. Also, recent research on measured sediment loads occurring during erosion and during deposition has demonstrated that the equilibrium load during the latter process is typically 50% higher than during the former.

3.1.3 Suspended Load

The suspended load is often computed by estimating the bed load and then using a dispersion-diffusion equation to obtain the sediment concentration in the remainder of the water column. Relationships differ depending on the assumed distribution of the water's eddy viscosity. Rouse (1937) assumed a parabolic diffusion coefficient; Kerssens et al. (1979), a parabolic-constant coefficient; Graf, (1971) presented a constant coefficient; and Laursen (1980) an exponential-type coefficient. The models of Rouse, Graf and Laursen are examined in some detail in chapters 7 and 8. In addition to the eddy viscosity, the value of von Karman's coefficient K (Yalin, 1986) and the relationship between the diffusion-dispersion of water and that of sediment (van Rijn, 1984b) have been the subject of recent debate. These issues are also discussed more fully in chapters 7 and 8.

For suspended load under unsteady flow conditions, Iseya (1984) has reported that "bursts" of sediment have been noted during the formation of dunes and that during this time, the suspended load can be well above that measured once dune conditions are established and stabilized.

3.1.4 Total Load

The total load can be obtained by adding bed load and suspended load. Some numerical models use this formulation because it allows the bed load to be computed based on local hydraulic conditions, while the suspended load may be obtained by using the convective-diffusive equation. The advantage of this approach is that the sediment transport rate is a function of time and distance as well as local hydraulic conditions. However, there are disadvantages. First, from a physical point of view, the distinction between "bed" and "suspended" load is somewhat ill-defined. Assuming that bed load consists of the sediment rolling along the river floor, then Einstein's definition (1950) is normally used. In this case, the bed load would be defined as that moving within 2 grain diameters of the bed. However, in sand-bed rivers this load is insignificant. Furthermore, when the reference level is chosen so close to the bed, substantial numerical problems arise (van Rijn 1984b and see chapter 8). Second, when using this formulation, the complexity of the numerical modelling increases dramatically since an additional boundary is required at the interface of the bed and suspended loads. Due to this computational difficulty, some models have, in the final analysis, gone full circle in so far as no real distinction between the two modes of transport is made (Holly and Rahuel 1989).

An alternate way of obtaining the total load is to use a "total load transport" expression directly. Due to the increased availability of data sets and computer statistical packages, recent formulae are superior to more traditional ones. Hansen and Engelund's (1967) formulae for flow resistance and sediment transport represent a significant contribution. Using an extended laboratory data set, Ackers and White (A-W) developed a dimensionless formula based on the concept of sediment mobility. Karim's (1981) equation implicitly incorporates bed forms and resistance to flow into the calculations. Yang and Molinas (1982) developed a very successful transport equation based on an extremal hypothesis. However, due to the complexities of the river processes, all of these formulae (which represent the best available) normally only estimate the actual sediment load within a factor of two.

When total load formulae are applied to sediment mixtures rather than to a unique grain size, some coefficients in the equations need modification. Day (1980) applied the A-W equation to sediment mixtures and noted that larger grains provided protection for smaller grains. This meant that the smaller ones were less mobile. On the other hand, the smaller grains forced the larger ones to be more exposed to the flow and hence the latter's mobility was increased.

Before leaving the subject of sediment transport, it should be emphasized that the above-referenced relationships have been developed for the "bed material load" (bml). However, this may be only a fraction of the full sediment load. In addition to the load that is in equilibrium with bed and hydraulic parameters (bml), an additional load referred to as the "wash load" (wl) is comprised of finer grains . The distinction between the two sediment load categories is normally based on grain size properties or alternatively on sediment availability. When the former criterion is used, grains less than 0.04 or 0.062 mm in diameter are normally categorized as wl (Richardson and Julien, 1986; Church et al., 1987). When the latter criterion is used, it is normally assumed that grains less than d_{10} form the wl.

It should be noted that these statements apply only on a reach-by-reach basis because what may be wl at one time or in one place may, in turn, become bml at another time and place. A fuller discussion of this matter in regards to data obtained on the Lower Fraser is presented in chapter 6. However, it should be added that though the wl is independent of hydraulic conditions, since it is supply dominated, it is dependent on hydrological and river basin conditions. Also, although the wl does not appear in the bed transient equation for the study reach simulated, it nevertheless may be very important with respect to river morphology further downstream and, since toxics are predominantly adsorbed to finer sediments, it is always important from a water quality viewpoint.

3.1.5 Geomorphological Processes

In some model applications total load formulae are applied to a specific class of grain sizes. In these cases total load formulae may need modifications of the type proposed by Day (1980) before being applied. When models incorporate this feature, it enables them to simulate hydraulic sorting. This is an important modelling capability when it is known that the character of river bed material is undergoing change. For example, in the simulation of a reservoir delta formation, it is well known that finer material is deposited on coarser material. Therefore there is a significant change in bed composition as a function of time and place.

In conjunction with hydraulic sorting, bed armouring often governs the rate and extent of bed degradation. Since the introduction of mobile-bed modelling, the necessity of incorporating this feature in many simulation processes has become evident. As a result, basic research into the bed armouring and grain sorting processes has increased in recent years. Although these processes are well understood conceptually, the functional relationships that are incorporated in numerical models to represent them are still being developed. The work by Karim and Holly (1986) is a notable example of the effort being made. They not only review recent research initiatives but also describe how they may be incorporated into a sub-model used in morphological modelling. In their work an attempt is made to quantify the effects of the stochastic nature of sediment transport in the near-bed zone and the effects of bedforms on the depth of the active mixing layer.

When modelling changes in bed elevation, it is often necessary to estimate the active channel bed width. Sometimes severe aggradation or degradation is occurring over only a small portion of the channel bed. If the model were to output only the corresponding average rise or fall in bed elevation, this would seriously limit the model's usefulness as a managerial tool.

Earlier it was noted that processes in gravel bed rivers often differ from those in sand bed rivers. The same could also be said of estuaries. When modelling estuaries, processes governing cohesive sediment transport are important. Some of these include flocculation, hindered settlement, and consolidation. These processes are very much related to water salinity and the Richardson Number. An example of a model which attempts to simulate this environment is that of Nicholson and

O'Connor (1986).

Finally, bank stability, bar formation, channel width and planform geometry are also important aspects of river engineering. For the most part, present day mathematical models are not sophisticated enough to simulate the dynamics of these river features. Accordingly, when addressing these particular aspects of river modelling, engineers must rely heavily on case histories.

3.2 Considerations in Mathematical Modelling

In the previous sections, important research contributions regarding considerations arising from the complexity of a river's behaviour have been outlined and some mathematical models have been mentioned. Ideally, a morphological river model would use the best available relationships and would attempt to simulate all important river processes. Before identifying which models incorporate which processes or which relationships, pertinent considerations regarding river modelling in general are presented.

Since hard data are not always available in sufficient quantity, an important first step in any mathematical modelling study is to get acquainted with the river's geomorphology and its unique character. Normally, mathematical river models are favoured when the reach to be modelled is long, e.g. a degrading reach downstream of a dam. On the other hand, a physical model is usually necessary when the problem is localized and highly complex, such as scouring in the vicinity of an intake structure. In other situations it may be most economical to combine the strengths of physical and mathematical models in a so-called "hybrid" system (McAnally et. al. 1986).

Whatever modelling approach is selected, when the concern is the river's response to engineering works and/or changes in watershed characteristics, the goals are always the same (Bray 1984): 1) to establish if there will be a significant change in the river's regime and to determine the nature of that change (i.e. aggradation or degradation), 2) to predict the new equilibrium state of the river, and 3) to quantify the predicted change as a function of time.

3.2.1 Scope of Models

Engineers must be able to identify the model(s) that will meet the objectives of their particular application. Typical questions which need to be addressed, vis a vis the choice of model are: What start-up time is required? How well is it documented? Does it have agency support? Will its use be acceptable to the client? Has it been successful in previous applications? What are the input requirements? Does it simulate the important processes governing this particular application? If it is a numerical model, is its numerical scheme consistent? How much human and computer resources are required? Is it "user-friendly" and/or "engineer-friendly"?

The engineer-friendly concept (Cunge and Holly 1986) is an important consideration in that river processes cannot be viewed as being purely deterministic; in fact they are often described as stochastic processes. Hence it is important that the model provides not only an estimate of the river's response, but also a "range" of potential responses, each, ideally, with an associated confidence level. At a less than ideal level, an engineer-friendly model might, for example, offer the user a choice in the transport functions and/or numerical schemes to be used.

In general, the more sophisticated a model is, the more data is required for its calibration and validation. Since large-scale data acquisition is expensive, this is a particularly important consideration when modelling sediment transport processes. In fact, more than any other item, advances in the modelling of mobile-boundary systems depend on the creation of river databases. The present scarcity of adequate databases is largely due to the fact that useful field data is normally collected over an extended period. Moreover, it is necessary that all pertinent parameters be measured, since the omission of any one parameter in the sampling process may ~~mean that~~ a particular model cannot be adequately calibrated and/or validated.

Assuming an 'in-channel' simulation model is selected, the next step is to decide on the level of sophistication required. At the very simplest level is the "rule of thumb" approach similar to that proposed by Lane (1955), namely:

$$QS_o \propto Sd_{50} \tag{3.1}$$

From this relationship it is clear that a change in a river's characteristic discharge Q or sediment load S will result in a re-adjustment of its bed slope S_o and/or its characteristic bed grain size d_{50}. At a second level, regime relationships (Blench 1971) may be used to provide a more quantitative and comprehensive description of the channel's response to a given change in sediment load or discharge. While the form of these relationships is well established, care is needed in assigning values to empirical coefficients since they are dependent on river location. At a third level, a "screening" model may be appropriate. Such models require a minimal amount of data while the functional relationships are fairly simplistic. At this level, the output is a semi-quantitative estimate of the river's response to various input scenarios. Screening-level analyses provide an initial insight into bed transient development should a more complete study of the river's response be warranted. Models at the screening level are rare, although analytical solutions presented in chapter 4 provide an ideal basis for their construction. Examples of screening-level applications are given by Torres and Subhash (1984), Lopez-Garcia (1977) and by de Vries (1981).

At the fourth level are the well-known "deterministic" models. This category of model simulates the in-channel water and sediment processes using the principles of conservation of mass and momentum as well as auxiliary relationships for resistance to flow and sediment transport. In the case of fixed-boundary models, they simulate the water discharge and elevations along a reach or, in the case of mobile-boundary models, temporal changes in the river's planform geometry, width and bed elevation. Both types of model are widely available and they will be discussed at some length later on. Their strength lies in the fact that they simulate as accurately as possible the actual behaviour of a river. However, it must be added that the solution generated is usually a singular one rather than a domain one and, in this sense, they are not engineer-friendly.

The next level of model sophistication includes "statistical" models. Although it is common practice to analyze data using statistical methods, very little development work has been undertaken in the area of statistical modelling, as applied to alluvial rivers.

Recent research on the nature of turbulence has led to a modelling approach quite distinct from the more traditional deterministic, statistical, or empirical approaches. In such cases phenomena, classically considered to have a statistical and deterministic component, have now been effectively described by applying the emerging theory of "chaos". While this relatively new theory has been successfully applied in such diverse areas as cardiology and economics, to the writer's knowledge this theory has not yet been applied to river engineering problems.

Due to the variety of river types, the complexity of the processes involved and the number of types of river engineering problems encountered, the ultimate river engineering management tool would be an "expert system". Drawing on extended data bases, hydraulic and sediment relationships, statistics and optimization routines, it would allow the user to systematically apply models of different scope to address the three questions outlined above. Expert systems (often called "artificial intelligence" or AI) have been developed in some areas of science with success but are still at the "infancy"-stage of development in most disciplines. Substantially more effort, experience and databases would be required before this tool would be available to the river engineer.

3.2.2 Types of Deterministic Models

For many years steady-state one-dimensional fixed-bed river models, such as HEC-2 (U.S. Corps of Engineers 1973), have been successfully applied to case studies. In the last twenty years, experience with similar unsteady models e.g. ONE-D (Gunaratnam and Perkins 1970), has meant that they also enjoy fairly wide acceptance among the engineering community. This is due largely to the fact that the input data needs are well known, techniques for the collection of data are well documented, and the governing relationships are well understood and are not too sensitive to errors in channel geometry and initial conditions. Moreover, the rules for the application of numerical schemes to solve the equations of motion are well known. The one major concern in applying these types of models is with regard to modelling overbank flow during floods.

Some interesting theoretical developments and applications have occurred in recent years regarding depth-integrated, 2-D models (Abbott et. al. (1985) and Falconer et. al. (1986)). Also, in the case of depth- or width-integrated, 2-D models, recent research contributions on the structure of turbulence has led to an improved estimate for the coefficients used in the increasingly popular k-e model (Rodi 1986). While some 3-D models are available, it is more difficult to assess their performance because of their limited application. For more information concerning fixed-bed models, the reader is referred to Hinwood and Wallis (1975).

It should be noted that the foregoing models are often used in conjunction with water quality routines to simulate the transport of pollutants and other constituents. There have been many successful applications in this area though, in some instances, the results could not be fully validated because of a lack of field data. The reader is referred to Ditmars et. al. (1987) for more information regarding this area of modelling.

The second major category of deterministic river models consist of "mobile-boundary" models. Since they include water transport simulation, the previous discussion also applies here. However, their primary purpose is to predict changes in bed elevation, channel width, and river planform geometry.

The ideal mobile-boundary model would simulate all of these changes. An example of a mobile-boundary model under development is TABS-3 (McAnally et. al. 1986). Such models are complex and require extensive field data for calibration and validation purposes. Therefore, other approaches have been used to model changes in planform geometry. Chang's model (1986), for example, indicates whether there will be a significant change in regime and hence planform geometry. The effects of changes in water and sediment input to a channel reach are analyzed in the context of regime threshold values. This is an important contribution in that it meets the first goal of river modelling, namely: estimating if there will be a significant channel response, then determining the nature of the response and the new state of equilibrium.

Regarding changes in channel width, some models simulate the physical processes of bank erosion (Hagerty et. al., 1986). However, the detail required to simulate the local bank stability and erosion processes is difficult to achieve and so these models are still at the developmental stage. Some models that attempt this exercise are not based on simulation of the physical processes; rather they predict changes in bed elevation and combine extremal hypotheses and regime relationships to estimate corresponding changes in channel width, e.g. FLUVIAL-11 (Chang 1984).

The more common approach used in simulating alluvial transport processes is to assume that the banks are fixed. This type of mobile-boundary model is called a "mobile-bed" model. In some applications, where suspended load is the dominant transport process, mobile-bed models may be based on a 2-D formulation of water movement, e.g. PROFILE (van Rijn 1986). However, most models of the mobile-bed type use a 1-D formulation as is the case for HEC-6 (U.S. Corps of Engineers 1977), IALLUVIAL (Karim and Kennedy 1982), MOBED (Krishnappan 1981) and Holly and Rahuel (1988). Whereas HEC-6 and IALLUVIAL are based on steady-state flow simulation, MOBED, FLUVIAL-11 and Holly and Rahuel are unsteady-flow models.

Much experience has been gained in the area of 1-D mobile bed modelling, especially with respect to data needs and the numerical schemes to be used. While it is not suggested here that all such models have equally effective numerical schemes, these particular models have received wider use. Krishnappan (1987), Lu and Shen (1986) and the Committee on Hydrodynamic Computer Models (1983) also review some of the better known fixed and mobile-bed models.

3.2.3 Model Components

In essence a mathematical model consists of relationships that transform input data into an output statement. Previously it was stated that input data requirements for mobile-boundary models are usually quite extensive. It should be added that boundary conditions are also frequently problematic (Lyn 1987). Moreover, because bed movement is slow compared to fluid transport, initial conditions in a mobile-bed model can often dominate the bed-transient solution for an inordinate amount of time; (note that the morphological time-scales of rivers can typically range from 50 to 500 years (de Vries 1981)). This problem does not exist for fixed-bed models, in that initial conditions are normally overtaken by the boundary conditions after a few simulation time steps.

Since the functional relationships incorporated in mobile-bed models are imprecise, the difference between the sediment inflow to a study reach and that leaving the reach can be compounded by the imprecision of the sediment transport function itself. As well, transport equations are very sensitive to the estimate in mean velocity. For example, a 5% error in velocity can easily translate into a 30% error in the related estimate of the sediment load. Also, if such flow resistance relationships are not properly calibrated, they are typically in error by 20% to 30%.

Regarding the equations of motion, whereas numerical schemes for fixed-bed models are well established, the same cannot be said for mobile-bed models. The difficulty arises from the fact that the characteristic bed velocity is proportional to the local sediment transport rate and hence is highly variable. The three most common methods used to solve the equations of sediment and water motion are (i) the method of characteristics (MC), (ii) the method of finite elements (FE), and (iii) the method of finite differences (FD). Since the MC provides an excellent insight into the governing processes, it is usually employed on a screening level. However, this approach is usually restricted due to computational difficulties.

FE schemes are becoming more popular as the power of computers increases.

The appeal of this method is that it is normally precise and versatile. However, models using this procedure require that the user be well acquainted with the FE method. FE models usually require a substantial effort in the preparation of the computational grid.

FD schemes can be of the "coupled" or "uncoupled" variety, and "explicit" or "implicit" in format. Most models use an uncoupled approach. In this case the equations of water movement are solved first, and the equations for the sediment transport processes are then evaluated. Lyn (1987) demonstrates that this approach cannot be used when bed development processes are rapid since the resulting solution is mathematically problematic. However models are often formulated in this way, the principle reasons being: the ease of programming, the saving in computer time, and the fact that the water-transport time step required to generate a consistent solution is usually orders of magnitude smaller than that required to meet the Courant criterion for bed processes. MOBED, among others, uses this format. A variation of the uncoupled format is to use an "iterative" solution. In this case, the solutions of water and sediment dynamics are solved separately but the model iterates until a convergence criterion is met. ONE-D-SED falls into this category.

In the case of the coupled approach, backwater effects are often ignored. As a result, the "known-discharge" model is normally used and solutions are often obtained using the "four-point" implicit numerical scheme, which is fully documented by Ponce et al. (1979b).

When an author documents the type of scheme(s) used in his model, qualifications are normally required. For example, an implicit scheme may be used to simulate water movement while an explicit scheme is employed to simulate bed movement (e.g., ONE-D-SED). Alternatively an implicit scheme may be used for both water and bed motion separately (e.g., MOBED) but, taken as a whole, the solution of the governing equations of motion can be said to be implicit only by analogy since not all variables are solved simultaneously. An interesting example is the model of Nicholson and O'Connor (1986), which uses the method of characteristics and both implicit and explicit formulations of the finite difference method.

Many explicit schemes have been developed over the years. ONE-D-SED offers the user a choice between de Vries' "pseudo-viscosity modified-Lax" scheme (1981) and Fromm's "zero-average-phase-error" scheme (1968). Both schemes are presented in chapter 4.

The main consideration when choosing a model is not the format or type of scheme used so much as the scheme's numerical properties and the provided documentation thereof.

3.2.4 Order of Computational Scheme

When selecting a model, it is important to recognize the "order" of the computational scheme used in the model's formulation. As was the case for the "type" of scheme used, the "order" of a scheme may refer to a portion of the solution or to the solution of all governing equations taken as a whole. An example of the former is Fromm's scheme for the solution of the bed transient, which is said to be second order (a function of the terms included in the discretization of the bed continuity equation). On the other hand, the overall solution of the water-sediment problem is said to be zero-order when uniform flow and transport based on equilibrium conditions are assumed (Koutitas 1986). For applications involving bed load transport only, or for simulations using large time steps, zero-order schemes are used. Many 1-D mobile-bed river models use a zero-order formulation.

A higher order representation of the transport processes is required in the case of more sophisticated models. A first-order model is one in which uniform conditions are assumed for water transport and non-equilibrium conditions are assumed for the simulation of the sediment transport. This means that only the concentration near the bed is assumed to depend on the local hydraulics, while the sediment in suspension is calculated based on a partial differential equation using the reference concentration as a boundary condition. The key to success in such applications is an accurate value of the reference concentration. An alternate first-order formulation would be to evaluate sediment transport based on equilibrium conditions while using unsteady flow equations for the solution of water motion. Finally, second-order schemes are employed when non-equilibrium conditions are assumed for both water and sediment dynamics.

3.3 Review of Mobile-Bed River Models

3.3.1 Analytical Models

The development of analytical morphological river models is presented in the next chapter. However, it is noted here that perturbation analyses have shown that the governing equations represent a third-order hyperbolic system. Moreover, depending on the assumptions made, the system can be simplified and the resulting bed transient process can be modelled by a simple wave or parabolic equation (de Vries 1981).

Culling (1960) proposed a degradation model based on the parabolic formulation of the morphological process. Although he presented a number of solutions based on different initial and boundary conditions, he failed to relate the diffusion coefficient to any hydraulic parameters. de Vries (1959, 1965, 1969 and 1981)) was the first to indicate the nature of the governing equations through perturbation analyses and to relate the coefficients obtained to meaningful hydraulic parameters. However with regard to his earlier efforts, re: applying the parabolic model to the case of degradation below a dam, his boundary conditions were erroneous (Torres and Subhash 1984). He also contributed a numerical model based on the method of characteristics.

Others, including Ashida and Michiue (1971) and Soni et al. (1980), have contributed to the development of the parabolic model. Soni et al. applied the model to Indian rivers subject to landslides, however, they made an error in the boundary conditions as did Gill (1980). Similar errors were also made by Vittal and Mittal (1980) in connection with a study of degradation below a dam, and Bejin et al. (1980, 1981) for a study of degradation due to a lowering of the water level at the downstream end of a channel.

The most authoritative work on the parabolic model is that of Torres and Subhash (1984), who introduced a second formulation of the parabolic model based on sediment flux rather than on bed elevation. As such, they were able to indicate clearly the appropriate boundary conditions that should be used in various contexts. They also used the method of moments in an FE scheme to compare analytical results to non-linear ones. However, the FE method adopted did not lead to unique solutions and was therefore of limited usefulness. On the other hand, they did compare their model's results with the experimental flume data of Newton (1951), Soni et al. (1981), and Garde et al. (1981). Lopez-Garcia (1977) analysed the 'known discharge' model and by comparing results to analytical solutions, developed correction coefficients to be applied to transients of finite height. However, due to inconsistencies in his parametric analysis, he was not successful (see chapter 5).

Lyn's (1987) main contribution was to study the effect of perturbations on the governing differential equations. This led to a more comprehensive analysis of the characteristic celerities and of boundary conditions.

3.3.2 Numerical Models

Regarding numerical models, Tinney (1962) and the U.S. Army Corps of Engineers (1976) developed models which first solved the backwater equation and then the sediment continuity equation using an uncoupled scheme. Lyn (1987) points out that, from a theoretical viewpoint, this approach is inconsistent. To avoid this inconsistency, one approach is to iterate when using a model of the uncoupled format. However, on a practical level, the experience gained from applying IALLUVIAL (Holly et al. 1984) indicates that there is no need to iterate unless bed armouring is simulated.

de Vries (1965, 1969) solved the equations of motion for low Froude Numbers by the MC and then developed a modified-Lax (pseudo-viscosity) FD scheme for shock-fitting purposes (see chapter 4). In subsequent publications, he addressed internal boundary conditions (1981). Chang (1969) and Chang and Richards (1971) also used the MC. They assumed a quasi-steady flow and neglected the change in bed slope in a short time interval. Gessler (1971) proposed a simple explicit model for aggradation in which (due to the numerical scheme employed) special care was required with respect to the selection of the time interval. Komura and Simons (1967) and Komura (1971) developed models for river bed degradation below dams, which included the effect of the bed armouring process. Hwang (1975) developed a similar model (and the Corps of Engineers (1977) later introduced this feature in HEC-6) based on the work of Gessler (1971). Sediment sorting was also introduced in a recent (1988) version of MOBED by Krishnappan.

Miloradov and Muskatirovic (1971) and Miloradov and Radojkovic (1975) built a conceptually realistic model that simulated unsteady and non-uniform flows in complex channel cross- ctions. However, the assumption of a horizontal water level, among others, was the reason for disagreement between model results and field data (Torres and Subhash 1984).

Cunge and Pedreau (1973) built a known-discharge, implicit model for aggradation studies. This was a major step forward, primarily because of the use of the Preissman four-point implicit scheme. Chen et al. (1975), Mahmood (1975) and Mahmood and Ponce (1976) developed similar models that accounted separately for the bed load and the suspended load. Cunge and Simons (1975) also developed a model based on the Preissman scheme, which accounted for varying roughness using the Engelund-Hansen (1967) approach. Bouvard et al. (1977) extended this model by incorporating Einstein's (1950) estimate for f.

Brown and Li (1979) proposed a "known discharge" uncoupled model which accounted for lateral sediment input due to tributaries. Puls et al. (1977) found the bottom shear stress based on a 2-D hydrodynamic formulation, which was then used to estimate the local sediment transport rate and hence the bed deformations. Chang and Hill (1976) and Chang (1982) developed the FLUVIAL series of models. FLUVIAL started as a 1-D model and then incorporated changes in channel width based on whether the channel was aggrading or degrading (FLUVIAL-3 and DELTA). The concept of minimum stream power was incorporated in FLUVIAL-14. The model was further modified (Chang 1984) to include the simulation of lateral migration. Kennedy (1983) also reported efforts at modelling bank erosion processes and the resulting model was presented by Hagerty et al. in 1986.

Ponce, Garcia and Simons (1979) developed a model similar to that of Cunge and Pedreau (1973), but corrected the error made by the latter with respect to the linearization of the upstream boundary condition. Ponce, Indlekofer and Simons (1979) added to this effort by performing an analysis on the numerical parameters of the four-point Preissman scheme. Tsai and Yen (1982) introduced the iterative approach in a quasi-steady formulation, while Vreugdenhil (1981) reported his numerical analysis on the modified-Lax (pseudo-viscosity) scheme. Simons et al. (1984) reported on how their HEC2SR model could be used to estimate scour at bridges and Gee (1984) elaborated on the role of calibration in numerical models.

A 2-D model was introduced by Ariathurai (1974) to simulate the transport of fine material. Simons et al. (1980) incorporated a watershed, sediment-yield sub-model to generate the wash load for an in-channel morphological model. The major contributions in the area of modelling fine sediment transport have been by Markofsky (1984 and 1985) and particularly by Nicholson and O'Connor (1986). Finally Krishnappan (1980) and Brownlie (1981) developed morphological models which incorporate varying friction factors and retain all the time derivatives in the governing equations.

Important contributions in model development have also originated in the Netherlands. Since 1975 a 1-D, all-purpose model (first called ZANTRI and then modified to RIVMOR) has been in use. It has been validated by flume experiments and has had field applications (Klaassen 1982). RIVMOR was extended to a 1.5-D model (Kerssens et al. 1979) for tidal applications in which the suspended load dominates. When the study reach is short, the adjustment of the suspended sediment profile to its equilibrium profile as a function of time is important. Van Rijn (1986) developed a vertical 2-D model (SUTRENCH), which was first based on a logarithmic velocity profile and a FD scheme for the convective-diffusive suspended sediment transport equation. This approach was later modified (PROFILE) for non-uniform flow applications.

Work in the area of morphological modelling continues to progress. Models reveal to the engineer parameters which must be characterized in order to simulate the morphological processes and hence there is important feedback between research and model application.

3.3.3 Summary

(a) The governing equations of river-bed transient motion form a third-order non-linear hyperbolic system.

(b) After linearizing the coefficients an analytical solution of the equations exist and depending on assumptions made, a simple wave, parabolic, or hyperbolic model results. Based on Lyn's (1987) analysis it is clear that numerical models simulating the non-linear version of the equations (i.e. no simplifying assumptions made) are theoretically inconsistent if an uncoupled approach is used. However, at the application level, good results nevertheless are achieved in most circumstances. Alternatively, the problem can be overcome by using an iterative method. Also, numerical effects have been quantified for the (explicit) modified-Lax (pseudo-viscosity) formulation.

Omitting backwater effects results in a solution of the parabolic type. This assumption is often made and has been presented in some detail by numerous authors. However, it is only recently that all the appropriate boundary conditions have been identified. Many non-linear numerical models of this type have been written. They usually incorporate the Preissman four-point implicit scheme, the numerical effects of which are well documented.

(c) The hydraulic sorting and bed armouring processes have been incorporated in some models. For certain applications this is a necessary step if meaningful simulations are to be achieved.

(d) Models simulating the transport processes of cohesive sediments in an estuarial context have been developed, however they have not been extensively validated.

(e) Models simulating the two-dimensional process of suspended sediment load transport have been proposed. These particular models are appropriate when the system being modelled contains strong non-uniformities, such as trench migration. They are also appropriate where flows are tidal and the area of interest is small.

(f) Although most existing models are of the mobile-bed type, some progress has been reported in regards to modelling changes in channel width and lateral migration.

(g) Currently available mobile-bed models have not been formulated to take channel networking into account.

Chapter 4

Theoretical Background

4.1 Governing Equations

Each deterministic river model uses a slightly different representation of the equations of motion. For one-dimensional models, the most complete representation of propagation of long water waves in open channel is described by the St. Venant equations. For the propagation of long river-bed waves, a form of the Exner equation is used in conjunction with a sediment transport relationship. The St. Venant equations represent the conservation of mass (4.1) and momentum (4.2) of fluid in the channel while the Exner equation (4.3) represents the conservation of mass of sediment. The following formulations of these equations are used in ONE-D-SED:

$$B\frac{\partial h}{\partial t} + \frac{\partial Q}{\partial x} - q_l = 0 \tag{4.1}$$

$$(\frac{\partial Q}{\partial t} + 2u\frac{\partial Q}{\partial x})/Ag + (1 - F^2)\frac{\partial h}{\partial x} - \frac{F^2}{B}\frac{\partial A_h}{\partial x} - S_f = 0 \tag{4.2}$$

$$\frac{\partial S}{\partial x} + (1-p)\frac{\partial Z}{\partial t} + \frac{\partial (CA)}{\partial t} - s_l = 0 \tag{4.3}$$

where:

A = channel cross-sectional area (m^2); A_h = channel cross-sectional area (m^2) evaluated at h constant as a function of x; B = channel top-width (m); C = sediment concentration (-) = S/Q; F = Froude Number (-) where $F^2 = Q^2B/(A^3g)$; g = acceleration due to gravity (m/s^2); h = water surface elevation from a fixed horizontal datum (m); p = sediment porosity (-); q_l = water discharge per unit channel length entering laterally due to overland flow (m^3/s/m); s_l = volumetric sediment transport rate per unit channel length entering laterally due to overland flow (m^3/s/m), note also that with modification to account for sediment porosity, s_l (≤ 0) could be used to represent dredging per unit length of channel; S_f = friction slope (-); t = time (s); u = water velocity = Q/A (m/s); x = coordinate axis along the length of a river (m); and, Z = change from reference conditions of cross-sectional area of the river's mobile-bed perimeter (m^2), for example, if the active river bed width is T_a (m), then z, the vertical change in river bed elevation (m), = Z/T_a.

Due to the uncoupled nature of the numerical solution method, the term $\partial z/\partial t$ has not been included in 4.1, though theoretically it should have been. However, since $\partial z/\partial t$ is orders of magnitude smaller than $\partial h/\partial t$, very little error is introduced in the solution through this omission.

With respect to the momentum equation, an additional relationship (normally called an equation of state) is required to determine the friction slope in equation

4.2. In ONE-D-SED,

$$S_f = \frac{u \mid u \mid}{C_h^2 R} \tag{4.4}$$

where, C_h is the Chezy coefficient ($m^{1/2}$/s) and R is the hydraulic radius (m). Note that the Chezy coefficient is used to express resistance to flow. In fact, the coefficient inputted to ONE-D-SED is Manning's n. The value of n is prescribed initially as a function of depth, which can be modified as a function of Q in a ONE-D-SED subroutine before being converted inside the model to an equivalent value of C_h.

With regard to the Exner equation, since ONE-D-SED is a one-dimensional formulation, change in river bed area Z is used instead of the more common parameter z which describes change in river bed elevations. The implication is that ONE-D-SED is incapable of determining the distribution of aggradation or degradation across the channel bed. It is up to the user to specify the active channel width T_a, then ONE-D-SED indicates only the average change in bed elevation z over the entire width W. Also, since $\partial(CA)/\partial t$ normally is orders of magnitude less than other terms, the user is given the option of excluding this term from calculations performed in ONE-D-SED.

In ONE-D, equation 4.3 is omitted, leaving only the St. Venant equations to describe the propagation of long water waves in a fixed-bed natural channel. The origin and role of each term in the St. Venant equations are discussed at some length in the ONE-D computer manual (Environment Canada 1988) and will not be repeated here. However, it is useful to state the fundamental assumptions made in deriving these equations (ONE-D manual, page 3):

"1) The flow is assumed to be one dimensional, i.e. the flow in the channel can be well approximated with uniform velocity over each cross-section and the free surface is taken to be a horizontal line across the section. This implies that centrifugal effect due to channel curvature and Coriolis effect are negligible.

2) The pressure is assumed to be hydrostatic, i.e. the vertical acceleration is neglected and the density of the fluid is assumed to be homogeneous.

3) The effects of boundary friction and turbulence can be accounted for through the introduction of a resistance force which is described by the empirical "Manning" or "Darcy Weisbach" Friction Factor Equations."

The characteristic velocities of water surface transients in fixed-bed applications are: u + $\sqrt{gY}$ and u - $\sqrt{gY}$, where Y is the river depth (m). Lyn (1987) has pointed out that for the mobile bed case, the value of $\sqrt{gY}$ is multiplied by the term $(1-\nu)$ in which ν is of the order of C (typically -3) for low Froude Numbers. Of particular interest to this study is the characteristic velocity of bed transients. Studies of the latter have been performed by many (de Vries 1981; Vreugdenhil 1982; and Lyn 1989). The following is a summary of some of their findings. For analytical purposes equations 4.1, 4.2 and 4.3 should be restated for wide prismatic channels having no lateral flow contributions. The continuity equation becomes:

$$\frac{\partial h}{\partial t} + \frac{\partial (Yu)}{\partial x} = 0 \tag{4.5}$$

In most mobile-bed analyses, the $\partial h/\partial t$ term of equation 4.5 is assumed to be negligible. However, Lyn (1989), through an 'order of magnitude' analysis, has shown that it would be more precise to say the coefficient of $\partial h/\partial t$ is asymptotic to zero for certain morphological calculations. In any case, assuming that the unit discharge q (m^3/s/m) varies only in t and not in x, 4.5 can be further simplified as follows:

$$\frac{\partial(Yu)}{\partial x} = 0 \tag{4.6}$$

Substituting equations 4.4 and 4.6 in 4.2 and assuming that the local acceleration term $\partial u/\partial t$ may be neglected (for the same reasons as those presented for $\partial h/\partial t$), then the momentum equation simplifies to:

$$\frac{\partial(\frac{u^2}{2} + gh)}{\partial x} + \frac{g \mid u \mid u}{C_h^2 Y} = 0 \tag{4.7}$$

Finally, for wide rectangular channels, equation 4.3 reduces to:

$$\frac{\partial s}{\partial x} + (1-p)\frac{\partial z}{\partial t} = 0 \tag{4.8}$$

where s is the unit sediment transport rate (m^3/s/m). In addition to the equations provided thus far, an equation of state is normally provided for the sediment transport rate, such as,

$$s = bu^m \tag{4.9}$$

where b and m are constants.

Eqns. 4.7 through 4.9 can be combined to give two characteristic velocities for water waves and a third for the bed wave, namely:

$$c = \frac{u\frac{ds}{du}}{y(1-F^2)(1-p)} \tag{4.10}$$

In linearized form, equations 4.6 through 4.10 can be combined and expressed as (de Vries; 1981):

$$\frac{\partial z}{\partial t} - \kappa\frac{\partial^2 z}{\partial x^2} - \frac{\kappa}{c}\frac{\partial^2 z}{\partial x \partial t} = 0 \tag{4.11}$$

where κ, a diffusion coefficient, is a linearized term given by:

$$\kappa = \frac{u\frac{ds}{du}}{3S_o(1-p)} = \frac{ms}{3S_o(1-p)} \qquad (4.12)$$

One method of obtaining a solution to equation 4.11 is by assuming a periodic initial condition and performing a perturbation analysis, seeking a solution of the form:

$$z(x,t) = Ue^{(ikx+rt)} \qquad (4.13)$$

where U is a complex amplitude function of k, and k is the wave number ($= 2\pi/l$), in which l is a wavelength (m) and r is a frequency (s^{-1}) to be determined. It has been found (Vreugdenhil 1982) that the expression:

$$r = -ikc_e - k^2K_e \qquad (4.14)$$

satisfies equation 4.11. Here c_e and K_e are respectively the effective bed velocity (m/s) and an effective diffusion coefficient (m^2/s), given by:

$$c_e = c\frac{4\pi^2}{P^2 + 4\pi^2} \qquad (4.15)$$

$$K_e = \kappa\frac{P^2}{P^2 + 4\pi^2} \qquad (4.16)$$

where P is the Péclet Number ($= cl/\kappa$). Though cl/κ is the standard expression for the Péclet Number, some researchers use alternate expressions such as $k\kappa/c$ or κ/cl. In this study the standard form is used.

Eqns. 4.13 and 4.14 when combined can be expressed as:

$$z(x,t) = Ue^{[ik(x-c_et)-k^2K_et]} \qquad (4.17)$$

When $x = c_e t$ and when 4.15 and 4.16 are substituted for c_e and K_e, then equation 4.17 becomes:

$$z(x, x/c_e) = U_e^{-P\frac{x}{l}} \tag{4.18}$$

Therefore, the role of the Péclet Number serves as the logarithmic decrement. For example, when the initial condition of equation 4.11 is $z(x, 0) = z_o cos(kx)$, then, from equation 4.18, $z(0, 0) = z_o$ while $z(l, l/c_e) = z_o e^{-P}$.

The greater the Péclet number, the more the bed wave attenuates as it moves downstream. For low values of P (i.e. $P \ll 1$), wave velocity is dominant in the solution of equation 4.11 while for high values ($P \gg 1$), dissipation best describes the motion of the transient. Though this result might seem paradoxical, as pointed out by de Vries (1981), an alternate expression for P (assuming $F^2 \ll 1$) is $P = 3lS_o/Y_o$. Hence low values of P mean primarily small (local) bed waves, while large values represent bed level changes occurring over a large distance. Many researchers (Lyn 1987; Ponce et al 1979; Ribberink and Sande 1985; Vreugdenhil 1982; de Vries 1981) have developed analytical solutions for equation 4.11 that reflect these considerations. The solutions, which have been successfully applied in the field (Gill 1983; Torres and Subhash 1984), form the theoretical background for any bed transient study. Since these solutions are based on bed waves of infinitesimal height, coefficients are required to correct for waves of finite height. In the numerical simulations (chapter 5), coefficients for velocity and diffusion are calculated and ONE-D-SED's capability to reproduce analytical values for small wave amplitudes is examined.

In this section, the characteristic bed velocity and wave attenuation have been identified. It is noted that the velocity of water waves is normally orders of magnitude greater than that of bed waves. This means that, whereas water waves may have a characteristic time measured in days, the time frame for bed wave development is normally measured in decades. From a mathematical modelling point of view, it is difficult to faithfully represent these two ends of the time spectrum. If typical bed wave development is modelled and water transients are not critical for obtaining the sediment load, then the simplifications to the governing equations outlined above (i.e., eqns. 4.6 and 4.7) are valid and the "known discharge" formulation is normally preferred in conjunction with the coupled implicit Preissman scheme. In this case the standard "backwater" curve must be used as the initial condition, since implicit in the assumptions is the fact that the water characteristic velocities have become infinite and hence water depth must correspond to the steady-state case.

On the other hand, if water transients need to be simulated, un-coupling of the Exner equation from the solutions of the St. Venant equations is theoretically inconsistent because such an un-coupling assumes that the characteristic velocity of the bed is zero. On a practical level, even though the result may still be acceptable (chapter 3), due to this theoretical inconsistency, ONE-D-SED is designed to iterate between the solution of each set of equations. Thus the difficulty can be overcome at the expense of increased computer effort.

4.2 Numerical Schemes

It is beyond the scope of this study to provide a detailed analysis of numerical schemes used in ONE-D for the solution of the St. Venant Equations. The schemes, discussed in Environment Canada (1988), are based on the work of Gunaratnam and Perkins 1970 (the authors of ONE-D) and subsequent reports discussing numerical effects (Wood et al. 1972; Daily and Harleman 1972). However, a few remarks are made here. In ONE-D, the solution within each reach is done separately from the solution of the nodes linking the reaches together. The basic technique has been described as "the method of superposition, ... it resembles the method of influence functions which is commonly used in structural analysis" (ONE-D manual, page 8), or alternatively as a scheme ..." obtained by applying a weighted residual method of optimization to a simplified linearized version of the governing equations and the discrete approximations" (Krishnappan et al. 1987).

From the user's point of view, the important fact to retain is the numerical accuracy of the scheme. In general, the performance of any numerical method is dependent on the spatial resolution expressed by a grid density N_x $(= L/\Delta x)$ and the Courant number $\sigma(= c\ \Delta t/\Delta x)$ where L is the half-wave length of interest (m) (see figure 5.4). Δt is the time step (s) and Δx is the distance between computational cross-sections (m). Analyses made by Gunaratnam and Perkins (1970) have shown that solutions of water transients are accurate when $N_x \geq 50$ and $\sigma \leq 5.5$. In fact, many applications of ONE-D have shown that accurate results are still obtained as long as $\sigma \leq 15$.

Of more interest to this study are those numerical schemes which model bed transients. Analyses of implicit schemes have been performed elsewhere (Ponce et al. 1979; and Lyn and Goodwin 1987). Though the performance of the implicit schemes is generally good, explicit schemes were chosen for ONE-D-SED. In 1982, Vreugdenhil performed perturbation analyses on a number of numerical schemes for the simulation of a simple wave which characterizes bed transients having small Péclet Numbers. He concluded that "...the modified Lax method (de Vries' scheme) ... and the 4-point method (Preissman's scheme) ... give relatively little numerical diffusion. The Fromm scheme gives the smallest (generation of secondary waves); moreover, with respect (to higher order errors), it compares well with the other schemes so that it is indeed among the better ones" (page 5.12). Also, it is noted that Ribberink and van der Sande (1985) and Wesseling (1973) indicated that de Vries' and Fromm's schemes had favorable numerical properties. Based on these findings, it was decided to use de Vries' (1981) and Fromm's (1968) schemes in ONE-D-SED. Though many researchers favor implicit schemes, explicit ones are quite appropriate in applications where the water dynamics are unsteady and hence the time step chosen is based on convergence criteria associated with the water motion.

4.2.1 de Vries' Scheme

A numerical representation of equation 4.8 is:

$$\frac{z_j^{n+1} - z_j^n}{\Delta t} + \frac{s_{j+1}^n - s_{j-1}^n}{2\Delta x}$$
$$-\frac{1}{4\Delta t}[(\alpha_{j+1}^n + \alpha_j^n)(z_{j+1}^n - z_j^n) - (\alpha_j^n + \alpha_{j-1}^n)(z_j^n - z_{j-1}^n)] = 0 \qquad (4.19)$$

where $z_j^n = z(j\Delta x, n\Delta t)$. This molecule represents Lax's original scheme when the dimensionless coefficient $\alpha = 1$; the Lax - Wendroff scheme when $\alpha = \sigma^2$; and de Vries' scheme when $\alpha_k^n = (\sigma_k^n)^2 + \beta$. The modified-Lax scheme has received much use in the solution of hyperbolic equations (Wesseling, 1973) however, since there is a tendency for numerically-generated secondary waves to develop, in de Vries' scheme the dimensionless pseudo-viscosity term β is introduced to counteract this tendency. This behaviour and other charateristics of the scheme are explored fully in chapter 5.

It should be noted that a difficulty with de Vries' scheme is that, when α is a function of the computational point (as is indicated in the formulation presented), then the scheme is non-conservative. That is, a slight error in the conservation of mass is introduced. Therefore, when conservation is important, a constant α can be used in equation 4.19. However, in this instance additional numerical damping may be introduced. The resulting modified version of (4.19) is:

$$\frac{z_j^{n+1} - z_j^n}{\Delta t} + \frac{s_{j+1}^n - s_{j-1}^n}{2\Delta x} - \frac{\alpha}{2\Delta t}[z_{j+1}^n - 2z_j^n + z_{j-1}^n] = 0 \qquad (4.20)$$

where α is normally the maximum of all calculated values of α_j^n. In order to give the user the option of using this conservative form of de Vries' scheme, equation 4.20 also is included in ONE-D-SED and its performance is discussed in chapter 5.

4.2.2 Fromm's Scheme

Another commonly used finite-difference scheme for the representation of equation 4.8 is Fromm's (1968) "zero-average-phase-error" numerical method. Whereas de Vries' scheme is a first order scheme, Fromm's is second order with the following molecule:

$$
\begin{aligned}
z_j^{n+1} = z_j^n - \frac{\Delta t}{2\Delta x}(s_{j+1}^n - s_{j-1}^n) \\
+\frac{1}{4}\left(\frac{\Delta t}{\Delta x}\right)^2 [(c_{j+1}^n + c_j^n)(s_{j+1}^n - s_j^n) - (c_j^n + c_{j-1}^n)(s_j^n - s_{j-1}^n)] \\
+\frac{1}{4}\frac{\Delta t}{\Delta x}[s_{j+1}^n - 3s_j^n + 3s_{j-1}^n - s_{j-2}^n] \\
-\frac{1}{4}\left(\frac{\Delta t}{\Delta x}\right)^2 [c_{j+1}^n s_{j+1}^n - 3c_j^n s_j^n + 3c_{j-1}^n s_{j-1}^n - c_{j-2}^n s_{j-2}^n]
\end{aligned}
\tag{4.21}
$$

Wesseling's (1973) perturbation analyses have shown that this formulation is a desirable one when applied to hyperbolic partial differential equations. However, Vreugdenhil (1979) demonstrated that it is prone to generate secondary waves when shock features are present. These and other properies of the scheme are explored in chapter 5.

Chapter 5

Application of ONE-D-SED to Test Cases

5.1 Model Description

5.1.1 Description of ONE-D

Since ONE-D-SED is the mobile-bed version of the fixed-bed model ONE-D, a brief description of the fixed-bed version is herein presented. As stated in the previous chapter, in ONE-D, water transients are simulated using the St. Venant equations. The fact that the complete form of the equations is used allows the model to simulate successfully most types of one-dimensional unsteady flow.

However, what really distinguishes ONE-D from other fixed-bed models is the fact that natural river systems may be fully represented. For example, in ONE-D, rectangular, circular, trapezoidal, as well as completely irregular channel geometry may be fully described. Also, the model permits the differentiation between areas that actively convey water and those storage areas which do not contribute to channel flow. Examples of the latter are swamp areas or some over-bank areas. In ONE-D Manning's n may be specified as a function of water surface elevation and cross-section location within a reach.

Various external boundary conditions may be specified at either the upstream or downstream ends of a simulated river network. These include the option of specifying stage or discharge as a function of time, a stage-discharge or a stage-routing boundary condition. The model also allows the simulation of control structures including weirs, dykes and culverts where calculations of discharge are performed internally. Lateral inflows, including point and non-point sources, may also be specified as a function of time throughout the modelled area. This permits incorporating minor tributaries in the simulation of the main channels or enables the linking of main channels by hydraulic structures.

Aside from its flexibility and the accuracy of its numerical schemes, what makes ONE-D particularly powerful is its ability to model river networks including bifurcations, trifurcations and looped channels. When this feature is combined with complete model documentation (in the form of a computer manual and full Federal Government agency support), the model becomes a very practical and valuable tool. For more detailed information, regarding the model's capabilities and limitations, see Gunaratnam and Perkins (1970), the ONE-D computer manual (Environment Canada 1988) and Krishnappan (1987).

ONE-D has been successfully applied to a wide variety of river networks. Applications include the Fraser River (multi- channel and tidal reaches; Sydor et. al.

1989), the Peace-Athabasca-Delta (consisting of a very large river network; ibid), the Truro River (including a very complex channel network system where channels are interconnected by dykes and culverts; ibid), the Red River (in which vast areas are flooded during the spring runoff; Morasse 1987) and the St. Lawrence/Ottawa river network (which includes lakes, dams, river rapids, trifurcations, confluences, lateral inflows, multiple channel looping, and five meter tides at the downstream end; Morse 1990a and 1990b). Although rapids can be simulated through the stage-discharge or stage-routing boundary condition, it should be noted that ONE-D is not able to simulate super-critical flow regimes per se.

5.1.2 Description of ONE-D-SED

To convert ONE-D to a mobile-bed model (ONE-D-SED), some fifty subroutines were added. The governing principle of the model extension was to minimize the number of changes to ONE-D's original code and to construct new distinct code in a modular format. For example, when applying ONE-D, input data is divided into nine "card groups" specified as cards "A" through "H". The only change made to this portion of the model input was the addition of a variable "in" card A-b (to specify whether the mobile-bed option is invoked). All additional sediment information is specified in a newly-created card group "J", documented in appendix A. Internally, the only change to ONE-D's code is to selectively call a sediment subroutine. Specifically, once cards A through H are read, the subroutine SEDINI is called to manage the input and initialization of sediment data. During the actual solution portion of the program, modified values of river bottom elevation, cross-sectional area and other channel geometry properties are obtained by call to MPARAM rather than the 'fixed-bed' version PARAM. Once water dynamics are solved, there is also a call to SEDMAN, which manages all calculations related to mobile-bed modelling (figure 5.1). Hence changes to the initial code were kept to a minimum. The reason the model was constructed in this way was for ease of maintenance and that future developments of ONE-D may be incorporated in ONE-D-SED.

SEDINI and SEDMAN are sediment subroutines written to manage all sediment transport calculations. The structure of the sediment routines can be seen by examining the calls made from SEDINI (figure 5.2) and SEDMAN (figure 5.3) to other sediment routines. For example, SEDINI first calls SEDRDR to read sediment input data. A call is then made to SEDNSN to move this data to the internal computational points of ONE-D-SED. Further calls are made to SEDNET, SEDTIM, SEDTR1 etc. to make all the necessary calculations regarding initial conditions. Calls from SEDMAN are a little more complex due to all the solution options available (figure 5.3). Note that either Fronm's, or one of the two versions of de Vries' schemes (outlined in the previous chapter) may be used, and also that the solution of the hydraulics and bed transients may be coupled by iteration.

A complete list and brief description of sediment subroutines added in ONE-D-SED and the related input variables, defined in a format consistent with that appearing in the ONE-D manual, are listed in Appendix A.

5.2 Numerical Properties of ONE-D-SED

The first application of ONE-D-SED was designed to test the numerical properties of de Vries' and Fromm's schemes and to quantify the non-linear behaviour of bed transients of finite height. In chapter 4, analytical solutions of bed transient motion were given for sinusoidal disturbances after certain simplifications were made to the governing equations. Based on those assumptions, recall that the effective theoretical bed velocity was given by:

$$c_r = c\frac{\pi^2}{P_e^2 + \pi^2} \tag{5.1}$$

where P_e is a modified version of the Péclet Number $= cL/K$; c is given by:

$$c = \frac{ms}{Y(1-F^2)(1-p)}; \tag{5.2}$$

and the diffusion coefficient is given by:

$$\kappa = \frac{ms}{3S_o(1-p)} \tag{5.3}$$

It was also seen that a wave, initially of amplitude z_0, would change in amplitude to $z_L = z_0 e^{-P_e}$ after travelling a distance L during a time L/c_r.

To validate the numerical schemes used in ONE-D-SED, two criteria were used. First, in the case of very small disturbances, simulated bed wave velocity (c_n) and bed amplitude at x = L (z_n) should correspond to analytical values c_r and z_L respectively. Second, when a finer computational grid is used, the schemes' performance should improve and the simulations should converge to a unique (exact) value.

In addition, since analytical solutions are based on bed waves of infinitesimal height, correction coefficients can be established for waves of finite height. In the numerical simulations which follow, coefficients for both velocity and diffusion are calculated. In sections 5.2.1 and 5.2.2 of this chapter, the numerical properties of de Vries's and Fromm's schemes are examined. In section 5.3 the schemes are applied to generate non-linear solutions, and values are assigned to the correction coefficients for wave velocity and attenuation.

5.2.1 de Vries' Scheme

In chapter 4 it was noted that de Vries introduced a pseudo-viscosity term (β) in the modified-Lax equation to counteract the tendency of Lax schemes to produce numerically-generated secondary waves at the expense of also introducing artificial damping in the transient's behaviour. Therefore the key to using de Vries' scheme is to choose a β large enough to inhibit numerical wave generation, yet small enough that numerical damping does not drown out the physical processes (de Vries 1981). Though de Vries suggested β-values in the order of 0.001 to 0.05, the following test cases serve as a more specific guide in the selection process.

The performance of the scheme, as it appears in ONE-D-SED, was tested. A parametric study was performed on the following test case: A steady flow acting on a single bed disturbance, (initially in the form of a half cosine wave of amplitude z_o and length L), see figure 5.4. This case differs in its initial conditions from the assumption made in deriving the analytical solution, namely a singular rather than periodic bed disturbance was assumed. This was done because unique disturbances are often found at the application level and because this analysis is analogous to the study made by Lopez-Garcia (1977) and reported by Ponce et al. (1979). In testing the numerical schemes the complete forms of the St. Venant equations were used. When reporting the findings of the non-linear (numerical) analyses, all important or pertinent parameters (i.e., L, N_x, P_e, c_e, K_e and σ) were calculated using the above equations for initial conditions and assuming 'small' waves.

Many alternatives of z_o and L were simulated with the hypothetical bed disturbance located near the upstream end of a straight reach of 'wide' alluvial channel on a predetermined slope (figure 5.4). A wide range of discharges and initial bed slopes was used in the parametric study, with the sediment discharge being dependent on the local fluid velocity as described above. Different values of m and b were also used, although m was usually set equal to 3 since the results appeared to be insensitive to the m-value tested. The values of all parameters selected for a typical run are given in table 5.1 and the simulated movement of the bed is shown in figure 5.5. The downstream boundary was chosen far enough away from the transient that the depth at this point could be held constant.

Table 5.1: Input Data for the Simulation of a Bed Transient

Y_o	=	3.048 m	u	=	0.914 m/s	q	=	2.787 m^2/s
S_o	=	0.00009	L	=	1.609 km	z_o	=	0.305 m
s	=	93.(10^{-6}) m^2/s	p	=	0.4	F	=	0.167
z_*	=	0.10	c	=	157. (10^{-6}) m/s	K	=	1.72 m^2/s
P_e	=	0.147	c_e	=	157. (10^{-6}) m/s	K_e	=	93. (10^{-5}) m^2/s
z_1	=	0.263 m	σ	=	0.1	N_x	=	40
m	=	3	b	=	121.6 (10^{-6}) s^2/m		=	

For each test a grid density N_x was chosen, and σ and β selected. The model was then run until either the peak of the initial bed wave reached a point equal to one wavelength L downstream, or alternatively had attenuated to half of its original height. The time to reach this point was noted and the average bed wave velocity c_n calculated. This, in turn, permitted comparison of numerical and analytical values by means of a velocity coefficient (Lopez-Garcia 1977):

$$R_c = \frac{c_n}{c_e} \tag{5.4}$$

The amplitude of the bed wave at this point z_n was also employed to define an attenuation coefficient:

$$R_d = \frac{z_n}{z_L} \tag{5.5}$$

Fig. 5.5 demonstrates that the numerical solution for $z(x,t)$ is a function of the β chosen. When the viscosity term is small ($\beta = 0.027$), the solution is just on the verge of being contaminated by secondary waves. In the case presented in figure 5.5 the emergence of secondary waves is just beginning at $t = 2L/c_e$. Not shown in the figure is the case of emergence of strong secondary waves (as found in figure 5.8) that would occur at even lower selected values of β. On the other hand, as the value of β was increased from 0.027 to 0.2 (figure 5.5), the resulting bed wave profiles display increasing numerical dissipation. The value of β corresponding to least dissipation while tolerating no secondary waves when the peak had moved a distance L downstream was deemed to be "optimal" and is denoted by β_*.

Figure 5.6 shows the resulting functional relationship between β_* and σ obtained for various bed wave amplitudes and for fixed P_e and F. In all cases the relationship between β_* and σ plotted as a straight line on log-log paper over three cycles. As shown in the figure, β_* is a function of z_* (defined as z_0/Y_0) because the higher the value of z_*, the more non-linear the system and hence the steeper

Table 5.2: β_* as a Function of F and z_*, for σ = 0.1

	β_*	
z_*	F = 0.167	F = 0.334
0.01	0.0275	—
0.05	0.03	0.06
0.10	0.04	0.06
0.20	0.12	0.16

the wave front. In the same way, as reported in table 5.2, β_* must also increase for higher values of F. Moreover, at higher P_e, β_* can be decreased since in this case the wave front is less steep. At the same time a higher β can be tolerated because the ratio of numerical to physical diffusion is less. β_* was not found to be a function of N_x.

However, due to the changing nature of bed transients, in practice it is virtually impossible to use an optimal β over the whole (x, t) domain. If a smaller value is chosen, usually it is readily apparent in the results in the form of secondary waves. On the other hand, it is important to quantify the numerical dissipation introduced when the β selected is greater than the optimal value. In this regard, two convergence coefficients are defined; one for bed attenuation (C_d) and one for bed velocity (C_c). Assuming for the moment that, when N_x=100 and $\beta = \beta_*$, the best solution of the governing equations is generated by the model, then the convergence coefficients could be defined as:

$$C_d = \frac{z_n(N_x, \beta)}{z_n(100, \beta_*)} \times 100\,\% \tag{5.6}$$

$$C_c = \frac{c_n(N_x, \beta)}{c_n(100, \beta_*)} \times 100\,\% \tag{5.7}$$

These coefficients are quantified in figure 5.7 and table 5.3 as functions of N_x and

Table 5.3: Convergence Characteristics of de Vries' Scheme

	C_c		C_d	
z_*	F = 0.167	F = 0.334	F = 0.167	F = 0.334
0.01	99	99	94	92
0.05	98	97	94	94
0.10	94	90	92	88
0.20	77	72	80	75

β/β_*. The figure shows that when the optimal value of β is used (i.e. $\beta/\beta_* = 1.0$), there is convergence for all $N_x > 20$ (which justifies the above assumption). Also, when $N_x = 100$, $C_d \geq 85\%$, even when $\beta/\beta_* = 12$. However when N_x is small, there is a high gradient in the degree of convergence for greater than optimal selected values of β. It should be added that C_c and C_d are also functions of z_* and F. As both the bed wave amplitude and the Froude Number increase, it becomes increasingly difficult to achieve a converged solution. On the other hand, for the reasons stated above, when P_e is larger convergence is easier to obtain.

Finally, an unexpected finding of the convergence study was the fact that C_d and C_c were virtually independent of σ. In other words figure 5.7, which was generated using $\sigma = 0.1$, would apply equally well for $\sigma = 0.01$, assuming β_* was chosen in accordance with its relationship to σ (figure 5.6). These analyses were made using the long form (equation 4.19) of the de Vries' scheme (i.e., α_j^n was a function of x). Some test case simulations were then repeated using the short form (equation 4.20) of de Vries' scheme (i.e., α = constant) to investigate the properties of this simpler formulation. For all cases tested, virtually the same performance was achieved.

5.2.2 Fromm's Scheme

Using the same set of test cases, bed transients were simulated using Fromm's scheme within ONE-D-SED. Recall that analytical analyses of the scheme indicated favourable results but a tendency for the scheme to generate secondary waves when shock features are present. Both these findings were confirmed in the present (non-linear) parametric study.

At higher Péclet Numbers, which usually preclude the generation of shocks, the scheme performs very well when the bed Courant Number is sufficiently low. For example, when $z_a = 0.1$, $P_r = 0.5$, $F = 0.167$, and $\sigma \leq 0.05$, the bed profiles generated were nearly identical to one another (in terms of bed wave velocity and damping) for all $\sigma \leq 0.05$ and all $N_r \geq 15$. However, when σ was increased beyond this threshold value, secondary waves would begin to contaminate the solution (figure 5.8). For larger amplitude waves the threshold value of σ continues to decrease for higher F and lower P_r. For example, when $z_a = 0.2$, $F = 0.334$, and $P_r = 0.146$, secondary waves were generated even for σ as low as 0.005. Therefore, when Fromm's scheme is free of secondary waves it performs remarkably consistently over a whole range of σ and N_r. On the other hand, as the system becomes more dominated by translation, it becomes increasingly difficult to select a σ below the threshold value that ensures secondary waves will not appear in the solution.

When appropriate choices of numerical parameters were made, both Fromm and de Vries' schemes gave virtually the same results. Whereas de Vries' scheme has the shortcoming of having to estimate, a priori, a fairly arbitrary parameter in the pseudo-viscosity term β, it does allow the user the flexibility of increasing β until all secondary waves are inhibited.

5.3 Non-Linear Behavior of Finite Transients

The linear values for the effective bed velocity c_e and wave attenuation z_L originate from a perturbation analysis which assumes infinitesimal bed disturbances. When, in ONE-D-SED, the full set of non-linear governing equations were used to simulate finite bed transients the actual bed wave velocity c_n and wave attenuation z_n could be significantly different from their linear counterparts c_e and z_L. To quantify this effect the converged solutions of the model were used to generate the correction coefficients R_c and R_d (defined above), so that actual values of velocity and attenuation could be obtained by applying the coefficients to those obtained by the perturbation analysis. The coefficients, which were derived as functions of z_*, F and P_c, appear in figs. 5.9, 5.10 and 5.11. The conclusions of this analysis differ from Lopez-Garcia's (1977) findings because, in the latter, the reported R_d and R_c were only made functions of z_* and F. As such, the sensitivity of the coefficients to F is confused with a much greater sensitivity to P_c.

Figure 5.9 shows the dependency of R_d and R_c on the dimensionless bed wave amplitude z_* for two different F and $P_c = 0.147$. First, as z_* approaches zero, R_c and R_d both approach 1.0. This confirms that simulations made using ONE-D-SED are accurate. With regard to the non-linear behaviour of transients of finite height, R_d was in the 0.95 to 1.0 range for all $z_* \leq 0.1$. As z_* increases non-linear effects become more significant, especially at higher values of F. When $z_* = 0.2$ and $F = 0.334$, R_d fell to 0.85.

From figure 5.9 it is clear that bed velocity (as expressed by R_c) is more sensitive to transients of finite height. This is evident from the required adjustment in c_r indicated for different z_*. For example, when $z_* = 0.05$, $R_c = 1.2$; whereas when $z_* = 0.2$, R_c increases to 2.4 (for F = 0.334). Some of these effects were expected because higher velocities occur over the crest of the bed wave, which in turn results in higher values of s. On the other hand, the linear values of c_r and P_r are obtained from the value of s calculated for the uniform depth.

The sensitivity of non-linear effects to F can be seen more explicitly in figure 5.10. When $P_r = 0.147$ and $z_* = 0.1$, F only begins to play a major role for $F \geq 0.2$, at which point there is a sharp exponential rise in the value of R_c. This confirms the statement made by numerous researchers, including de Vries (1981) and Lyn (1989) that the analytical solution (equation 4.11) is particularly valid for low F values. Finally, the sensitivity of R_d and R_c to the Péclet Number is shown in figure 5.11 for $z_* = 0.1$. For $P_e \leq 2.0$, R_d is in the 90% to 110% range; however, as diffusion starts to dominate the system (at higher P_e), R_d increases dramatically. On the other hand R_c shows a high degree of sensitivity to P_e for both high and low P_e.

5.4 Discussion

For the conditions examined in this chapter, the convergence characteristics of de Vries' scheme are favourable for a grid density $N_x \geq 40$. Even when there is very little diffusion present in the physical system good results can be achieved (figure 5.7) if β is chosen according to the selection criteria implied in figure 5.6 and table 5.2. In general, convergence was found to be a function of the relationship of β to σ. Convergence is easier to achieve when F and z_m are small and when P_e is large.

For Fromm's scheme, simulated results are consistent when $N_x \geq 15$, as long as there is no generation of secondary waves. This is achieved by lowering the Courant Number until secondary waves disappear, which is an easier task when shock features are not present (i.e., at lower F and z_m and higher P_e).

In most of the cases tested, the analytical formulation (equation 4.11) of the bed transient problem provided a good representation of the governing equations. However, non-linearities became significant when the bed wave amplitude z_m was large, F was large and P_e was either high or low (figure 5.9 to 5.11). In such cases the bed wave velocity c_r may under- or over-predict the actual velocity c_n by 100%, while wave attenuation z_L may under- or over-predict actual bed attenuation z_n by 35% to 10% respectively.

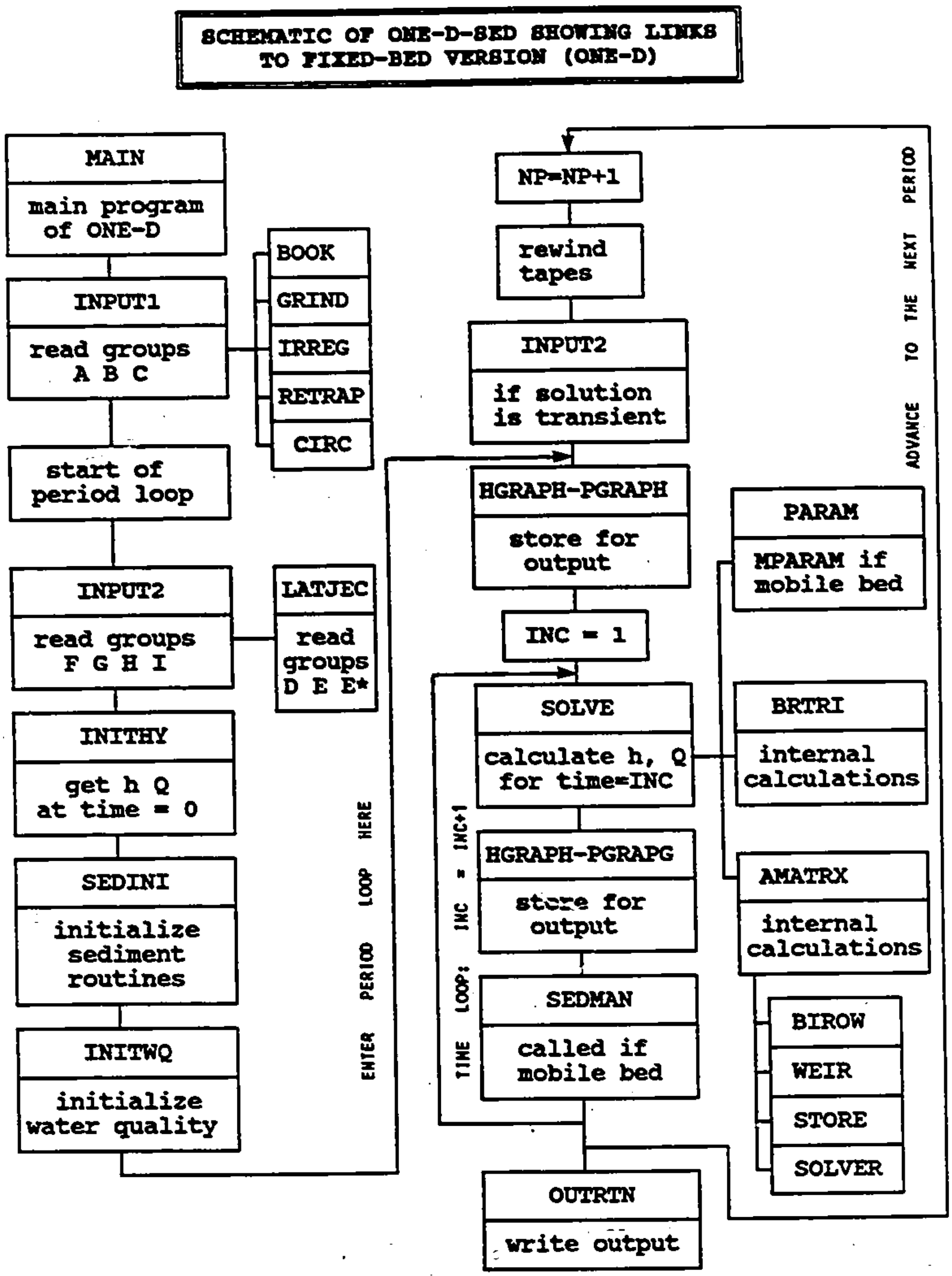

Figure 5.1: Flow Chart Showing ONE-D Links to Sediment Subroutines

*Note: See Appendix A for description of Subroutines.

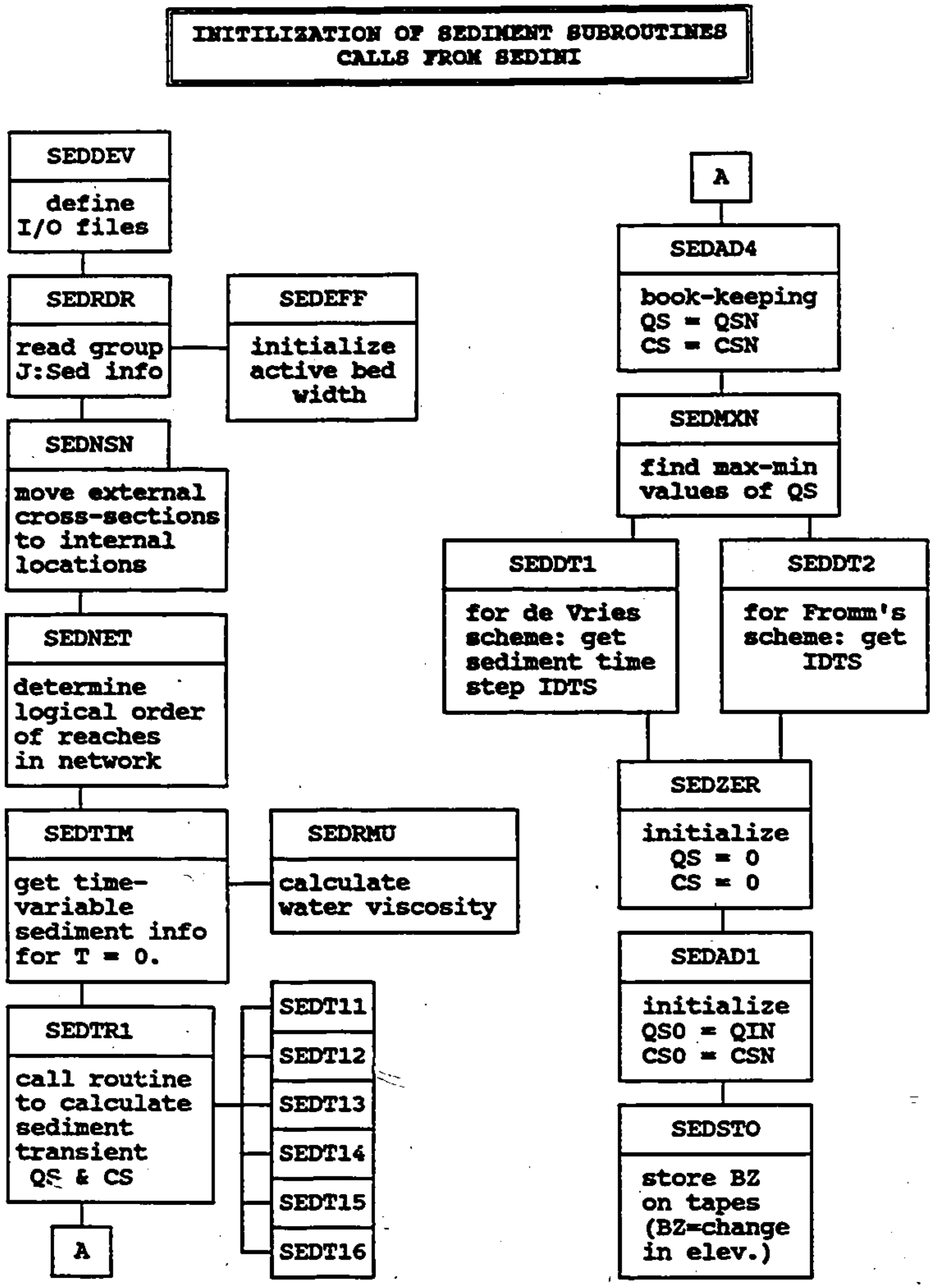

Figure 5.2: Flow Chart of Sediment Subroutines for Initial Conditions

*Note: See Appendix A for description of Subroutines.

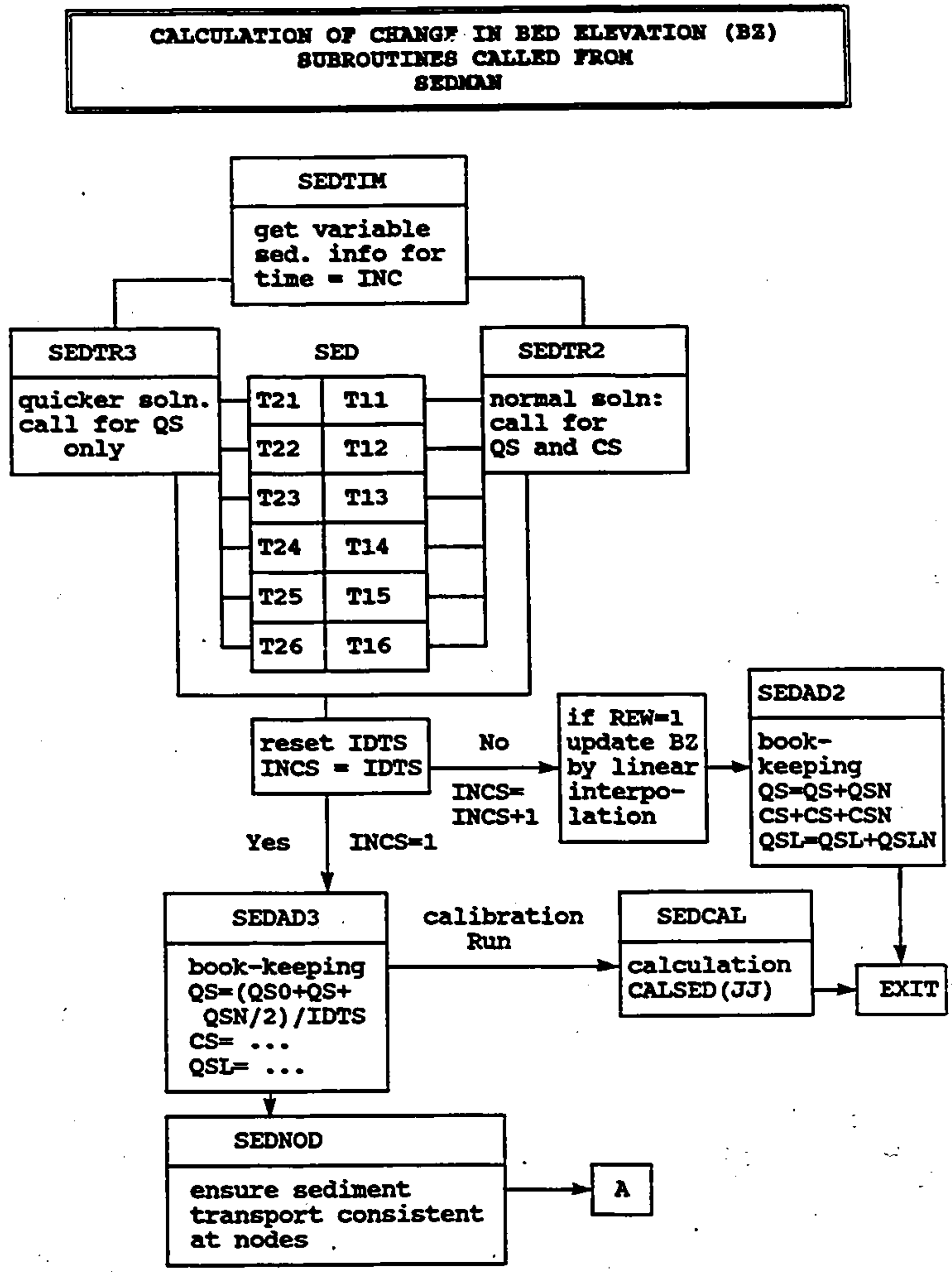

Figure 5.3: Flow Chart of Sediment Subroutines during Time Loop

*Note: See Appendix A for description of Subroutines.

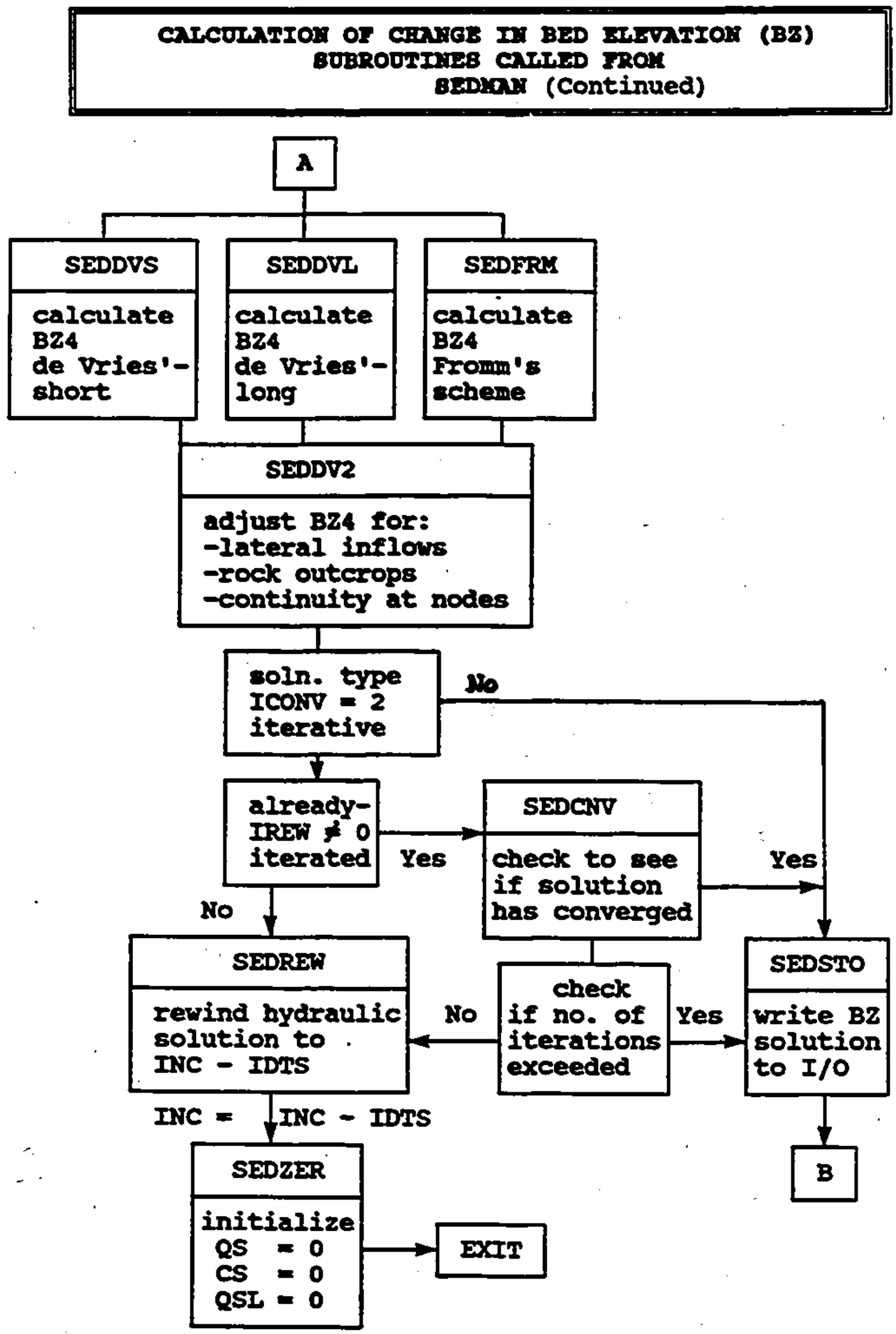

Figure 5.3: Flow Chart of Sediment Subroutines during Time Loop (Continued)

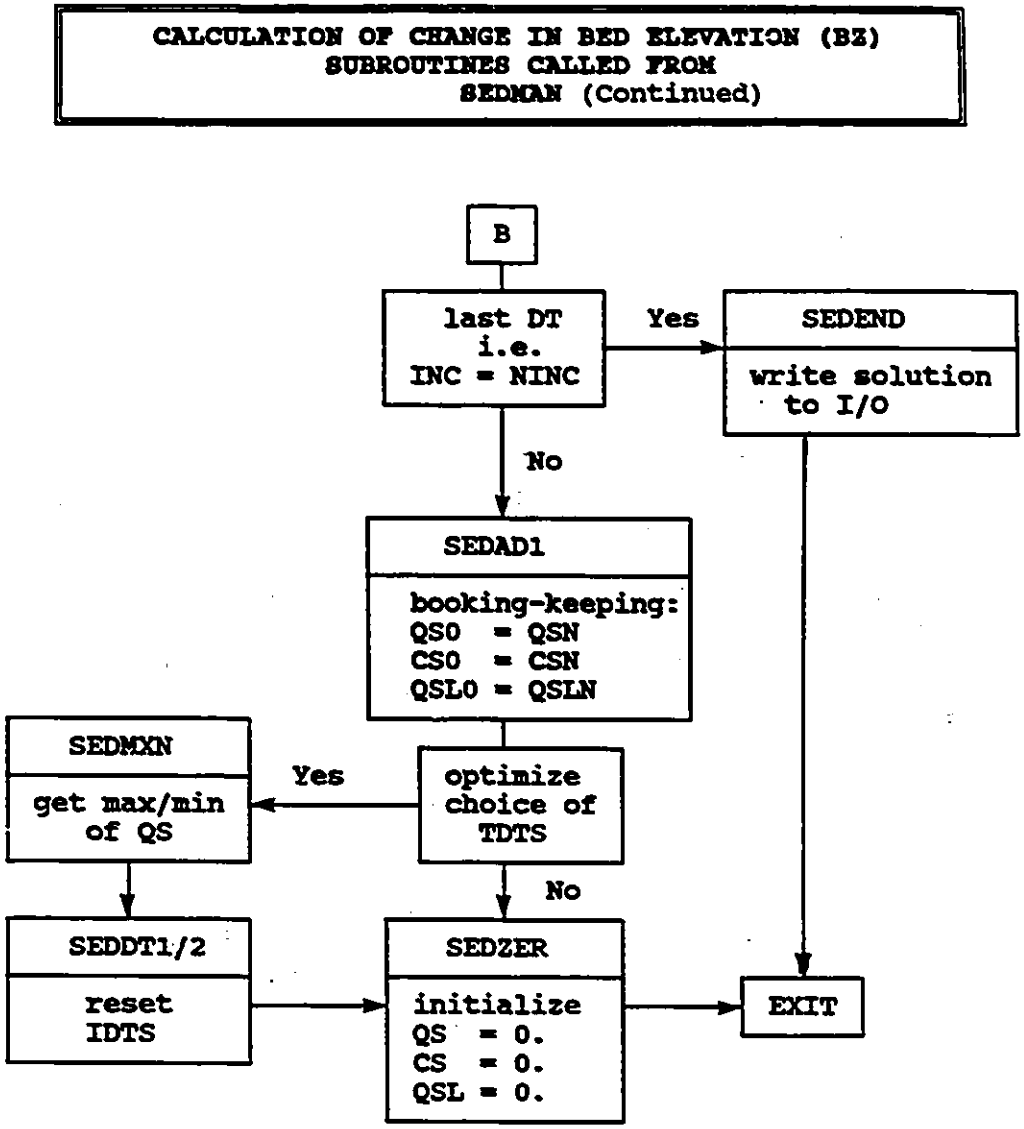

Figure 5.3: Flow Chart of Sediment Subroutines during Time Loop (Continued)

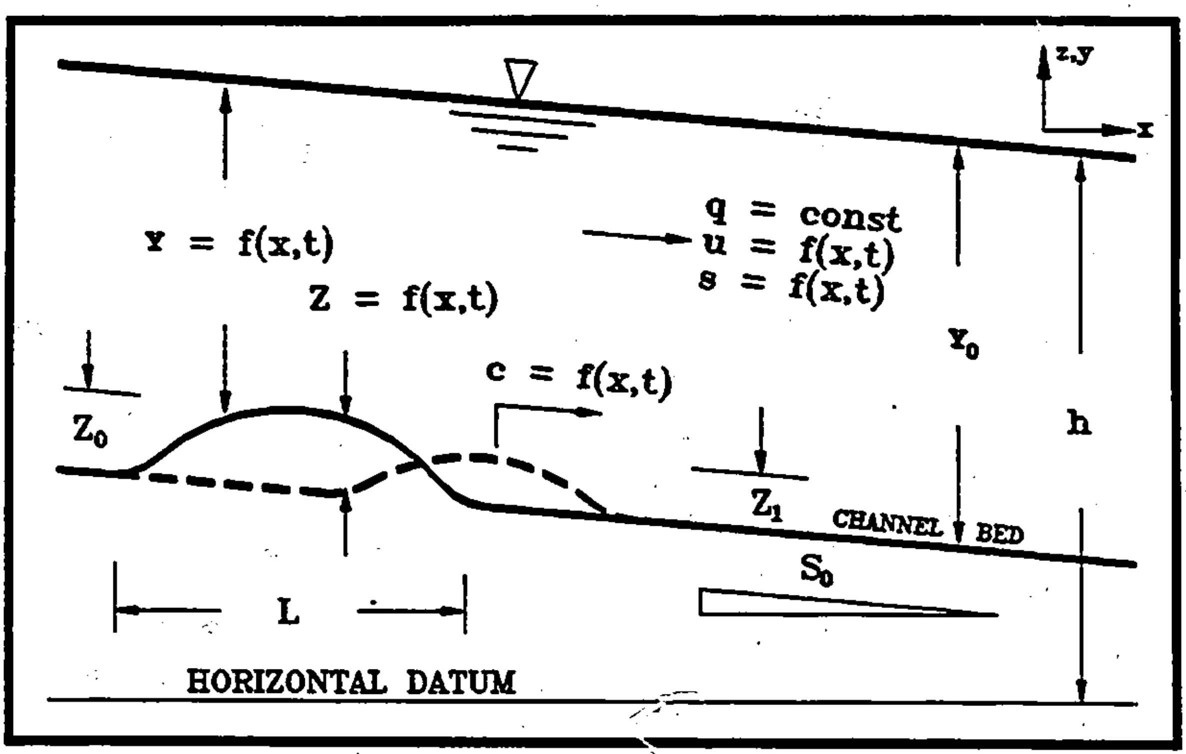

Figure 5.4: Definition Sketch

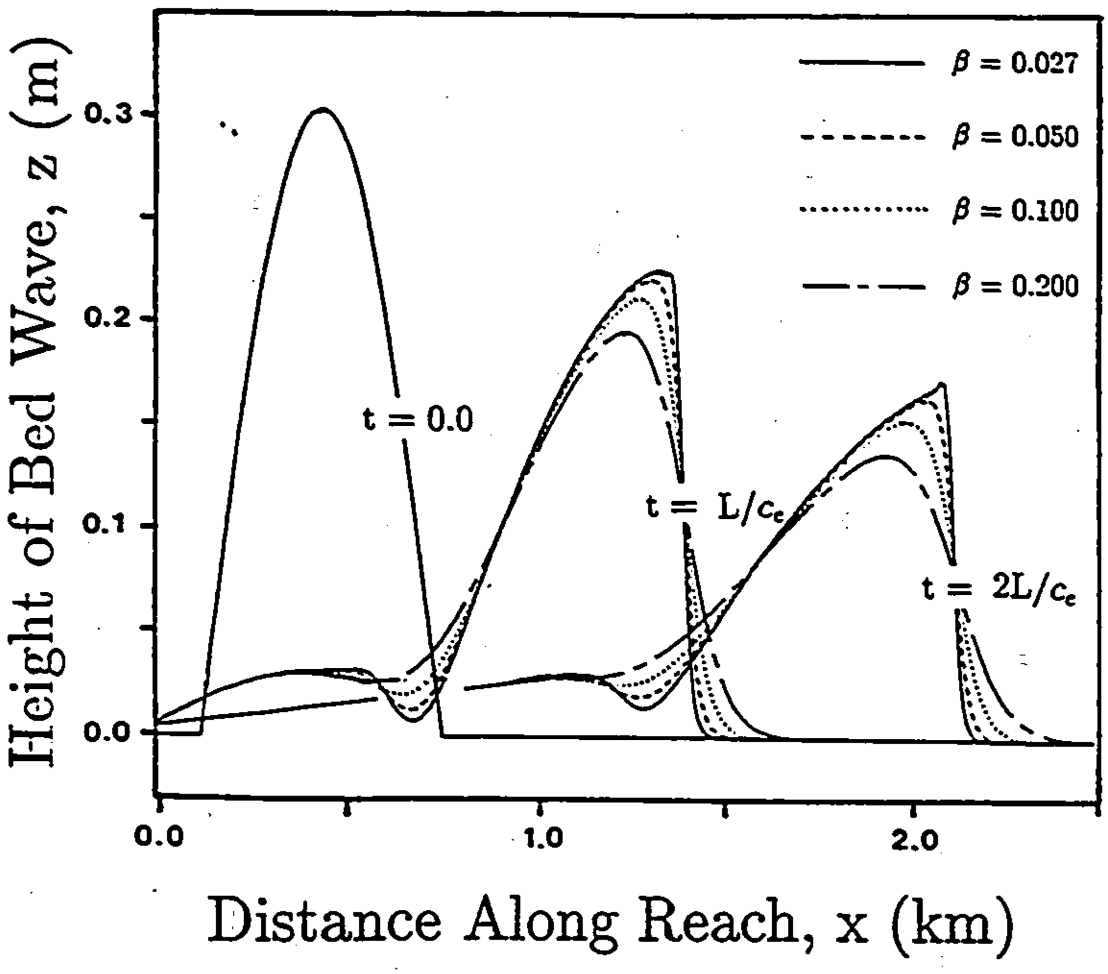

Figure 5.5: Attenuation of Sinusoidal Bed Wave Showing the Influence of Numerical Diffusion - de Vries' Scheme

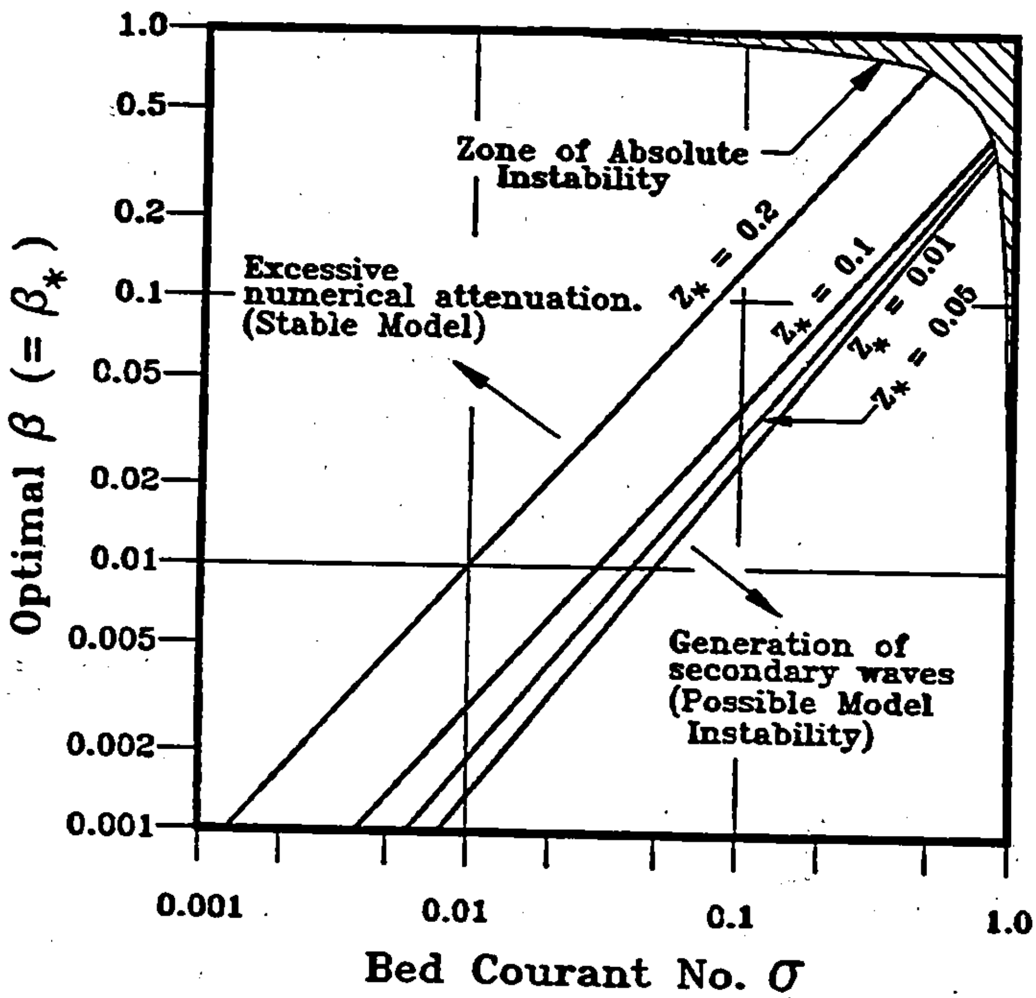

Figure 5.6: Relationship Between β_* and σ for Different z_*; with $F = 0.167$ and $P_c = 0.146$

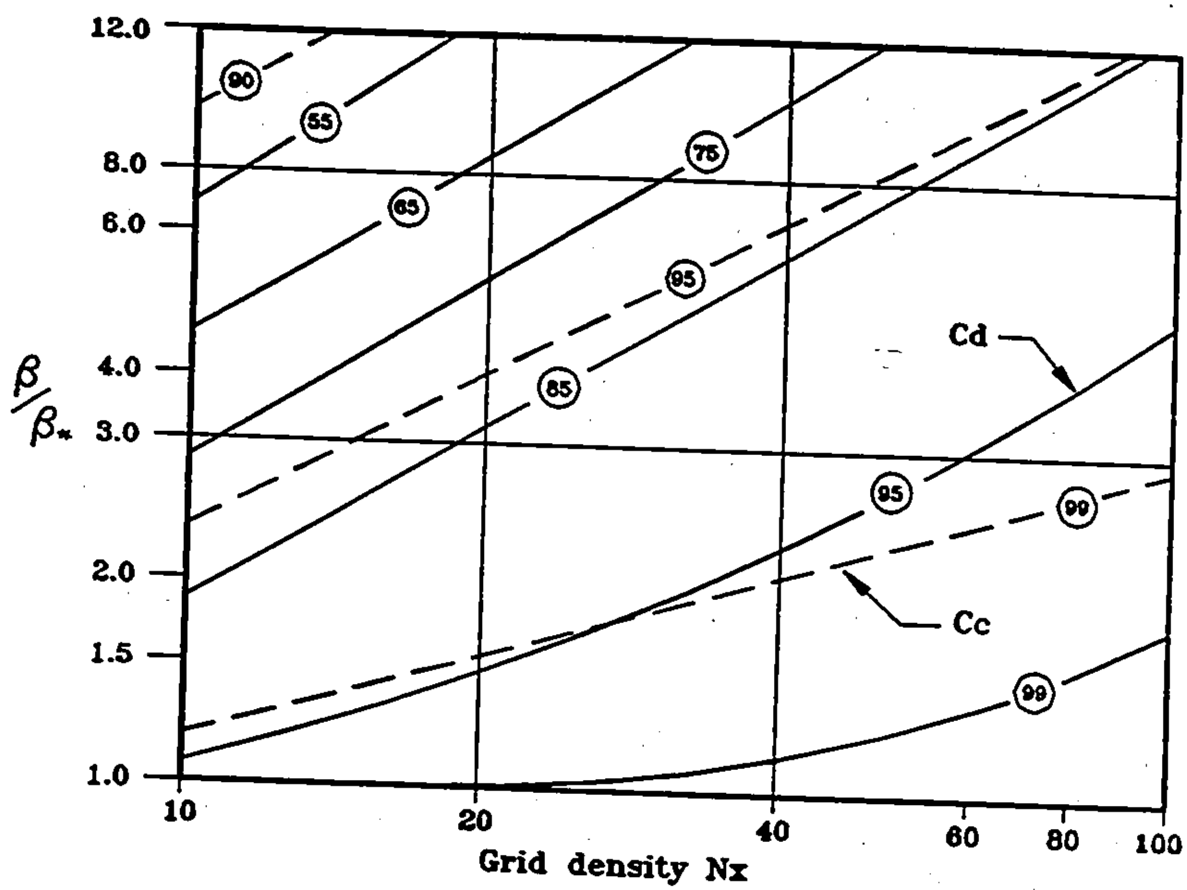

Figure 5.7: Convergence Characteristics for de Vries's Scheme as Function of N_x and β/β_*

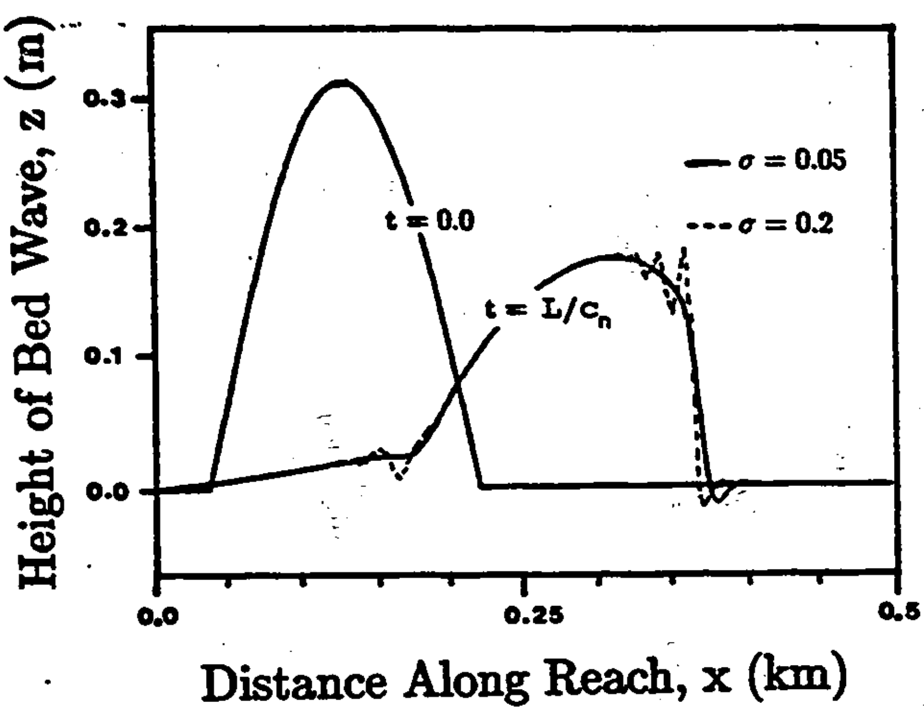

Figure 5.8: Attenuation of Sinusoidal Bed Wave Showing Effect of σ on Solution Stability - Fromm's Scheme

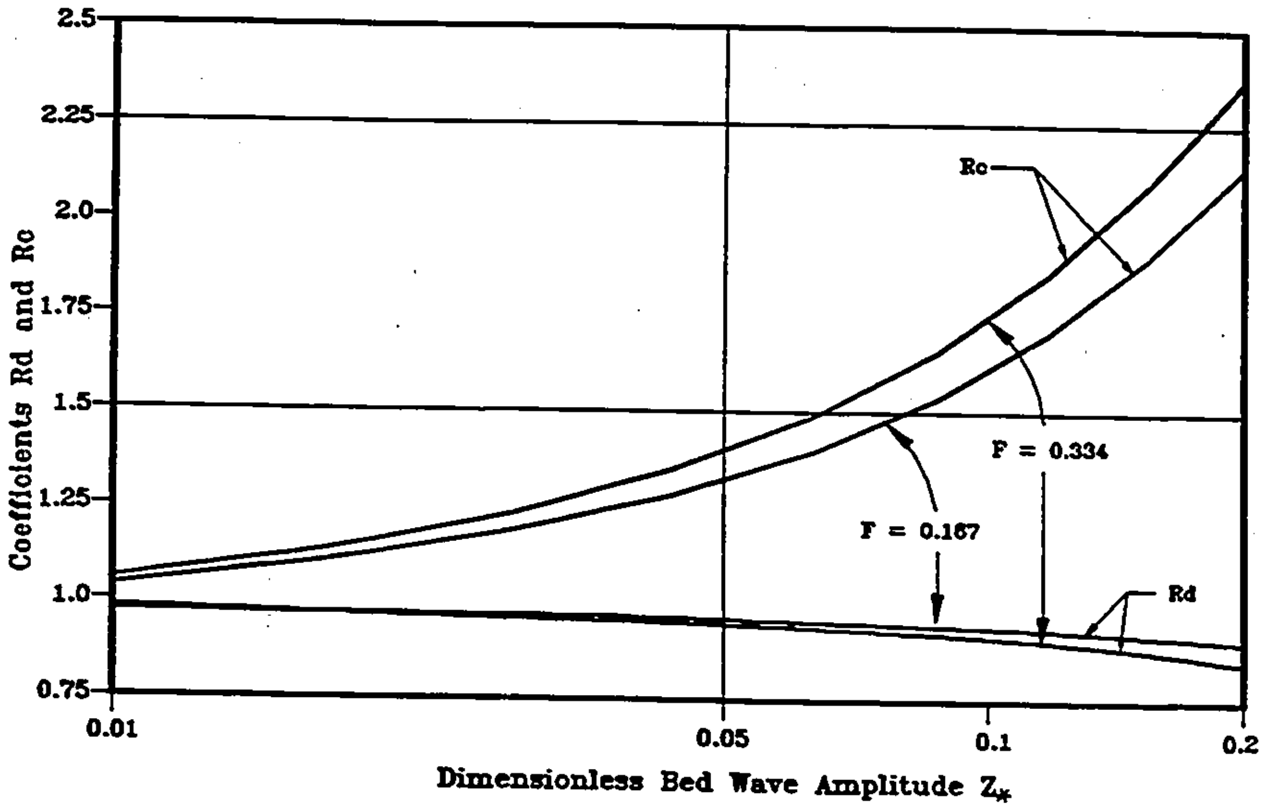

Figure 5.9: Influence of z_* on Attenuation and Velocity ($P_c = 0.146$)

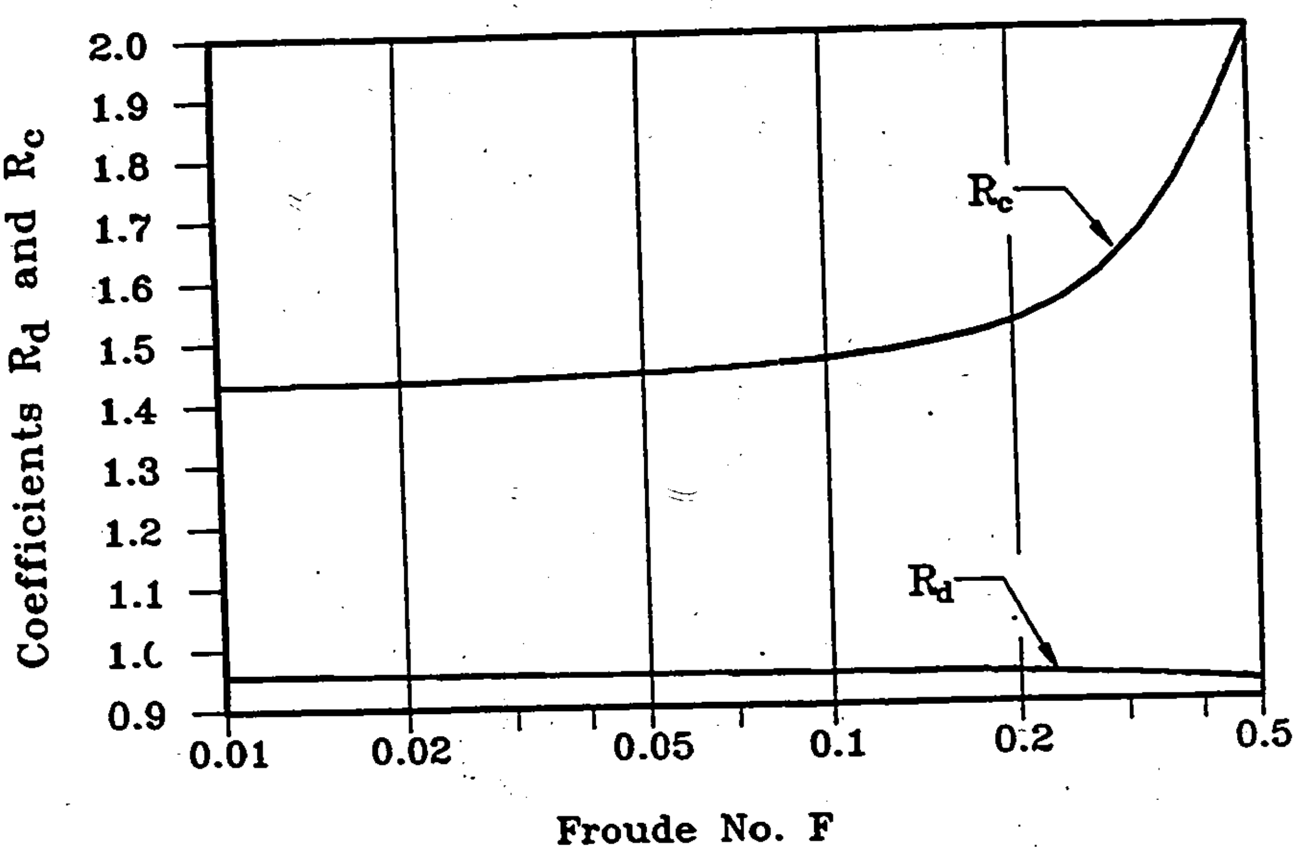

Figure 5.10: Influence of F on Attenuation and Velocity ($P_e = 0.146$) for $z_* = 0.1$

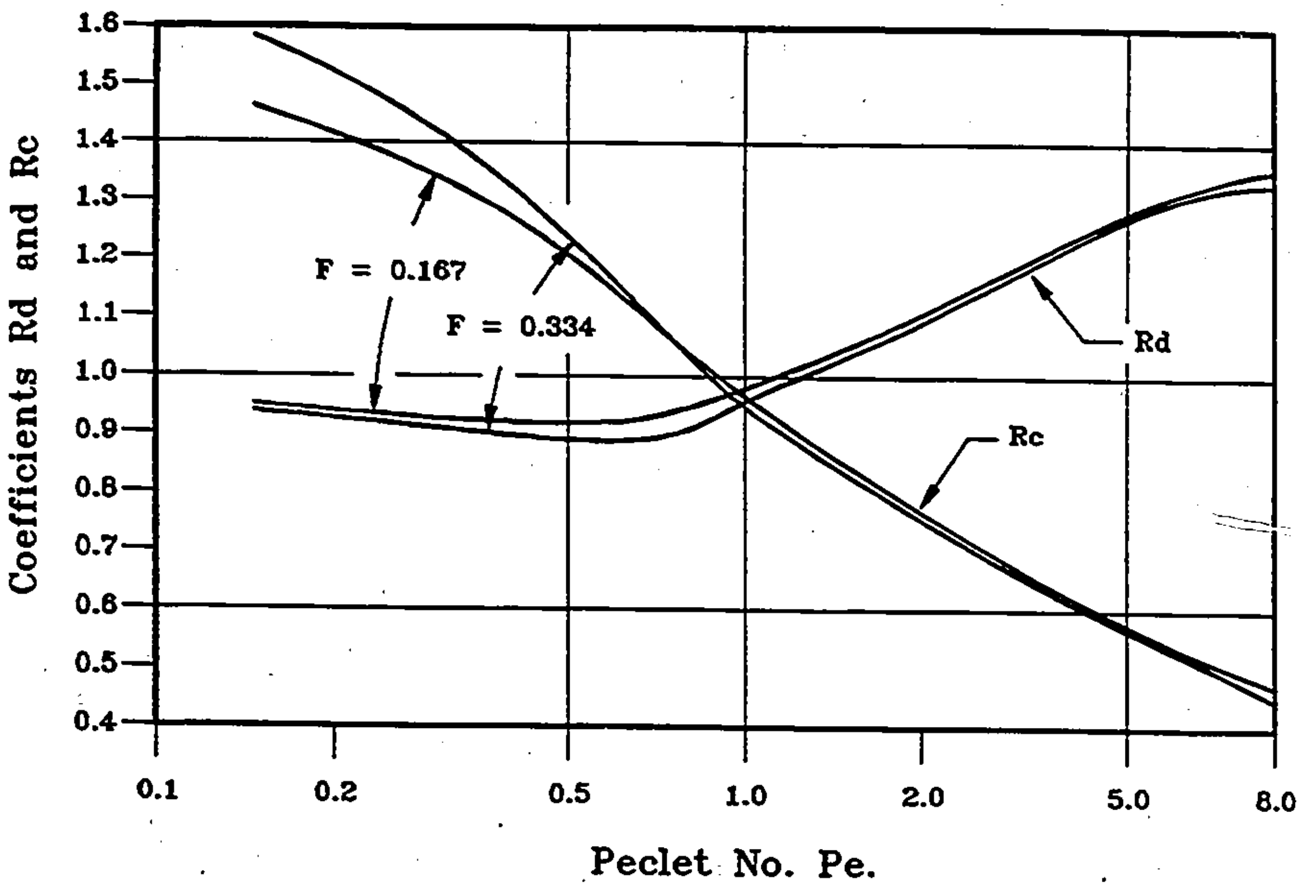

Figure 5.11: Influence of P_e on Attenuation and Velocity ($z_* = 0.1$)

Chapter 6

The Suspended Bed Material Load at Mission City

In this chapter, the sediment transport at Mission City is discussed. The Mission station is the most reliable source of sediment transport data for the Lower Fraser. Also, since this station is well defined in terms of hydraulic parameters, it forms the basis for simulating sediment transport processes in the Lower Fraser, beginning at Mission and extending down to the channel trifurcation area where the influence of the salt wedge becomes important.

Many factors make assessment of the sediment load complicated. First, there is the question of which sediment data set to use. Often data are missing important information such as grain size and local hydraulic conditions. Therefore, to obtain the bed material load (bml), unknown parameters must first be estimated. Finally, sediment transport functions must be calibrated to measured values.

The principle objective of analyzing sediment data at Mission is to determine the bml transport along the Lower Fraser River study reach. Since the bed material is fairly uniform in this reach, sediment transport equations developed for Mission can be applied to points further downstream. After making certain assumptions regarding the reach's state of dynamic equilibrium, bed river processes can then be simulated.

6.1 Available Data Sets

Five types of data are available for the determination of suspended bed material load (sbml). Within these 5 data sets, WSC distinguishes two groups based on the sampling method applied. First, samples may be obtained by the Point Integrating (PI) method. This consists of sampling sediment and velocity at five or six known depths in the water column. The sediment concentration is then determined by integrating the measurements over the total depth. This is a very labour-intensive sampling method that may or may not be repeated for different verticals in a given channel cross-section. This particular data set has been used to determine correction coefficients to be applied to data obtained through the second sampling method (since the latter do not measure the near-bed zone).

The second sampling method used by WSC is called the Depth Integrating (DI) method. In this case the sampler is lowered to the river bed, raised about 6 inches from the bed, activated and then gradually raised through the water column to the mid-point. A second sample is then taken from the mid-point to the water surface. Results from the two samples are subsequently combined and averaged.

The vast majority of sediment data collected uses the DI method.

Within the DI-type data, WSC further distinguishes two categories of data. The first, taken at five verticals within a channel cross-section, is known as "R" data. When R samples are taken, velocity, depth, water temperature and occasionally stage are also measured. The concentration from each vertical is then discharge-weighted to obtain a mean concentration for the entire cross-section. The second type of data consists of "K" samples. In this case, the DI method is employed at one vertical only. Since the vast majority of sampling is of the K type, this vertical is referred to as the "Daily" vertical.

To compensate for the inherent bias of sampling at one vertical only, K data is normally adjusted by means of a cross-stream distribution factor φ. This factor is calculated using R data. Normally the mean concentration obtained through R data is divided by the concentration measured at the Daily vertical. This quotient (and the discharge) is then plotted as a function of time. Based on the assumption that φ is a function of time and discharge, a line is fitted through the plotted quotient values. [This line is drawn based on the experience and best judgement of the technician assigned to this task]. The plotted φ line is then digitized and applied to measured K concentrations. The resulting product is published annually by WSC.

For the Mission site, there was a problem with this procedure that will be discussed later. For now, suffice it to say that it was the practice of WSC to use one of the five R verticals in the calculation of the φ quotients. Clearly, the Daily vertical should have been used. In the case of Mission, since the Daily vertical is located some 300 m downstream, φ values calculated by WSC should not used. (This matter was discussed with WSC personnel, and since 1984 the practice has been corrected).

For the purposes of determining sbml, the distinction should also be made between those data sets which do and those which do not have a grain size analysis. Such analysis is essential in order to separate the wash load (wl) from the sbml. Regarding the evaluation of the sbml, certain implications relating to 4 categories of DI data must be considered. At the first level is the R data which includes grain size analysis. In this case, the sbml can be determined directly. At the second level (R data without grain size analysis), a way must be found to estimate the percentage of the measured concentration contributing to the sbml. Towards this end Tassone and McLean (1989) developed appropriate relationships based on seasonal and hydrological factors. Though this procedure was well-suited to their hindcasting and forecasting purposes, it is not directly applicable to a hydraulically-based mathematical model.

To obtain sbml using the third data set (K data with grain size analysis), a relationship must be established between the measured sbml at the Daily vertical, and the mean sbml calculated using level-1 data. Note that the φ value used for this purpose should be one based on the sbml, rather than being based on the total concentration. Using the fourth data set (K samples without grain-size analysis) to obtain the sbml is even more difficult. This requires establishing the percentage of the concentration contributing to the sbml as a function of time at the Daily vertical and then using φ calculations to transform the former into a mean value for the entire cross- section.

6.2 Distinction between Wash and Bed Material Load

On the basis of grain size, some river engineers would identify only the clay fraction ($d \leq 0.062$ mm) as wl. Accordingly, for the Lower Fraser, 69 % of the suspended load would be considered wl and the remaining 31 % sbml. However, there is an alternate approach to distinguish between the wl and sbml in a river. In the second method, the distinction is based on whether or not the load is "supply" dominated. The grain size, which identifies the limiting size for the initiation of transport, is considered the "threshold" value. Since hydraulic conditions are changing continuously, so is the threshold grain size and therefore the distinction between wl and sbml. Since this particular approach enables the load to be quantified from a modelling view point, it is superior to the first method.

In this approach, the model must 'track' all the components of the sediment load and bed material composition as a function of grain size. Normally, the sediment load is divided into three to ten grain size classes. Depending on prevailing conditions, sediment in a given class may change from wash load (at high stream velocities) to sediment which is fully deposited and at rest on the channel bed (at lower velocities). As the load in each grain-size class is tracked, so too is the composition of the river bed. Normally this is done by dividing the bed into an active layer (at the surface) and other temporarily dormant layers below this layer. This method of distinguishing between wl and sbml is normally adopted in more sophisticated computer models. It obviously requires an enormous amount of bookkeeping, computational effort and special knowledge of boundary conditions. Its application is particularly appropriate for two- and three-dimensional modelling where, for example, wl is transferred to the sides of the channel or to minor channels where it may be deposited. It is also appropriate for reservoir modelling, insofar as the wl in a river feeding the reservoir eventually becomes bed material load in a downstream section of the reservoir.

The third way of distinguishing between wl and sbml combines some elements from each of the preceding methods. Einstein (1950) proposed that the division between wash and bed material load could be estimated by noting the d_{10} grain size of the bed material. Though this value is somewhat arbitrary, it is based on the observation that there will always be some fine material hidden between larger grains in the river bed. As such, this material is not available for transport. On the other hand, the fine material already in transport cannot deposit in the bed because there are no longer the required voids to receive it.

This classification scheme provides a basis for simple mobile-bed modelling. On one hand, the sbml is considered that which is in dynamic equilibrium with the bed. This allows for the calibration of a total sediment transport function. On the other hand, it is assumed that, while conditions may temporarily allow for the deposition of fine material, once channel velocity increases, this same material will be once again swept downstream. In this case, if there is a long-term trend in bed material gradation, the d_{10} value will also change with time.

Table 6.1: Bed Material Composition in the Lower Fraser River

Mission		Port Mann	
Distance from left marker (ft)	d_{10} value (*mm*)	Distance from left marker (ft)	d_{10} value (*mm*)
300	0.15	400	0.19
600	0.17	700	0.24
900	0.23	1000	0.30
1200	0.33	1300	0.26
1500		1600	0.17

Given the inherent limitations of Einstein's approach, in this study the distinction between wash and bed material load was based on the d_{10} value. This decision is consistent with the current stage of development of ONE-D-SED, which does not allow for tracking the sediment load as a function of grain size.

An analysis of 1968 bed material samples revealed the distribution of d_{10} values at the Mission and Port Mann sampling stations as noted in table 6.1:

When this analysis was first presented, it was suggested to WSC that a d_{10} value of about 0.2 mm should be used for the threshold between wl and sbml. Prior to this recommendation, McLean and Church (1986) were using 0.125 as the threshold value. Subsequently to the 0.2 mm threshold- value recommendation they changed their threshold value from 0.125 mm to 0.19 mm (Tassone and McLean 1989).

For one-dimensional models, a single d_{10} value must be selected. However, it is clear from table 6.1 that the bed material shows a cross-stream gradation. At Mission, even though the river reach upstream is straight for some 4 km, the grain size distribution is skewed across the channel width. The straight reach at Port

Mann, on the other hand, shows the more usual distribution, i.e. larger grains in the middle of the channel and smaller grains near the bank. The gradation of grain size across the channel suggests that hydraulic and sediment processes are highly three-dimensional and that using a one-dimensional model such as ONE-D-SED implies that the simulation of bed material load and bed processes are greatly simplified.

6.3 Estimating Hydraulic Parameters

When R samples are obtained, water temperature is recorded and both depth and mean velocity are measured at each sampling vertical. The total instantaneous discharge is also calculated by WSC personnel. To calibrate a sediment transport function, the area, wetted perimeter, hydraulic radius and top width must be known. Though WSC was most accommodating in providing original data for this study, the above noted parameters were not obtained in some cases. Since for 1968 all parameters were obtained for all 61 R samples, relationships between these parameters and the average measured depth $\bar{D}$ were calculated by linear regression (Figures 6.1 to 6.4). The relationships are:

$$A = -4281 + 1751.55 \times \bar{D}; \tag{6.1}$$

$$R = 3.48 + 0.8335 \times \bar{D}; \tag{6.2}$$

$$WP = 1434 + 8.7000 \times \bar{D}; \tag{6.3}$$

$$T = 1429 + 8.5339 \times \bar{D}. \tag{6.4}$$

where D = (D300 + D600 + D900 + D1200 + D1500) × 0.2; D300, D600, D900, D1200 and D1500 are the measured depths (ft) at the sampling verticals located 300, 600, 900, 1200 and 1500 ft respectively from the left marker; A is the cross-sectional area (sq. ft); R is the hydraulic radius (ft); WP is the wetted perimeter (ft) and T is the top width (ft). It should be noted that the WSC data was normally in imperial units (although sometimes also found in a mixed format). The WSC values reported in this work used the original symbols and units. Moreover, in order to conform with the internal calculations of ONE-D (and the Fraser ONE-D model in particular), ONE-D-SED was developed for imperial units. Hence, in this study, it was more appropriate to work in imperial rather than S.I. units.

Even though it takes about an hour to sample at all five verticals, and the stage can change quite rapidly during that period (particularly at small depths), figures 6.1 to 6.4 demonstrate that relationships 6.1-6.4 provide good estimates of measured parameters. The difference between observed and predicted values is small in nearly all cases.

These relationships were used to obtain missing information when calibrating the sediment transport function. However, since the relationships used in ONE-D-SED Fraser model are not identical to those reported above, the transport function was also calibrated using the relationships contained in ONE-D-SED. In ONE-D-SED, all cross-section geometry is related to stage. So, for the calibration based on the model's internal relationships, stage was obtained by noting that the mean bed elevation was -24.46 ft in relation to the Geodetic Survey of Canada (GSC) datum. This value was obtained using known stage and $\bar{D}$ throughout 1968. Tests

Table 6.2: Distribution of Panel Discharge at Mission

Vertical	*Percent Discharge*
300	15.388
600	20.807
900	20.423
1200	21.991
1500	21.391

confirmed that there was virtually no trend of mean bed elevation as a function of discharge during 1968 and hence the average bed elevation value was adopted throughout.

Earlier it was stated that the mean observed suspended sediment load was obtained by adding the products of the measured concentration at each vertical and the associated panel discharge. The panel discharge was obtained by multiplying the measured velocity at each vertical by the area of each vertical's panel. Since panel discharges were only obtained from WSC for 1968, they had to be estimated for other years. Analysis of the 61 R data of 1968 revealed the distribution of panel discharges found in table 6.2.

The analysis indicated that the measured values departed from those quoted here by less than 1.5 % . When these mean values were used in lieu of the measured panel discharges, only a slight error was introduced in the computed total load. For example, suppose the measured concentrations for a given R data set were 50, 60, 70, 80 and 100 mg/l at verticals 300 through 1500 respectively. Further suppose that measurements indicated the following distribution of panel discharge: 16, 20, 20, 22 and 22 % respectively. Then the mean concentration would be (50×0.16)

+ (60 × 0.20) + (70 × 0.20) + (80 × 0.22) + (100 × 0.22) = 73.60 mg/l. Using average panel discharge percentages, the computed mean concentration would be (50 × 0.15388) + (60 × 0.20807) + (70 × 0.20423) + (80 × 0.21991) + (100 × 0.21391) = 73.46 mg/l. In this example, even though the assumed concentration was quite skewed, the error introduced in the calculated mean concentration when using average panel discharge values is a mere 0.2 %. This error is typical of errors noted when actual 1968 concentration and discharge panel data were used. Therefore, it was concluded that using average panel discharge values introduced no appreciable error in the computed mean sediment concentration.

Once the mean concentration was calculated, only one item remained to be determined. When sediment is sampled using the DI method, the sampling begins some 6 inches from the river bed. Thus, a systematic underestimation of the actual mean sediment concentration is introduced. To eliminate this "near-bed" bias the measured concentration was increased by a certain amount. The overall adjustment was found to be about 7 %. This adjustment was based on analysis of PI data which is documented in the next chapter.

To obtain the total bml, the bed load should also be added to the sbml. For most sand-bed rivers the bed load, defined as that material moving within 2 grain diameters of the channel bottom, is negligible. In the case of the Fraser River study reach, bml is virtually identical to sbml.

6.4 Calibration of the Sediment Transport Function

ONE-D-SED provides the user with the option of selecting from five sediment transport functions. For the Fraser River application, the Akers-White (A-W, see appendix B) expression was selected. Documentation of sediment transport relationships (White et al. 1975) indicated that the A-W expression is one of the superior relationships available.

Constants used in the A-W relationship were developed based on laboratory data wherein the representative bed material size d_r corresponded to d_{50}. Subsequent applications of the relationship to field studies indicated that when d_{50} was used for d_r, bed material loads were generally under-estimated. The authors, therefore, suggested that for field applications a better choice for d_r might be d_{35}.

Virtually all sediment transport formulae employ a representative grain size. Usually these relationships were developed using laboratory data, where the representative grain size to be employed was usually well defined because gradation in bed material was usually very small. However, when applying relationships to field studies little guidance is available regarding selection of the representative grain size to be used. Ackers and White are among the few sources to address this question.

The problem of applying sediment transport relationships in the field is the fact that suspended sediment in rivers usually has a wide grain-size gradation. In this doctoral program, in order to determine d_r, a special analysis was made to quantify it for field studies (chapter 8).

By applying different eddy viscosity models, it is shown that the representative fall velocity of a sediment mixture depends on: the fineness of the sediment mixture, the amount of grain gradation within the suspended load, and the ratio of the mean fall velocity of the sediment mixture to the bed shear velocity in the channel. Moreover, it is demonstrated that the larger the grain gradation, the smaller to be the d_r should be chosen. Such analysis confirms Ackers and White's observation that bed material loads would be under-estimated in natural channels if the d_{50} were used. However, it is further concluded (chapter 8) that depending on hydraulic conditions and the actual grain gradation in a particular river, the representative grain size might well differ from the d_{35} value. d_r varies depending on the river studied and the period analyzed.

Cognizant of these findings, the strategy adopted for the calibration of the A-W relationship was to choose a representative grain size initially based on the d_{50} value and then to apply a correction coefficient to computed values to account for any under-prediction of the sediment load.

d_{50} values of individual bed samples in the Fraser River study reach varied a great deal as a function of location and time. Though a slight decrease in value was detected in samples taken closer to the mouth of the Fraser, no systematic variation of d_{50} was found as a function of discharge or time. Data in the study reach indicated that d_{50} fell somewhere between 0.3 to 0.4 mm.

Before reporting the results of the said calibration, it is of interest to report the findings of a parametric analysis of the A-W relationship. In this analysis a single parameter was varied while holding all others constant (Figure 6.5 to 6.9). Figure 6.5 demonstrates how the computed bed material concentration increases as a function of discharge when the specific gravity of the grains (SG) is 2.65, the temperature is 3° C, the hydraulic mean depth (HD defined as A/T) is 35 ft and the d_r is 0.35 mm. For this case, initiation of motion is indicated at about 100,000 cfs and the computed concentration increases exponentially thereafter.

Figure 6.6 demonstrates that when the discharge is held constant at 300,000 cfs, there is an inverse relationship between computed concentration and the HD. The effect of water temperature on computed transport rates is indicated in figure 6.7. When other parameters are held constant, there is a fairly uniform drop of about 23 % in computed concentration when the temperature rises from 3° C to 18° C. In ONE-D-SED and in this analysis, water viscosity is computed as a function of water temperature based on a non-linear interpolation of published values (Vanoni 1975). Finally, the effect of d_r on computed values is displayed for different discharges in figures 6.8 and 6.9. Computed concentrations for $d_r \leq 0.25$ mm indicate a marked sensitivity to d_r. For values ≥ 0.3 mm, predicted rates are not as sensitive to d_r.

The parametric analysis indicates that computed concentrations are dominated by the discharge and are marginally sensitive to water temperature. It also indicates that the computed bed material concentration will be in error by about 10 % when normal variations in river bed elevation occur (of approximately 1 foot) and they are not incorporated into the calculations.

Noting that the A-W function was stable for values of d_r greater than 0.3 mm, the calibration of the equation was undertaken. Initially, a trial d_r of 0.3 mm produced good agreement between computed and predicted mean loads. However, it was found that the computed rate of increase in concentration as a function of discharge was higher than that observed. When 0.4 mm was used for d_r, the predicted load using A-W grossly under-predicted the mean concentration. In addition, the computed rate of increase of concentration as a function of discharge was lower than that observed. Clearly the appropriate d_r, was between these two values.

The final value chosen for d_r was based on matching the computed rate of increase of concentration as a function of discharge to that observed. The method consisted of choosing a d_r and obtaining computed concentrations. A linear regression was then made between computed and measured values. This regression was made using a 'no-intercept' option. The factor obtained was such that once computed concentrations were multiplied by it, they equalled, on the average, those observed (Figure 6.10).

Next the ratio of measured to modified-computed values were plotted as a function of discharge (Figure 6.11). Any trend of the ratio indicated that computed concentrations were not increasing as a function of discharge at the same rate as those observed. The foregoing procedure was then repeated using different values of d_r until any trend was removed. The final d_r value chosen was 0.345 mm. Using this value, modified computed values displayed the same sensitivity to discharge as those observed (figure 12).

It was noted that an exception to this general rule occurred at very low discharges. In this case, the modified computed values were still systematically low. The interpretation of this anomaly was that the A-W equation was not accurately predicting the onset of sediment motion. To remedy the problem, the initiation of motion parameter "CA" (internal to the A-W equation) was modified from CA = $0.14 + 0.23/D_{gr}$ to CA = $0.175 + 0.23/D_{gr}$ (where D_{gr} is the dimensionless grain size defined in the A-W equation).

It was found that, in order to match the sbml at Mission (adjusted for the near-bed DI sampling bias), the modified A-W relationship should be multiplied by a factor of 2.02. Since it is further assumed that the sbml only relates to 90% of the actual bed composition, the calibration factor was increased by 100%/90% to account for additional material $\leq d_{10}$ being deposited or removed from the channel bottom along with those grains included in the sbml. Hence for the Fraser the A-W computed load in ONE-D-SED is multiplied by the calibration factor 2.25 (= 2.02/0.9).

Secondary data sets were used to verify the calibrated relationship. As stated beforehand, once cross-stream distribution factors φ are obtained, K data with grain size analysis can provide an estimate of the sbml. In the following section, the value of φ is quantified. Then using K data from 1968, the validity of the calibrated A-W is examined.

6.5 Cross-Stream Distribution Factors

Typical measured velocities at Mission are shown in figure 6.13. The shape of the cross-section is quite regular and the isovels are distributed in a standard manner. In the associated figures 6.14 through 6.17, the sediment concentrations for different grain sizes are also plotted. Though these figures provide only a sample (instantaneous) representation it is noted that the gradation of fine material is much less pronounced than that for coarser material. The example provides an indication of how the total and bed material load may be distributed in a given cross-section of the Lower Fraser. To obtain mean values of the total, sand, bed or suspended loads at Mission from a measurement at a single vertical, it is first necessary to quantify how the load is distributed at this particular cross-section.

Figure 6.18 shows the mean distribution of the various types of sediment loads at the Mission station, based on the analysis of the 78 point R data set used in the previous section. It is noted that the coarser the load investigated, the more the cross-stream gradient increases. The distribution of the loads at this sampling station is of interest because the daily vertical is only 300 m downstream. Though the distribution of sediment there would be somewhat different than at the sampling station, a comparison between the two locations can be made. In particular, a comparison of φ factors calculated for vertical 900 (φ_9) can be made with those calculated for the Daily vertical (φ_D).

As indicated at the beginning of this chapter, φ represents the ratio of the mean concentration at the sampling station to the measured concentration at the reference vertical (either vertical 900 of the sampling station itself or preferably, the Daily vertical located downstream). The mean concentration used is that based on the panel discharge weighting method outlined earlier. Table 6.3 summarizes the calculated mean φ values and their associated standard deviations. In the table the subscript "t" represents φ calculations based on total suspended load, "s" represents calculations based on the suspended sand load only, "c" represents calculations based on the suspended load coarser than 0.125 mm and "b" represents calculations based on the sbml.

Table 6.3: Cross-Stream Distribution Factors (φ)

Reference Vertical: 900	*Reference Vertical: Daily*
φ_{9t} = 0.90 +/- 0.10	φ_{Dt} = 0.79 +/- 0.08
φ_{9s} = 0.77 +/- 0.16	φ_{Ds} = 0.62 +/- 0.13
φ_{9c} = 0.75 +/- 0.24	no data
φ_{9b} = 0.74 +/- 0.26	no data

Values calculated for vertical 900 (φ_9) were based on the full R data set from 1965 to 1984. However, simultaneous measurements of concentration and the Daily vertical were introduced only in 1978. As a result, φ_D values were only based on 25 measurements between 1978 and 1984. To verify that there is a basis for comparison, φ_9 values were recalculated based on this 25 point data set and were found to be within 1% of those values quoted here. φ_{Dc} and φ_{Db} values were not calculated because certain necessary information at the Daily vertical was missing.

It was stated previously that φ used by WSC assumed that φ varied gradually as a function of time and discharge; hence the practice of drawing a smooth φ line between measured quotients. Clearly the WSC assumption was reasonable. Using the 78 point R data set, φ_9 and discharge were plotted as functions of time for the various years. It was noted that φ was indeed dependent on both discharge and time, although no consistent pattern was evident. Figures 6.19, 6.20 and 6.21 are an indication of the global results obtained for φ_{9f}, φ_{9s} and φ_{9c} respectively. While there is a small reduction in φ_{9f} and φ_{9s} as a function of discharge, the reduction is dwarfed by the scatter of the points around the regression line and, in the case of φ_{9c} , the linear regression indicated a small increase (rather than a decrease) in value.

It may be argued that these figures are misleading in that they represent values obtained from different years. However, φ_{9f} was calculated using a 60 point R data set in 1968. The resulting quotients are plotted in Figure 6.22. Clearly, in this case, the time-discharge dependence implemented by WSC is over-stated. In fact any trend in φ_{9f} for 1968 is difficult to quantify.

Given the above findings, it is concluded that it is appropriate to use an average φ, in lieu of a time-discharge dependent value, particularly for those calculations requiring the reduced R data set including grain size analysis.

The scatter in the calculated φ (figures 6.19 to 6.21) is quantified by the standard deviation of φ given in table 6.3. It should be noted that there is a marked increase in scatter, with respect to the grain size class for which φ was calculated. This may simply be due to the fact that the cross-stream distribution of the coarser load is more variable than that of the finer load. However, there may also be a numerically-based reason originating from the error made in estimating the grain distribution of given samples. Consider that, as a result of the sampler shape, the sampling technique used, or errors introduced in the laboratory analysis, there is an error of 3 % in the estimate of the grain size distribution. If this error was an absolute value, since 31 % of the load is sand and 18 % of the load is coarser than 0.125 mm, the relative error of the sand portion of the total load would be 3 % × 100 % / 31 % = 10 %. Similarly the relative error of load greater than 0.125 mm would be 3 % × 100 % / 18 % = 17 %. Hence the error for the coarser load would be nearly double the error associated with the finer load.

This example also suggests another source of bias in the computations: Since measurement of small quantities is difficult, the normal practice at WSC is to perform grain size analyses only on those samples whose concentration is greater than 100 mg/l. Hence computed φ are weighted towards the more significant sediment discharge periods.

Having identified some of the inherent limitations of the φ-factors and their application, a φ_{Db}-value is nevertheless required if K data sets that include grain size analysis are to be used. Due to the limitations of certain data, φ_{Db} must be extrapolated from other available φ_D values. In table 6.3 it is noted that, while the φ_{9s} is significantly lower than φ_{9t}, there is only a marginal difference between φ_{9s}, φ_{9c} and φ_{9b}. This suggests that, at the sampling station, the distribution of the sand load is a very good indication of the distribution of the sbml. If the same can be said for the Daily vertical, then it follows that φ_{Db} should be marginally less than the φ_{Ds} obtained. With this in mind, the φ_{Db} selected was 0.60.

6.6 Validation of the A-W Equation

Having estimated the cross-stream distribution factor φ_{Db}, the 48 K data with grain size analysis sampled during 1968 could be used to validate the A-W equation (calibrated based on R data obtained between 1965 and 1983). Suspended sediment transported coarser than 0.19 mm was calculated using 1968 K data. The value was subsequently multiplied by $\varphi_{Db} = 0.60$ to obtain an estimate of the mean sbml at Mission. The product was plotted along with 1965-183 R (figure 6.23). The plotted points suggest that both data sets have the same depency on discharge. This observation confirms the methodology used.

The adjusted 1968 K data were further increased by 7% to account for the near-bed bias introduced by DI sampling. The resulting values were then plotted as "measured" values in Figure 6.23 along with measured R data values for 1968. Computed-modified A-W values are included in the same figure. In should be noted that, in this case, hydraulic parameters were based on measured stage rather than measured mean depth $\bar{D}$ when computing predicted values. This was done because $\bar{D}$ was not available for the time the K samples were collected. $\bar{D}$ was estimated using known stage and by assuming that the mean bed elevation at Mission was -24.6 ft GSC (see discussion above).

In general predicted sbml concentrations reproduce those observed. The limitation of the A-W sediment function is its failure to reproduce the full range of the observed load particularly at high discharges. Some of the observed scatter is simply due to the statistical nature of sediment transport processes. However, in this case the observed scatter is probably due in part to the increased sediment load associated with dune formation and to the extra sand load originating in the gravel-bed portion of the river a few kilometers upstream of Mission. During the quieter months preceding the spring freshet, sand deposits in the braided channel reaches (McLean and Church 1986). When the freshet occurs, an excessive amount of sand is swept into the study reach. Equilibrium of local sbml transport is probably only established after a period of time and some travel distance. In 1968 there was an abnormally high "first flush" effect to compound this particular "feature". Concentrations calculated based on local hydraulic conditions alone will never fully simulate all of these natural processes.

6.7 Sediment Load for the Entire Study Reach

Thus far, the discussion relating to bml has been confined primarily to the simulated and observed sbml values at the Mission survey station. In order to model the Fraser study reach from Mission to Port Mann, a sediment transport function must be obtained for each computational point in the reach. One approach is to assume a gradation in d_r as a function of distance and use the same sediment function throughout. However, due to the high variability in the cross-sectional geometry of natural channels, this approach leads to grossly unrealistic estimates of the sediment load as a function of distance. In these circumstances, the transport function would predict very different loads every few hundred meters, which would translate into severe degradation followed by severe aggradation all the way down the channel. Clearly this is not representative of the natural processes.

To overcome this difficulty an alternate sediment transport calibration approach is required. In this study it was postulated that the river was in dynamic equilibrium for the period preceding the major channel improvements made during 1969 to 1972. In this scenario the assumption is made that, while the river bed may adjust to transient phenomena, the governing bed slope remained essentially constant over a period of time. Since large-scale morphological processes are generally slow, normally the period of time selected should be measured in decades. However, due to other constraints, an equilibrium was assumed for the 1968 calendar year. This period contains the complete annual sediment and discharge cycle and corresponds to a time when there had been no dramatic river training works or over-dredging in the area.

ONE-D-SED was run in the "calibration" mode for the entire 1968 year. Since the bed is assumed to be in equilibrium for that period, calibration coefficients were calculated for each computational point such that the river's transport was the same as that computed at Mission for the entire year. Using these coefficients the model was then re-run to verify that no significant net change in bed elevation was simulated. In this way the bml for Mission was obtained and the A-W relationship was calibrated for the entire study reach.

This page is intentionally left blank.

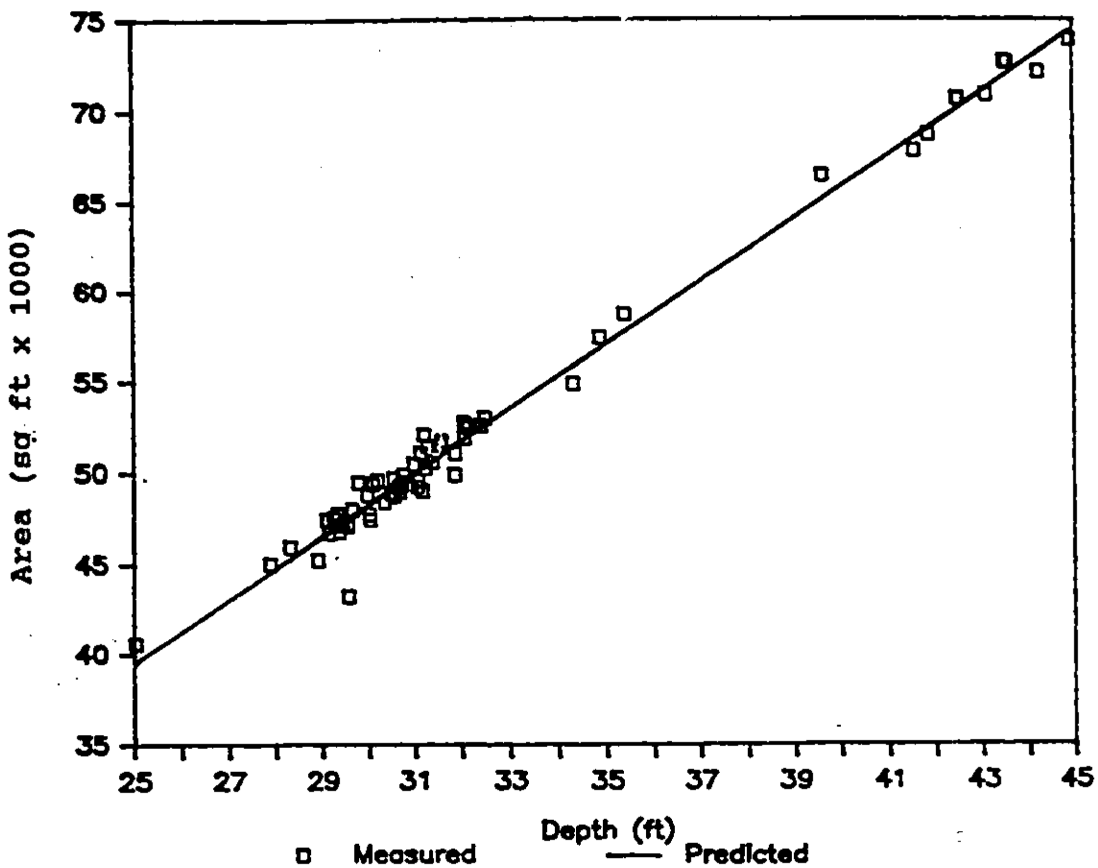

Figure 6.1: Regression of Cross-Sectional Area to Mean Depth - Mission 1968

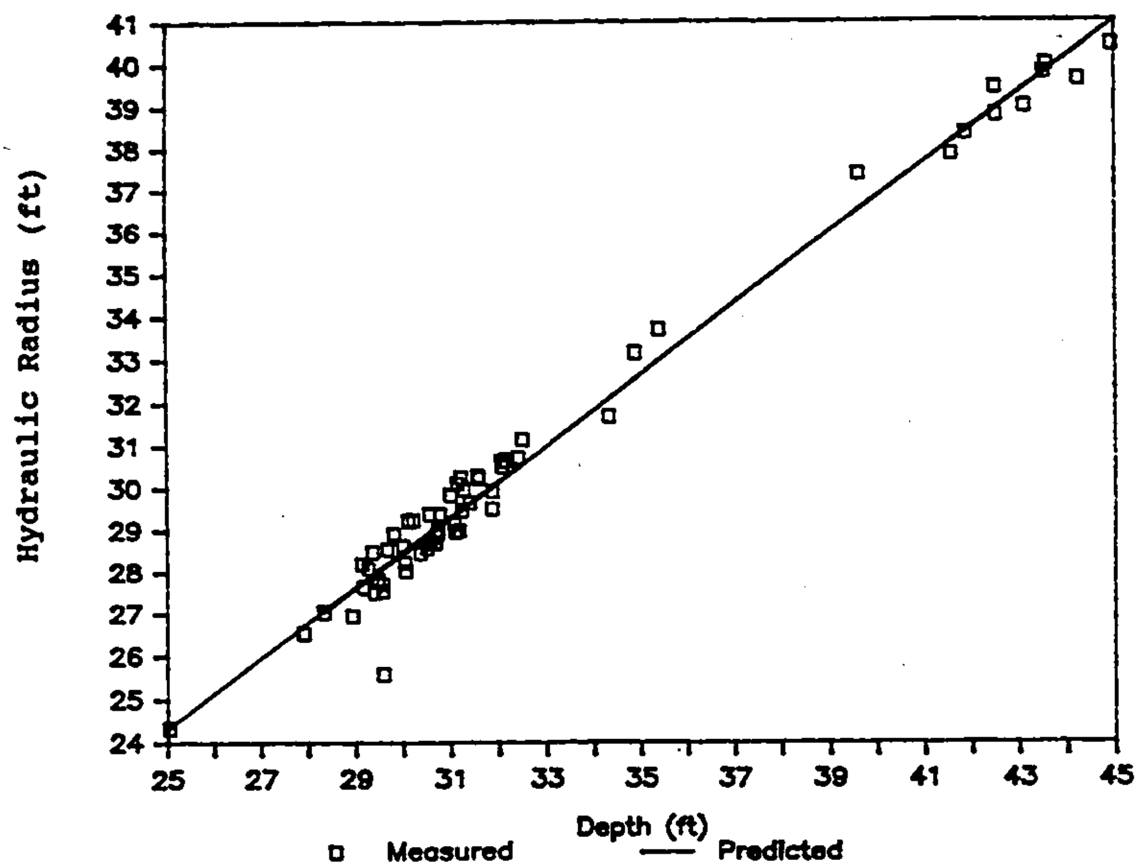

Figure 6.2: Regression of Hydraulic Radius to Mean Depth - Mission 1968

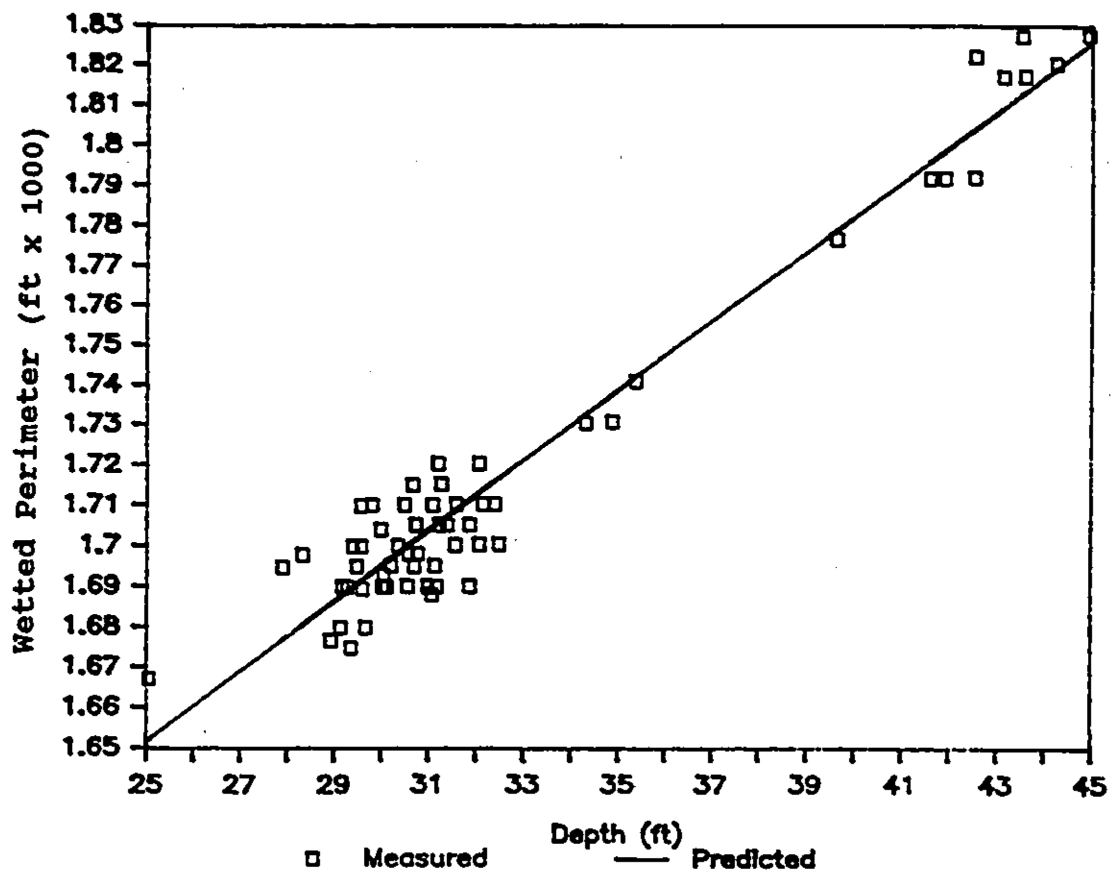

Figure 6.3: Regression of Wetted Perimeter to Mean Depth - Mission 1968

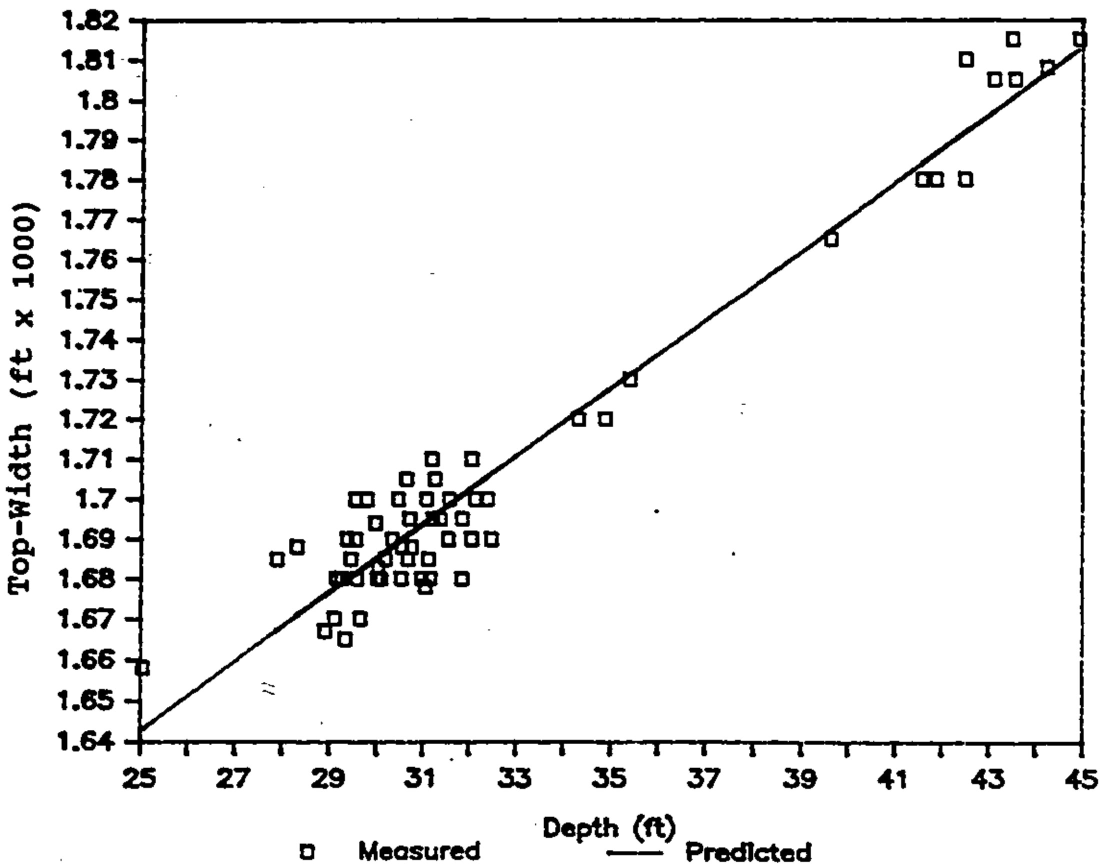

Figure 6.4: Regression of Top-Width to Mean Depth - Mission 1968

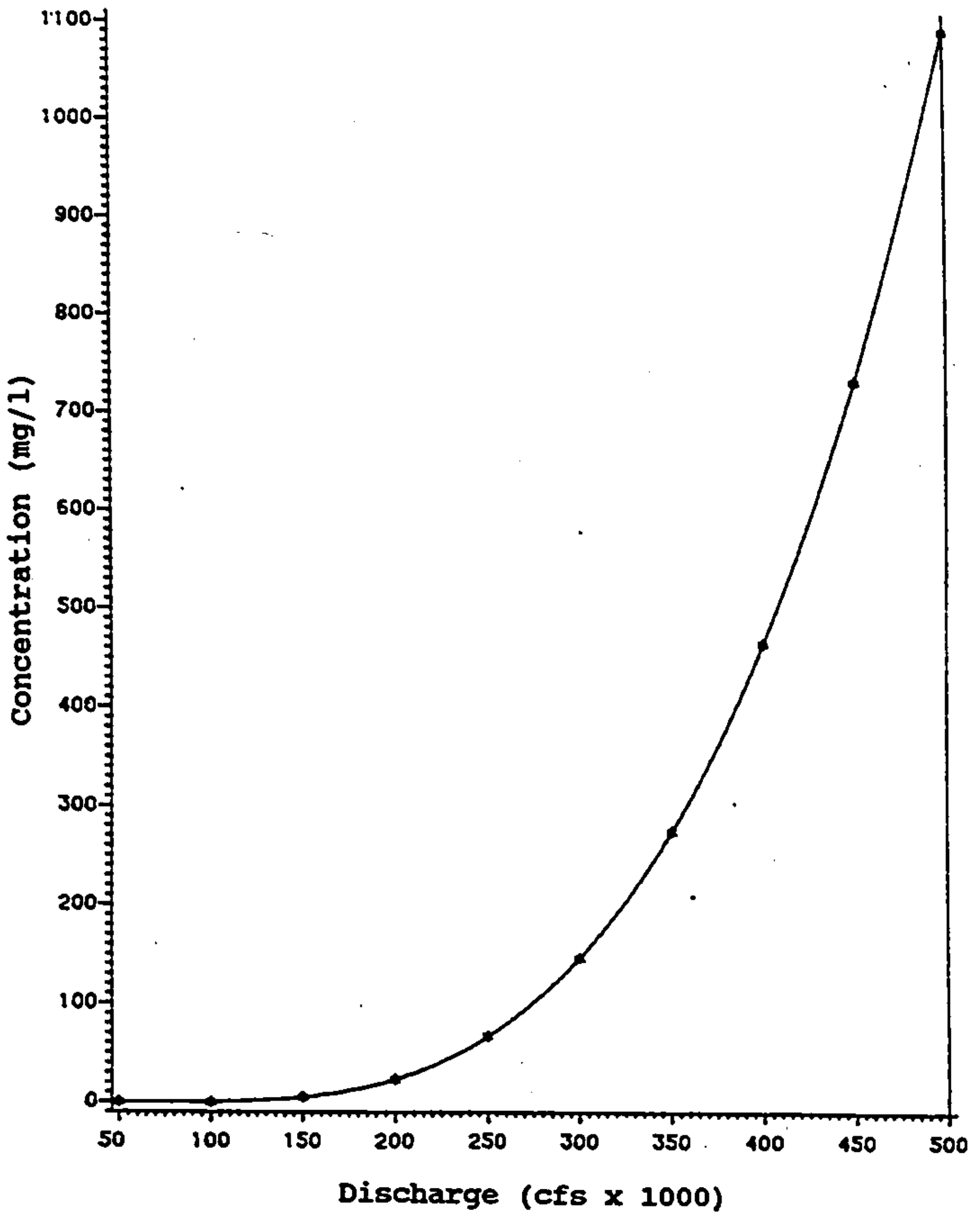

Figure 6.5: Parameteric Analysis of A-W Equation - Sensitivity to Discharge

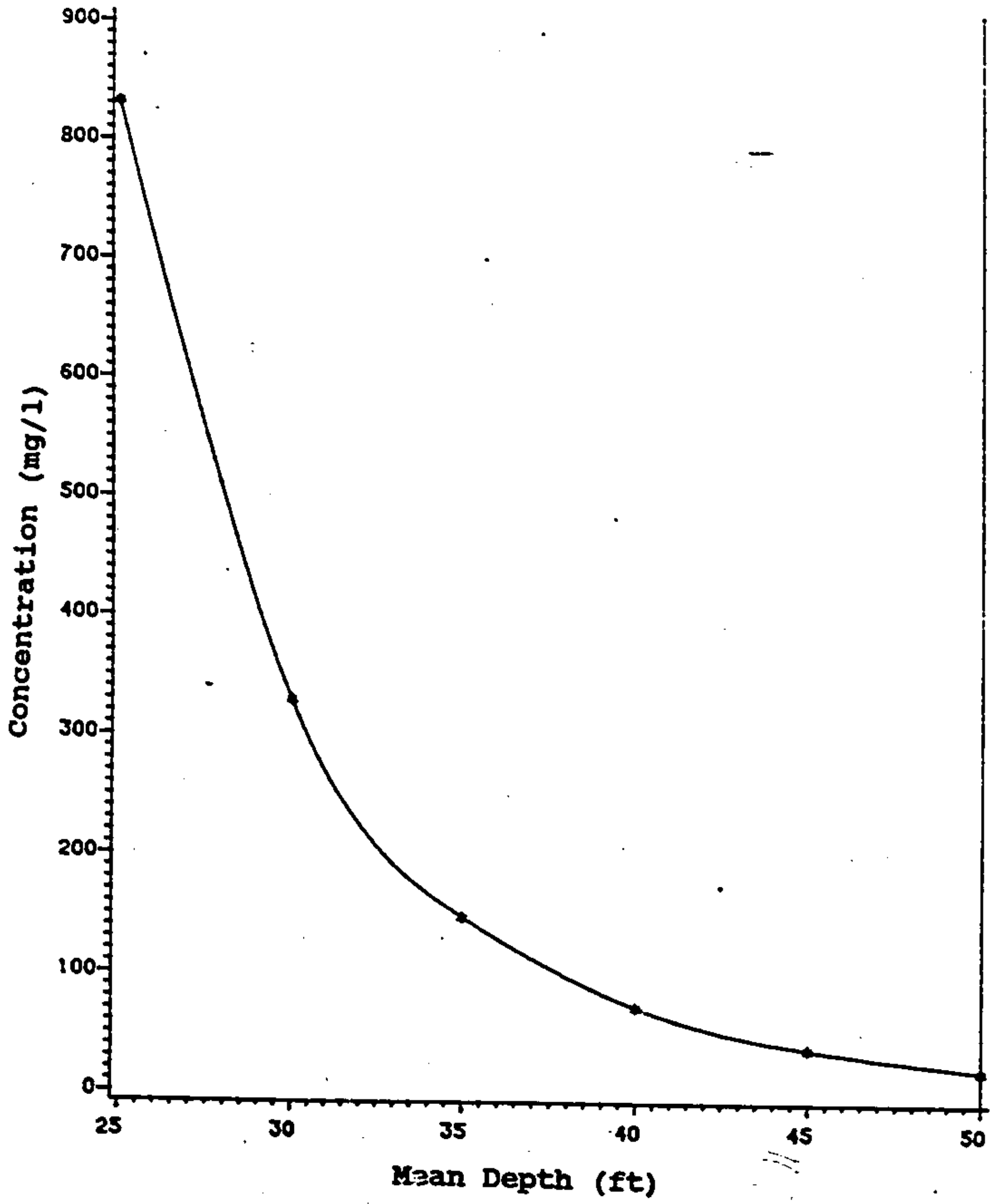

Figure 6.6: Parameteric Analysis of A-W Equation - Sensitivity to Depth

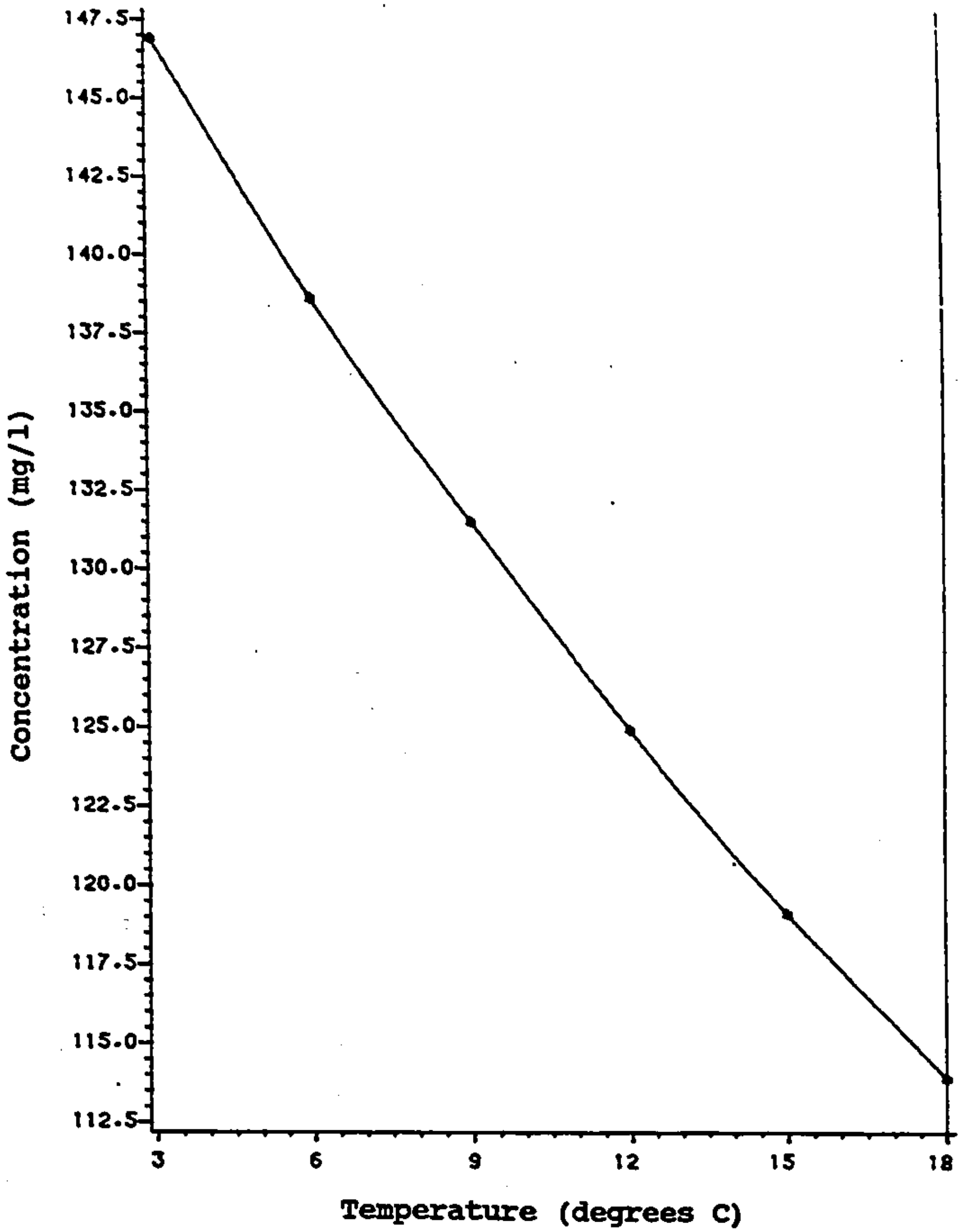

Figure 6.7: Parameteric Analysis of A-W Equation - Sensitivity to Temperature

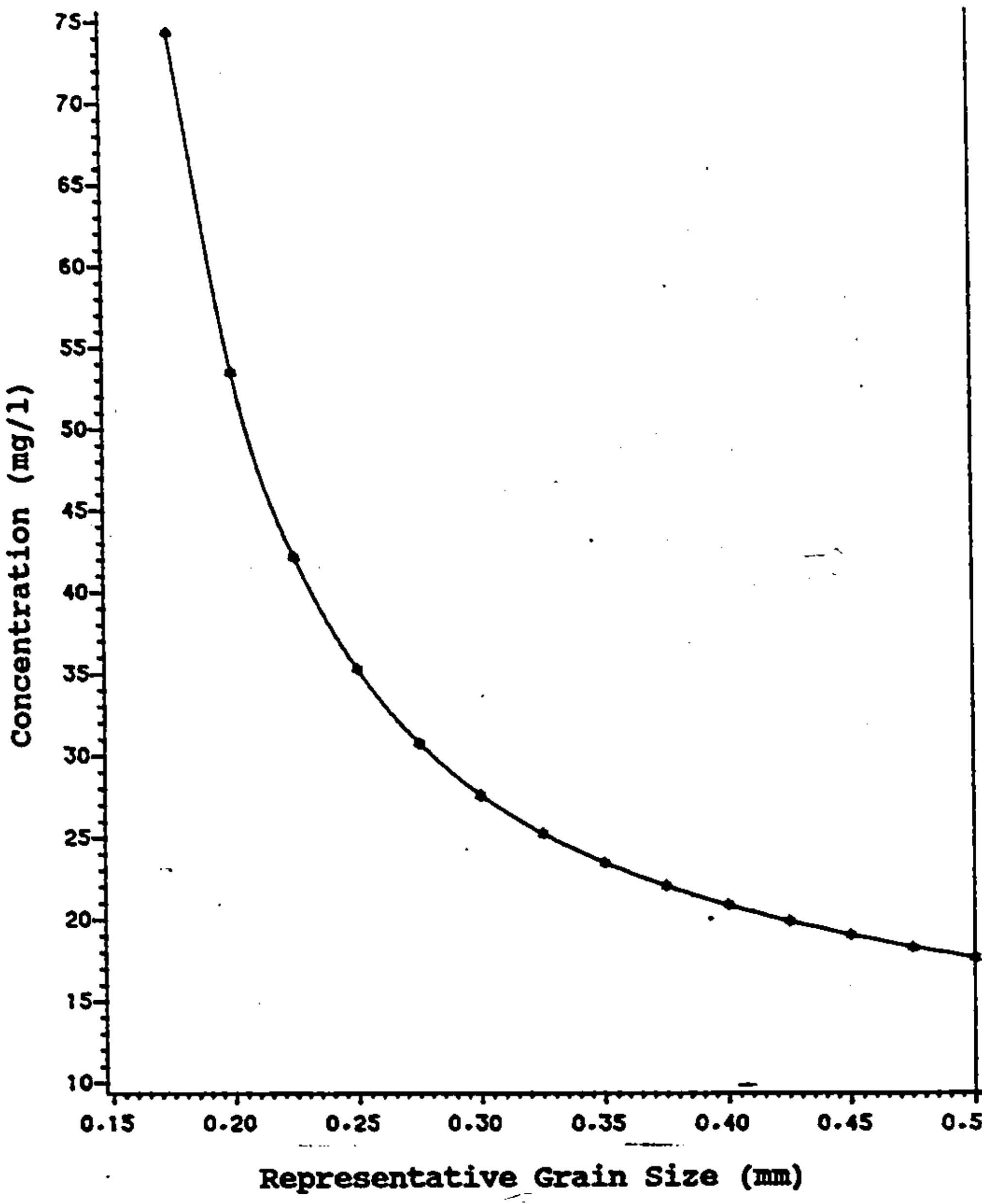

Figure 6.8: Parameteric Analysis of A-W Equation - Sensitivity to Representative Grain Size for $Q = 200{,}000$ cfs

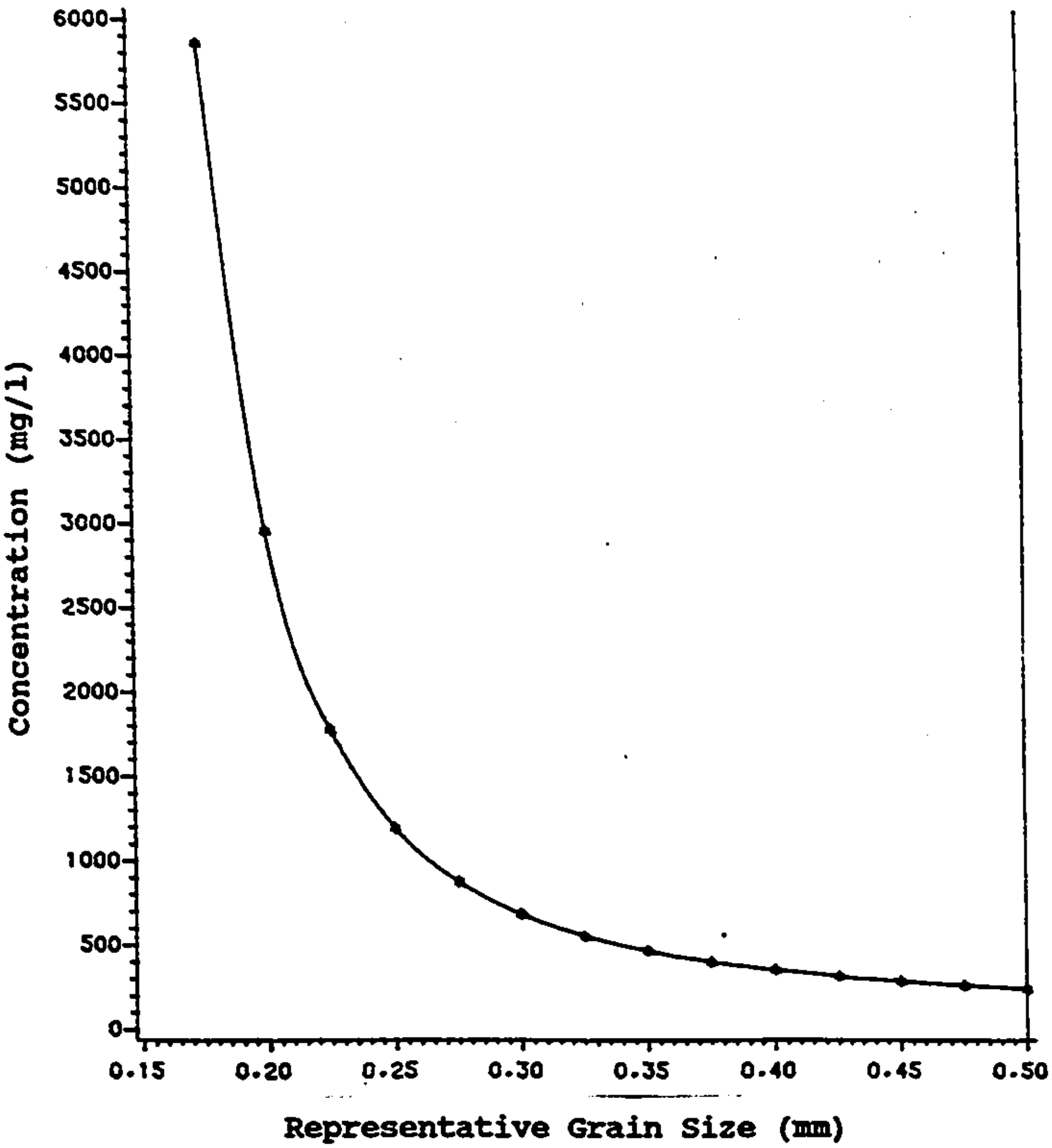

Figure 6.9: Parameteric Analysis of A-W Equation - Sensitivity to Representative Grain Size for $Q = 400{,}000$ cfs

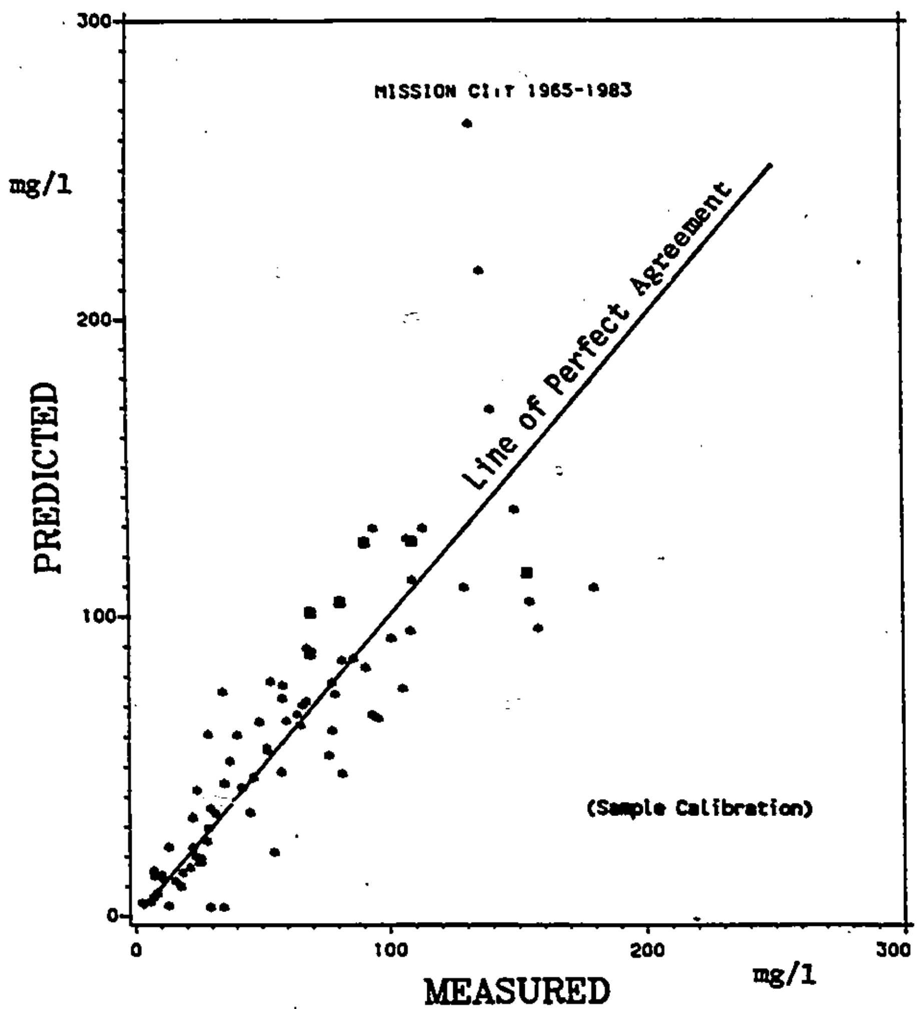

Figure 6.10: Predicted versus Measured SBML

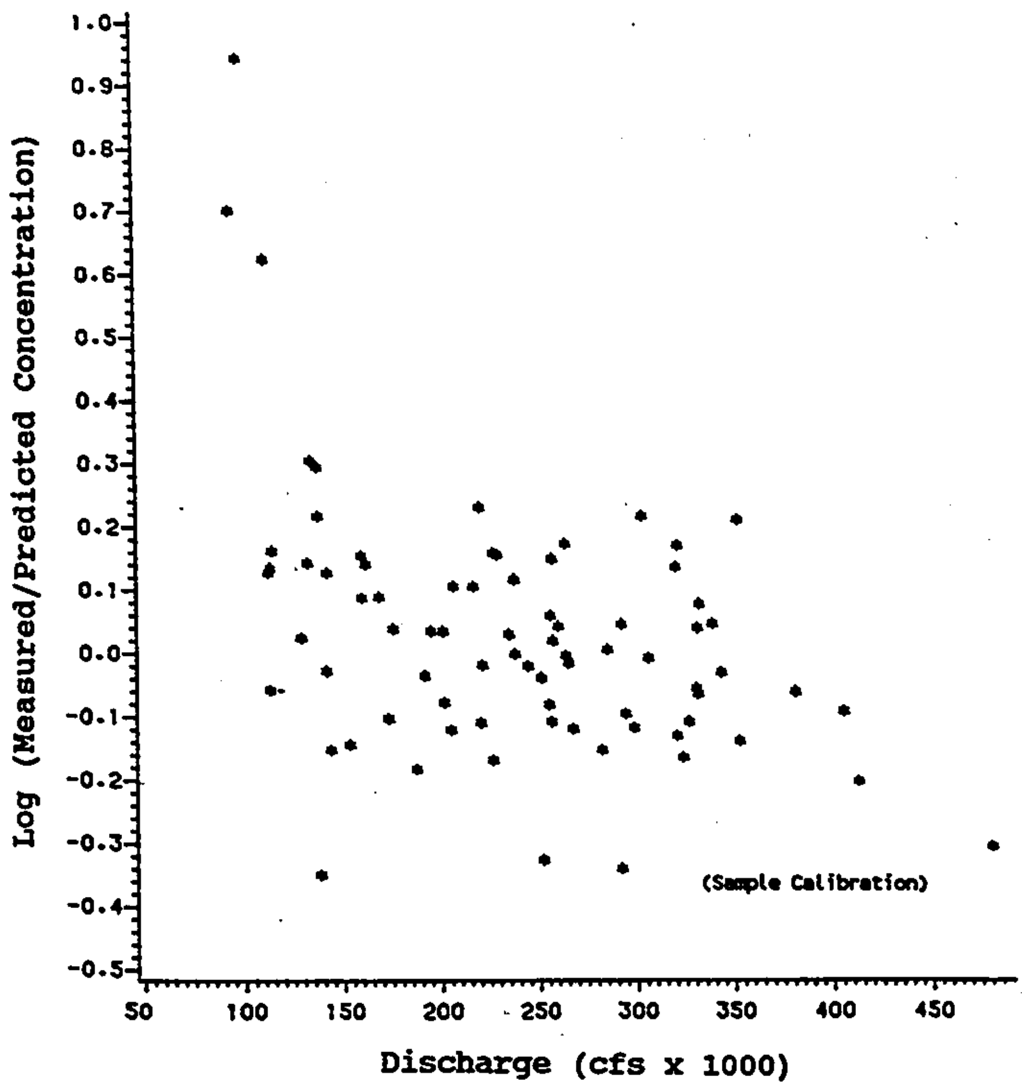

Figure 6.11: Ratio of Measured to Predicted SBML versus Discharge

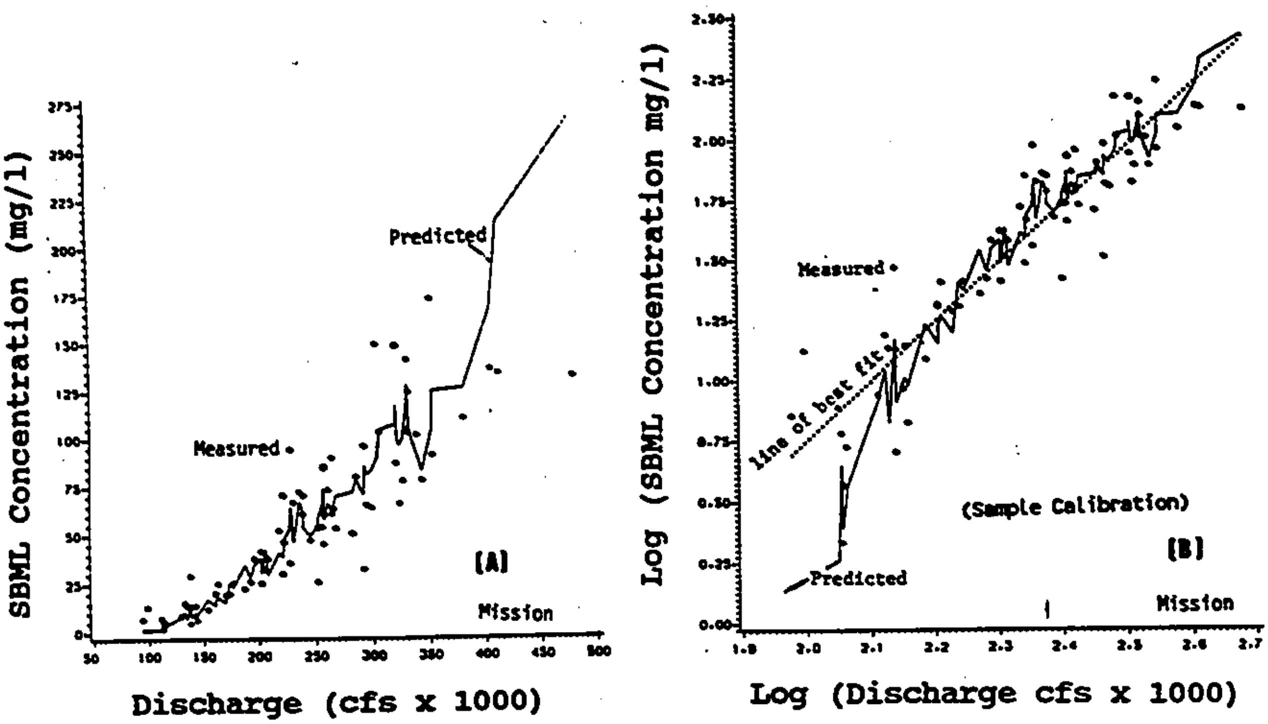

Figure 6.12: Comparison of Measured and Computed SBML Concentration versus Discharge (1965 - 1983)

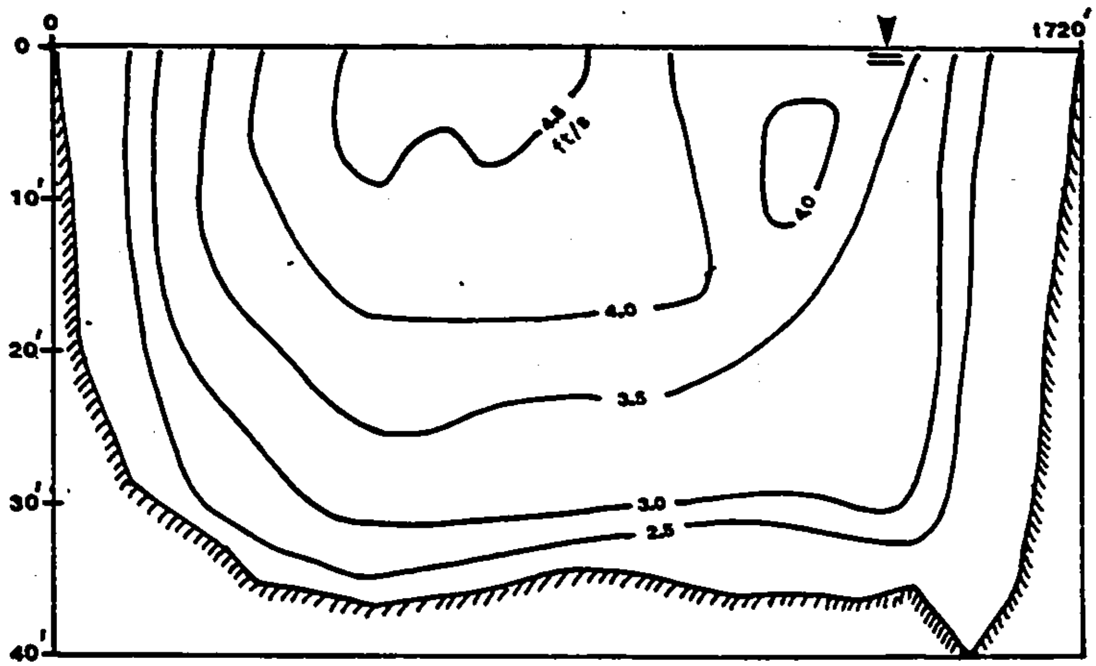

Figure 6.13: Cross-Sectional Velocity Distribution at Mission (1968-05-17)

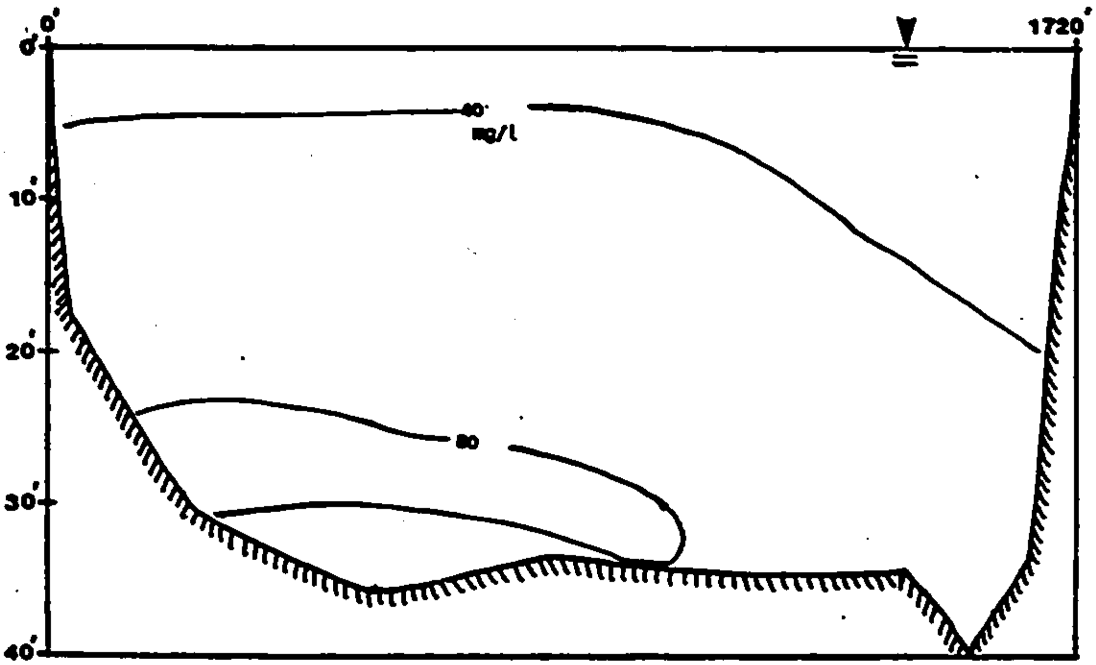

Figure 6.14: Cross-Sectional Suspended Sediment Distribution for (1968-05-17) $0 < d < 0.062$ mm

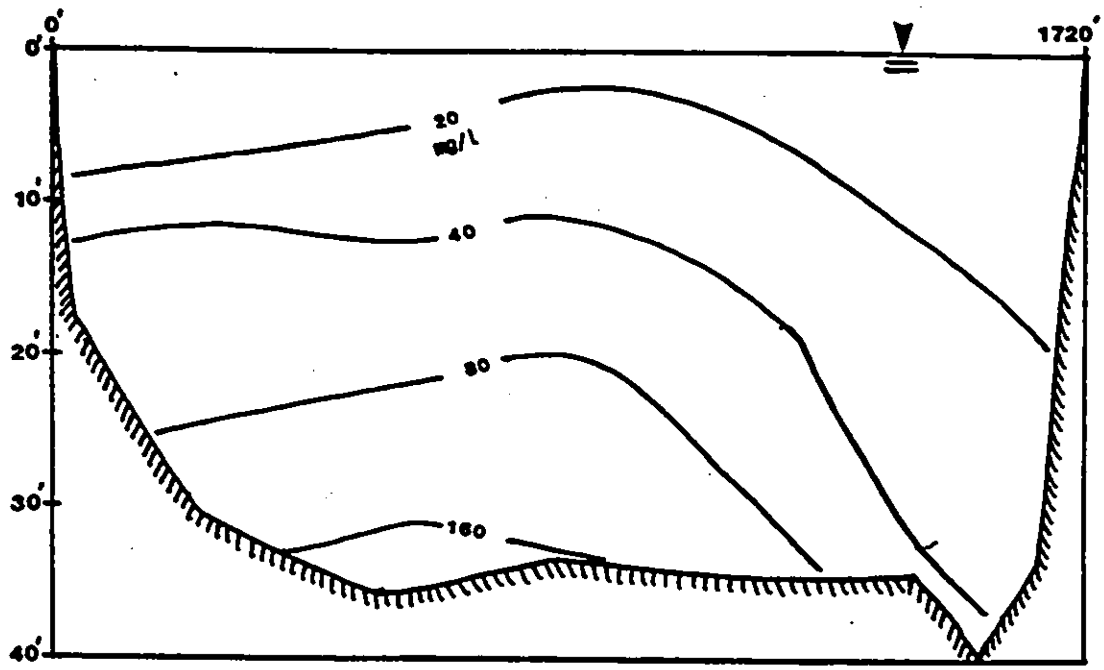

Figure 6.15: Cross-Sectional Suspended Sediment Distribution for (1968-05-17) $0.062 < d < 0.125$ mm

This page is intentionally left blank.

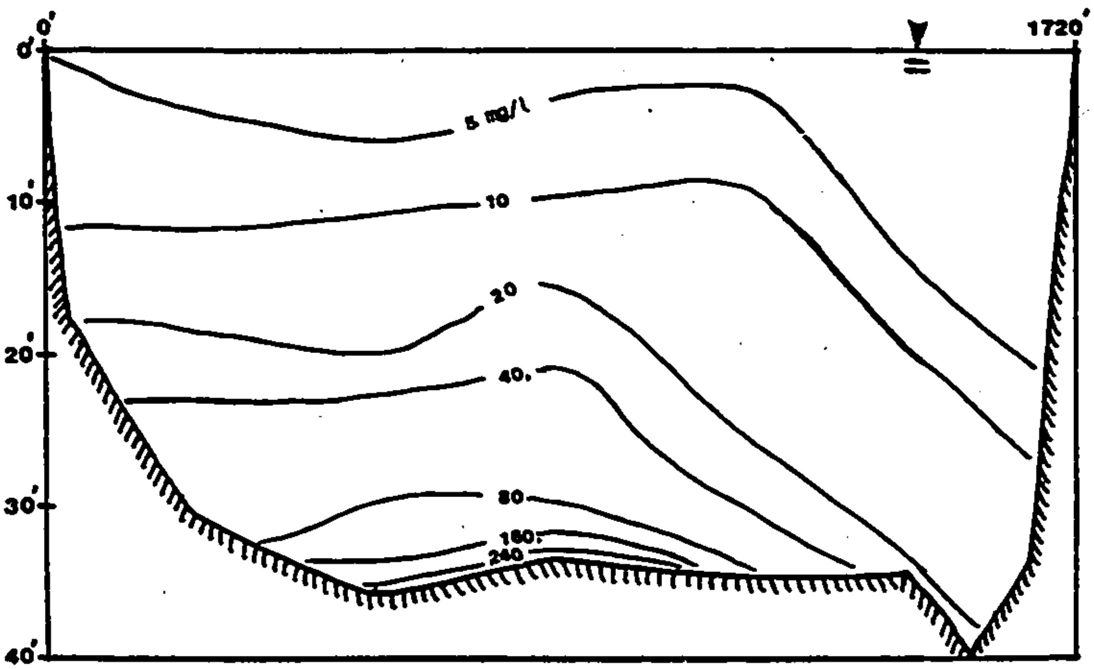

Figure 6.16: Cross-Sectional Suspended Sediment Distribution for (1968-05-17) $0.125 < d < 0.250$ mm

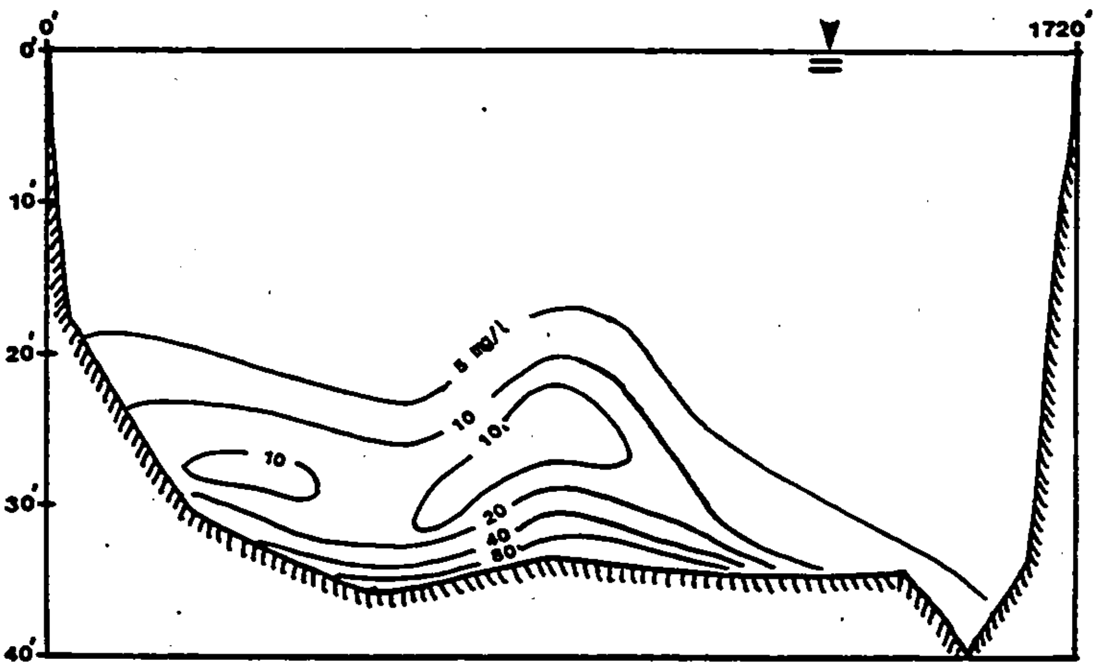

Figure 6.17: Cross-Sectional Suspended Sediment Distribution for (1968-05-17) $0.250 < d < 0.500$ mm

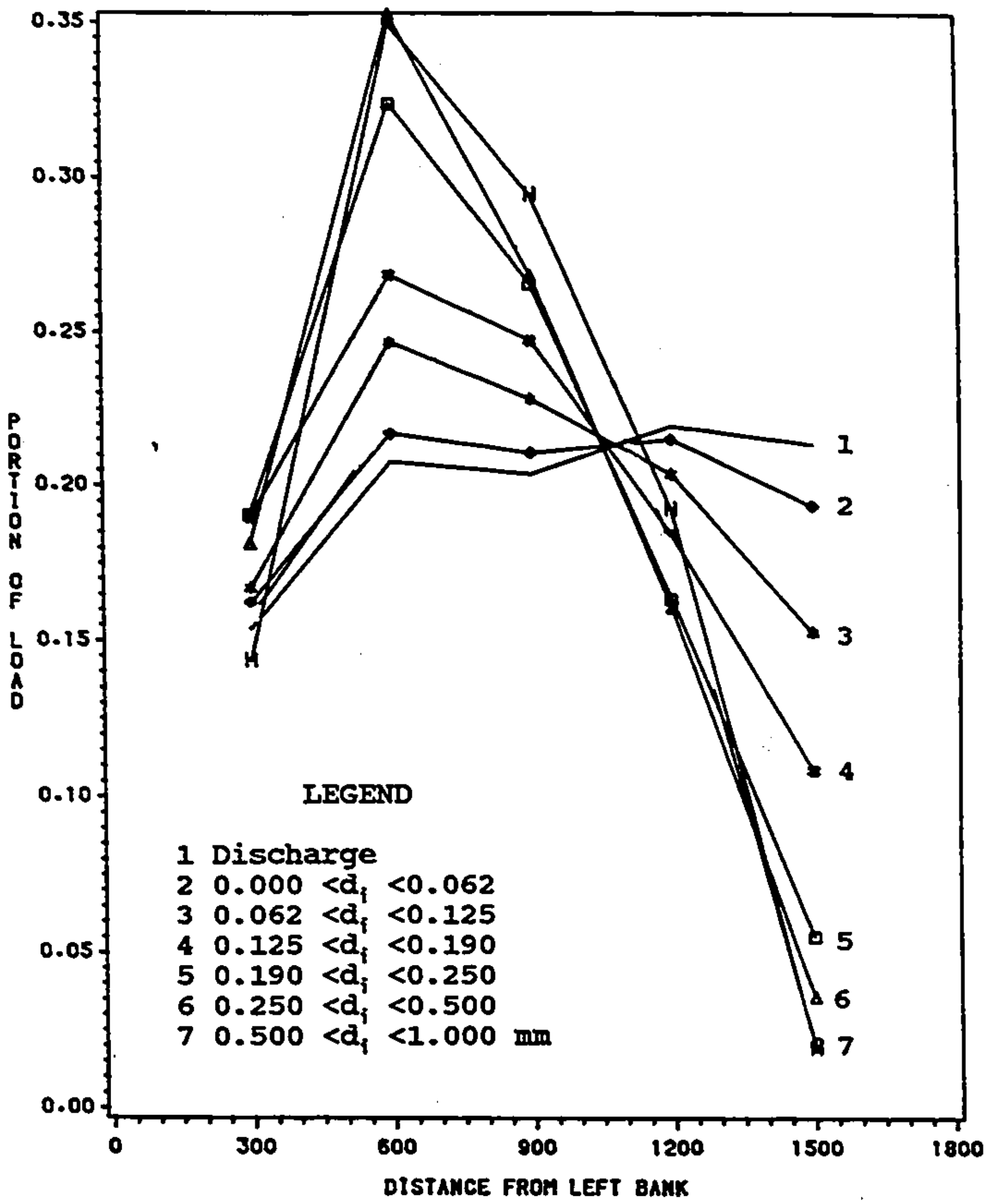

Figure 6.18: Cross-Sectional Distribution of Sediment Load at Mission (1966-1983)

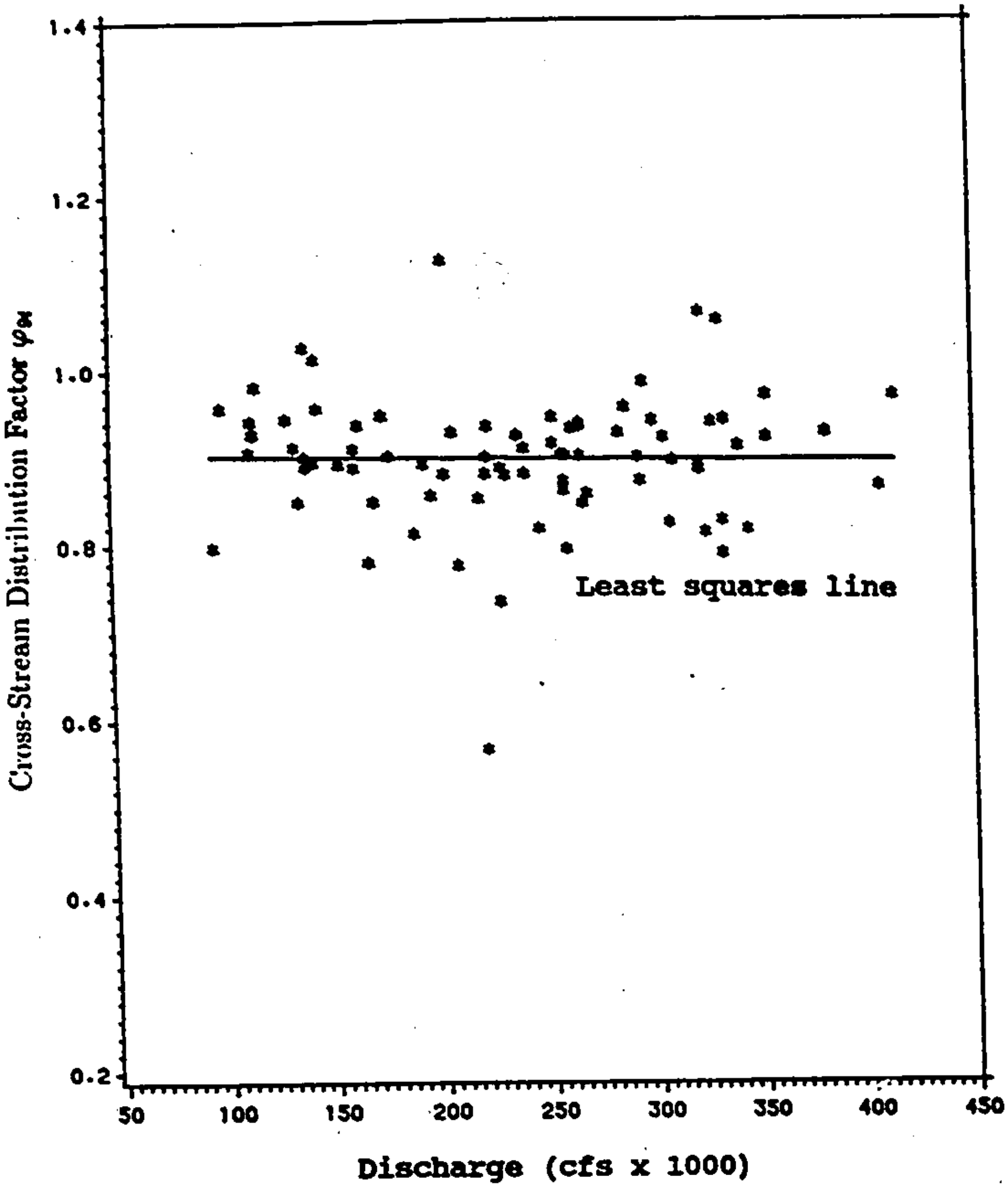

Figure 6.19: Cross-Stream Distribution Factor φ_{9t} at Mission (1965-1983)

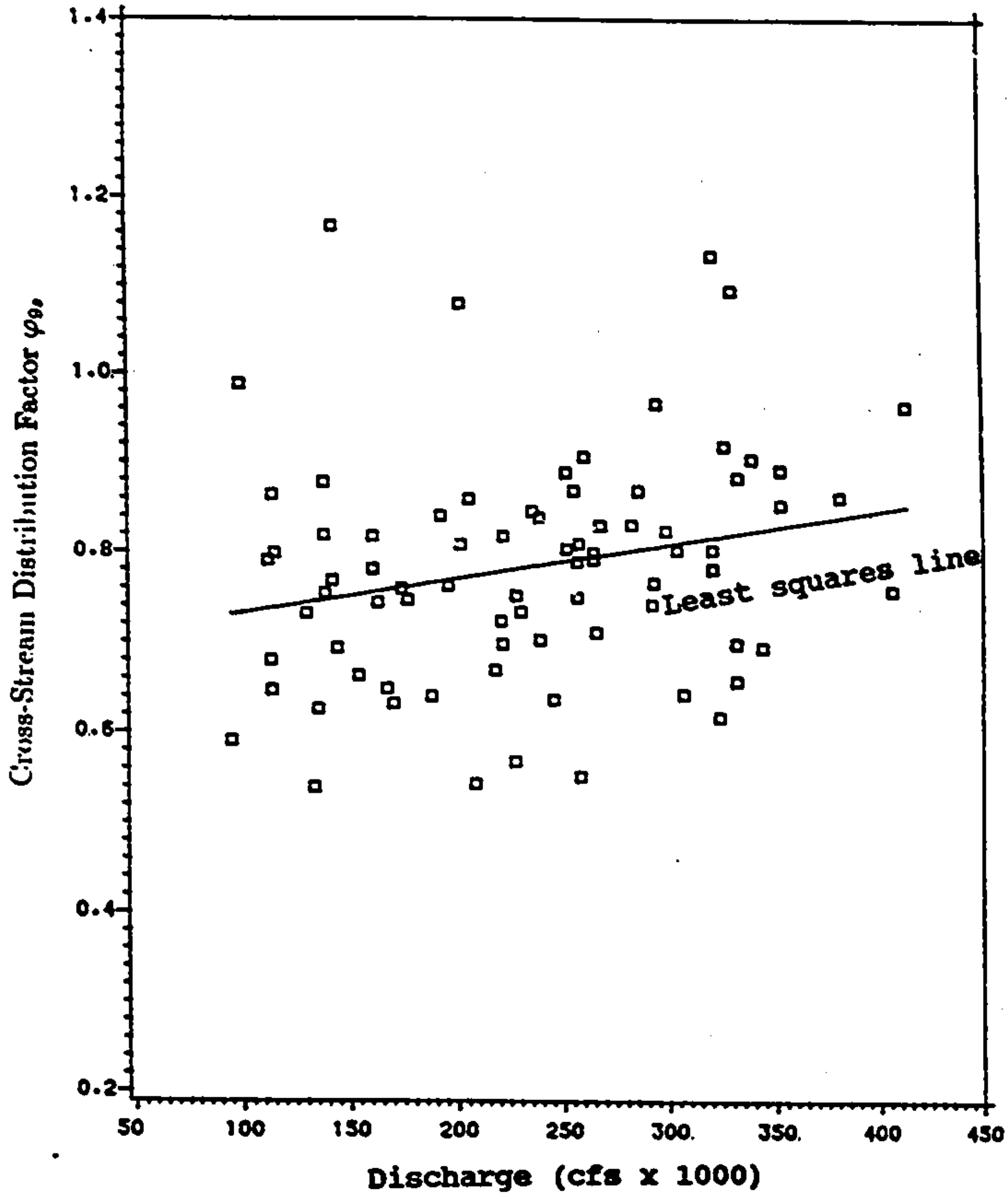

Figure 6.20: Cross-Stream Distribution Factor φ_{9s} at Mission (1965-1983)

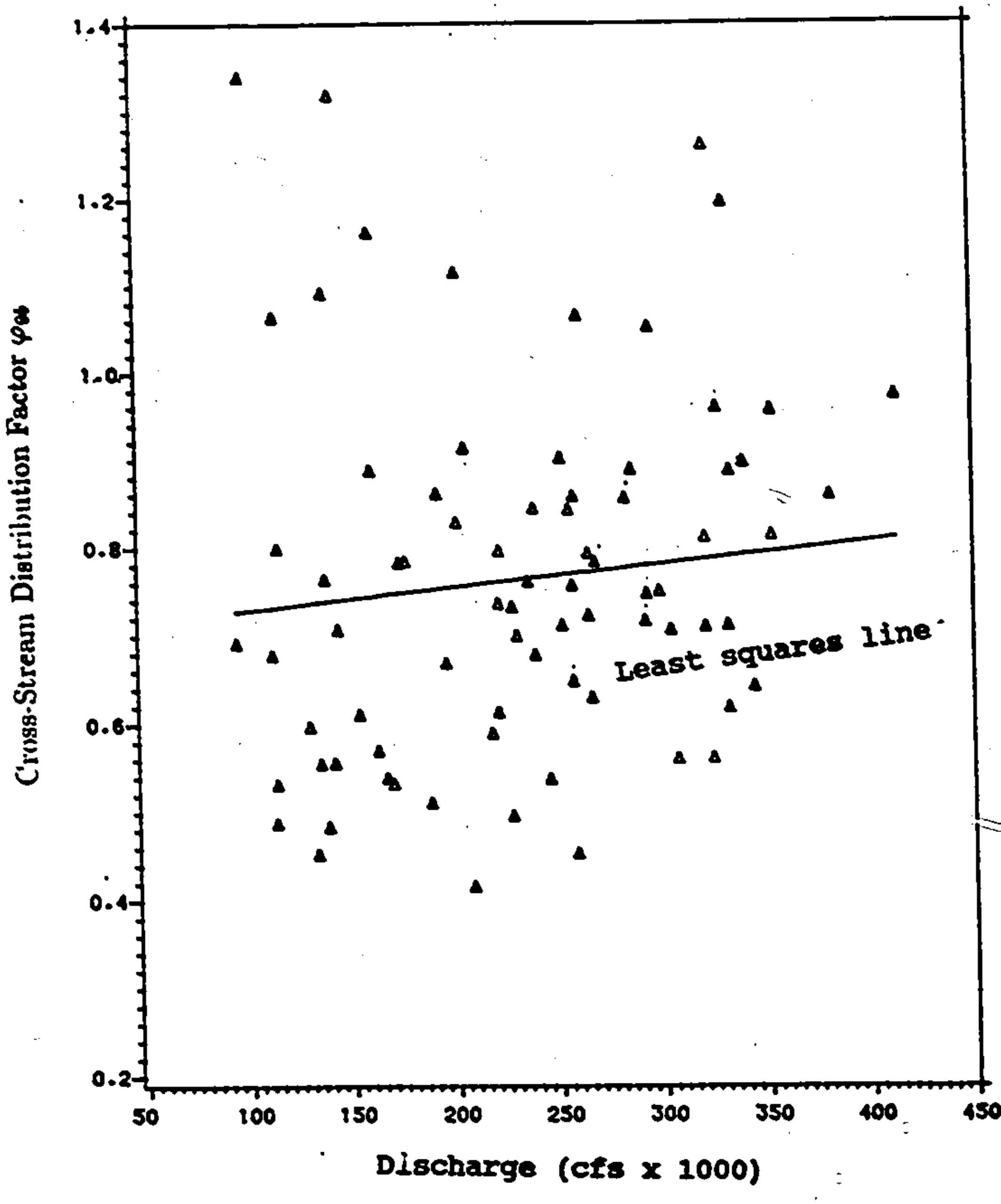

Figure 6.21: Cross-Stream Distribution Factor φ_{96} at Mission (1965-1983)

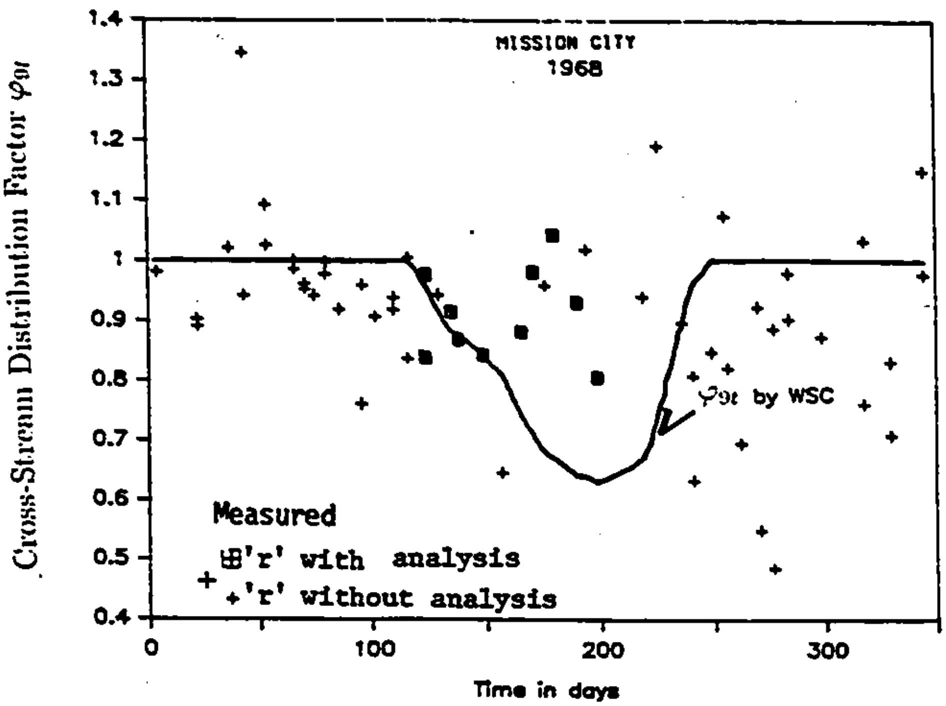

Figure 6.22: Cross-Stream Distribution Factor φ_{9t} at Mission (1968)

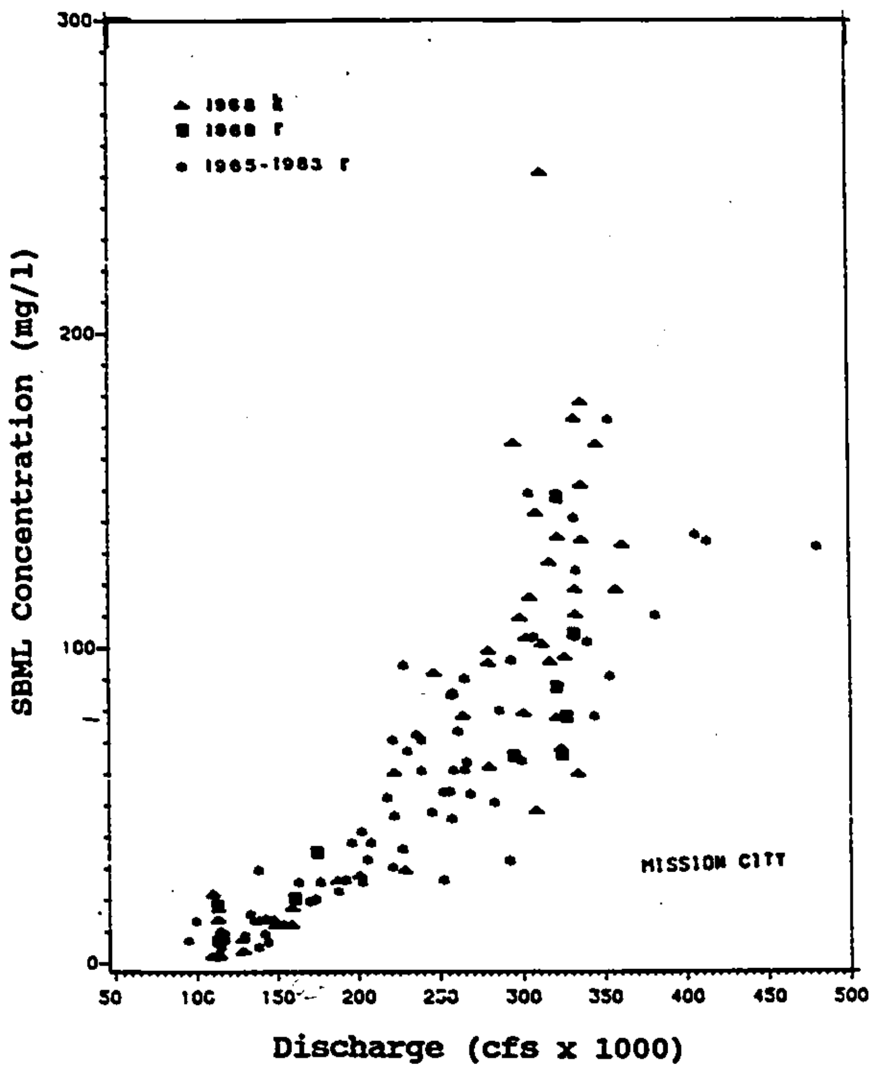

Figure 6.23: Measured SBML Concentration versus Discharge: 1965-1983 Compared to 1968

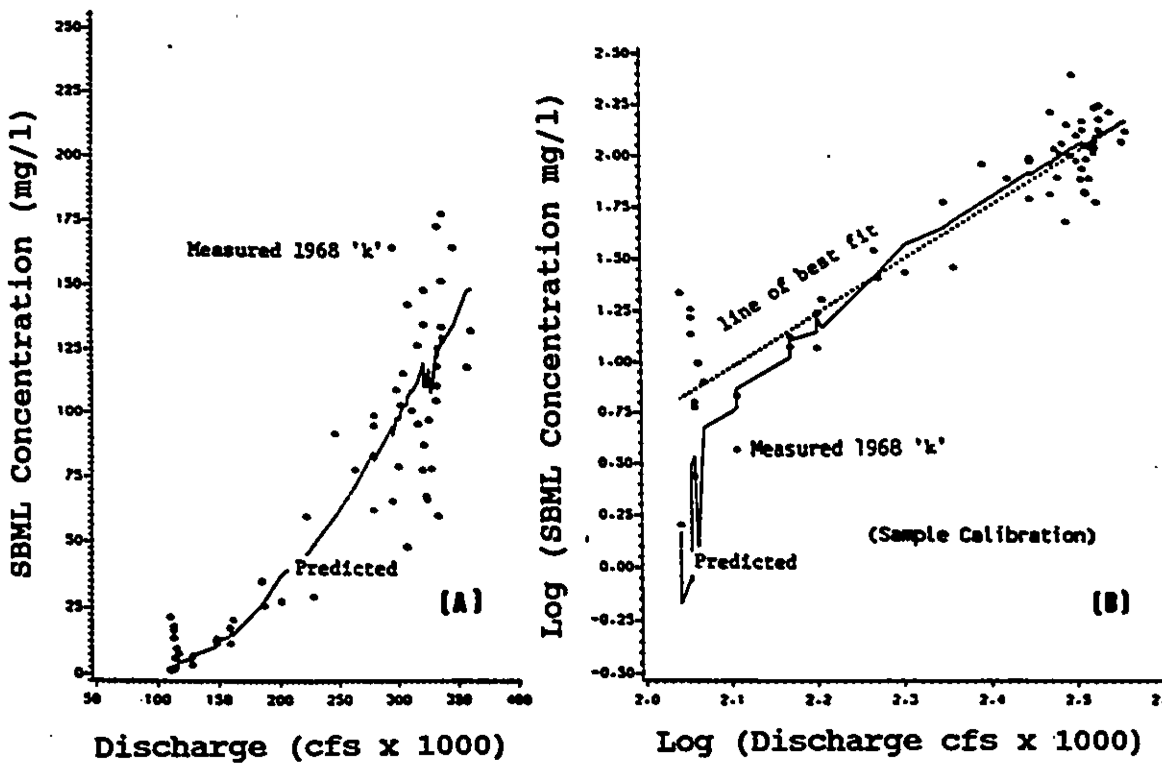

Figure 6.24: Measures and Predicted SBML Concentration at Mission (1968)

Chapter 7

Distribution of Suspended Sediment in the Water Column

This chapter reviews, based on an investigation of Point Integrating (PI) data for the lower Fraser, the applicability of conventional suspended sediment distribution theories to the study reach. Also included is the approach taken to adjust for the bias in Depth Integrated (DI) sampling that results from the fact that the near-bed portion of the water column is not sampled.

Traditionally the concentration of suspended sediment is obtained by applying Rouse's (1937) relationship:

$$\frac{C(y,d)}{C_a(d)} = \left(\frac{1-y}{1-a}\frac{a}{y}\right)^{\Xi(d)} \tag{7.1}$$

where $C(y,d)$ is the suspended concentration of sediment of diameter d at relative depth y (defined as Y/Y_0), $C_a(d)$ is $C(y,d)$ evaluated at $y = a$, a is the relative reference depth, and $\Xi(d)$ is the Rouse number. This states that the concentration decreases exponentially as a function of water depth. Although the relationship is consistent from a theoretical viewpoint, at the application level Ξ is difficult to determine a priori. Also, other field applications have indicated that the assumption of zero turbulence near the water surface should be modified. In this chapter, the applicability of this equation and the variability of the Rouse number is quantified. Calibrated values of the expression are then employed to determine concentration in the near-bed region and the associated correction factors to be employed when using DI measurements.

It should be stated at the outset that there are two limitations in these analyses. First, analyses were based on an assumed logarithmic velocity distribution. In fact, three separate velocity zones can be distinguished in the Lower Fraser river. The first two zones are both logarithmically distributed but the first (in the lower 15% of the water column) has a significantly different logarithmic slope than the middle zone. In the third zone (the upper 5 % to 10 % of the column), the velocity can remain virtually constant, or more frequently, due to the shear stress at the air-water interface, can decrease in the near surface region. The first zone probably differs from the middle zone due to the local effect of dunes. Examples of the velocity distribution observed at the Mission gauging station are shown in figures 7.1 to 7.5 (raw data was obtained from WSC).

The second limitation of the analyses is that no provisions were made in the estimate of the sediment fall velocity to account for the fact that grain size fractions (rather than unique grain sizes) were employed. This omission led to systematic biases in results that motivated additional research in this area (presented in the following chapter).

7.1 Data Sources

Analyses of the suspended sediment distributions were made using PI data sets. PI data is normally obtained at a given vertical by first noting the total water depth and then sampling sediment and velocity at 7 pre-determined levels in the water column. Generally, WSC obtains PI data at all verticals of a sampling station. This was the case in the Lower Fraser for the Mission site, but normally only the Daily vertical was sampled at Port Mann. At Mission, the 5 verticals were sampled at 20 unique flow rates during the 1965 to 1983 period. At Port Mann, the Daily was sampled on some 50 occasions. When possible, WSC also determined the associated instantaneous discharge. In the case of PI measurements at Mission, the discharge varied from a minimum of 187,000 cfs to a maximum of 459,000 cfs. At Port Mann, due to changes in velocity direction, it was not always possible to estimate the discharge. For 16 of the 50 occasions when PI data was collected there, the range in discharge varied from 155,000 to 345,000 cfs.

In order to estimate shear velocity U_*, the mean velocity $\bar{u}$ and average depth Y_0 are required (equation 7.6). Accordingly linear regressions for $\bar{u}$ and Y_0 as a function of the discharge Q were performed. The data used in this exercise was based on 60 R samples collected in 1968. It should be noted that WSC has also developed a stage-discharge relationship for this station that applies during the freshet season. The relationship has been found to be quite stable over the long-term although there has been a small (5%) increase in discharge as a function of stage in the late 1970's. This change is due principally to a change in bed elevation at the station.

Therefore, the corresponding change in the depth-discharge relationship would not be as severe. The result of the linear regression for Y_0(ft) is (figure 7.6):

$$Y_0 = 25.27 + 5.413 \times 10^{-5} Q \tag{7.2}$$

Note that the scatter of depths about the regression line is about 2 ft. This error is not very significant since it represents a relative error in depth of about 6%. Now, since U_* is proportional to $Y_0^{-1/6}$, the resulting error in U_* is only about 1.0 %. Using the same data, based on a non-linear regression, the following expression was obtained for the mean velocity $\bar{u}$ (ft/s):

$$\ln(\bar{u}) = 0.75693 \ln(Q) - 9.713 \tag{7.3}$$

As demonstrated in figure 7.7, there is very little scatter of the points around the estimate.

7.2 Theory

7.2.1 Mean Velocity Profile

Many functions have been proposed to describe the velocity profile. The most traditional among them is the logarithmic velocity distribution proposed by Keulegan and Patterson (1943). This model assumes a linear rate of change in velocity with distance from the river bed (Y):

$$\frac{du}{dY} = \frac{U_*}{KY} \tag{7.4}$$

where u is the velocity (ft/s) at level Y, U_* is the boundary shear velocity (ft/s) and K is the von Karman constant (normally equated to 0.4). Integrating between level

Y and the water surface Y_0 (where the velocity is maximum U_m), the expression becomes:

$$u = \frac{U_*}{K}\ln(Y) + U_m - \frac{U_*}{K}\ln(Y_0) \tag{7.5}$$

Using Manning's equation, the boundary shear stress (ft/s) is given by:

$$U_* = \frac{\bar{u}ng^{1/2}}{1.486Y_0^{1/6}} \tag{7.6}$$

7.2.2 Eddy Viscosity

Various functions are used to describe the distribution of the eddy viscosity (E) in the water column. At the simplest level, a constant value can be used for the entire depth:

$$E_c = \eta U_* Y_0 K \tag{7.7}$$

where η is a constant of proportionality (evaluated in equation 7.16 as 1/6). The more traditional expression is to assume a parabolic distribution developed as follows (Graf 1971):

First, a linear shear stress profile is assumed in the water column:

$$\frac{t_y}{t_0} = \frac{Y_0 - Y}{Y_0} \tag{7.8}$$

where t_y and t_0 are the local and boundary shear stresses respectively. Next, the logarithmic velocity profile assumption (equation 7.4) is adopted together with the Reynold's analogy given as follows:

$$t_y = \rho E \frac{du}{dY} \tag{7.9}$$

where ρ is the fluid density. Combini these three equations and solving for E gives:

$$E = Y_0 K U_* y(1 - y) \tag{7.10}$$

Note that this expression suggests that $E = 0$ at $y = 0$ or $y = 1$ and E is maximum at mid-depth. This expression is one of the principal building blocks for the Rouse expression (equation 7.1) describing the suspended sediment profile.

More recently, researchers use a combination of the parabolic eddy viscosity distribution in the lower half of the water column and a constant (maximum) value in the upper half. That is, E is described by equation 7.7 for $y \leq 0.5$ and by $0.25 Y_0 K U_*$ for $y \geq 0.5$. This combination of 7.7 and 7.4 results from the analyses of suspended sediment distributions and from noting that the presence of water surface waves implies that there is mixing in the upper portion of the water column.

A fourth expression for E, developed by Laursen (1980), is described in the next chapter. Only the constant and parabolic distributions are investigated in this chapter.

7.2.3 Suspended Sediment Distribution

Using the principle of conservation of mass in a control volume and the Eulerian diffusion equation combined with Reynold's analogy, the dispersion-diffusion equation in three dimensions for open channel imcompressible flow is:

$$\frac{dC(x_j, d)}{dt} = -u_{sj}\frac{\partial C(x_j, d)}{\partial x_j} + \frac{\partial}{\partial x_j}(E_{sj}\frac{\partial C(x_j, d)}{\partial x_j}) \tag{7.11}$$

where the subscript s represents solids, the subscript j represents each of the three directions, and E_s is the coefficient representing the combined effect of molecular and turbulent diffusion.

Assuming that $C(x_j, d)$ is virtually constant in time and that gradients in the longitudinal and cross-stream directions are an order of magnitude less than gradients in the vertical direction, then for a given d, if the still-water settling velocity of that grain size $W(d)$ is representative of the settling velocity of d in turbulent flow, equation 7.10 reduces to the following well-known equilibrium equation:

$$W(d)C(Y,d) = -E_{s2}\frac{dC(Y,d)}{dY} \tag{7.12}$$

Also, assuming a relationship between the vertical dispersion coefficient and the eddy viscosity ($E_{s2} = \mathcal{B}E$, where $\mathcal{B}$ is a constant of proportionality), then equation 7.12 becomes:

$$w(d)C(Y,d) = -\mathcal{B}E\frac{dC(Y,d)}{dY} \tag{7.13}$$

When equation 7.13 is combined with equation 7.10, the well-known Rouse equation describing the sediment concentration distribution is obtained:

$$\frac{C(y,d)}{C_a(d)} = y_{*R}^{\,z(d)} \tag{7.14}$$

where, y_{*R} is the normalized Rouse expression for depth, given by:

$$y_{*R} = \left(\frac{1-y}{1-a}\frac{a}{y}\right) \tag{7.15}$$

When a constant eddy viscosity is assumed, the expression for concentration in the vertical becomes:

$$\frac{C(y,d)}{C_a(d)} = \exp^{-\Xi(d)\eta[y-a]} \tag{7.16}$$

where the inclusion of η in the exponent allows the use of Ξ in both 7.14 and 7.16. It is given by:

$$\Xi = \frac{w(d)}{BU_*K} \tag{7.17}$$

Note that for the case of parabolic eddy viscosity E, average value $\bar{E}$ of E is obtained by integrating equation 7.10 over the full water depth giving:

$$\bar{E} = \frac{U_*KY_0}{6B} \tag{7.18}$$

If the hypothesis is made that the constant eddy viscosity E_c is equal to the average value given by equation 7.18, then from equation 7.7, $\eta = 1/6$. In the following pages this hypothesis is tested against PI measurements obtained in the Lower Fraser.

Regardless of the expression used, the key for successfully modelling the suspended load is to evaluate Ξ(d) (equation 7.17). Recently, there has been controversy over the value of the von Karman constant. Some researchers (e.g., Yalin, 1986) have begun to refer to it as the von Karman "parameter". Traditionally, a value of 0.4 is assigned to K though some studies indicate that its value may be much lower (Einstein, 1950). For the Lower Fraser, preliminary analyses indicated that K may range between 0.24 and 0.45 (table 7.1).

Second, the value of B is also receiving attention. Arguments are put forward that sediment turbulence differs from water turbulence because of inter-particle interference and/or because of increased momentum of the solids over that of water. In practice, the value of B is usually obtained experimentally by first calibrating equation 7.14 for a given grain size and then obtaining the Rouse number for other grain sizes according to the following relationship (Graf 1971):

$$\mathcal{Z}_{i/j} = \frac{\mathcal{Z}_i}{\mathcal{Z}_j} = \left(\frac{w(d_i)}{w(d_j)}\right)^{\psi} \tag{7.19}$$

where subscripts i and j relate parameters to grains of size i and j respectively and $\mathcal{Z}_{i/j}$ is the ratio of Rouse number's of grain size i and j respectively. From an examination of 7.17, the theoretical value of ψ should be 1.0. However research has shown that a value of 0.7 is more appropriate (Graf 1971).

In this chapter, grain size fractions will be examined. A comparison will be made of the behaviour of the suspended of grain fractions rather than grain sizes. Accordingly subscripts i and j denote fractions characterized by (1) $d \leq 0.062$ mm, (2) $0.062 \leq d \leq 0.125$ mm, (3) $0.125 \leq d \leq 0.250$ mm and (4) $0.250 \leq d \leq 0.500$ mm. Note that according to equation 7.19, $\mathcal{Z}_{i/j}$ should be independent of local hydraulic parameters.

Finally, for equation 7.17, Einstein (1950) proposed using the 'skin' shear velocity (U_*') in lieu of the total shear velocity U_*. Noting that the relationships used to develop the equation were based on total shear stress, Einstein's assumption should be avoided.

In the following section two suspended sediment distribution models are examined. The first, known as the Rouse equation, assumes a parabolic distribution of

E, while the second more convenient expression uses a constant eddy viscosity E_c. However, for the successful application of either model, it is necessary to quantify Ξ. In the following section, Lower Fraser PI data will be used to study the behaviour of the suspended sediment, evaluate Ξ, and assess the performance of the two models.

7.3 Observed Concentration Distribution

As stated above, the suspended sediment profile in the Lower Fraser was measured more than 150 times by WSC. Certain data manipulations were undertaken to see if the theory presented in the previous sections conformed with PI data obtained. Some manipulations were for the purpose of statistical analyses while others were made in order to plot points for visual (subjective) interpretations.

To test the Rouse and constant eddy viscosity models against grain fractions 1 through 4, equations 7.14, 7.15 and 7.16 were manipulated. Taking the log of each side of equation 7.14, the following expression was obtained:

$$\log(C_{ri}) = \log(\frac{C_{yi}}{C_{ai}}) = \Xi_i \log(y_{*R}) \tag{7.20}$$

where C_{yi} is the concentration of grain fraction i at local relative depth y, C_{ai} is C_{yi} evaluated at $y = a$ (normally corresponding to the sample depth closest to the river bed), C_{ri} denotes the relative concentration of grain fraction i, and i represents one of the four grain fractions (defined above). The validity of 7.20 was tested in two ways. First, when log (C_{ri}) is plotted against log (y_{*R}) (or against log $[(1-y)/y]$, the points should fall on a straight line. A visual inspection was made of the plots to determine their linearity. Second, the scatter of the points about the estimate was measured by performing a linear regression analysis. The goodness of fit was indicated by the value of the correlation coefficient r, defined as follows:

$$r^2(\Phi) = \frac{\sum_{i=1}^{n}(\Phi_i - \Phi_m) - \sum_{i=1}^{n}(\Phi_i - \Phi_p)}{\sum_{i=1}^{n}(\Phi_i - \Phi_m)^2} \tag{7.21}$$

where Φ_i are the individual data points (in this case, $\Phi_i = \log[C_{ri}]$), Φ_m is the mean value of Φ_i in the vertical, and Φ_p is the predicted value of Φ_i according to the linear regression. It should be noted that since no intercept is present in equation 7.16, when regressions were performed the "zero-intercept" option was normally chosen. This option (known as a "regression with zero degrees of freedom") forces the line of best-fit to pass through the origin. As such, some cases occur where the mean value of Φ_i (Φ_m) is a better estimate of Φ_i than the line of best fit (given by Φ_e). In such cases, r^2 may have the unusual character of being less than zero.

The same analytical approach (both subjective and statistical) was used to evaluate the performance of equation 7.16 after making the following manipulation:

$$\log(C_{ri}) = -Z\eta(y-a)\log(e) \tag{7.22}$$

In this case Φ_i was plotted against $(y-a)$.

7.4 Results of Visual Inspection of the Data

Due to space constraints, all 150 plots of each grain fraction for each model can not be included here. Sample plots of PI data according to equations 7.21 and 7.22

are shown in figures 7.8 and 7.9 respectively. If the theory on which they were based is well founded, the equation. should plot as straight lines. However, visual inspection revealed that some profiles plotted equally well (or equally poorly) under either formulation, while some tended to follow the Rouse and others the simplified expression more closely (figure 7.10).

For the first grain fraction ($d \leq 0.062$ mm), the Rouse expression revealed a definite advantage in 5 % of the cases, the simplified expression in 2 % of the cases and either performed equally well (or poorly) in 93 % of the cases. For the second fraction ($0.062 \leq d \leq 0.125$) Rouse was favored 26 % of the cases while the simplified expression was favored in 10 % of the cases. For i = 3 ($0.125 \leq d \leq 0.250$ mm), the expressions were favored in 45 % and 24 % of the cases respectively, while for the fourth fraction ($0.250 \leq d \leq 0.500$ mm) the expressions were favored in 43 % and 27 % of the cases respectively. Stated differently, the Rouse expression was applicable to 95 % of the data, when i = 1 or 2, and was applicable to 75 % of the larger fractions. On the other hand the simplified expressions were applicable to 85 % and 55 % respectively.

This analysis indicated a clear preference in favor of the Rouse expression over the simplified one. Though this result was expected, it is interesting to note that in some cases the assumption of a constant eddy viscosity provided the better model. An insight into this observation is obtained by examining the data at Mission (figure 7.11) and at Port Mann (figure 7.12) separately. For the latter, where there is a more efficient mixing process (due to tidal effects), both models were found to be equally appropriate.

The results of the statistical analyses are reported in figures 7.13 through 7.16, for fractions i = 1 through 4 respectively. In each of the figures the frequency distribution of r is plotted for each model. Contrary to the subjective analysis, r was generally found not to be a function of the grain fraction examined. The mean, median and modal values of r were 0.7, 0.8 and 0.9. This indicates that for most measured profiles, the models are a fair representation. On the other hand, the statistical analysis confirmed that in some cases, neither model was applicable since 20 % of the r values were less than 0.5. The statistical analysis indicated only a marginal preference of the Rouse model over the simplified one.

Visual analysis of the PI data revealed additional information. Examination of the data plotted according to equations 7.21 and 7.22 revealed that the scatter of the data about the estimate was not "normally" distributed. In fact, in a significant number of cases, data showed a persistent trend towards non-linearity. In the case of the first fraction, since the grains were so fine, they were very well mixed and the non-linearity did not reveal itself to a great extent. However, for the coarser the grain fractions, not only was the effect stronger but it was found in increasing frequency. According to the inspection (using either model), skewed results were observed in 10, 38, 61 and 57 % of the cases for grain fractions 1 through 4 respectively. When this effect was observed, the Rouse equation was virtually always superior in performance to the simplified one. At the time of the analysis, it was hypothesized that the skew may be due to the limitations of the models investigated or may be due to the effect of analyzing grains by fractions. The numerical consequences of using grain fractions in suspended sediment modelling was therefore studied in depth and is presented in the next chapter.

The ratio $\Xi_{i/j}$ (the quotient of Ξ_i and Ξ_j) may also be effected by the distribution of grains within a fraction. On the other hand, it can give an indication of the consistency of Ξ since, on the surface, the ratio is independent of hydraulic parameters K, U_* and to a certain extent B. Since the statistical analysis indicated the models performed poorly 20 % of the time, it is expected that $\Xi_{i/j}$ would also be inconsistent about 20 % of the time. As such, only the central 80 % of the data was used (figures 7.17 and 7.18) and the error in the computed value of $\Xi_{i/j}$ was estimated by subtracting the 10 percentile value from the median value.

When $0.125 < d < 0.250$ mm was chosen as the reference (j) fraction, $\Xi_{1/3}$ was 0.14 +/- 0.17, $\Xi_{2/3}$ was 0.45 +/- 0.24 and $\Xi_{4/3}$ was 1.7 +/- 1.2. Note that the errors represent 120, 50 and 70 % of the *median* values respectively. To verify that the large relative errors were not due to the particular choice of the j-fraction, the analysis was repeated for j = 2. This analysis confirmed that there is a very large relative error in the computation of $\Xi_{i/j}$. Moreover, one reference size did not lead to greater consistency than another. However, on the positive side, the median values of $\Xi_{i/j}$ are surprisingly consistent. Whether the calculations were performed at Port Mann or Mission, or based on one or zero degrees of freedom in the regression of Ξ_i, median values for a given i/j combination only varied from one site to another by about 20%.

Finally, an analysis was made of the value of η. Recall that the theoretical value of this constant was obtained by assuming that the mean eddy viscosities of the two models were equal. As such, the expected value of η was 1/6. Figures 7.19 and 7.20 show the observed value of η for fractions 2 and 3 respectively. η performs well between the 10 and 90 percentiles. On the other hand, because the tails are so long, the median rather than the mean value of η is a better estimate of the constant.

When all profile data were used and Ξ was calculated based on a regression of one degree of freedom, the median value of η was 1/7.3. When Mission data is used exclusively, η was 1/7.2, whereas at Port Mann η was 1/7.6. When Ξ was obtained using a zero-intercept option, η dropped to 1/7.9 overall. Therefore, there is a fair agreement between the theoretical and observed values.

Thus far in the analysis the applicability of the models has been evaluated and the behaviour of the Rouse number examined. In order to characterize the grain fractions for estimating bias in DI samples, it would be useful to establish functional relationships between Ξ_i and $1/Q$. Theoretically, Ξ should be related to U_* (since $\Xi = w/(\beta K U_*)$, equation 7.15), however due to the nature of the shear stress dependency on discharge at Mission, this more practical form of the relationship can be obtained. From equation 7.6,

$$U_* = \frac{\bar{u} n g^{0.5}}{1.486 Y_0^{-1/6}} \tag{7.23}$$

substituting equation 7.3 for $\bar{u}$ and 7.2 for Y_0 and the following expression for Manning's n (obtained through calibration of ONE-D to the Lower Fraser):

for $Q > 199,500 cfs$

$$n = 0.01971 + 2.4 \times 10^{-8} Q \tag{7.24}$$

or for $Q < 199,500cfs$

$$n = 0.0245 \tag{7.25}$$

then, for $Q > 199,500cfs$

$$U_* = \frac{6.05 \times 10^{-5} Q^{0.75683} (0.01971 + 2.4 \times 10^{-8} Q) g^{0.5}}{(25.27 + 5.4 \times 10^{-5} Q)^{1/6}} \tag{7.26}$$

or, for $Q < 199,500cfs$, equation 7.6 becomes:

$$U_* = \frac{6.05 \times 10^{-5} Q^{0.75683} (0.0245) g^{0.5}}{(25.27 + 5.4 \times 10^{-5} Q)^{1/6}} \tag{7.27}$$

At first glance, equations 7.26 and 7.27 would indicate a very non-linear relationship between U_* and Q. However, as displayed in figure 7.21, the relationship can be well represented by a linear dependency and hence the feasibility of formulae relating Ξ_i to $1/Q$ in lieu of Ξ_i to $1/U_*$.

Based on calculated values of Ξ_i, linear regressions relating Ξ_i to $1/Q$ were performed (figures 7.22 through 7.25). The estimated values of the slope and the intercepts are listed in table 7.2. The table also indicates that the average r value for the Ξ_i - $1/Q$ regression was about 0.5. Given the scatter in the data displayed in figures 7.22 to 7.25, the low value of r is not surprizing. The derived value Ξ_i differed from that estimated within the 10 to 90 percentile range by about 100%. This may imply that a second parameter should have been included in the analysis. On the other hand, the trends represented by the estimates are definitive and the scatter associated with each line is quite uniformly distributed for all values of $1/Q$. This suggests that the general form of the relationship is appropriate. The fact that scatter is present means that the results are not as precise as desired, nevertheless, if these regressions have the same properties as others made above, there is a degree of confidence that the mean values obtained are reliable and representative.

7.5 Estimating the Bias in DI Measurements

WSC has addressed the issue of discrepancies between mean sediment concentrations obtained using DI and PI data. To obtain the mean sediment concentration from PI data, the product of measured concentration and measured velocity was plotted as a function of depth, manually integrated and then divided by the unit discharge q:

$$C = \int_0^{Y0} C(Y)u dY/q \tag{7.28}$$

Durette concluded that, in general, values obtained by each sampling method were within 5 % of each other.

In this study, an alternate comparative method was employed. It consisted of using values obtained above for Ξ_i as a function of $1/Q$ in combination with the Rouse suspended sediment distribution model. The latter was applied to calculate the ratio between the theoretical mean concentration of the entire water column, and the mean concentration of the DI sampled zone only. The ratios obtained were then related to the grain fraction, the extent of the unsampled (near-bed) zone, the von Karman K and the discharge. The ratios were subsequently applied to DI data obtained in the 1965 to 1983 period and the overall bias in measured concentration was estimated.

7.5.1 Theoretical Development

The suspended sediment load S_A in a portion of the water column extending from $Y = \mathcal{A}$ to $Y = Y_0$, is given by the integration of the product of local velocity and sediment concentration:

$$S_A = \int_{\mathcal{A}}^{Y_0} \frac{Y_0}{\mathcal{A}} C(Y) u dY \tag{7.29}$$

where A is the reference depth. Assuming that the velocity in the water column is logarithmically distributed and that the Rouse sediment model is applicable, Einstein (1950) expressed equation 7.29 in integral form as:

$$S_A = 11.6 C_a U'_* \mathcal{A}[P_E I1(\mathcal{A}) + I2(\mathcal{A})] \tag{7.30}$$

where $I1$ and $I2$ (functions of $\mathcal{A}$) are Einstein's integration factors and P_E is a transport parameter given by:

$$P_E = \ln\left(\frac{30.2 Y_0}{\Delta}\right) \tag{7.31}$$

where Δ is the apparent roughness of the bed.

As stated above, the full shear velocity U_* should be used in equation 7.30 in lieu of the skin shear stress U_*' indicated by Einstein. Also, hidden in the value

11.6 (equation 7.30) is the assumption that von Karman's K is 0.4. Otherwise, 11.6 would be replaced with 1 / (0.216 K). P_E can also be expressed in an equivalent yet more practical form. Integrating equation 7.5 over the depth and dividing by Y_0 gives:

$$\bar{u} = U_m - U_*/K \tag{7.32}$$

Hence, an alternate form of equation 7.5 is:

$$u = \frac{U_*}{K}(\ln(Y) + \frac{K\bar{u}}{U_*} + 1 - \ln(Y_0)) \tag{7.33}$$

This is equivalent to Einstein's formulation of the logarithmic velocity profile:

$$u = \frac{U_*}{K}\ln(\frac{30.2Y}{\Delta}) \tag{7.34}$$

and hence the transport parameter can be expressed as:

$$P_E = \frac{K\bar{u}}{U_*} + 1 \tag{7.35}$$

Replacing $[P_E I1(\mathcal{A}) + I2(\mathcal{A})]$ by $I(\mathcal{A})$ and using the modified expressions, equation 7.30 can be re-written as:

$$S_{\mathcal{A}} = \frac{C_a U_* \mathcal{A}}{0.216K} I(\mathcal{A}) \qquad (7.36)$$

Assuming that the reference depth $\mathcal{A} = M$ corresponds to the depth in which DI sampling occurs, then S_M represents the theoretical suspended sediment load in the measurable portion of the water column (denoted by S_M). To obtain the theoretical load in the entire water column, the lower limit of integration ($\mathcal{A}$) should be zero. However, based on Rouse's relationship, the theoretical value of $C(0, d)$ is undefined. Accordingly, the load in the entire water column (S_F) is obtained (equation 7.36) by choosing a value of $\mathcal{A}(= F)$ a few median grain diameters above the bed. The validity of this simplification was confirmed by a sensitivity analysis of S_F with respect to F.

Noting that the mean sediment concentration is the load divided by the unit discharge, the theoretical mean concentrations in the measurable portion of the water column (C_M) and the full water column (C_F) are given by:

$$C_M = \frac{S_M}{q_M} \qquad (7.37)$$

and

$$C_F = \frac{S_F}{q} \qquad (7.38)$$

where q_M is the unit discharge obtained by integrating the local velocity over the measurable portion of the sampling vertical. Defining Θ as q_M/q and noting that $q = uY_0$, then from equation 7.33,

$$\Theta = 1 - \frac{M}{Y_0} - \frac{MU_*}{Y_0 K \bar{u}} \ln(M/Y_0) \qquad (7.39)$$

Having developed expressions for S_M, S_F and Θ, the theoretical bias in the DI samples ($B_i = C_F/C_M$) can now be expressed in the following form:

$$B_i = \frac{S_F \Theta}{S_M} \qquad (7.40)$$

After substituting for the appropriate limits of integration (i.e., $\mathcal{A} = M$ and $\mathcal{A} = F$) in equation 7.36 and noting that $C(M, d) = y_{*R}^{\mathcal{Z}_i} C(F)^d$, equation 7.31 becomes:

$$B_i = y_{*R}^{\mathcal{Z}_i} \left(\frac{FI(F)\Theta}{MI(M)} \right) \qquad (7.41)$$

Hidden in expression 7.41 is the fact that the theoretical bias in DI samples is a function of several parameters: i.e. $B_i = f(\bar{u}, Y_0, U_*, \mathcal{B}, w_i, K$ and $M)$. Since $\bar{u}$, Y_0 and U_* are functions of Q and $\mathcal{B}$ can be replaced by $\mathcal{Z}_i$ (which in turn can be expressed as a function of Q for a given grain fraction i), then the parametric dependency can be simplified to $B_i = f(Q, i, K$ and $M)$. Using equation 7.41, a parametric study of the value of the B_i was performed and is reported in the following section.

7.5.2 Parametric Study of the Bias in DI

To calculate the estimated bias (B_i) in DI measurements, values of Q, i, K were assumed. In addition, based on relationships reported above, Y_0, u, Manning's n and Ξ_i were obtained for the Mission station. $I(\mathcal{A})$ was calculated by estimating P_E according to equation 7.35 and $I1(\mathcal{A})$ and $I2(\mathcal{A})$ were obtained by numerical integration. Θ was calculated using equation 7.39. Finally B_i was obtained according to equation 7.41. As stated above, results were insensitive to the choice of F. For the sake of convenience, a standard value of $M = 1$ ft. was normally selected in the analysis. It should be noted that other M-values were used and it was determined that B_i was directly proportional to the M-value. (Normally M ranged between 0.5 and 1.0 ft. when DI samples were obtained at Mission and hence the appropriate M-value was adopted when Bt was applied to correct the DI data).

Empirical relationships obtained for Y_0, $\bar{u}$ and Ξ_i for discharges between 190,000 and 330,000 cfs were extrapolated for the purpose of the parametric analysis of B_i. The reported behaviour of B_i for discharges outside the quoted range should be viewed as being less authorative than those obtained within the range. The results of the parametric study are presented in figures 7.26 through 7.28 and the following general conclusions apply:

(i) For a given grain fraction i and a given K, the larger the flow rate (Q) the more B_i approaches unity (figures 7.26).

(ii) Although B_i is always greater than 1.0 for a given K, M and Q, the smaller the grain diameter the more B_i approaches unity (figure 7.27).

(iii) For a given i, Q and M, the smaller the value of K the more B_i approaches unity (figure 7.28)

(iv) For a given i, Q and K, B_i is essentially directly proportional to M.

Figure 7.27 is a contour plot of B_i as a function of grain fraction (i) and discharge. Assuming $K = 0.4$ and $M = 1$ ft, figure 7.27 shows that B_i is greater than 1.05 when Q is less than 60,000 cfs, 160,000 cfs, 330,000 cfs and 700,000 cfs for each grain fraction respectively. Similarly, B_i is greater than 1.1 when Q is less than 40,000 cfs, 110,000 cfs, 200,000 cfs and 460,000 cfs respectively. Also, B_i is greater than 1.15 when Q is less than 60,000 cfs, 90,000 cfs and 230,000 cfs for fractions 2 through 4 respectively.

Therefore, for all values of Q, there is no appreciable error in the measured DI concentrations of the silt and finer loads. For flows in the spring freshet range ($Q \geq 200,000$ cfs), there is no appreciable error in the measured wash load ($d \leq 0.19$ mm). However, for the suspended bed material load (sbml), appreciable errors (in the order of 5 to 15 %) can be expected even during the freshet period.

This would be less if a smaller value of the von Karman constant was assumed. For example, if $K = 0.3$, then for fractions 1 through 4, B_i would be greater than 1.1 if Q was less than 30,000 cfs, 90,000 cfs, 130,000 cfs and 260,000 cfs respectively.

To highlight the dependence of B_i on Ξ, B_i was expressed as a function of Ξ and K. For example, when Q = 200,000 cfs, B_i can be as low as 1.05 (for $\Xi \leq 0.3$ or $K \leq 0.3$) or as high as 2.45 (for $K = 0.4$ and $\Xi \geq 1.2$).

7.6 Summary

7.6.1 Sediment and Velocity Profiles

PI data indicate that the vertical velocity profile in the Lower Fraser has three distinct zones. Firstly, the bottom 15 % of the water column is logarithmically distributed. Secondly, in the core area (also logarithmically distributed) because this zone is free of dune effects, the dependence of u on Y is different than that observed in the lowest region. In the third zone, the top 5 to 10 % of the water column, the velocity profile is frequently distorted due to wind-generated shear stress. Therefore, direct application of the traditional logarithmic velocity profile to the entire vertical flow field of Lower Fraser has its limitations. Accordingly, alternate expressions for representing the vertical velocity profile should be explored.

Of the two suspended sediment models investigated, the Rouse model (based on a parabolic distribution of the eddy viscosity) was found to be better than the simpler model (based on an assumed constant eddy viscosity). However, in most cases both models were equally able (or unable) to represent the vertical gradation in sediment concentration. In other cases, each model displayed a marked advantage over the other.

For each model there was a systematic skew in the plot of normalized concentration versus normalized depth in about 50 % of the PI grain fraction profiles examined. It is hypothesized that the bias may be due, in part, to the fact that grain fractions rather than distinct grain sizes were used in the analyses. Further study of this effect was undertaken and the results are reported in the next chapter.

The Rouse Number Ξ showed a marked variability in all of the analyses undertaken. Even the ratio of Rouse Numbers obtained for one grain fraction to that obtained for another grain fraction ($\Xi_{i/j}$ determined at the same time and same location) showed a marked variability. For example, the 10 percentile value of $\Xi_{i/j}$ differed from the median value by about 100 %. Some of the variability is certainly due to limitations associated with the collection of the data, the laboratory analyses (often involving the measurement of very few grains), and statistical procedures used to estimate Ξ. It could be due to the fact that B may not vary in the same way as a function of discharge from one grain size to the other. It may also be because the relative proportion of the sediment sizes within a grain fraction may be a function of discharge. Finally, the variability of $\Xi_{i/j}$ may be due to poor or inadequate theoretical assumptions inherent to the models used. However, even though $\Xi_{i/j}$ showed a great deal of variability, median values were quite consistent from one data subset to another. This fact lent credibility to the analyses and reliability to the median values obtained.

The hypothesis that the Rouse number used for the constant eddy viscosity model should be multiplied by $1/6$ $(= \eta)$ was confirmed. Analyses showed that η using Mission data was $1/7.2$, while that for the Port Mann data was $1/7.6$. Although a frequency distribution analysis of the ratio revealed that 20 % of the data were outliers, most values were clustered around the median value. This reaffirmed the conclusion that the median estimates of the Rouse number are generally reliable.

From an examination of the relationship between U_* and Q, it was determined that Ξ could be related to $1/Q$ in lieu of $1/U_*$. While subsequent analyses revealed a large scatter of points, the regression lines displayed consistent trends. Since the Ξ was uniformly scattered about the estimate for all values of $1/Q$ (and given the consistency of the trends found in other analyses of the Rouse number), a fair degree of confidence can be placed in the derived Ξ_i - $1/Q$ relationships even though the 10 percentile values differed from the estimates by about 100 %.

7.6.2 Bias in DI Sampling

Based on Rouse's model for suspended sediment concentration distribution and empirical relationships derived for the Mission station, the potential bias (B_i) in DI measurements was quantified through a parametric study of B_i versus grain fraction i, and parameters K, Q and M. The bias was directly proportional to the magnitude (M) of the unsampled near-bed zone.

B_i was also found to be greater for higher values of the von Karman coefficient, for coarser grains, and for lower discharges. The analyses indicated that no appreciable bias in Mission DI measurements of wash load would occur during the spring freshet period. On the other hand, for the sbml (grains coarser than 0.19 mm), a bias in the order of 5 to 15 % was indicated, even during freshet conditions. To obtain a better estimate of the sbml in the Lower Fraser, B_i should be applied to actual DI measurements.

This page is intentionally left blank.

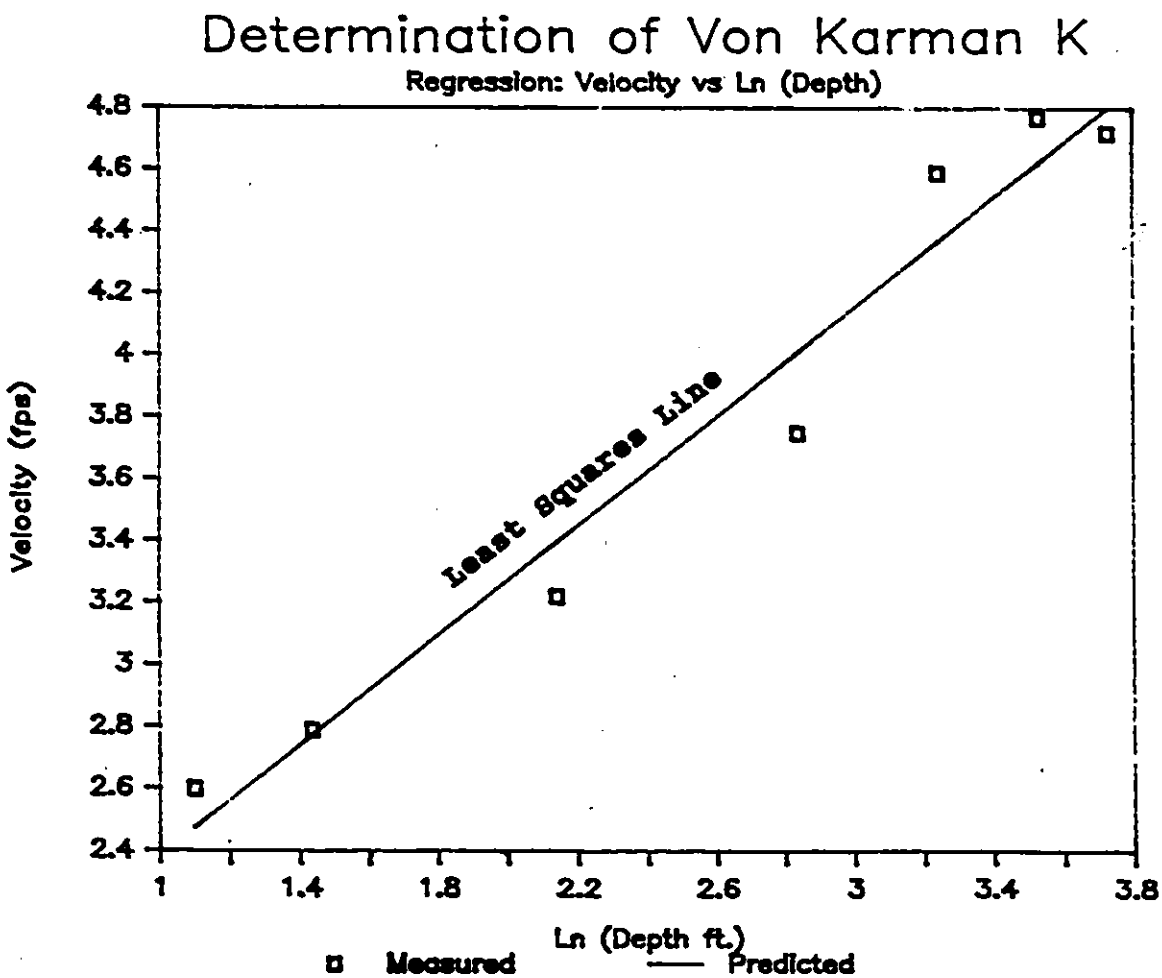

Figure 7.1: Regression of Velocity versus ln(Local Depth) at Mission - *Vertical* 300

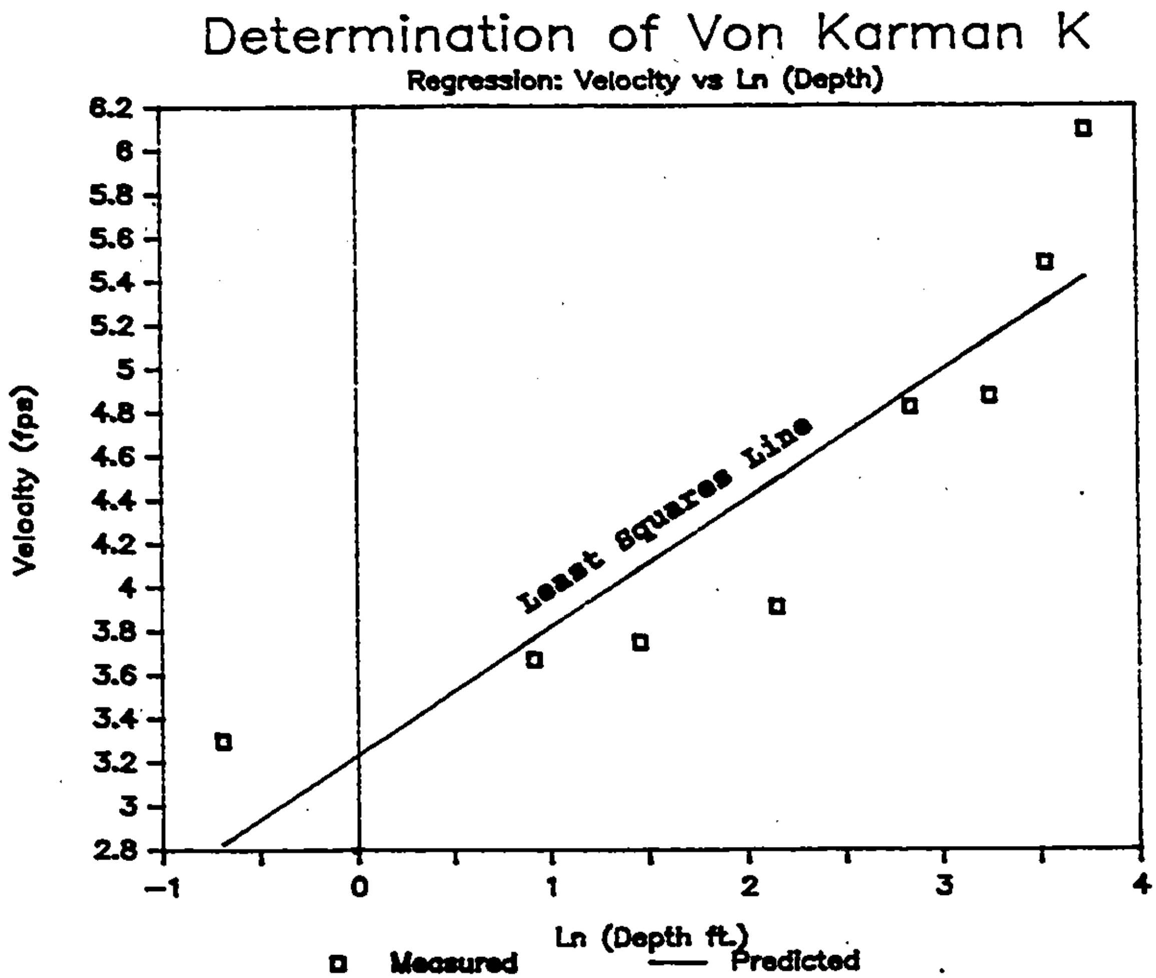

Figure 7.2: Regression of Velocity versus ln(Local Depth) at Mission - *Vertical* 600

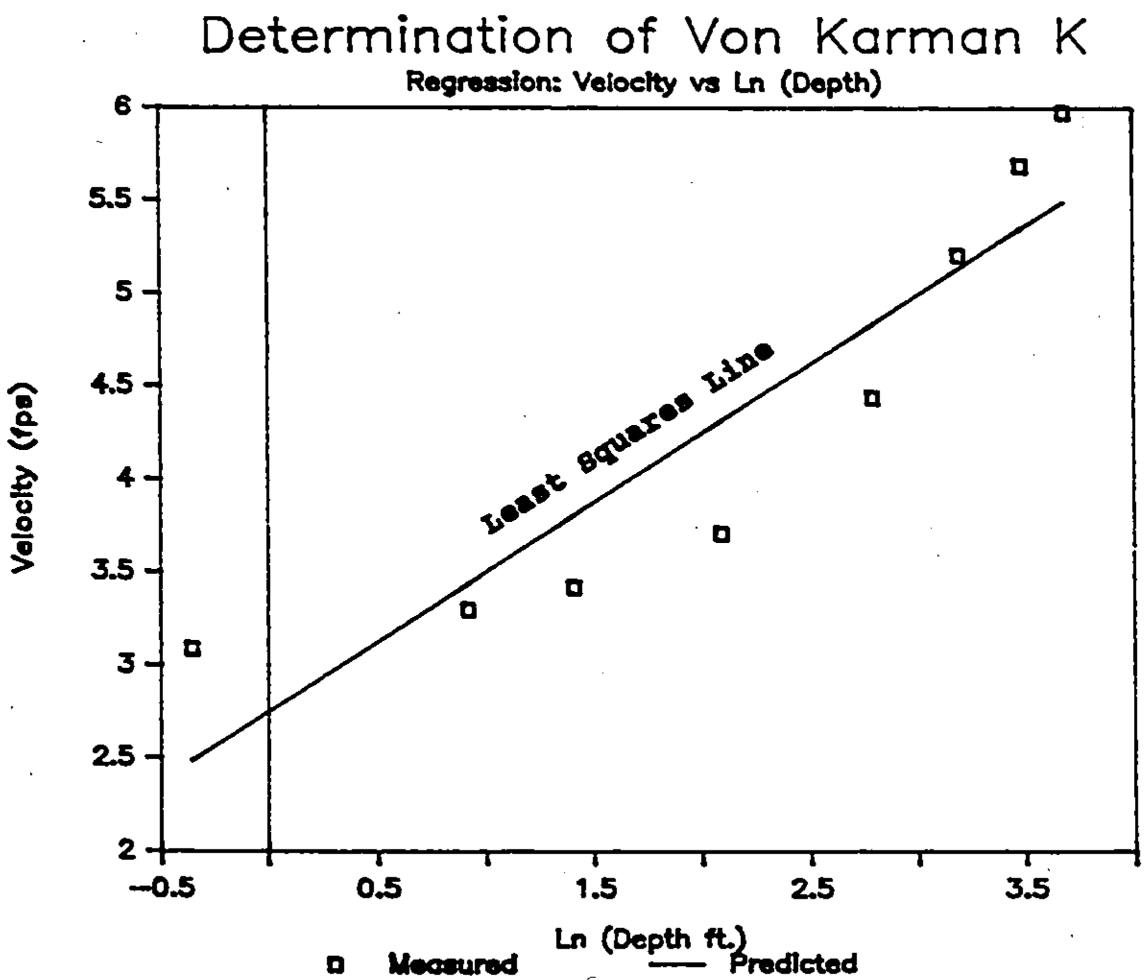

Figure 7.3: Regression of Velocity versus ln(Local Depth) at Mission - *Vertical* 900

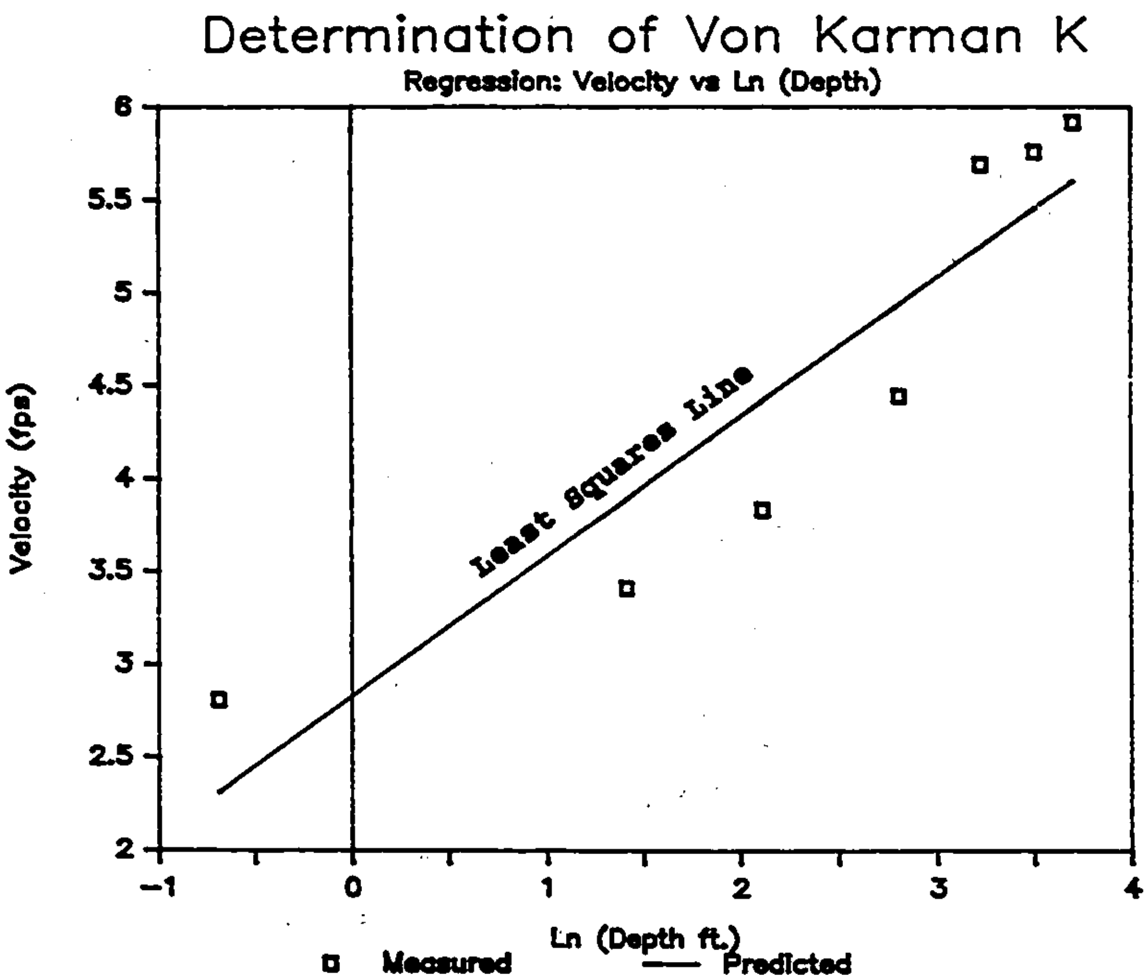

Figure 7.4: Regression of Velocity versus ln(Local Depth) at Mission - *Vertical* 1200

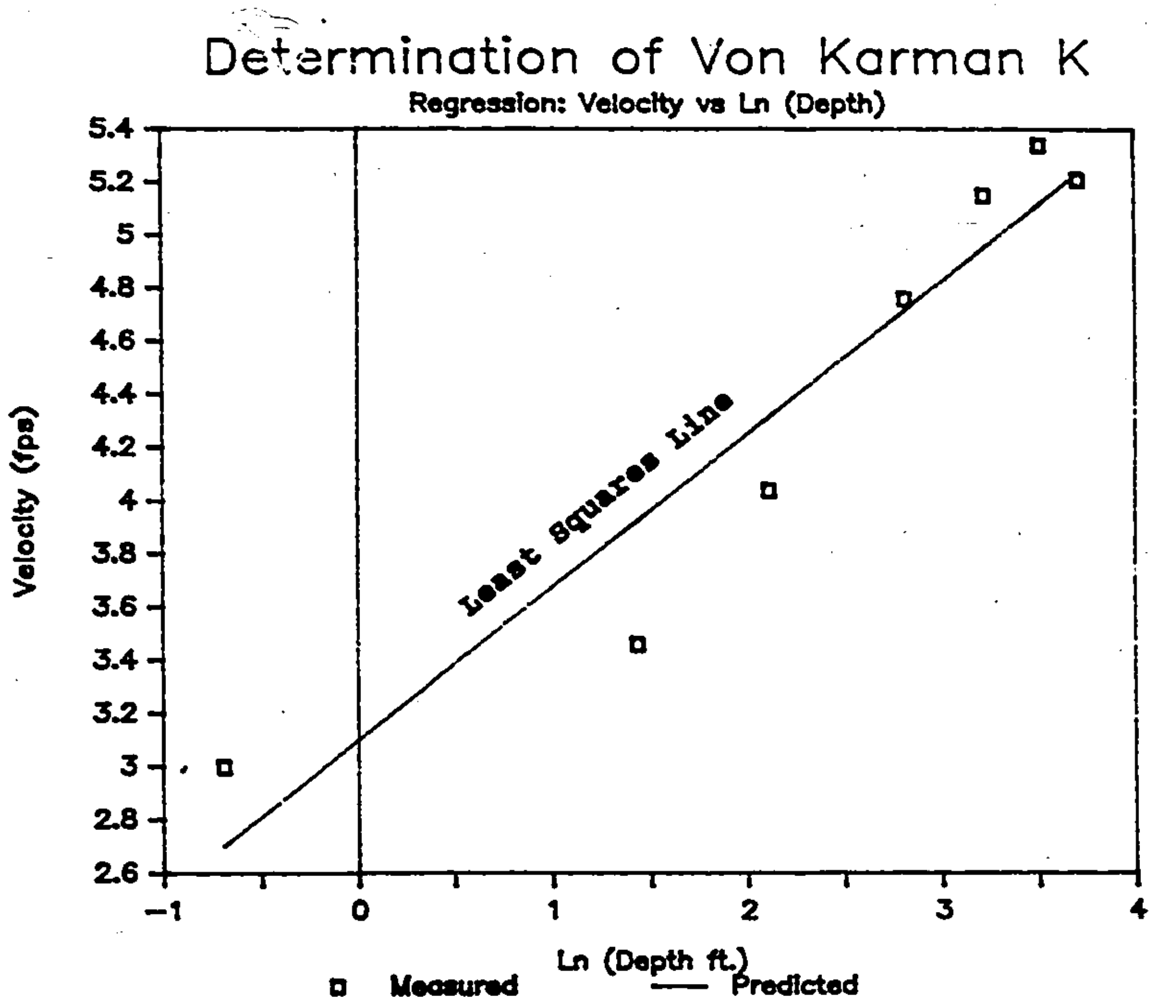

Figure 7.5: Regression of Velocity versus ln(Local Depth) at Mission - *Vertical* 1500.

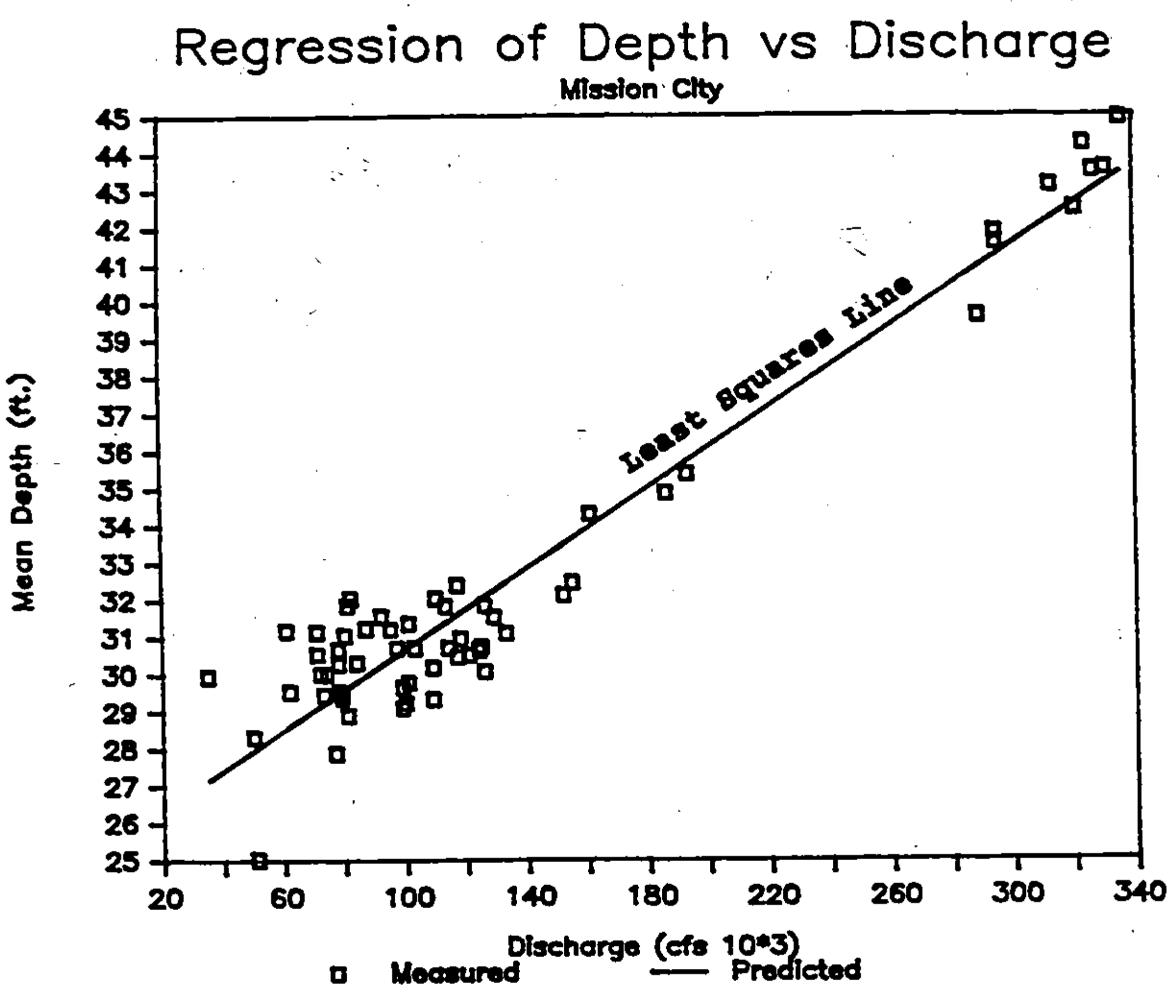

Figure 7.6: Regression of Mean Depth versus Discharge at Mission (1968)

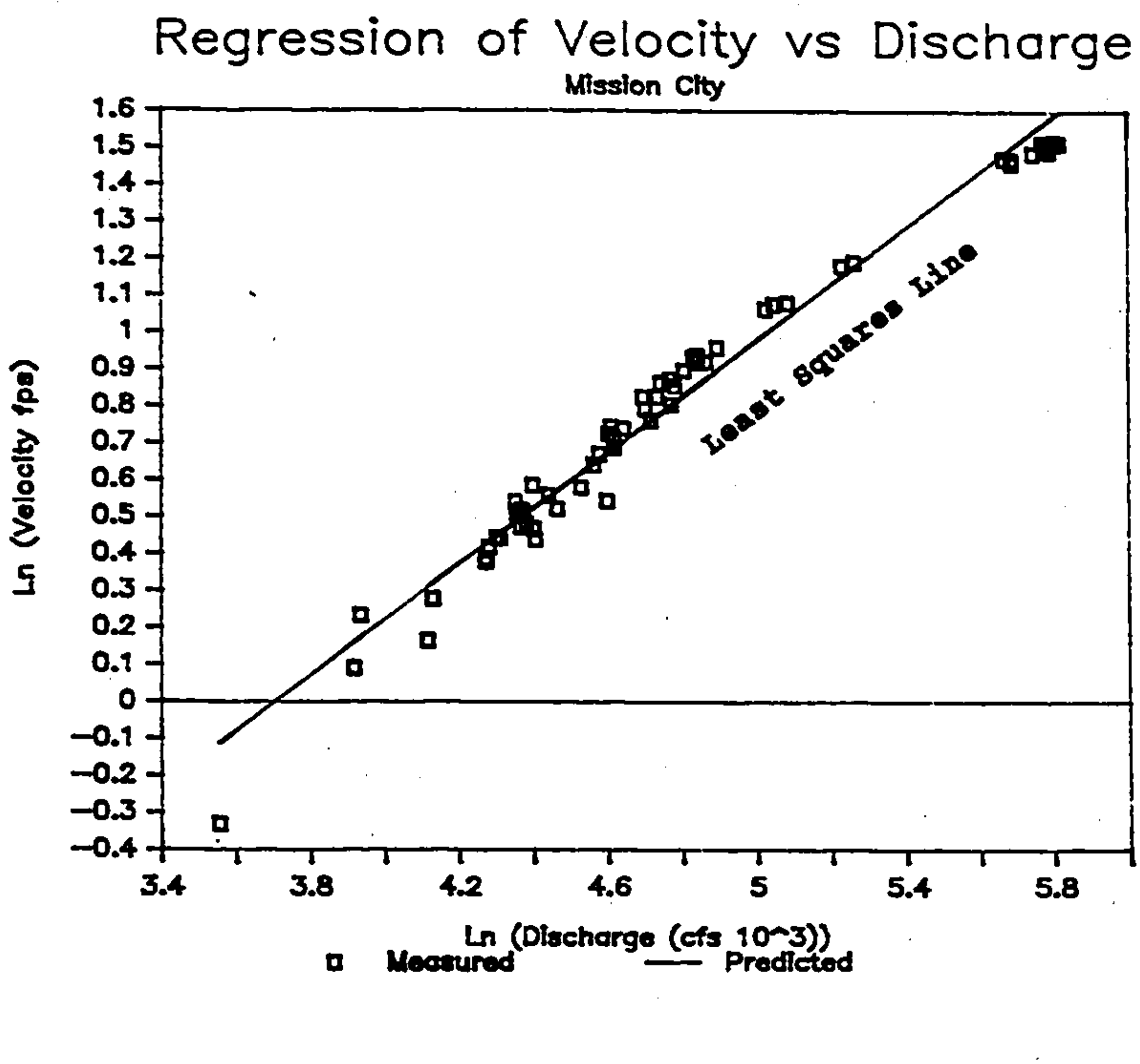

Figure 7.7: Regression of Velocity versus Discharge at Mission (1968)

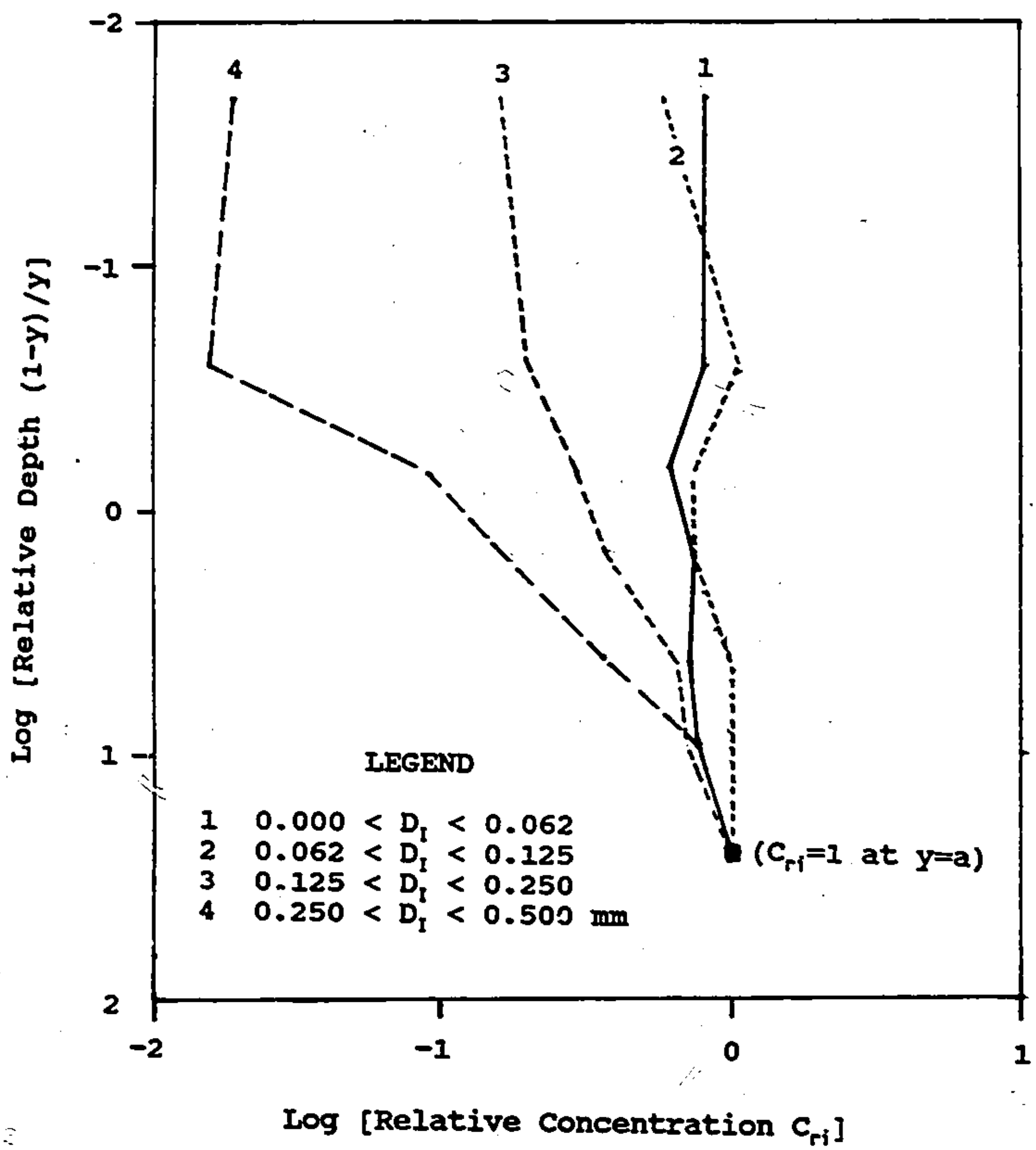

Figure 7.8: Relative Depth versus Relative Concentration according to the Rouse Model

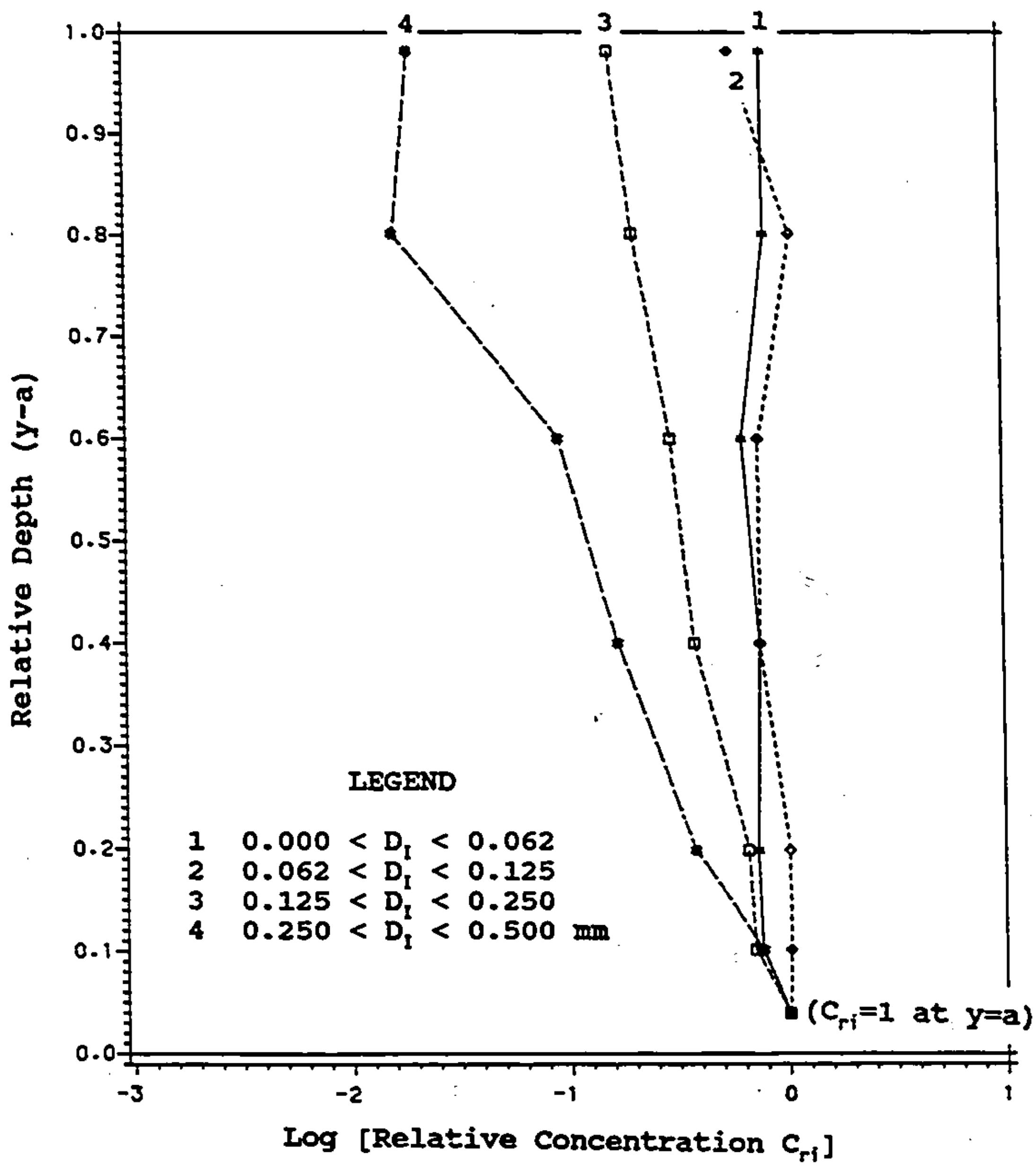

Figure 7.9: Relative Depth versus Relative Concentration according to the Constant Eddy Viscosity Model

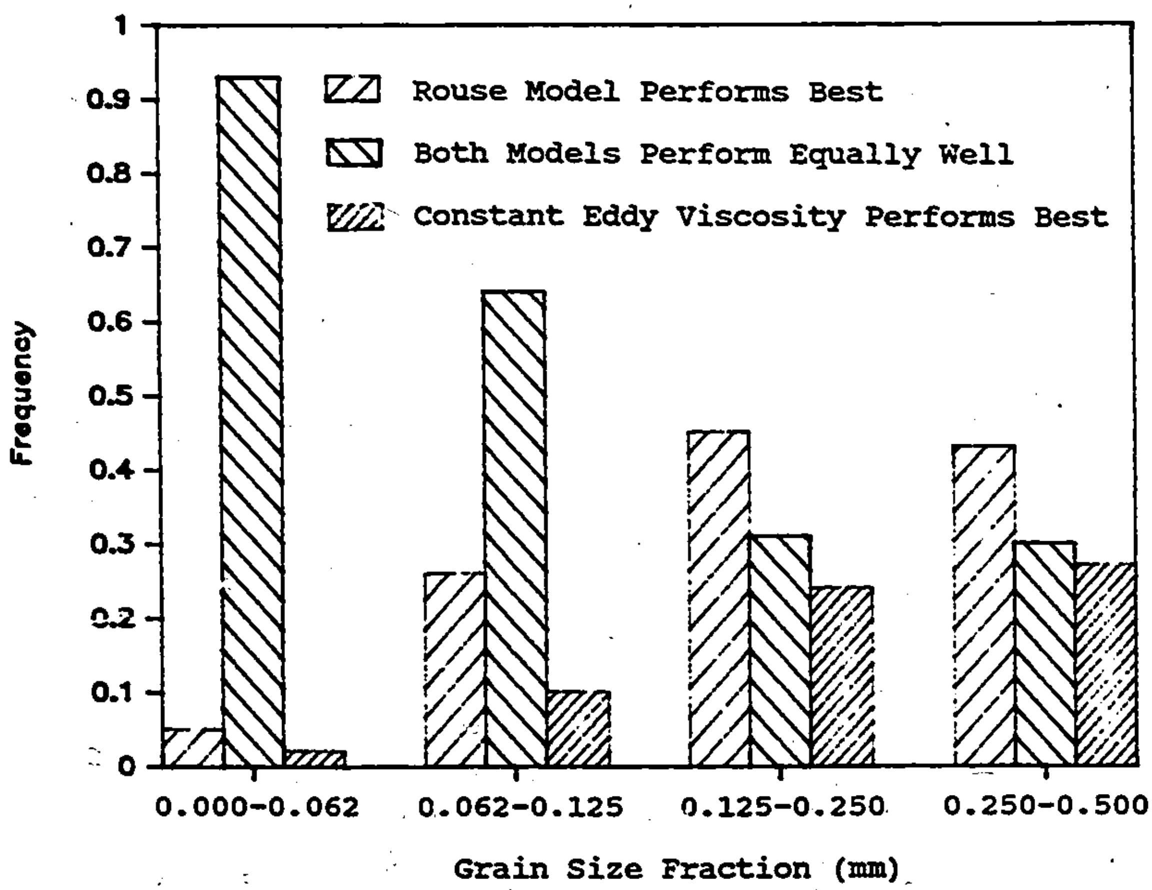

Figure 7.10: Comparison of Diffusion-Dispersion Models; Visual Inspection - Mission and Port Mann

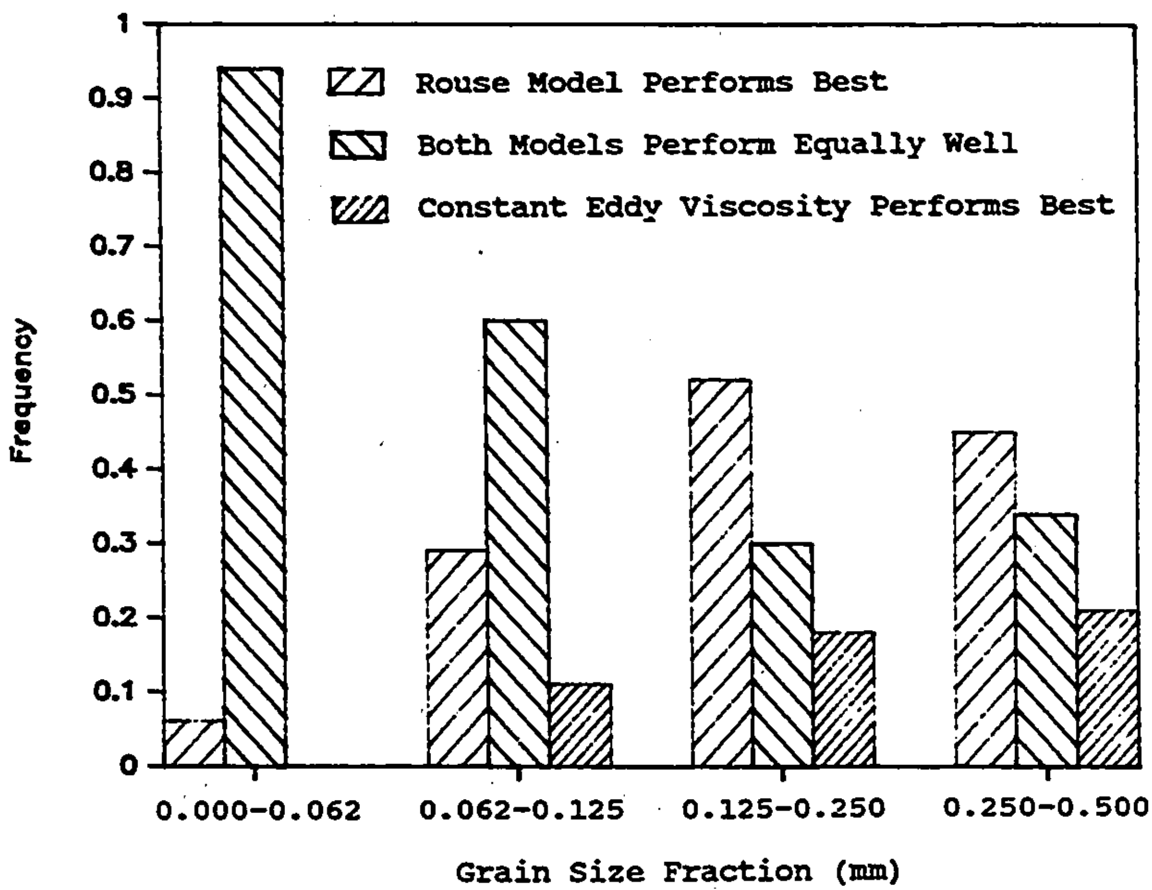

Figure 7.11: Comparison of Diffusion-Dispersion Models; Visual Inspection - Mission only

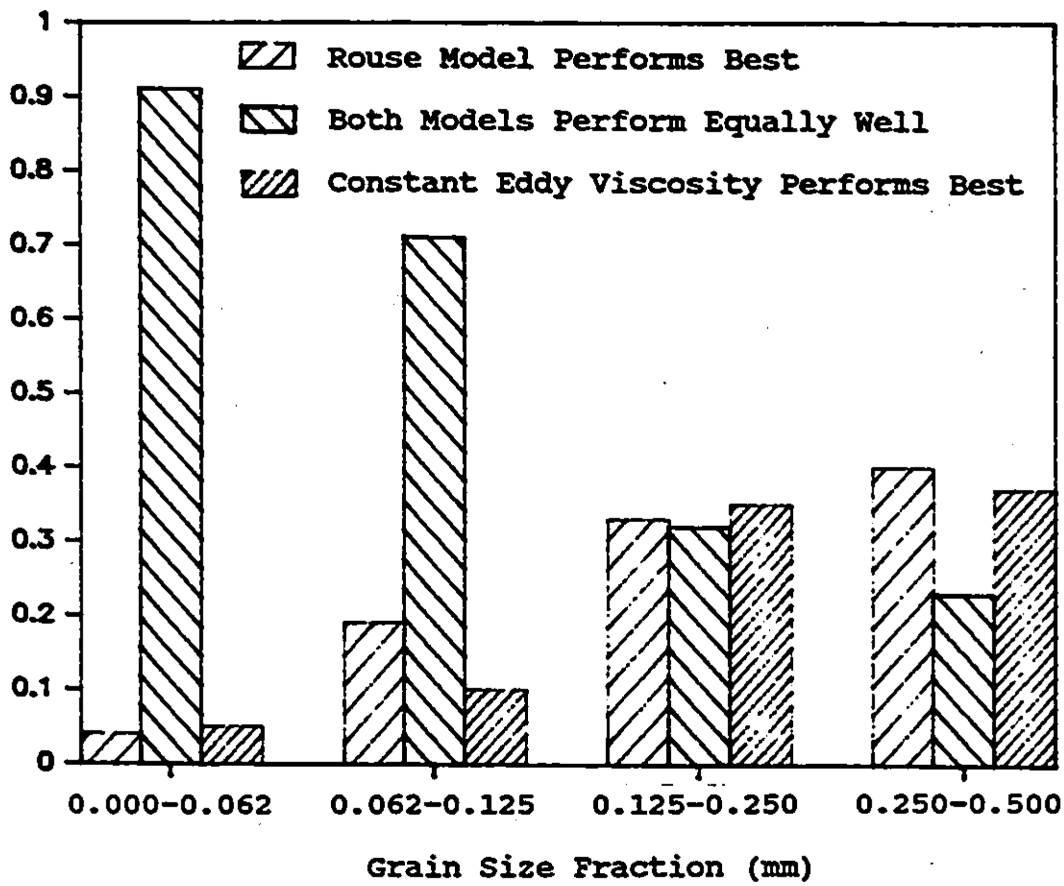

Figure 7.12: Comparison of Diffusion-Dispersion Models; Visual Inspection - Port Mann only

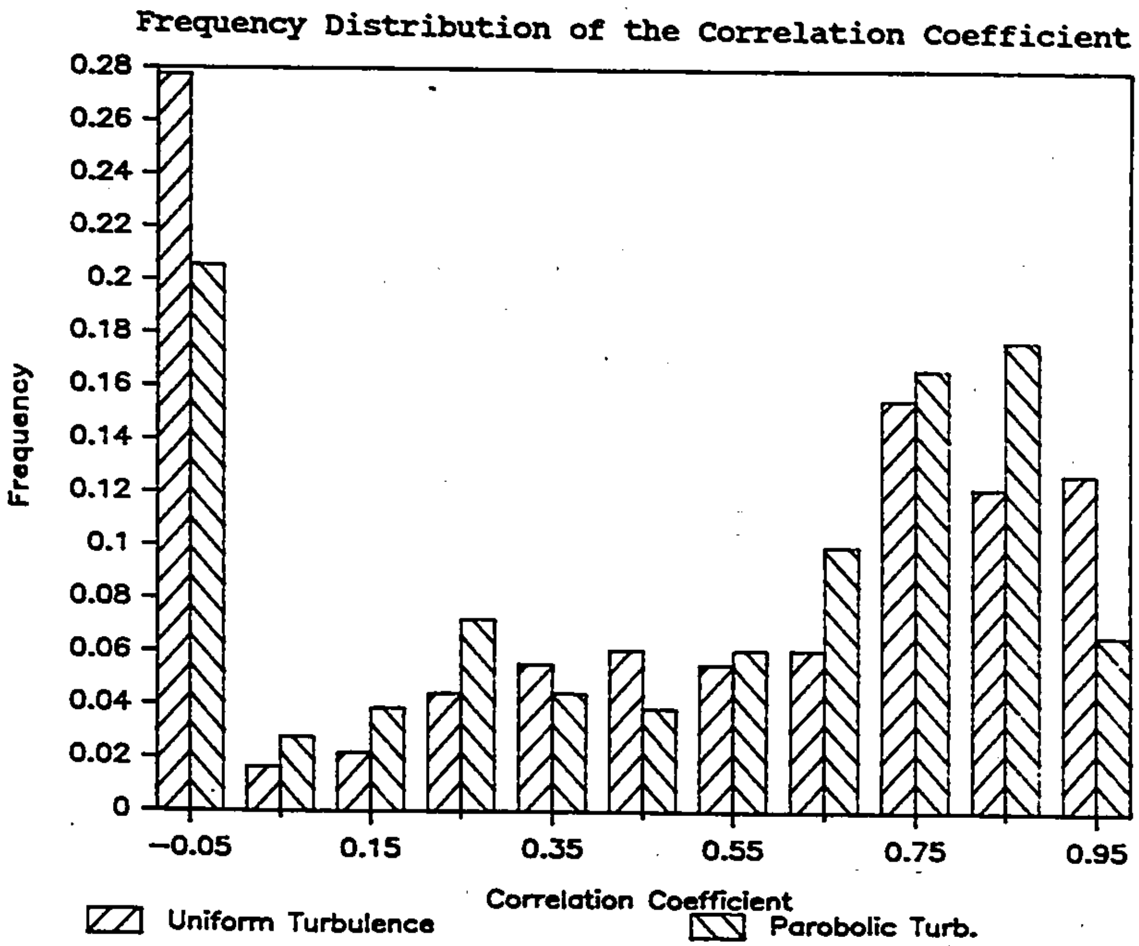

Figure 7.13: Comparison of Diffusion-Dispersion Models; Statistical Analysis - $0 < d < 0.062mm$

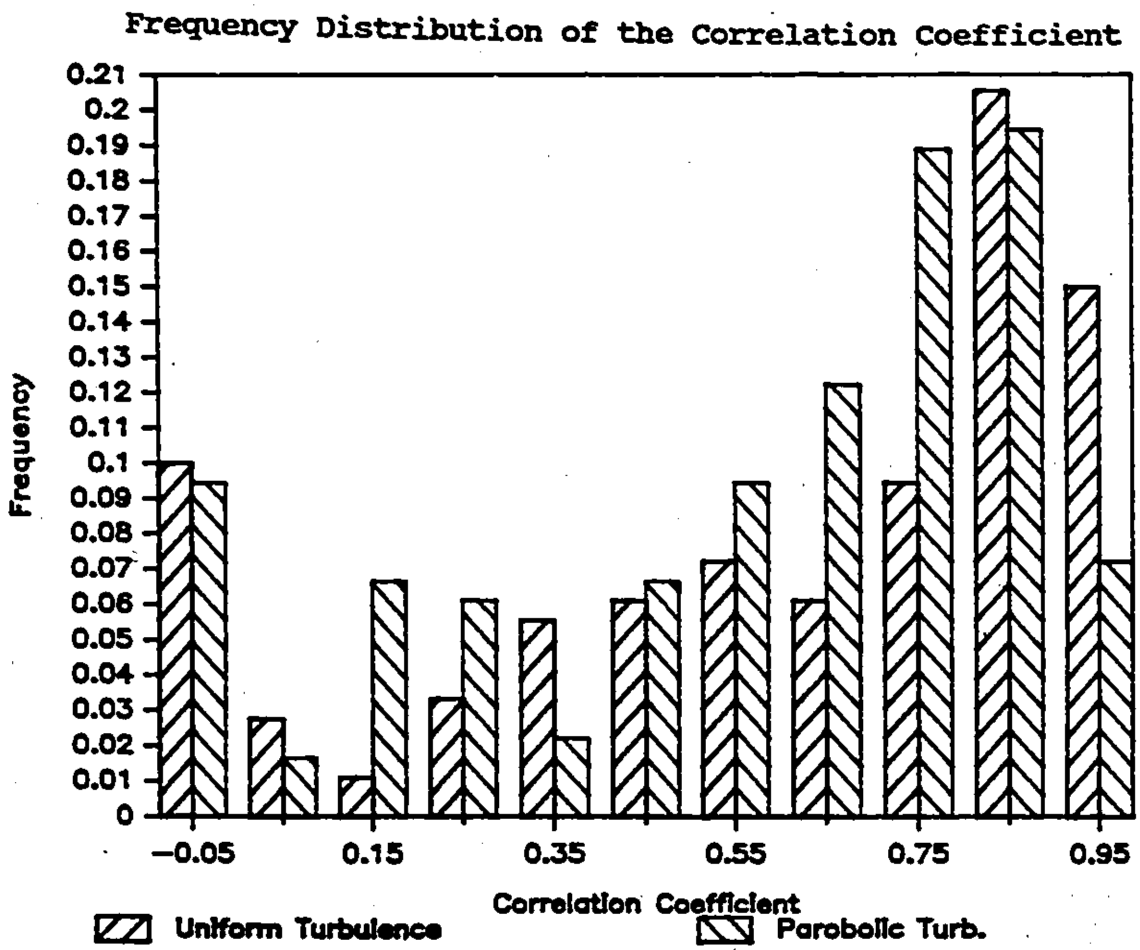

Figure 7.14: Comparison of Diffusion-Dispersion Models; Statistical Analysis - $0.062 < d < 0.125mm$

This page is intentionally left blank.

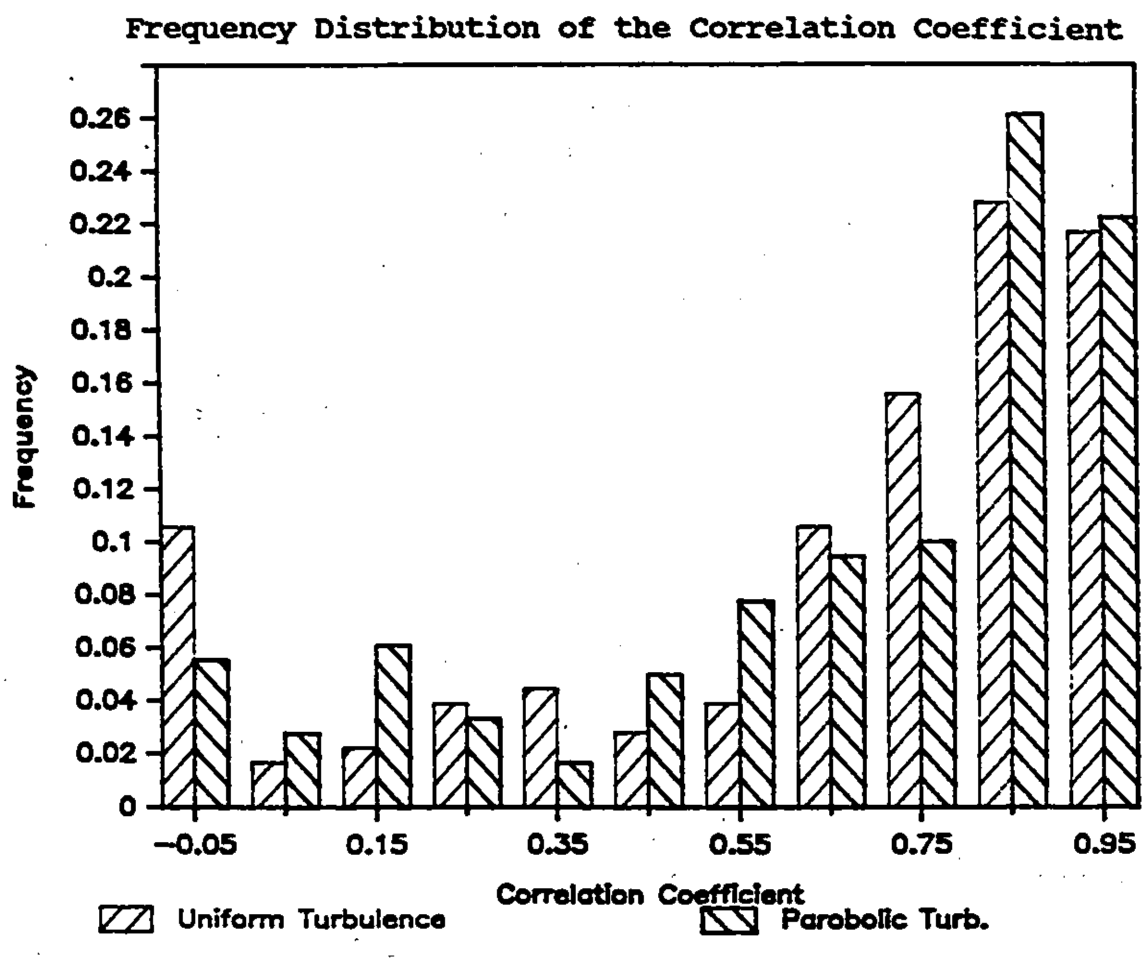

Figure 7.15: Comparison of Diffusion-Dispersion Models: Statistical Analysis - $0.125 < d < 0.250mm$

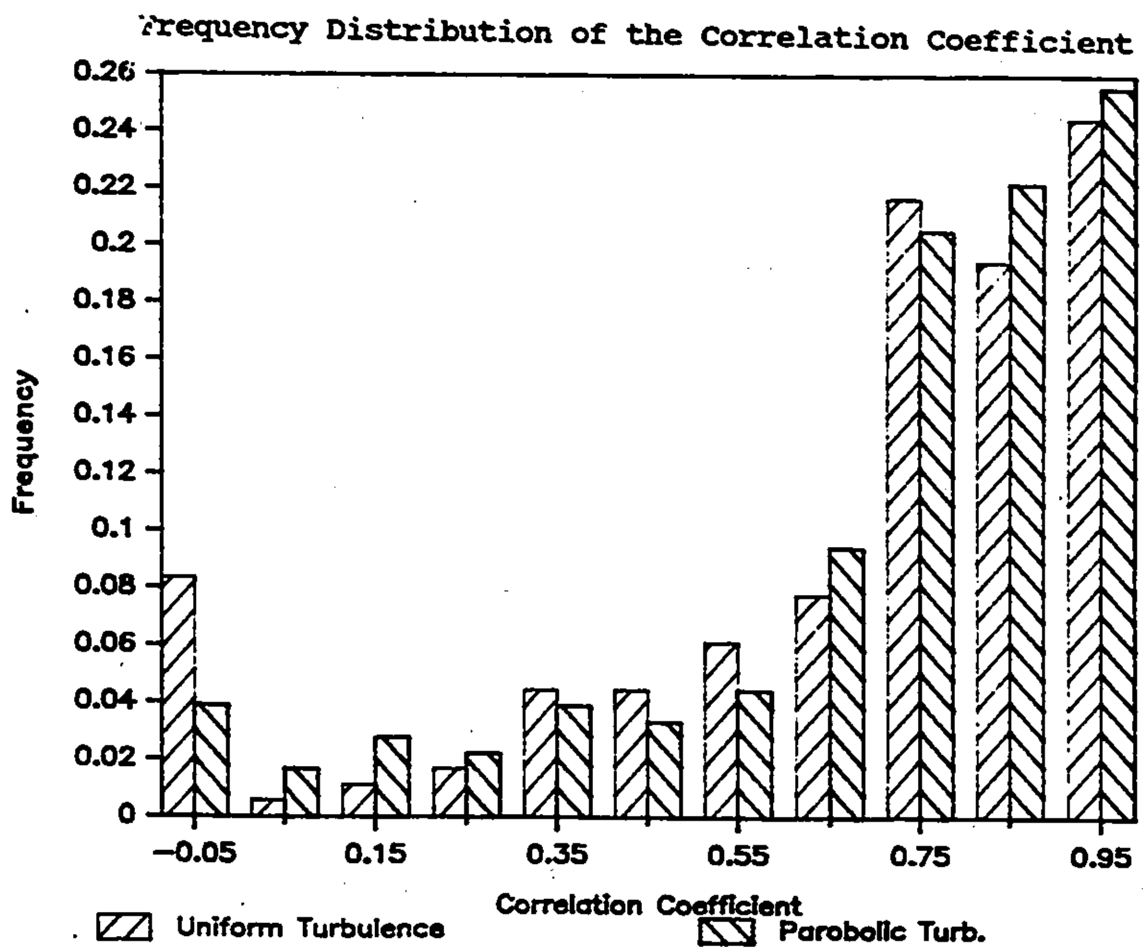

Figure 7.16: Comparison of Diffusion-Dispersion Models; Statistical Analysis - $0.250 < d < 0.500mm$

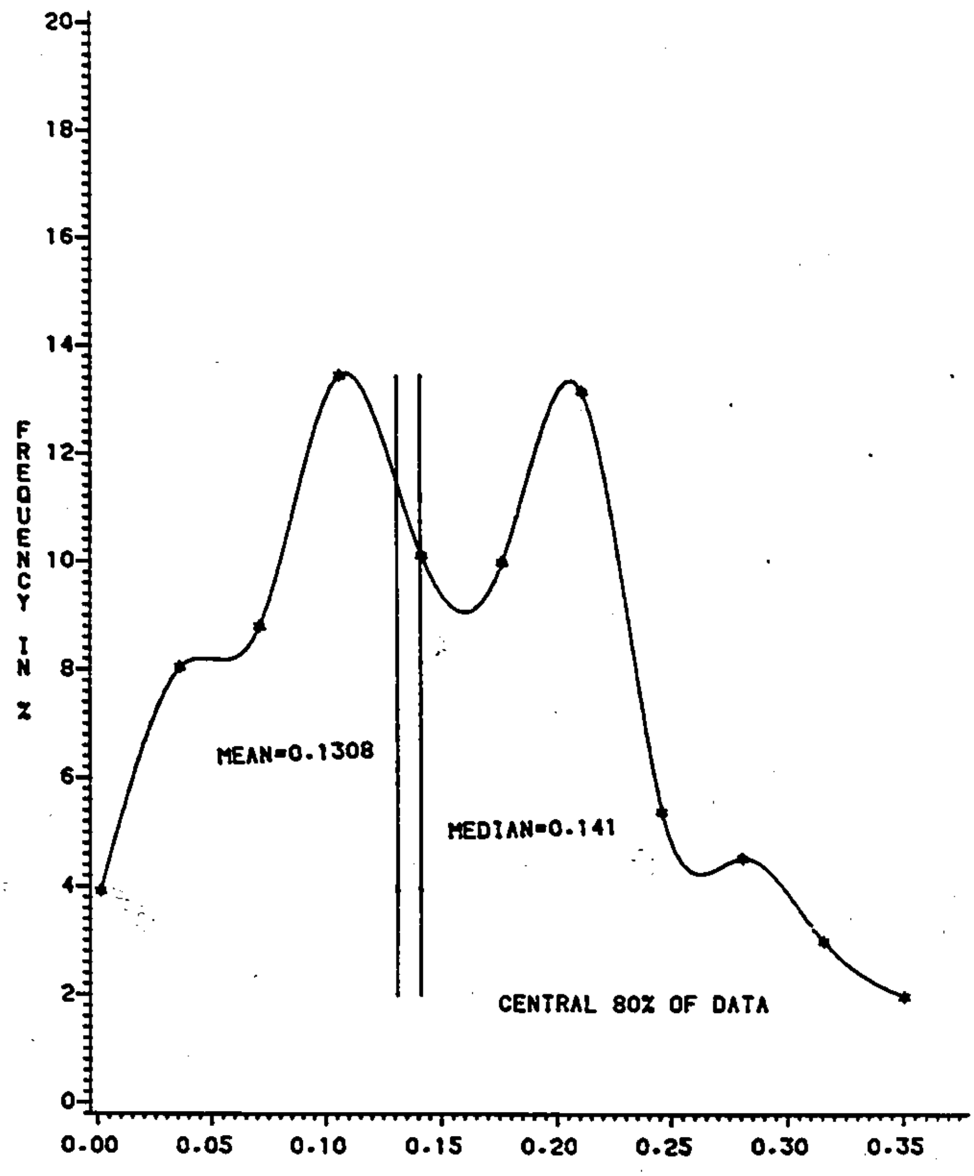

Figure 7.17: Frequency Distribution of the Ratio of Rouse Numbers: $\Xi_{1/3}$

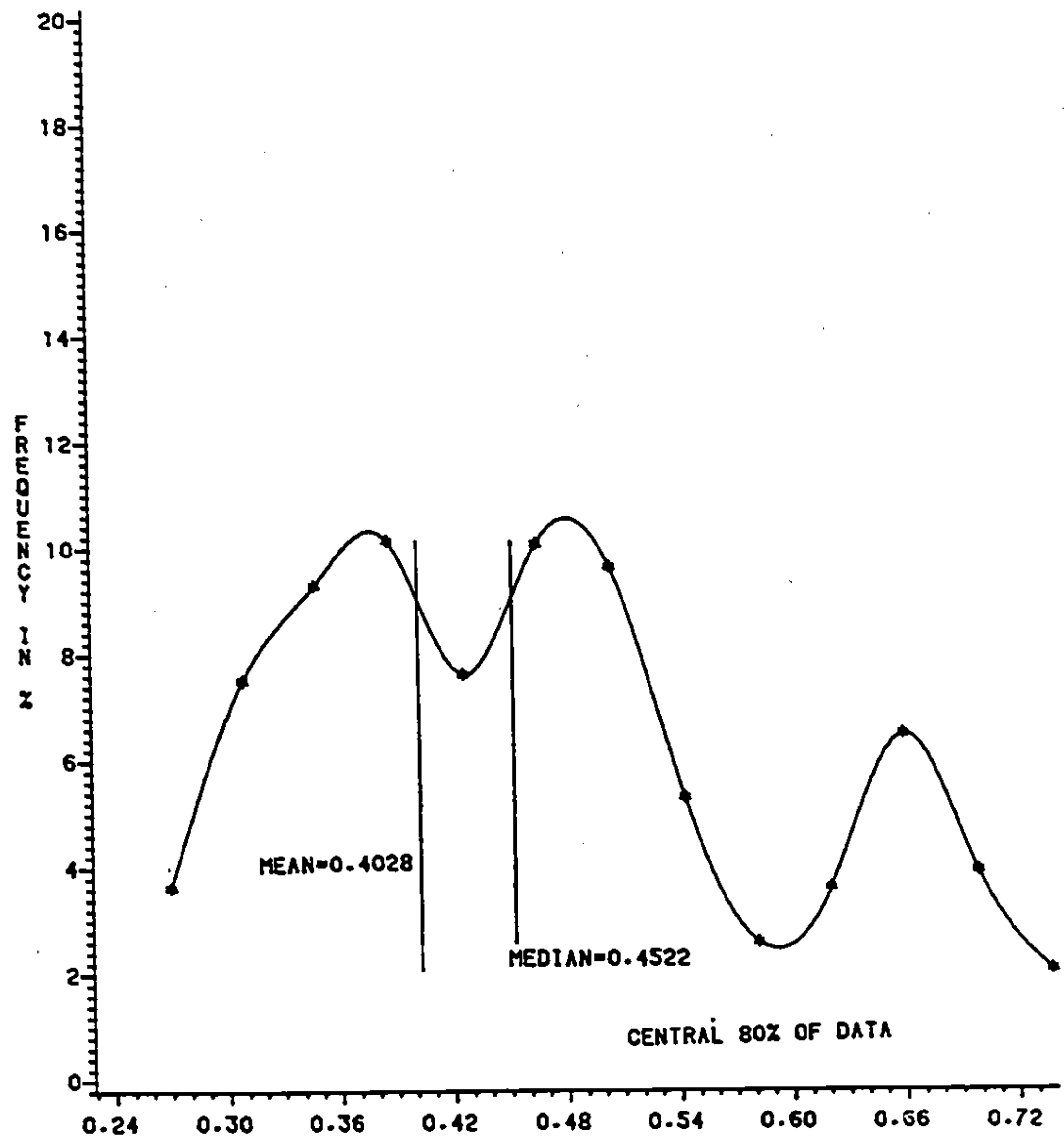

Figure 7.18: Frequency Distribution of the Ratio of Rouse Numbers: $Z_{2/3}$

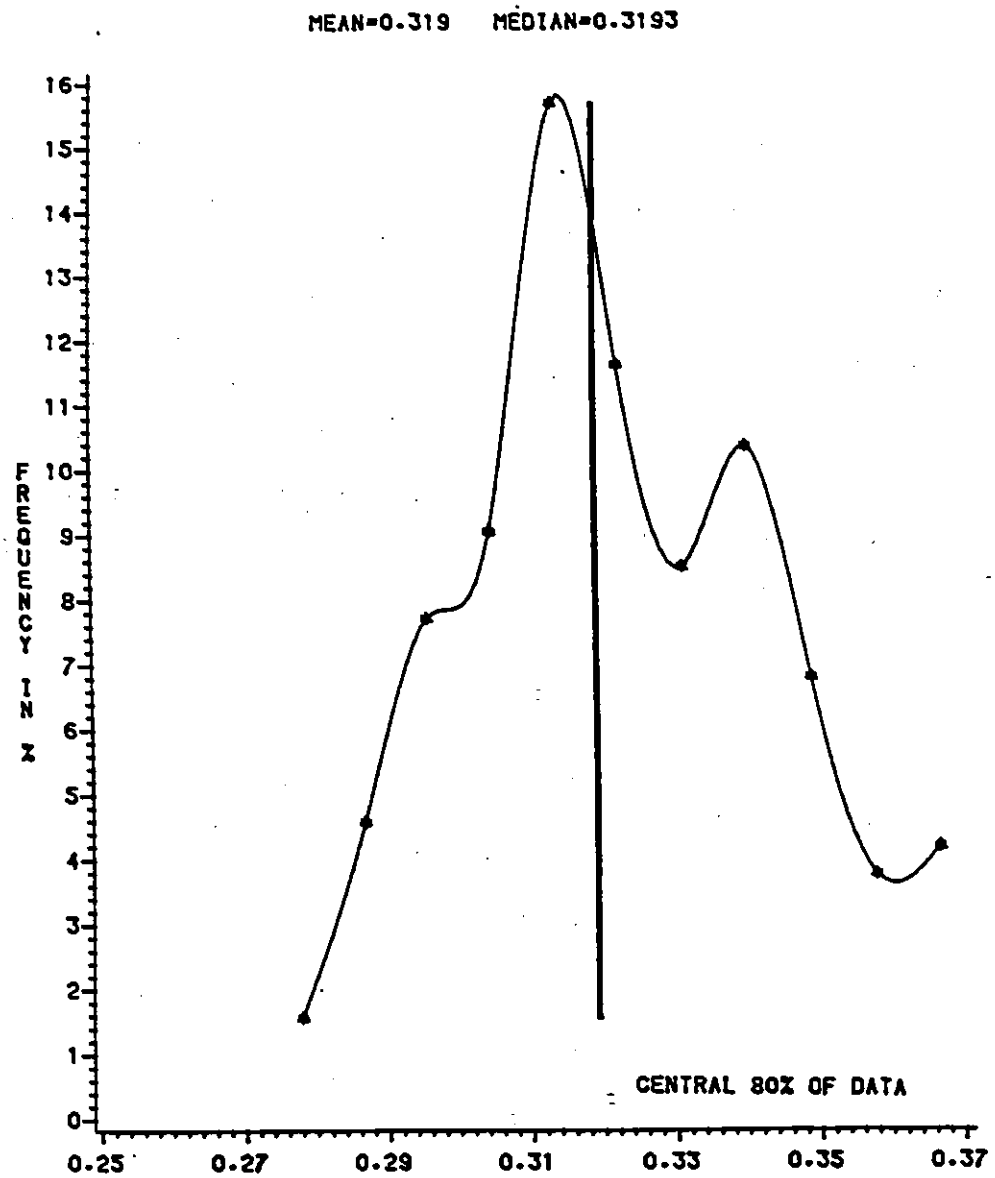

Figure 7.19: Frequency Distribution of η for $0.062 < d < 0.125$

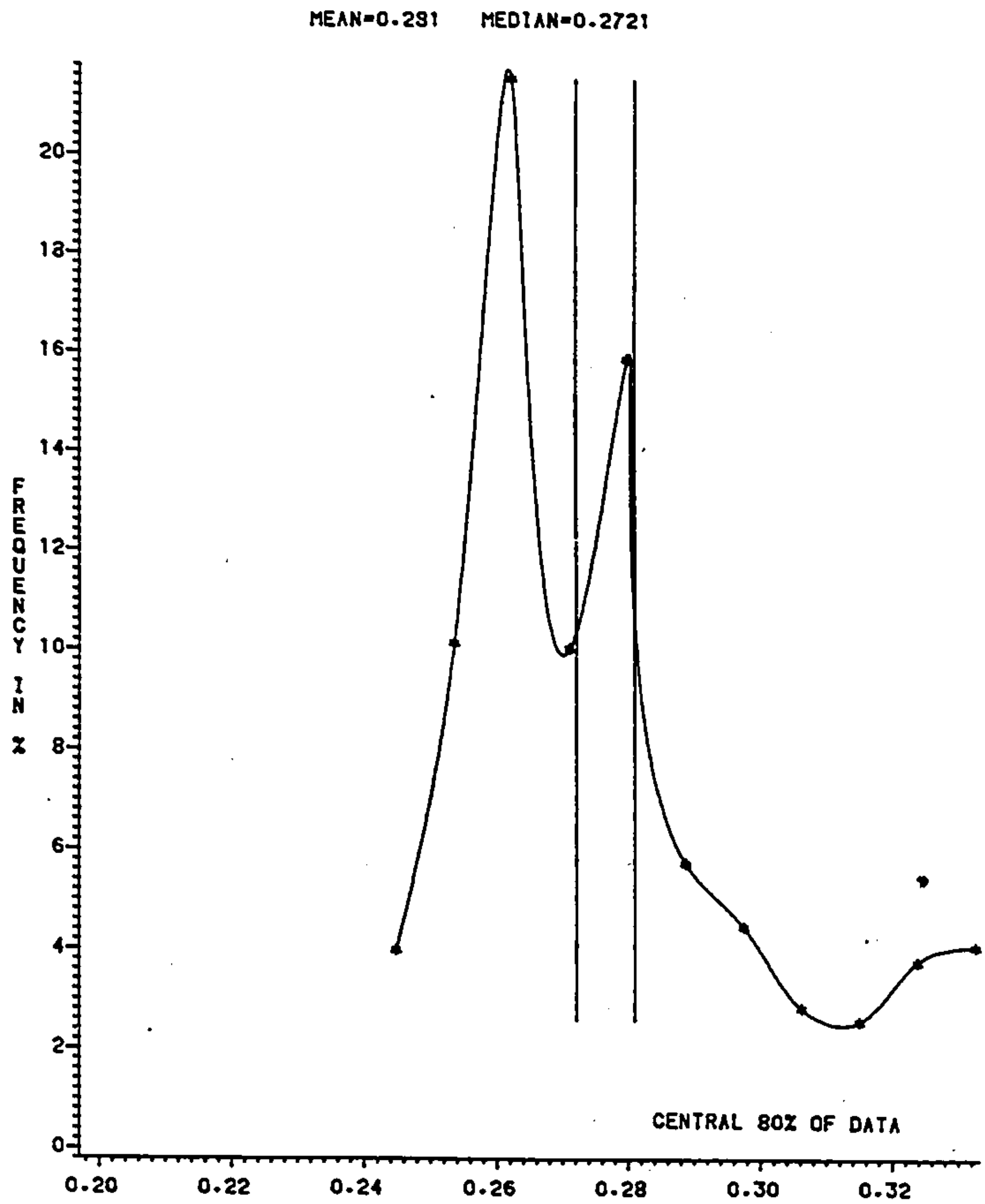

Figure 7.20: Frequency Distribution of η for $0.250 < d < 0.500$

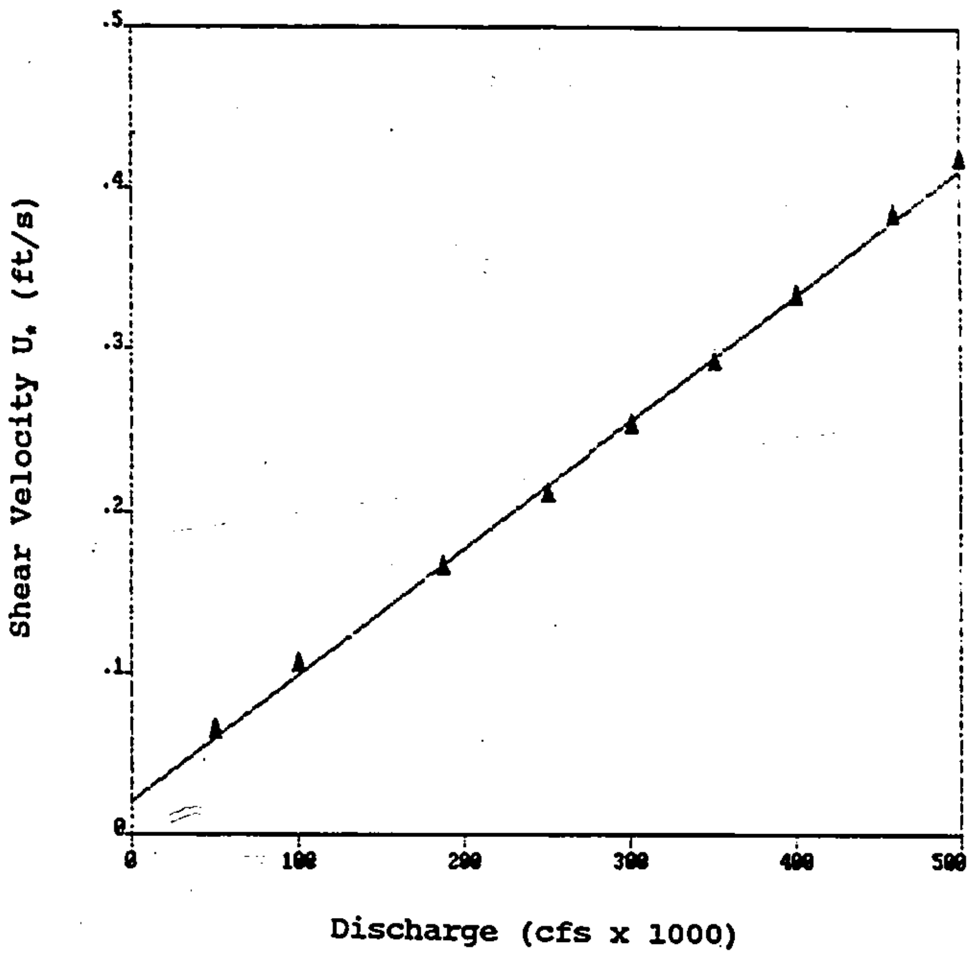

Figure 7.21: Regression of U_* versus Q at Mission (1968)

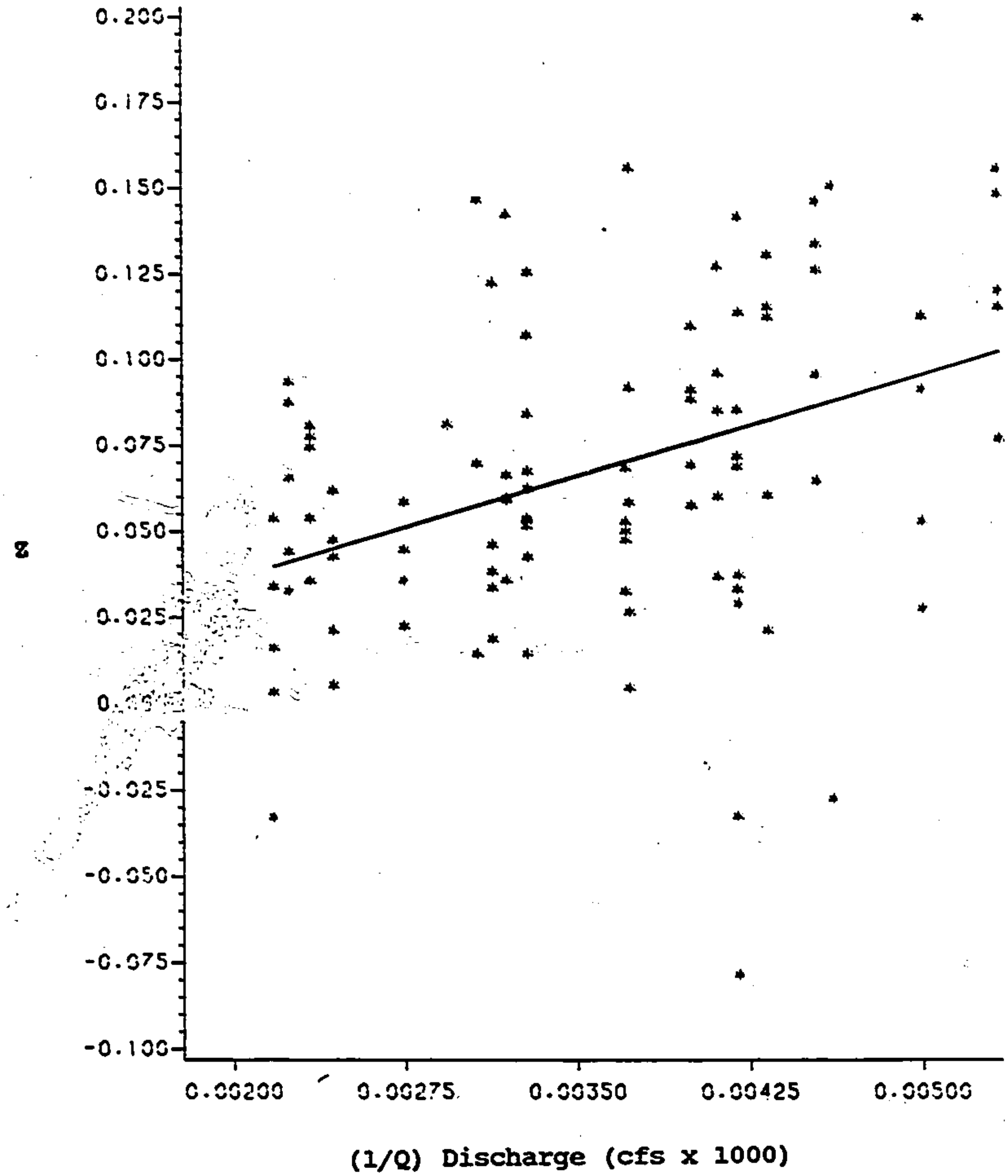

Figure 7.22: Regression of Rouse Number versus 1/Q for $0 < d < 0.062$

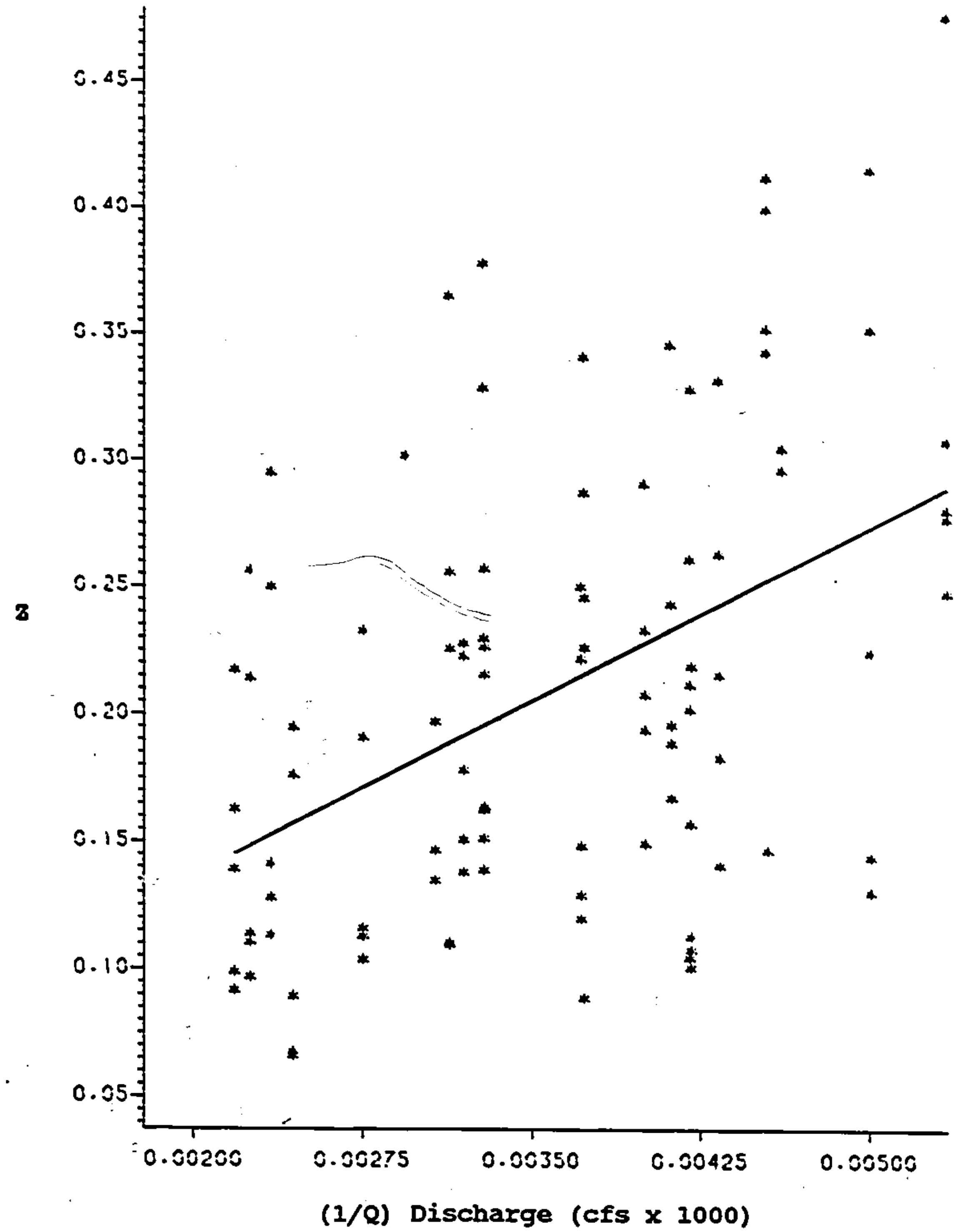

Figure 7.23: Regression of Rouse Number versus 1/Q for $0.062 < d < 0.125$

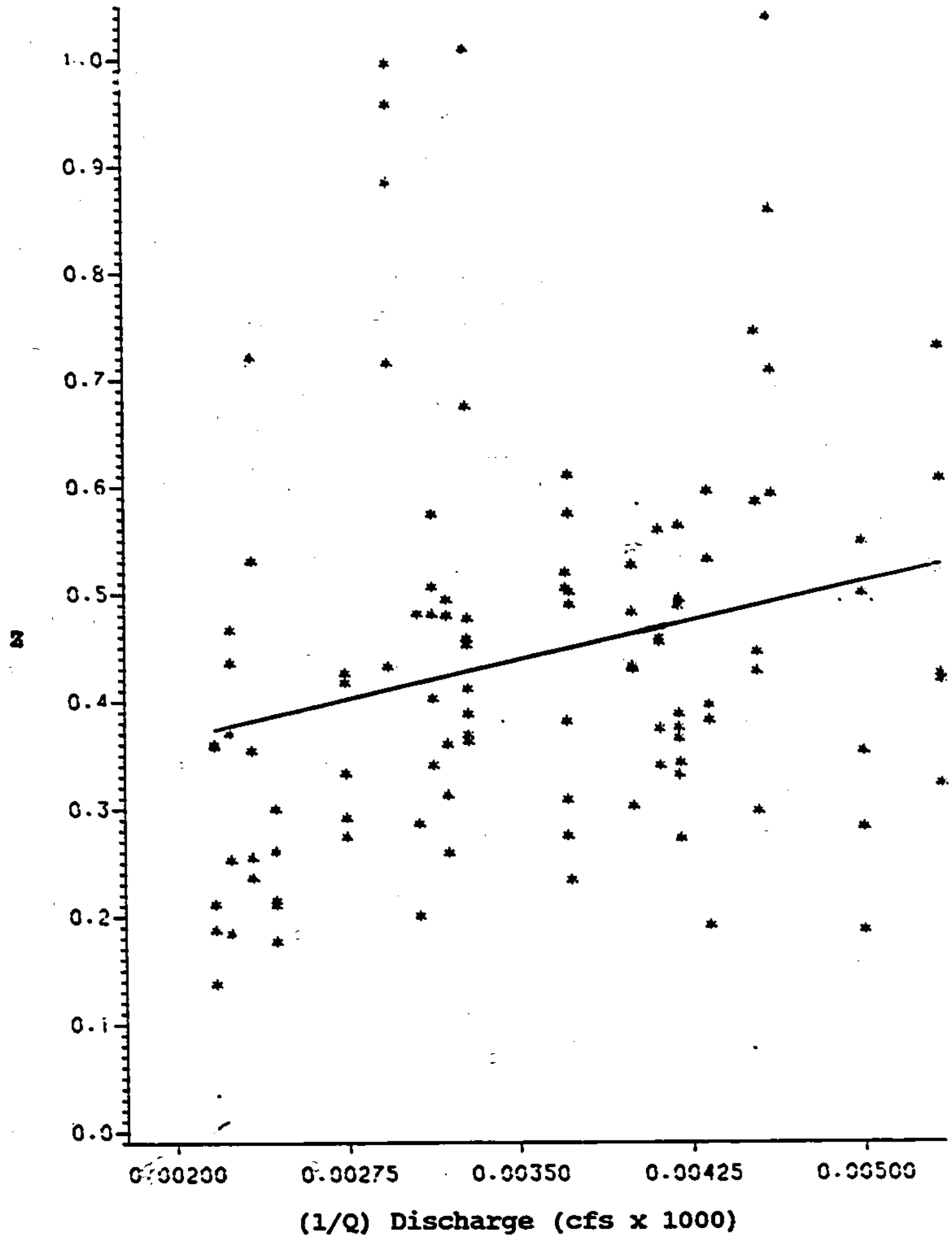

Figure 7.24: Regression of Rouse Number versus 1/Q for $0.125 < d < 0.250$

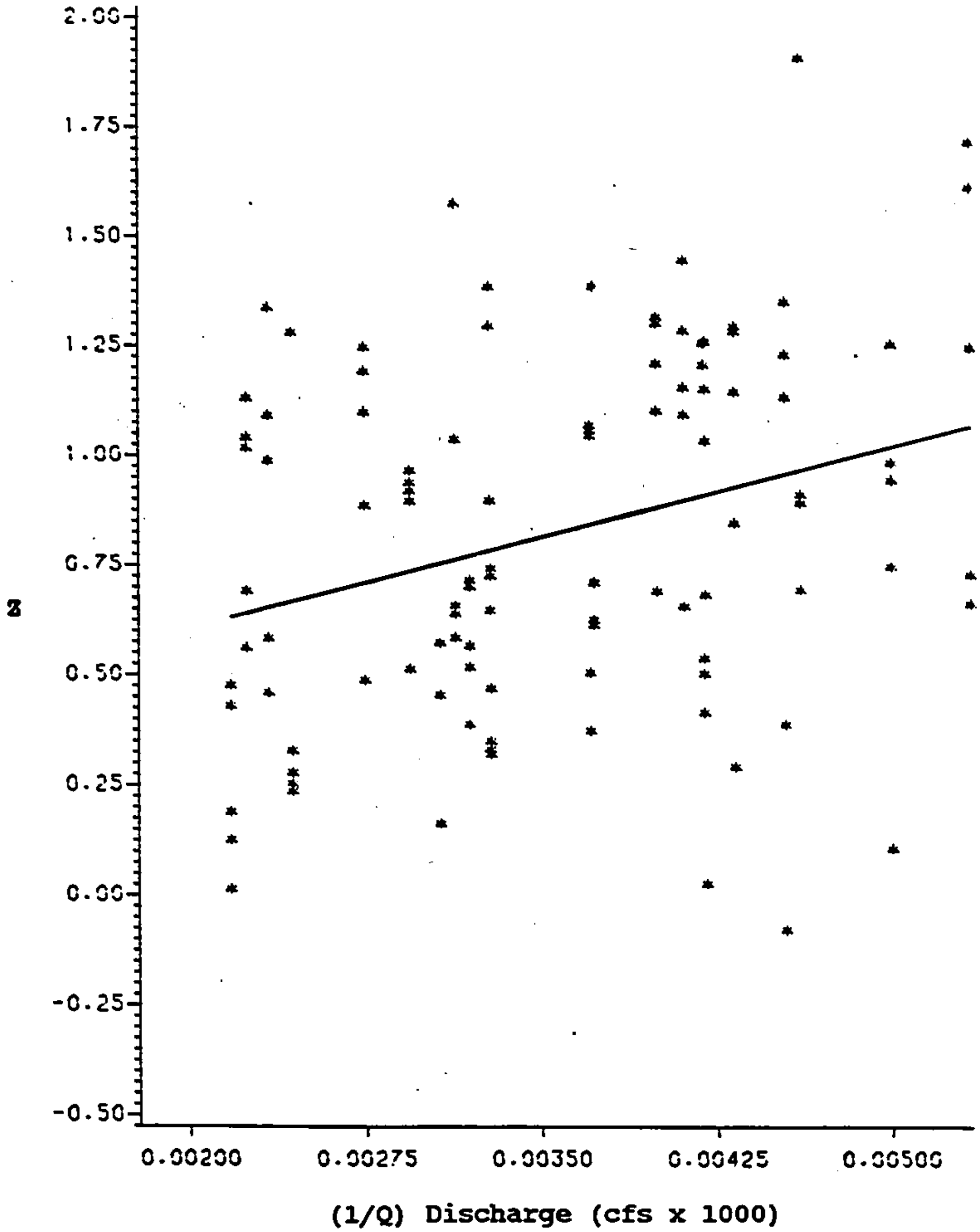

Figure 7.25: Regression of Rouse Number versus 1/Q for $.250 < d < 0.500$

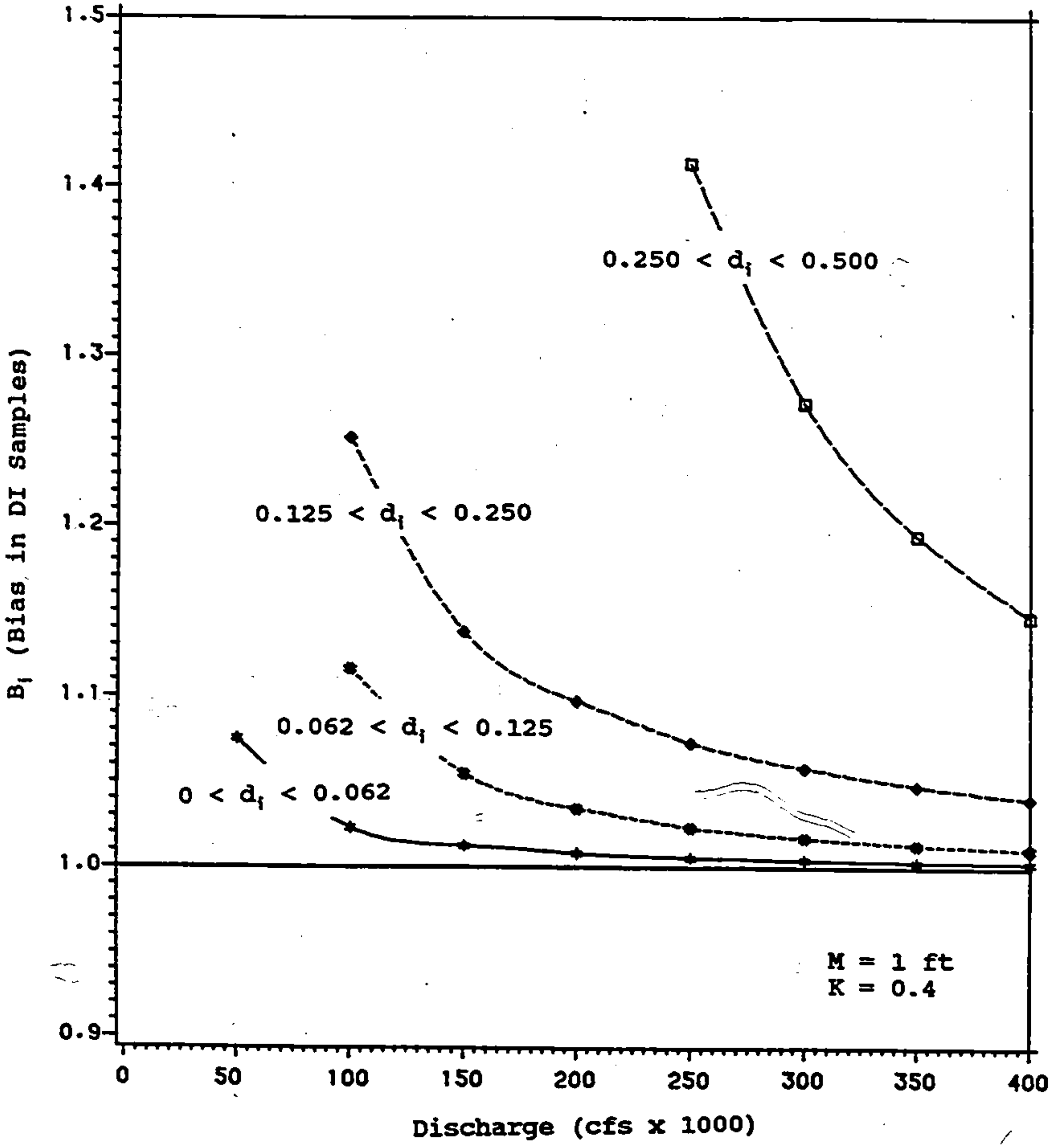

Figure 7.26: Correction Coefficient to DI Measurements versus Discharge

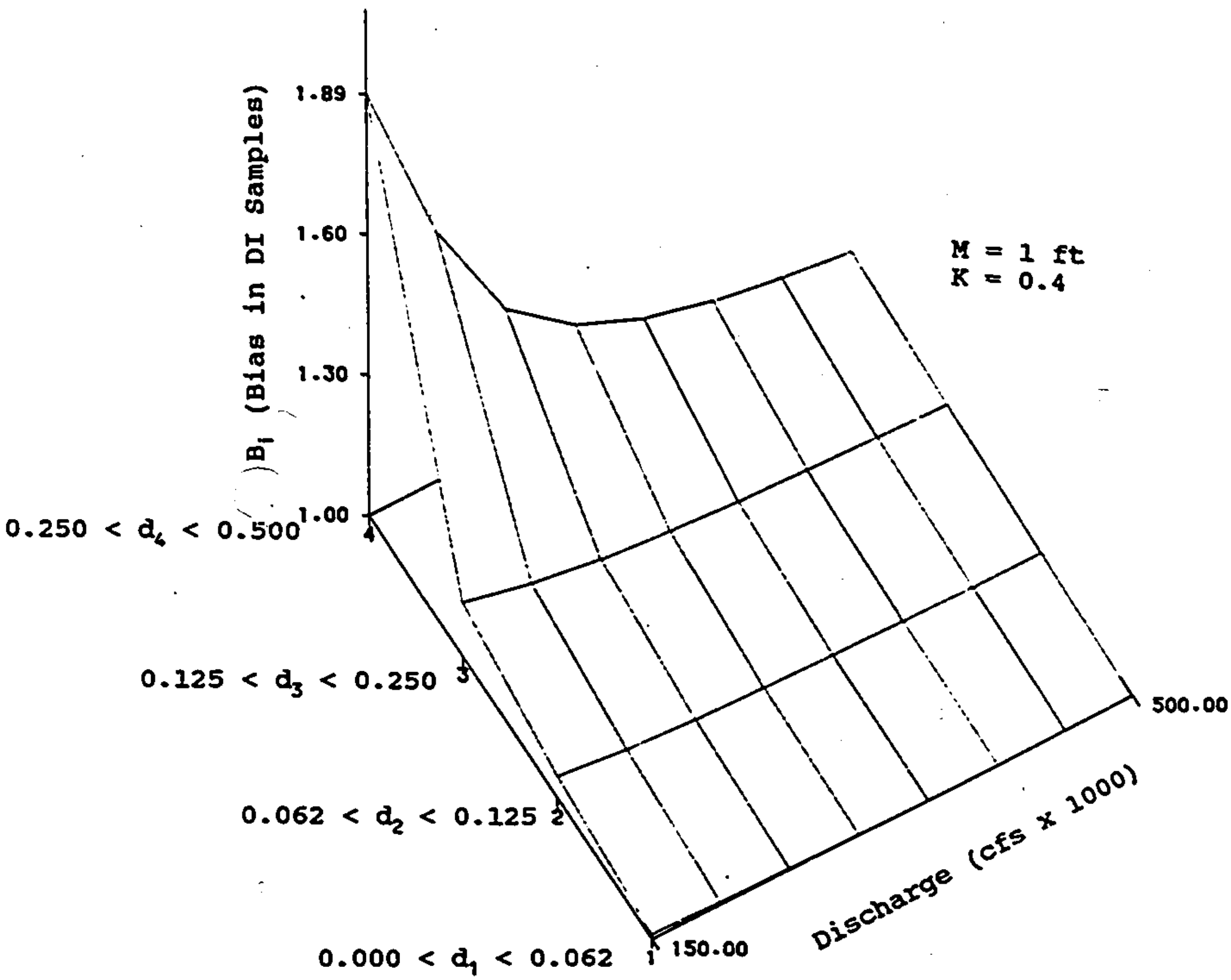

Figure 7.27: Correction Coefficient to DI Measurements versus Discharge and Grain Fraction

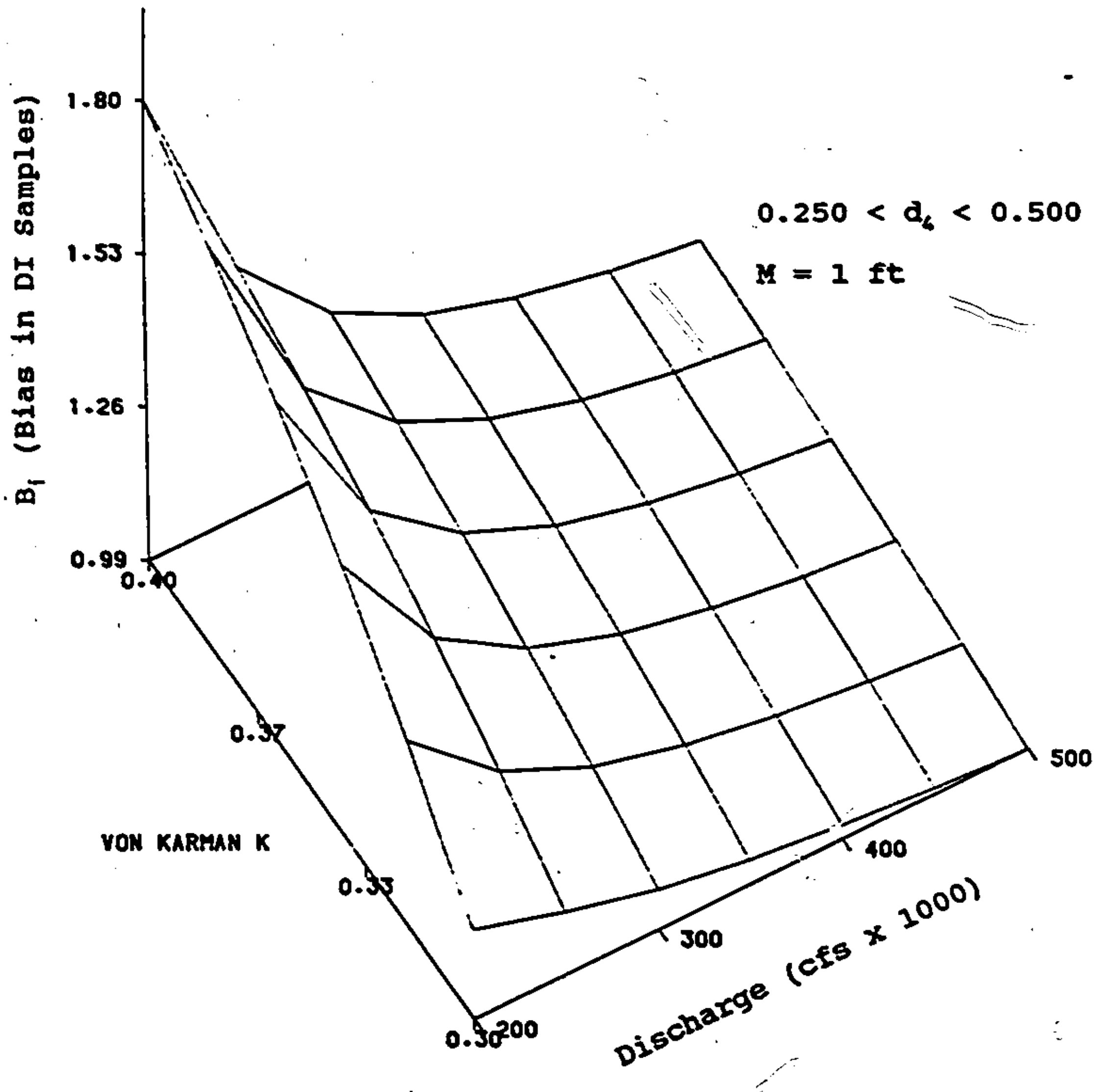

Figure 7.28: Correction Coefficient for to DI Measurements versus Discharge and von Karman

Table 7.1: Estimation of von Karman's K at Mission

	Vertical 300	*Vertical* 300	*Vertical* 300	*Vertical* 300	*Vertical* 300
Y_0 (ft)	42.5	43	40.7	41.5	41.6
$\bar{u}$ (ft/s)	3.95	4.75	4.66	4.78	4.67
u_* (ft/s)	0.216	0.260	0.257	0.263	0.267
Intercept (ft/s)	1.50	3.23	2.75	2.83	3.10
Slope = $\frac{u_*}{K}$ (ft/s)	0.885	0.584	0.745	0.750	0.750
K	0.24	0.44	0.35	0.35	0.45

Table 7.2: Regressions of Ξ_i versus $1/Q$ (Q in 1000 cfs)

	Grain Fraction	Intercept	Slope	Correlation Coefficient	Error on Intercept
Mission City	$0.000 < d < 0.062$	-0.003	19.65	0.64	
All Verticals	$0.062 < d < 0.125$	0.046	45.71	0.38	
No. of data	$0.125 < d < 0.250$	0.27	43.30	0.41	
= 101	$0.250 < d < 0.500$	0.33	138.9	0.48	
Mission City	$0.000 < d < 0.062$	-0.002	15.66	0.77	0.38
Vertical 900	$0.062 < d < 0.125$	-0.30	62.79	0.29	0.075
No. of data	$0.125 < d < 0.250$	0.16	72.17	0.39	0.10
= 20	$0.250 < d < 0.500$	0.11	186.7	0.43	0.35
Port Mann	$0.000 < d < 0.062$	0.004	7.80	0.81	
Vertical 700	$0.062 < d < 0.125$	0.018	27.88	0.40	
No. of data	$0.125 < d < 0.250$	0.18	37.17	0.28	
= 16	$0.250 < d < 0.500$	0.62	31.0	0.60	

Chapter 8

Modelling Mixed Sediment Suspended Load Profiles

8.1 Preamble

At present, ONE-D-SED calculates the sediment transport rate based on total load formulae. When employing such equations, a representative grain size must be used. In chapter 6, it was noted that the representative size d_r is a function of several parameters including the extent of the grain size distribution. It was indicated that both the Ackers and White and Day findings indicated that representing the sediment grain size for natural rivers needed further examination.

It was postulated that the choice of the representative grain size d_r could be related to the representative fall velocity W_r of the suspended sediment since for sand-bed streams, virtually all sediment load moves within the water column. A mathematical analysis was therefore performed to determine d_r of a suspended load consisting of a range of grain sizes. This is the subject of this chapter and, as will be shown, the results not only will provide a mathematical basis for the choice of d_r, but also will provide required information should ONE-D-SED be up-graded to include the modelling of the sediment load by grain-size class and/or for modelling the suspended load (including the wash load) separately from the bed load.

The vertical suspended sediment concentration profile in a river flow is often described by a diffusion-dispersion model. Such models are normally formulated on the basis that the material is of uniform size. However river sediments are invariably mixtures of different-sized grains. The usual approach is to divide the entire grain size distribution into an appropriate number of size ranges, or "fractions", and then characterize the latter by their respective geometric mean sizes d_g.

This chapter examines, based on an assumed log-normal distribution of grain sizes, the possible errors in calculated suspended sediment concentrations arising from the choice of d_r or the representative grain size for sediment mixtures in the application of diffusion-dispersion models. Under certain conditions errors are found to be significant and a correction factor is proposed to account for the resulting discrepancies.

8.2 Theory

In some diffusion-dispersion models, the sediment transfer coefficient E_{s2} is assumed to be constant over part of the water column (Kerssens et al. 1979), while in others E_{s2} is assumed to vary throughout the whole depth. Its value can be based on a stochastic analysis (Bechteler and Farber 1985), although most models assume a direct relationship between the sediment transfer and momentum transfer coefficients as follows:

$$E_{s2} = BE \tag{8.1}$$

in which E is the momentum transfer coefficient and B is a coefficient of proportionality reflecting the difference between the diffusion of sediment particles and that of momentum (Itakura and Kishi 1980; Kerssens et al. 1979; Laursen 1980; McTigue 1981 and Rouse 1937).

Assuming equation 8.1 applies and that the velocity in the channel is logarithmically distributed and is steady and uniform, for moderate concentrations the sediment concentration profile in the water column is given by:

$$\frac{C(y,d)}{C_a(d)} = y_*^{z(d)}. \tag{8.2}$$

Based on pseudo-theoretical analyses, Rouse (1937) and Laursen (1980) give the following expressions for y_* respectively:

$$y_{*R} = \left(\frac{1-y}{1-a}\right)\frac{a}{y} \tag{8.3}$$

$$y_{*L} = \frac{a}{y} \tag{8.4}$$

Although the form of the y_*-expression is not the most critical component of the model (Jobson and Sayre 1970), the choice of expression does influence the computed concentration to a certain extent. It should be noted that the Laursen version not only is simpler, but also it better reflects the findings of many researchers (Coleman 1970; Kerssens et al. 1979; Laursen 1980), namely that the suspended sediment is more uniformly mixed in the upper region of the water column.

What is usually considered critical however is the estimate of the Rouse number Ξ which for a particular grain size can be expressed thus:

$$\Xi(d) = \frac{W(d)}{\phi B U_* K} \tag{8.5}$$

where ϕ (y) is a function which has been introduced to account for the generally assumed damping of fluid turbulence by higher concentrations in the "near-bed" zone (van Rijn 1984).

Estimating Ξ can be difficult. Not only has K to be estimated but also B and ϕ. The estimates are uncertain for a number of reasons, including: the stochastic nature of turbulence (Petkovic and Bouvard 1985), the influence of bedforms on local velocities and sediment concentrations (Ikeda and Takashi 1983), the effect of turbulence and the proximity of other grains on the value of the grain fall velocity (Graf 1971), the interference of one size on another (Samaga et al. 1986), the effect of secondary currents which promote transverse mixing, and the fact that no direct comparison can be made between the constants of proportionality of one diffusion-dispersion model and those of another (Karim and Kennedy 1987). Therefore, although equation 8.5 is used in this work, its limitations are recognized. Although at high concentrations $\phi(y) < 1.0$ (van Rijn 1984). in the analysis that follows. for the sake of convenience. ϕ was assumed equal to unity for all values of y . Also the product BK was taken as 0.4. but this assumption was made only for the purposes of presentation and does not represent any loss of generality in the results presented.

As noted in the previous section, in practice the relevant grain size distribution is divided into fractions and equations 8.2 and 8.5 are then applied to these in turn. (The number of fractions employed in any given situation is to a large extent dependent on the degree of accuracy required and what level of analysis is feasible). A fraction can be characterized by its "band width" I_{1-2} $(= d_2/d_1)$ and by its geometric mean size d_g $(= \sqrt{d_1 d_2})$, where d_2 and d_1 are the fraction's upper and lower bounds respectively.

Normally, for each fraction, the representative fall velocity W_r is assumed approximately equal to that for d_g , i.e.

$$W_r \simeq W_g \tag{8.6}$$

Since this assumption is not necessarily valid (van Rijn 1984) it would be more correct to write

$$W_r = \frac{W_g}{\gamma} \tag{8.7}$$

where γ is a fall velocity coefficient introduced to account for any discrepancy between the representative fall velocity and that for the geometric mean size. Although engineers are generally aware of the over-simplification contained in equation 8.6, little effort has been directed towards quantifying numerical (computational) errors that result from its use. The present study addresses this particular issue by examining the relationship between W_r and W_g. It was found that in some cases the simplification represented by equation 8.6 is quite justified while in others the value of γ departs substantially from unity.

The study's main goal was to determine the order of errors that may be introduced in the analysis as a result of applying equation 8.6 and hence provide a framework for selecting a suitable number of grain size fractions in a given situation. The study also quantified the behaviour of γ with respect to certain parameters that assist in the selection of an appropriate W_r to be used in evaluating Ξ for a given grain fraction.

8.3 Analysis

8.3.1 Fall Velocity Coefficient γ

In the analysis that follows it was assumed that the sieved grain size distribution at the reference level was log-normally distributed, i.e.

$$C_a(d) = \frac{C_0 e^{-\frac{\zeta^2}{2}}}{d\sqrt{2\pi}\ln\sigma_g} \tag{8.8}$$

where ζ is the normal variate ($= \ln\frac{d}{d_{50}}/\ln\sigma_g$), σ_g is the geometric standard deviation of the distribution ($= d_{84}/d_{50}$). d_{50} and d_{84} are the grain sizes for which 50 % and 84 % by weight respectively of the sediment is finer and C_0 is some arbitrary concentration. Substituting the value for $C_a(d)$ in equation 8.2 and numerically integrating from d_1 to d_2 yields the exact value of the local concentration $C_{1-2}(y)$ for that sediment fraction:

$$C_{1-2}(y) = \int_{d_1}^{d_2} y_*^{\frac{W(d)}{\phi BU_* K}} \frac{C_0}{d\sqrt{2\pi}\ln\sigma_g} e^{-\frac{\zeta^2}{2}} dd \tag{8.9}$$

If, however, the correct representative fall velocity ($W_r = W_g/\gamma$) was chosen for the fraction, $C_{1-2}(y)$ could be obtained more simply by

$$C_{1-2}(y) = y_*^{\frac{W_g}{\gamma(y)\phi BU_* K}} \cdot C_0 \cdot F_{1-2} \tag{8.10}$$

where F_{1-2} is the area under the normal distribution curve between $\zeta(d_1)$ and $\zeta(d_2)$.

Equations 8.9 and 8.10 are equivalent and hence a solution for $\gamma\ (y_*)$ is obtained directly:

$$\gamma(y_*) = \frac{W_g}{\phi BU_* K} \frac{\ln y_*}{\ln \int_{d_1}^{d_2} y_*^{\frac{W(d)}{\phi BU_* K}} \cdot d^{-1} \cdot e^{-\frac{\zeta^2}{2}} \cdot dd - \ln(F_{1-2}\sqrt{2\pi}\ln\sigma_g)} \tag{8.11}$$

Various equations are available to estimate W as a function of d. In this analysis a shape factor of 0.7 was assumed for those grains larger than 0.026 mm and a standard settling diameter was obtained (Vanoni 1975). The drag coefficient C_d associated with fully turbulent settling was equated to 0.4; for settling that was not fully in the turbulent region, $W(d)$ was evaluated based on Schiller's equation

(Schiller and Naumann 1933): $C_d = \frac{24}{R_e}(1 + 0.15 R_e^{0.687})$, where R_e is the grain Reynolds Number. Based on these values of C_d, a relationship was established according to Yalin's recommendation between two dimensionless parameters and hence the fall velocity was obtained without the usual "trial and error" approach (Yalin 1972). It should be noted that when the distribution of the grain sizes is log-normal, the corresponding distribution of the fall velocities generally deviates somewhat from the log-normal one (Kennedy and Koh 1964).

Referring to equation 8.11, it can be shown that

$$\gamma(y_*) = f(I_{1-2}, \frac{W_g}{U_*}, d_g, \zeta_{d_g}, \sigma_g) \tag{8.12}$$

in which $\frac{W_g}{U_*}$ is called the "dimensionless fall velocity" and ζ_{d_g} is ζ evaluated at $d = d_g$. Equation 8.12 is a function of several dimensionless variables and the dimensional variable d_g (mm). Since it is not feasible to display such a function directly, a parametric study was performed holding four variables constant and plotting γ as a function of y_* for different values of the fifth variable. For example, in figure 8.1, γ is shown as a function of y_* for various values of the grain fraction width (I_{1-2}). The other four variables were held constant at $\frac{W_g}{U_*} = 0.3$, $d_g = 0.05$ mm, $\zeta_{d_g} = 0.0$ (i.e. $d_g = d_{50}$) and $\sigma_g = 2$. For $I_{1-2} = 1.5$, γ (y_*) is fairly close to unity. It varies from 0.98 at $y_* = 1$ (i.e. y = a) to 1.07 at $y_* = 0.01$ (i.e. y = 0.5 according to equation 8.3, or y = 1 according to equation 8.4). Hence there is a trend that as y increases, so does γ and it is noted that the trend is more pronounced at larger values of I_{1-2}.

There is some support in the literature for this trend of γ (y_*) in that, when equation 8.6 is used to characterize the Rouse number for a grain fraction, measurements have shown that the diffusion-dispersion equation in its original form (i.e. equation 8.2 in conjunction with equations 8.1 and 8.3) under-predicts the actual concentration in the water column (Antsyferov and Kos'yan 1980; Coleman 1970; Kerssens et al. 1979; Laursen 1980). Therefore, in order to overcome this deficiency van Rijn (1984), for example, increased the value of ε_s in the upper half of the water column and introduced ϕ (y) in the lower regions of the flow. Though these modifications may have a psuedo-theoretical basis (Karim and Kennedy 1987), it is noted that introducing γ (y) would have the same effect and hence may partially explain some of the measured values.

In figure 8.2, I_{1-2} is held constant at 2.0, and γ is plotted against y_* for different values of the dimensionless fall velocity $\frac{W_g}{U_*}$. For low values of $\frac{W_g}{U_*}$ the suspended sediment concentration profile is flat and hence there is little variability in γ (y_*). However, as $\frac{W_g}{U_*}$ increases (and hence the concentration gradient increases), γ (y_*) shows a marked departure from unity. This result is also confirmed by others. Though Samaga et al (1986) used a different approach, their analysis of measured concentrations confirm the increased variability of γ (y_*) as $\frac{W_g}{U_*}$ increases. Clearly therefore there are conditions under which the assumption that $\gamma = 1$ is appropriate and others where this assumption will lead to biases in the predicted concentration.

In figure 8.3, $\frac{W_g}{U_*}$ is again held constant at 0.3 and the absolute value of d_g is varied. In this case $\gamma(y_*)$ is more sensitive at lower values of d_g. This is explained by the fact that for small grains, $W(d) \propto d^2$, whereas for larger grain sizes, $W(d) \propto \sqrt{d}$.

However this result should not be confused with the former, since in this case the dimensionless fall velocity is held constant and therefore the concentration gradient of the mean grain size does not depend on the absolute size of d_g .

Finally, in figure 8.4 the effect of ζ_{d_g} on γ (y_*) is shown. Since $C_a(d)$ is log-normal, the distribution of $C_a(d)$ with respect to d is quite skewed. Hence the location of d_g in relation to d_{50} can alter the value of γ (y_*) in a fairly significant way. This result suggests that should a constant value for $\gamma(y_*)$ be employed for all fractions, a bias will still be present in the computed concentrations. It might also be noted that for grain fractions that are coarser than the mean size of the distribution (i.e. $\zeta_{d_g} = 1$ and 2), the corresponding fall velocity coefficient is always greater than 1.0 for $y > a$.

The parametric study showing the effect of σ_g on γ (y_*) is not included here since it was found that γ (y_*) increased only very marginally as σ_g increased, while holding the other four parameters constant. Therefore the effect of the standard deviation of the distribution σ_g is only indirectly (or implicitly) important in that, as σ_g increases so does the required number of fractions (to maintain an equivalent fraction width) and so does the spread in the values of ζ_{d_g} over the range of fractions in the distribution.

8.3.2 Depth-Averaged Fall Velocity Coefficient $\bar{\gamma}$

In the preceding section it was shown that γ is a function of the local depth. However, when estimating average sediment concentrations in the flow, it would be preferable to express $\gamma\ (y_*)$ as a depth-averaged value ($\bar{\gamma}$). Consider the load q_{s1-2} (corresponding to grain fraction I_{1-2}), moving in suspension between depths $y = a$ and $y = 1$. The load is obtained by integrating the product of the local concentration for this fraction $C_{1-2}\ (y)$ and local velocity $u\ (y)$ between these depth limits. For the purpose of analysis, a logarithmic velocity distribution throughout the water column (with a mean velocity $\bar{u}$) was assumed. Therefore, within the limits specified, the suspended load is given by:

$$q_{s1-2} = \int_a^1 C_{a1-2} \cdot y_*^{\frac{W_g}{\gamma(y_*)\,\phi\beta U_* K}} \cdot \left(\frac{U_*}{K} \ln y + \frac{U_*}{K} + \bar{u}\right) dy \qquad (8.13)$$

Once q_{s1-2} is determined, γ (which is a function of y_*) can be replaced by $\bar{\gamma}$ using a trial and error procedure. In the analysis it was found that convergence to an accurate value was quite quick (2 or 3 iterations) using the Newton-Raphson technique.

For the analysis of the variability of $\bar{\gamma}$, d_g was set equal to d_{50} (i.e. $\zeta_{d_g} = 0$) and I_{1-2} was equated to $(n\sigma_g)^2$, where $n = 1, 2, 3$ etc. Hence the values obtained for $\bar{\gamma}$ are representative of the grain sizes contained within n standard deviations of d_{50}. Therefore, referring to equations 8.7, 8.11 and 8.13 and given these additional restrictions:

$$\bar{\gamma} = f(\sigma_g, n, \frac{W_g}{U_*}, d_{50}, a, \frac{\bar{u}}{U_*}) \qquad (8.14)$$

Included in this functional relationship is a hidden parameter in the choice of the

y_*-expression . In the analysis, both Rouse's and Laursen's expressions were used (equations 8.3 and 8.4 respectively). In the former case, the upper limit of integration of equation 8.13 was taken as 0.99, since y_* is infinite at $y = 1.0$

Once again the results are presented in the form of a parametric study. In this case $\bar{\gamma}$ is the ordinate and $\frac{W_g}{U_*}$ the abscissa. Figure 8.5 is representative of the results obtained. Here Laursen's expression was used for y_*, a was set equal to 0.1, d_{50} had a value of 0.05 mm, while σ_g took on typical field values (1.5, 2 and 4). Normally $\frac{\bar{u}}{U_*}$ can have a value between 10 and 30, however since $\bar{\gamma}$ was essentially insensitive to $\frac{\bar{u}}{U_*}$ for $\frac{\bar{u}}{U_*} > 20$, $\frac{\bar{u}}{U_*}$ was set equal to 20 throughout. Also a sensitivity analysis was performed with regard to the value of n. Though results could significantly differ in the range $1 \leq n \leq 2$, they were essentially the same for $n = 2$ and 3. The analysis chosen for presentation was n equal to 2, as this accounts for 95 % of the grain sizes in the distribution. The results presented are particularly appropriate when computations are based on the total concentration at a reference level without separating the grain distribution into fractions.

Referring to figures 8.5 and 8.1 respectively, there is a parallel between the functional relationships for $\bar{\gamma}$ versus $\frac{W_g}{U_*}$ and γ versus y_* . For low values of $\frac{W_g}{U_*}$, $\bar{\gamma}$ is small and increases as $\frac{W_g}{U_*}$ increases; this is also the general trend for γ (y_*). More significant however is the parallel between $\bar{\gamma}$ ($\frac{W_g}{U_*}$) and the reported behaviour of β ($\frac{W_g}{U_*}$). For small values of $\frac{W_g}{U_*}$, β has sometimes been found to be less than or close to unity whereas at large values, many researchers have found β to be greater than unity and that β increases as a function of $\frac{W_g}{U_*}$ (Ghosh 1986; Graf 1971 and van Rijn 1984). An example of this finding is the expression reported by van Rijn

(1984), namely $B = 1 + 2(\frac{W_g}{U_*})^2$ for $0.1 < \frac{W_g}{U_*} < 1.0$. This is not to suggest that B is equivalent to γ. On the contrary, B is a 'physical' parameter (equation 8.1) while $\bar{\gamma}$ represents a correction to the Rouse exponent based on a computational simplification (equation 8.7). Nevertheless, because B may have been mistaken for γ in past studies, for the sake of comparison, van Rijn's relationship is included in figures 8.5 through 8.8.

The variability of $\bar{\gamma}$ $(\frac{W_g}{U_*})$ increases significantly as σ_g (and therefore I_{1-2}) increases. This result lends limited support to the current practice of using d_{50} as an input variable in the calculations for total sediment load in a laboratory context (where σ_g is small) but employing d_{35} when the same formulae are applied to natural rivers (where σ_g is normally substantially larger). Of course $\bar{\gamma}$ can be easily transformed into a characteristic grain size d_x to be used in lieu of d_{50}. This calculation, however, is not presented here because d_x would be as variable as $\bar{\gamma}$ $(\frac{W_g}{U_*})$ and hence no unique characteristic grain size would result. Therefore the use of d_{35} as the representative size for a particular distribution can be only partially endorsed.

In figure 8.6, σ_g is held constant at 4 while d_{50} takes on different values. Once again, due to the sensitivity of W with respect to d in this range, $\bar{\gamma}$ $(\frac{W_g}{U_*})$ is more sensitive at lower values of d_{50}.

It is also important to note that the choice of a significantly affects the computed value of $\bar{\gamma}$ (figure 8.7). At this time, there is no consensus as to the value of a. Ideally, a should be small so that the transport of sediment between the bed and a can be considered "bed load" and hence only a function of local conditions. Though a is often assumed to be proportional to the roughness element (eg. d_{90} or dune height), this analysis is further evidence (see also van Rijn 1984) that, for the sake of consistency, low values of a should be used with caution.

As evidenced in figures 8.5 and 8.8, when Rouse's rather than Laursen's formulation for y_* is used, there is more variability in $\bar{\gamma}$. This results from the fact that, when equation 8.13 is applied using Rouse's formulation, there is a greater range in y_* and therefore $\gamma(y_*)$, and this produces a greater variability in $\bar{\gamma}(\frac{W_g}{U_*})$. Table 8.1 summarizes the value of $\bar{\gamma}$ for $n = 2$ and $\frac{u}{U_*} = 20$ as a function of $\frac{W_g}{U_*}$, $d_g = d_{50}$, σ_g and a for y_{*R} and y_{*L}. The errors resulting in the calculated depth-averaged concentration, based on the assumption that $\bar{\gamma}$ is unity, are also presented. The error is presented as a ratio of the exact value of C (based on the actual value of $\bar{\gamma}$) to the assumed mean concentration $\bar{C}_1$ (based on a value of $\bar{\gamma} = 1.0$). For small values of the relative fall velocity ($\frac{W_g}{U_*} \simeq 0.05$), $\bar{C}$ is less than C_1 by a factor as low as 0.84, whereas for large values of $\frac{W_g}{U_*}$ (i.e. $0.3 \leq \frac{W_g}{U_*} \leq 0.6$), C_1 is less than $\bar{C}$ by a factor of up to 15. Accordingly errors in calculation become significant when the concentration gradient in the vertical is large, which is normally the case for flows involving 'large grain' sediment transport and/or small mean flow velocities.

Finally it was reported earlier that choosing Rouse's rather than Laursen's expression for y_* resulted in a greater variability in $\bar{\gamma}(\frac{W_g}{U_*})$. The resulting error in $\bar{C}$ however, may in some cases be less than that obtained when using Laursen's expression. This is because the greater variability in $\bar{\gamma}(\frac{W_g}{U_*})$ is counter-balanced by Rouse's under-prediction of the concentration in the upper region of the water

Table 8.1: Value of $\bar{\gamma}$ and Error in the Average Concentration $\bar{C}$ when $\bar{\gamma}$ is assumed equal to 1.0

$\frac{u}{U_*}=20,\ d_g=d_{50}$; $y_{*R}=\frac{1-y}{1-a}\cdot\frac{a}{y}$; $y_{*L}=\frac{a}{y}$			Depth-averaged fall velocity coefficient: $\bar{\gamma}$				Factor for under-estimation of $\bar{C}$: $\bar{C}/\bar{C}_1$			
			$a=0.01$		$a=0.1$		$a=0.01$		$a=0.1$	
$\frac{W_g}{U_*}$	$d_{g(mm)}$	σ_g	y_{*R}	y_{*L}	y_{*R}	y_{*L}	y_{*R}	y_{*L}	y_{*R}	y_{*L}
0.05	0.05	2	0.904	0.840	0.782	0.701	0.94	0.92	0.93	0.92
0.05	0.05	4	0.866	0.766	0.653	0.528	0.92	0.87	0.85	0.84
0.05	0.5	2	1.000	0.980	0.968	0.945	1.00	0.99	0.99	0.99
0.05	0.5	4	0.995	0.949	0.917	0.864	1.00	0.98	0.97	0.97
0.05	1.0	4	1.003	0.970	0.948	0.911	1.00	0.99	0.98	0.98
0.1	0.05	2	1.142	1.051	0.935	0.814	1.14	1.04	0.96	0.92
0.1	0.05	4	1.268	1.117	0.905	0.715	1.25	1.10	0.94	0.86
0.1	0.5	2	1.075	1.043	1.013	0.974	1.07	1.04	1.01	0.99
0.1	0.5	4	1.178	1.101	1.025	0.934	1.17	1.09	1.01	0.97
0.1	1.0	4	1.133	1.078	1.025	0.960	1.13	1.07	1.01	0.98
0.3	0.05	2	1.786	1.652	1.336	1.152	2.97	2.55	1.35	1.14
0.3	0.05	4	2.435	2.157	1.616	1.279	4.57	3.67	1.60	1.25
0.3	0.5	2	1.304	1.261	1.143	1.080	1.72	1.61	1.15	1.08
0.3	0.5	4	1.760	1.628	1.357	1.189	2.90	2.50	1.37	1.17
0.3	1.0	2	1.204	1.178	1.097	1.055	1.47	1.41	1.11	1.05
0.3	1.0	4	1.543	1.457	1.258	1.141	2.34	2.09	1.27	1.13
0.3	2.0	2	1.148	1.131	1.073	1.044	1.34	1.30	1.08	1.04
0.3	2.0	4	1.399	1.342	1.197	1.115	1.96	1.81	1.21	1.11
0.6	0.05	2	2.410	2.272	1.700	1.505	7.16	7.61	1.97	1.74
0.6	0.05	4	3.710	3.324	2.362	1.906	15.27	14.93	2.83	2.26
0.6	0.5	2	1.512	1.496	1.256	1.205	2.57	2.88	1.35	1.30
0.6	0.5	4	2.387	2.239	1.698	1.503	7.02	7.39	1.96	1.73
0.6	1.0	2	1.326	1.328	1.167	1.139	1.89	2.11	1.23	1.21
0.6	1.0	4	1.951	1.879	1.481	1.364	4.59	5.03	1.66	1.54
0.6	2.0	2	1.229	1.234	1.120	1.103	1.59	1.74	1.16	1.15
0.6	2.0	4	1.666	1.637	1.345	1.274	3.22	3.61	1.47	1.40

column.

8.4 Discussion

In the case of channel flows with mixed sediment suspended loads, when estimating local suspended sediment concentrations the representative fall velocity W_r for a grain fraction can be substantially different from that for the fraction's geometric mean size W_g. As the depth y, the fraction width (I_{1-2}), the dimensionless fall velocity $(\frac{W_g}{U_*})$, the relative coarseness of the grain fraction within the sediment mixture ζ_{d_g} and the standard deviation of the distribution σ_g increase, so does the ratio $\frac{W_g}{W_r}$ $(= \gamma)$. Therefore, when a standard diffusion-dispersion model is being applied the analysis should incorporate γ for greater accuracy.

The behaviour of $\bar{\gamma}$ should be considered where calculations using depth-averaged concentrations are performed. In this study $\bar{\gamma}$ is shown to increase in value as a function of the relative fall velocity $\frac{W_g}{U_*}$ and the geometric standard deviation σ_g. Also, $\bar{\gamma}$ shows a greater sensitivity to these parameters when d_{50} and the lower limit of integration (a) decrease in value. Hence if W_r is assumed to be equal to W_g, an error is introduced in the estimation of the depth-averaged concentration of the suspended load $\bar{C}$. As evidenced in table 8.1, the error in depth-averaged concentration $\bar{C}$ is significant for the combination of smaller d_{50} and relatively lower transport rates (values of $\frac{W_{50}}{U_*} > 0.3$). For higher transport rates (values of $\frac{W_{50}}{U_*}$ < 0.2), the error in depth-averaged concentration is normally negligible (ie. the under-estimation factor is generally within 10% of unity). On the other hand, for low transport rates the value of C can be under-estimated by a factor as large as 15.

This implies that the recommended representative grain size may vary as a function of hydraulic conditions when using total-load formulae. This would be particularly true if the application involved modelling a natural river in which a significant portion of the load moves in the near-bed zone. In this case, the value of $\frac{W_s}{U_*}$ is high and hence a larger bias may otherwise be introduced if the total load formula was developed in a laboratory context. On the other hand, if the mobile-bed model simulates the suspended load separately and/or models grain-size classes, the calculated value of $\bar{\gamma}$ documented as a function of hydraulic conditions may be used. In chapter 7 it was shown that, on the surface, $\Xi_{i/j}$ is independent of hydraulic conditions. However, the scatter in measured values indicated that there may be some dependency of hydraulic conditions. The findings of this chapter have confirmed and quantified that effect.

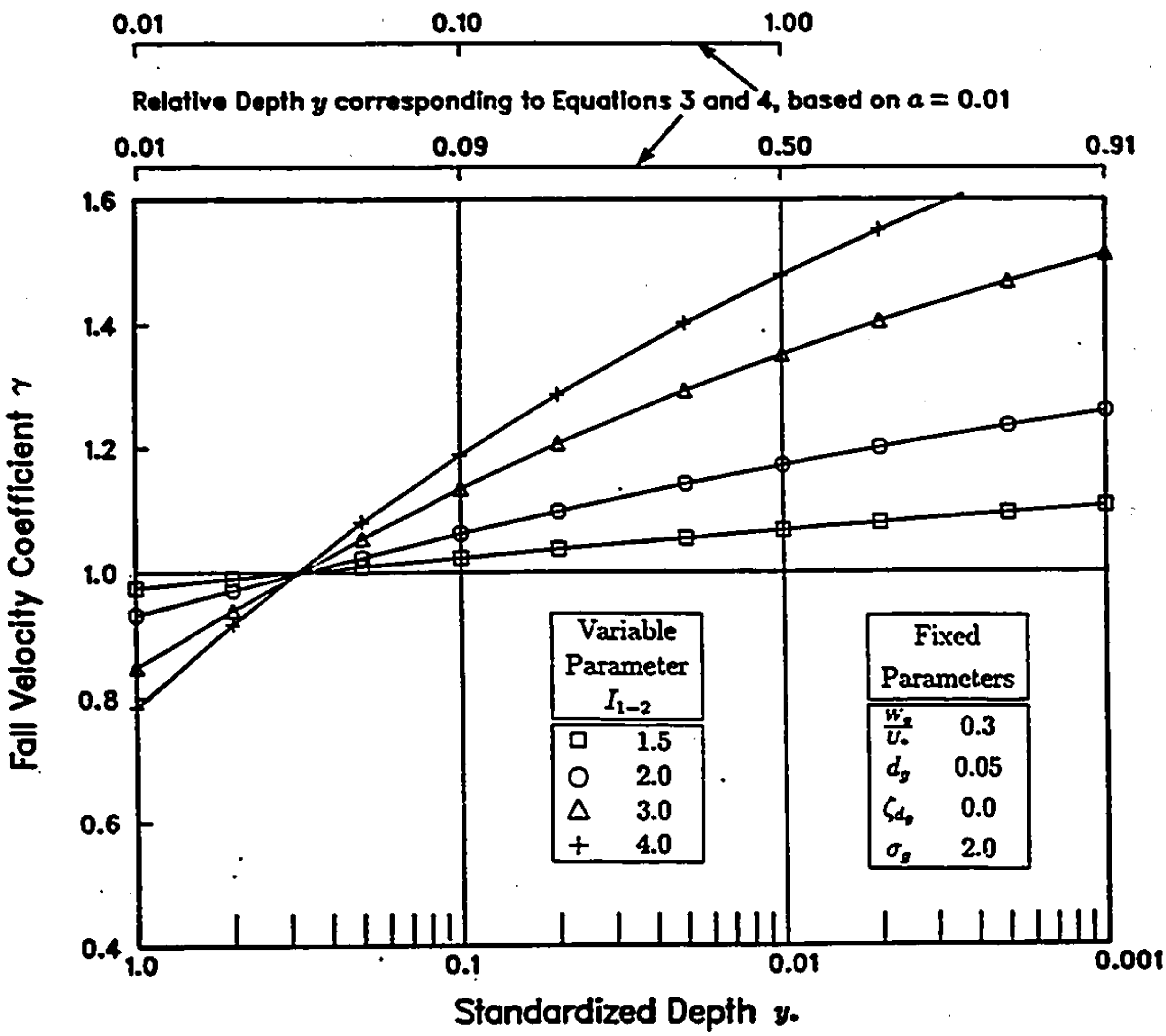

Figure 8.1: Fall Velocity γ versus Standardized Depth y_*; with Variable Parameter I_{1-2}

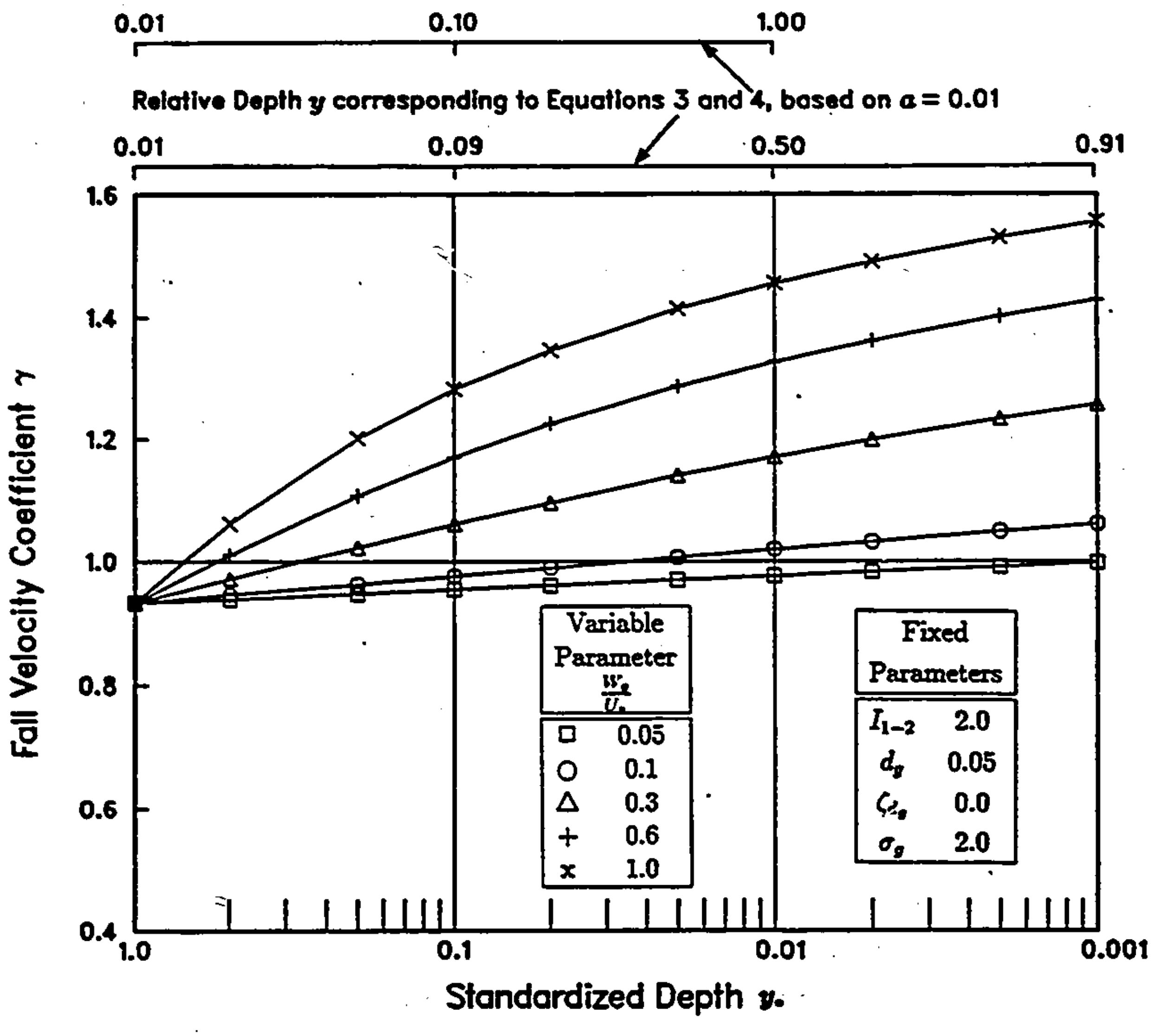

Figure S.2: Fall Velocity γ versus Standardized Depth y_*; with Variable Parameter $\frac{W_g}{U_*}$

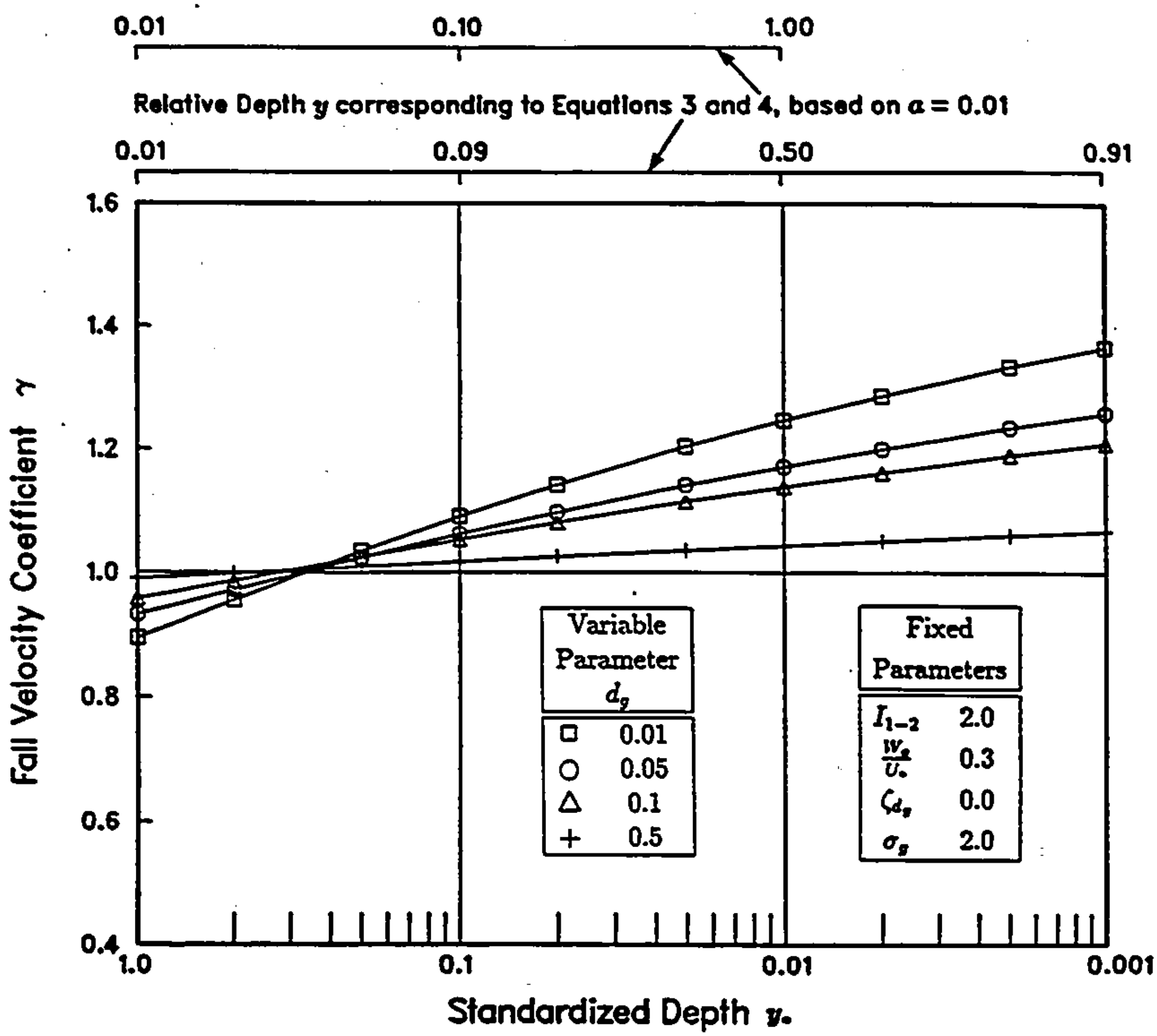

Figure 8.3: Fall Velocity γ versus Standardized Depth y_*; with Variable Parameter d_g

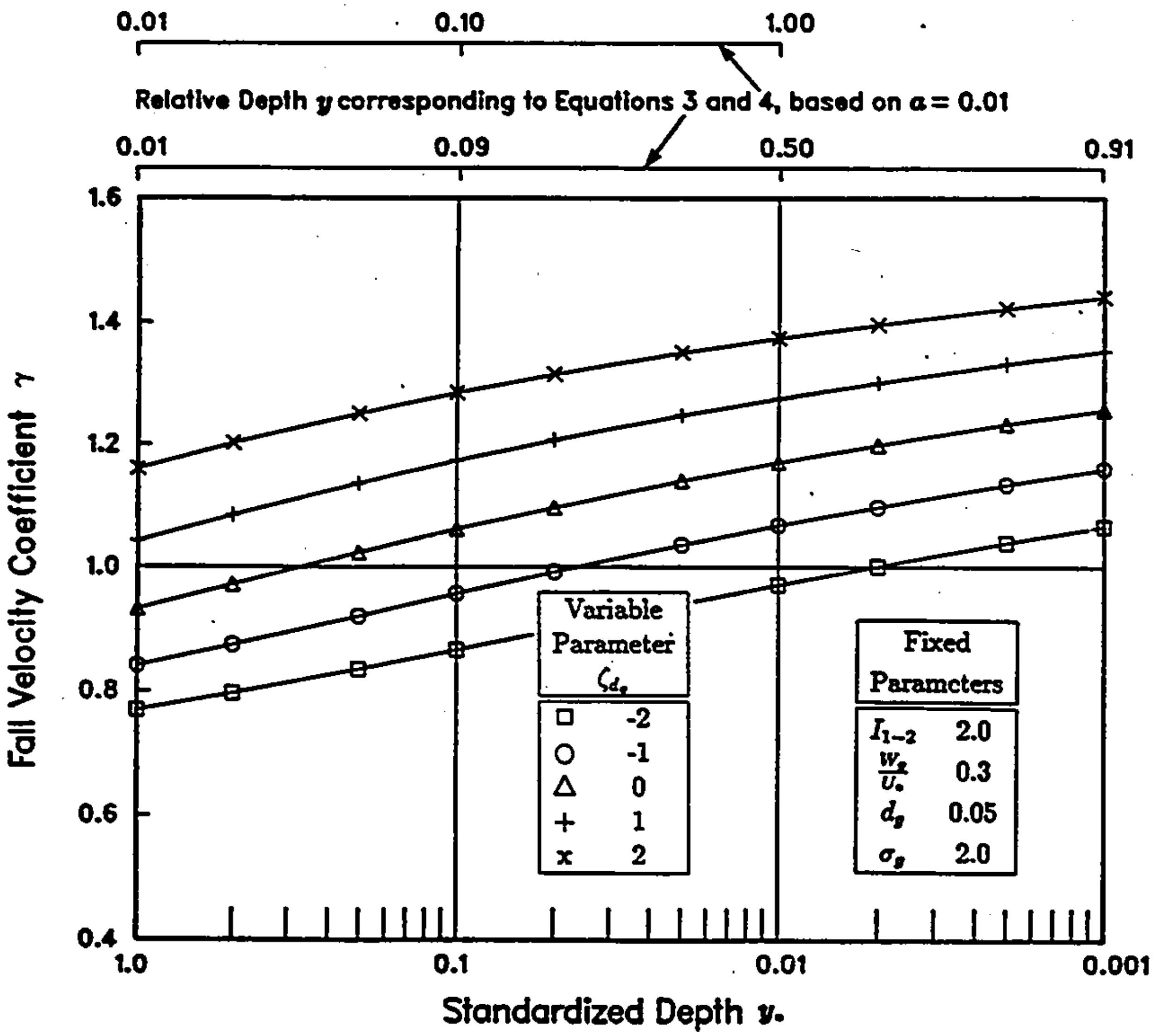

Figure 8.4: Fall Velocity γ versus Standardized Depth y_*; with Variable Parameter ζ_{d_g}

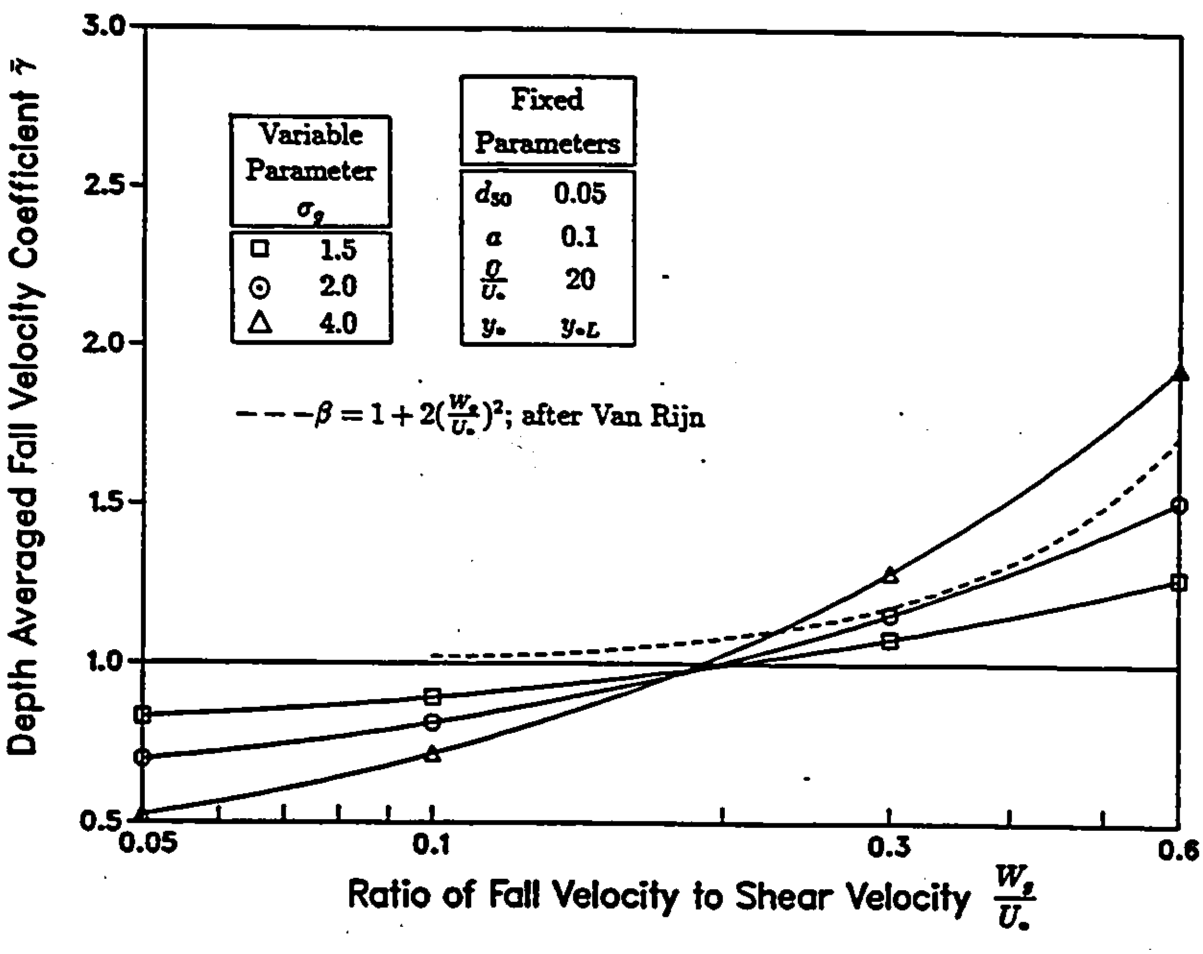

Figure 8.5: Depth-Averaged Fall Velocity Coefficient $\bar{\gamma}$ versus Dimensionless Fall Velocity $\frac{W_s}{U_*}$, after Laursen; with $a = 0.1$ and Variable Parameter σ_g

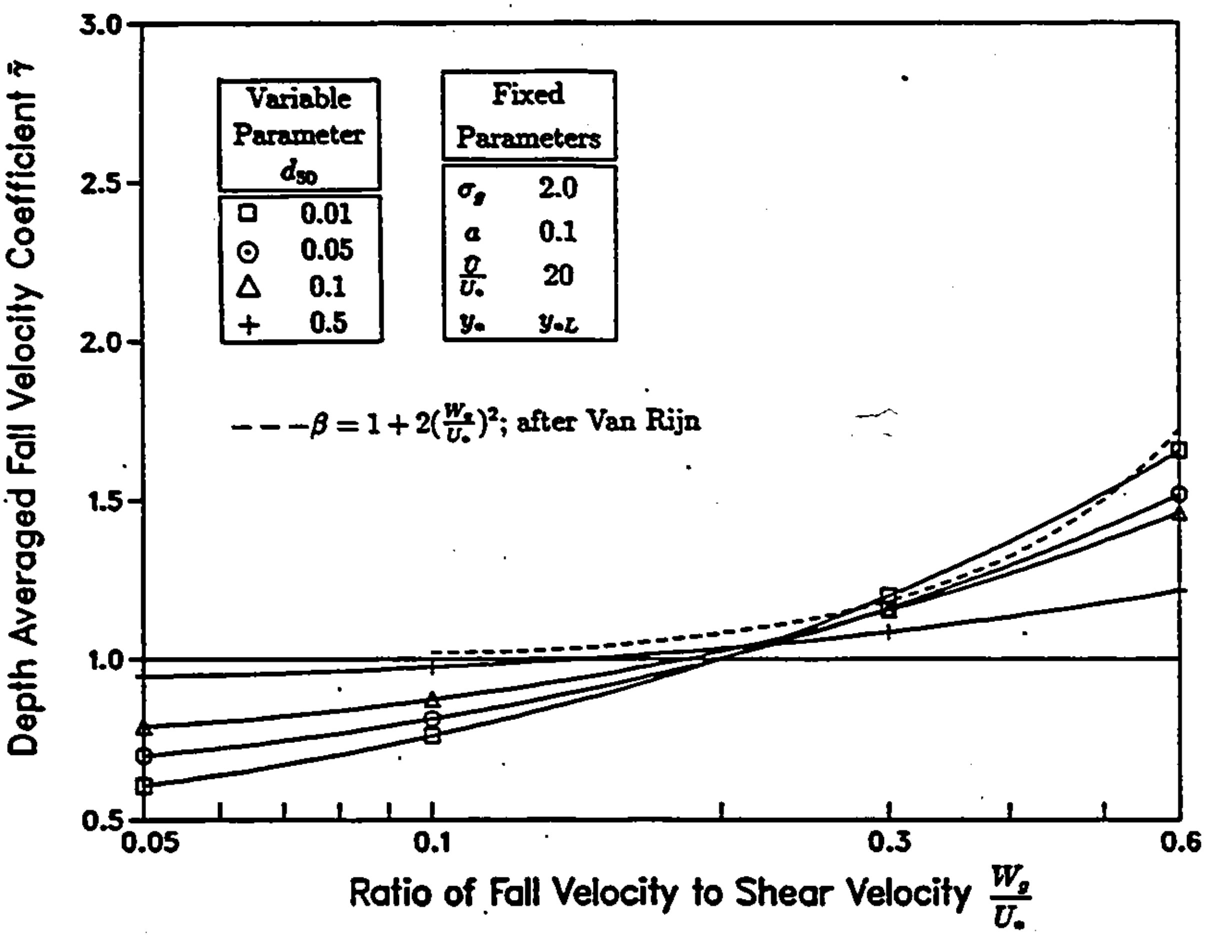

Figure 8.6: Depth-Averaged Fall Velocity Coefficient $\bar{\gamma}$ versus Dimensionless Fall Velocity $\frac{W_g}{U_*}$, after Laursen; with $a = 0.1$ and Variable Parameter d_g

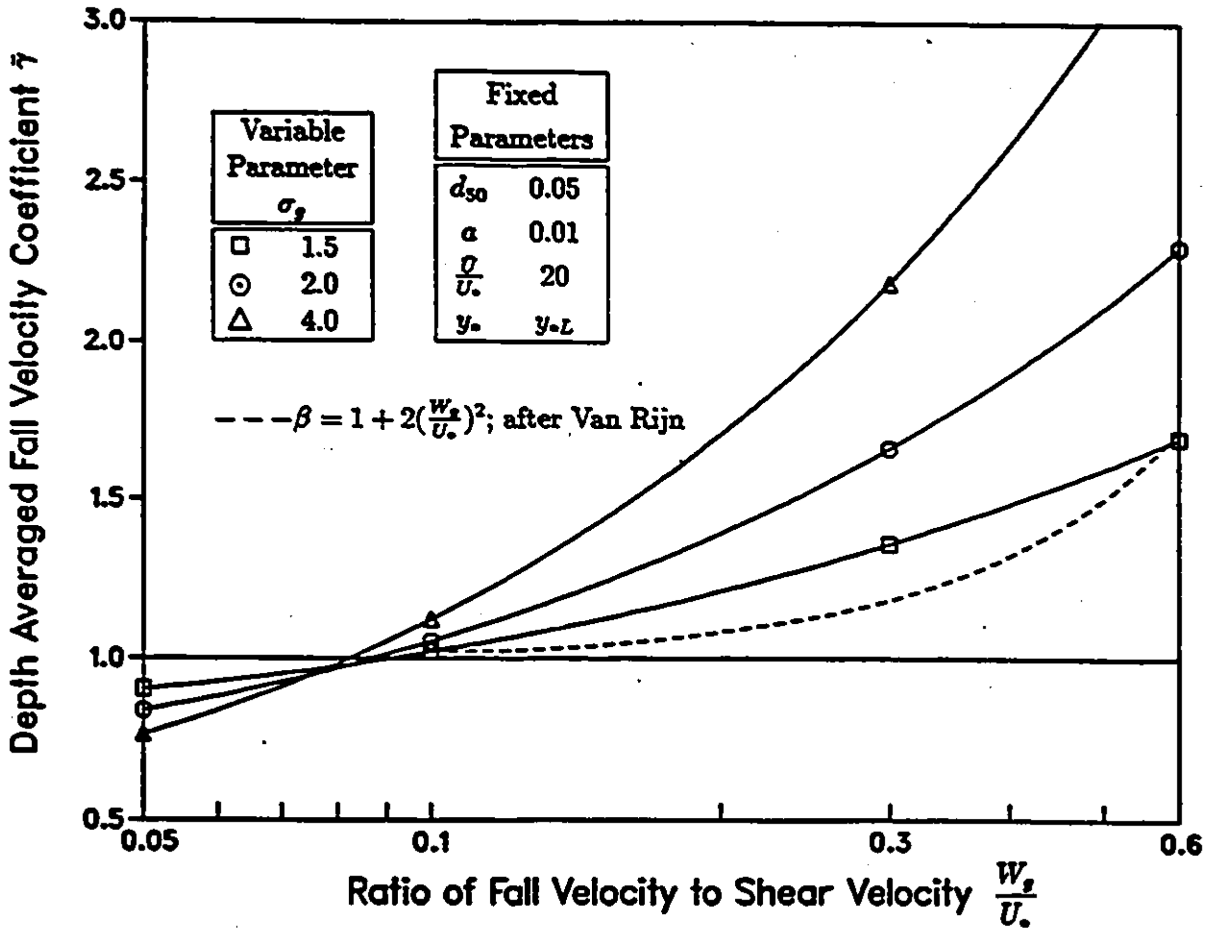

Figure 8.7: **Depth-Averaged Fall Velocity Coefficient $\bar{\gamma}$ versus Dimensionless Fall Velocity $\frac{W_s}{U_*}$, after Laursen; with $a = 0.01$ and Variable Parameter σ_g**

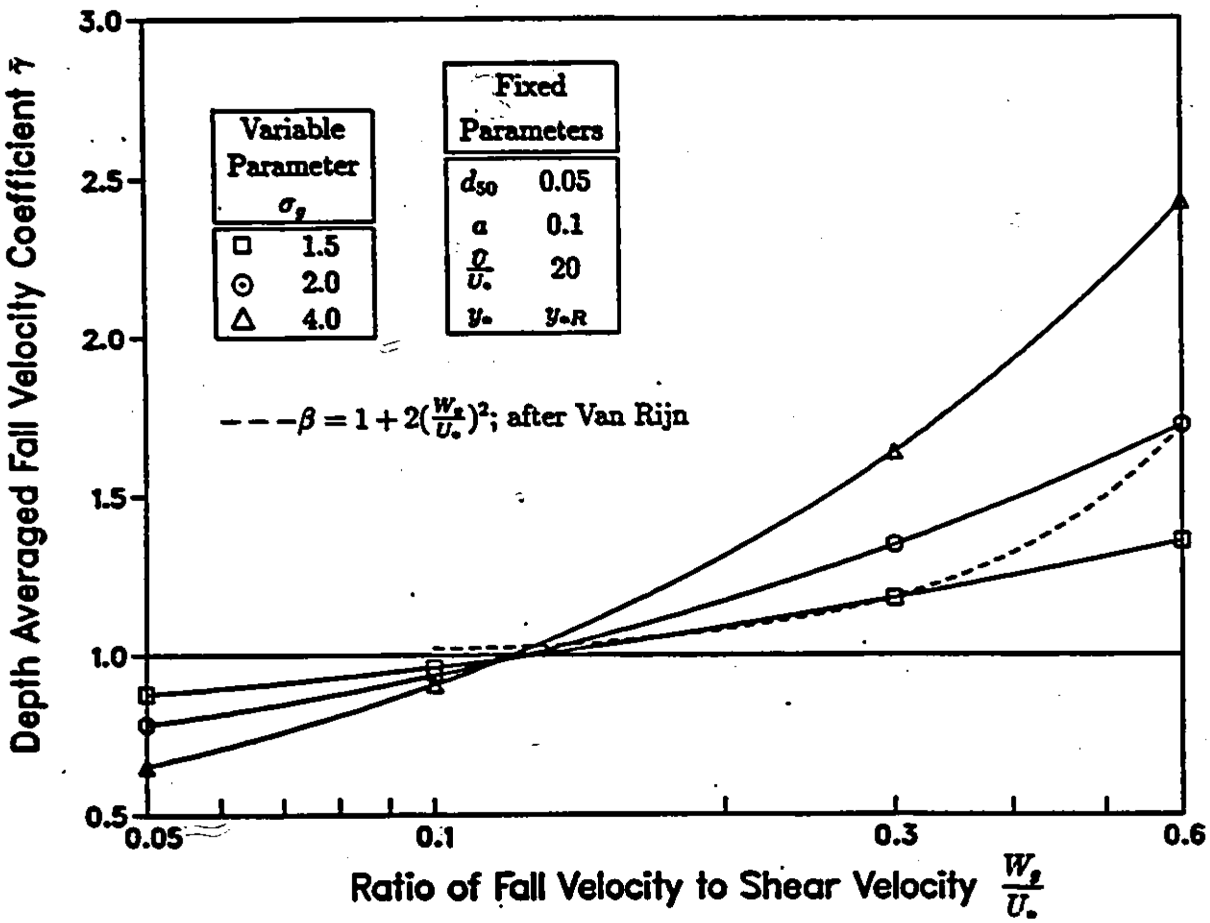

Figure S.S: Depth-Averaged Fall Velocity Coefficient $\bar{\gamma}$ versus Dimensionless Fall Velocity $\frac{W_g}{U_*}$, after Rouse; with $a = 0.1$ and Variable Parameter σ_g

Chapter 9

Screening-Level Simulations of the Lower Fraser

9.1 Preamble

Prior to performing detailed simulations of the Lower Fraser River, two 'screening'-level studies were performed. In the first, simple channel geometry and constant discharge were used to represent the river. This study provided an ideal framework for investigating (i) the time-frame for bed degradation processes on the Lower Fraser, (ii) the general effect of islands on degradation patterns, and (iii) the effect of channel non-uniformities on temporal and spatial changes in river-bed elevations. In the second screening-level study, the complete Lower Fraser channel network geometry was represented in its entirety and the hydrometric data used to described the flow regime was that observed during 1968 only. The objective was to provide a more realistic appraisal of the effects of man-made changes on bed elevation processes in the study reach.

During the early 1970's extensive river training works and navigational dredging were carried out downstream of Port Mann while in the study reach itself (figure 9.1), borrow dredging occurred on an intermittent basis. As a result of the river works, the average water level at Port Mann was reported to be about 0.3 m lower than its historical mean value (personal communication from Tassone though after further analysis he later estimated the drop to be approximately 0.5 m). The question addressed in this chapter is how this change in the downstream water level would affect, over the long term, the river bed elevations in the Port Mann to Mission study reach.

9.2 Screening-level Application No. 1

Due to the approximate 0.3 m general lowering of the water level at the downstream end of the study reach (Port Mann), theoretically the bed elevation should also eventually drop by 0.3 m. To obtain a first estimate of the time required for the bed to erode and how this erosion would move upstream, ONE-D-SED was applied to a very simplified representation of the Lower Fraser river system.

9.2.1 Degradation in a Uniform Single Channel

In this application the reach upstream of Port Mann was represented by a single uniform channel having a width of 710 m, a depth of 9.144 m, a length of 245 km and a Manning's n of 0.025. The annual discharge hydrograph was represented by a constant discharge of 8500 m^3/s flowing for only 7 weeks. These values were chosen to represent the freshet period which is when most of the annual sediment transport takes place. Sediment transport was calculated using the calibrated A-W equation. The representative grain size of the bed material was taken as $d_r = 0.345$ mm. Sediment transport values generated by A-W were increased by a factor of 2.25 to reflect the findings of the sediment transport calibration study. The water surface elevation imposed at the downstream boundary was 0.305 m lower than the uniform depth value for this particular flow. The simulated (3-year interval) bed profiles obtained using ONE-D-SED are shown in figure 9.2. For this simulation, an 'open' boundary condition was used to describe the change in bed elevation at the upstream end of the system (245 km from Port Mann).

This screening-level study revealed that bed degradation could travel a considerable distance upstream relatively quickly although the bed degradation process, even after 18 years, had not yet reached two thirds of its final equilibrium value (0.305 m) at the downstream end. The time-dependency of the degradation process at Port Mann is depicted more clearly in figure 9.3. The figure reveals that the degradation process is relatively rapid at first but slows down in later years. After a period of 9 to 12 years, the bed approaches its equilibrium level in an asymptotic manner.

However, since the Fraser river-bed is gravel upstream of Mission, the Mission to Port Mann reach of the screening model was re-run using a non-degrading (i.e. 'fixed') bed condition at the Mission station (also shown in figure 9.2). Implicit is the result that the predicted bed degradation near Mission (e.g. km 30-45) is substantially lower in this case than it was in the former scenario. While the effect of the fixed-bed condition is felt immediately in the vicinity of Mission, it takes about 9 years before it influences the degradation process in the vicinity of Port Mann (figures 9.2 and 9.3). Once the effect is felt, it takes only a few more years for the fixed-bed condition at Mission to arrest all further degradation in the vicinity of Port Mann (and the entire study reach). For the fixed-bed condition, the final river bed profile is obtained after 12 years, at which time the bed has degraded by only two thirds of its theoretical value.

9.2.2 Degradation in a Prismatic Channel with an Island

The next step of the screening-level analysis No. 1 was to run the model for the same prismatic reach which, in this case, divided unevenly around a hypothetical 10-km long island. On one side of the island the channel was made 470 m wide, while on the other it was 240 m wide. When the water surface elevation was again lowered by 0.305 m at the downstream end, results indicated that the overall erosion pattern was essentially unchanged from the 'single channel' case, except that there was slightly more erosion in the larger channel (than in the smaller channel) around the island.

As evidenced in figure 9.4, at the tips of the island (km-18 and 28), there are no 'steps' in the change in bed elevation. This is due to one of the internal boundary conditions developed for ONE- D-SED, namely that at a nodal point (i.e., bi-functions, confluences etc.), bed elevations in all adjoining reaches are the same. Though this is a useful assumption, in nature sand-bars can form at the upstream end of minor channels. Since the Lower Fraser has a large wash-load component, the frequent formation of bars in these locations has been observed. The minor channel can act as a sediment trap in such cases. However, given the fact that wash load was not simulated in the present study and that bed elevation compatibility is assumed in ONE-D-SED, the presence of islands in and of themselves did not change the overall predicted degradation pattern.

9.2.3 Degradation in a Non-Uniform Channel

Finally, screening model No.1 was used to simulate bed sediment dynamics in a non-uniform channel. In a central portion of the simplified 45 km study reach, the single channel was assumed to be half its standard width of 710 m. Under uniform-flow conditions, ONE-D-SED was run until the equilibrium bed profile in the constricted section of the river was established (about 7 m deeper than normal, see figure 9.5). In order to study the bed profile development, the water level at the downstream end of the system was again lowered by 0.305 m. The simulated bed elevations are shown in figure 9.5 and the changes from the equilibrium position are shown in figure 9.6.

Two important results were observed. First, the deep (constricted) portion of the channel (km-18 to km-26) was quite resistant to erosion. In fact, this particular section actually showed some areas of minor aggradation. Second, in the wider channel section downstream of the constricted area, initially there was less erosion than in the 'uniform reach' case (presented earlier) but then the degradation process accelerated and reached final equilibrium after only 4 years (compare figure 9.6 with figure 9.2).

These results were obtained by mathematically modelling the simplified Lower Fraser system. Channel non-uniformities have, in the last few years, been targeted for further research (Shen 1986). The state-of-the-art review (chapter 2) indicated that this is an area of river engineering that is not well understood. In the review, no concrete information was found to provide any indication of how the non-uniformity of channel width and/or depth affects river-bed dynamics. If the 'mathematical' behaviour reported herein is representative of nature, channel non-uniformity is very important in the prediction of the time-frame of river bed processes. Although in a uniform channel, only two thirds of the total change in river-bed degradation had occurred after 18 years, in this case, full degradation at Port Mann is predicted to occur in only 4 years. On the other hand, deep (constricted) zones of the channel are expected to suffer virtually no degradation at all.

9.3 Screening-Level Application No. 2

After applying ONE-D-SED to a simple representation of the Lower Fraser river, a more detailed physical representation was used to simulate the actual Lower Fraser study area with all its variability in cross-sectional channel geometry and including all five islands and the Pitt River system. In this more detailed screening level application, water levels and discharges were based on 1968 historical values. Recall that 1968 preceded the construction of the river training works and extensive dredging undertaken from 1969 to 1972. In view of this, it was postulated that the river was in dynamic equilibrium during 1968.

In this particular exercise, a previously calibrated version of the ONE-D Fraser River model was used. In 1984, Bernard Morasse of Environment Canada used the 1980/81 version of the ONE-D Fraser River model and recalibrated it for 1968 conditions (Morasse 1985). It should be noted that the 1980/81 version of the model is based on cross-sectional geometry obtained using river surveys made in 1961/62. Knowing that the river had subsequently degraded, the 1980/1981 model cross-sectional geometry was adjusted to account for some of the observed degradation that had occurred in the intervening period. Rather than using the un-adjusted (1961/62) cross-sectional data, Morasse continued to use the larger cross- sectional representations found in the 1980/81 model version. Morasse was forced to increase the Manning's n value by 10% throughout to account for the descrepancy in river conveyance between 1968 and 1989. In this way he succeeded in reproducing historically observed discharges. A copy of this version of ONE-D (hereafter referred to as the '1968 version') was made available to the present study.

In order to predict changes in river-bed elevations in the Mission to Port Mann study reach, the 1968 version formed the basis for developing a mobile-bed version of the model (i.e., ONE-D-SED). However, for the mobile-bed application, the hydrodynamic boundary conditions were changed. Morasse had described the system by water surface boundary conditions at Port Mann, Port Coquitlam and Mission, however, for the present study it was more appropriate to use discharge boundary conditions at Mission and Port Coquitlam. The reason for this is the fact that the historically observed water levels at Port Mann, had to be reduced by 0.305 m to predict (at the screening-level) the effects of a lowered water level on bed profile dynamics. These effects should be distinguished from those that would occur as a result of a change in discharge at Mission or Port Coquitlam. For this reason Morasse's computed discharges for Port Coquitlam were used to describe the boundary conditions.

In addition to the description of the river's geometry provided by the '1968 version', the sediment components were added to form a mobile-bed version of the study area. As before, the sediment load was determined by multiplying A-W computed values by a factor of 2.25 at Mission and using a representative grain size of 0.345 mm. In addition, 1968 water temperatures were noted and used as input to the A-W equation.

In order to obtain multiplying factors for the A-W equation in the rest of the river network, the model's calibration option was invoked. (This assumes that during 1968, the Lower Fraser was in dynamic equilibrium). The coefficients generated by ONE-D-SED were generally within the 0.5 to 2.0 range, although there was one location where the coefficient generated was very small and another where it was very large. This indicated that the cross-sectional area used in ONE-D may have been in error. Therefore, at these locations, the cross-sectional areas were themselves modified and the calibration procedure repeated. In subsequent communications with Tassone it was established that the model had failed at these locations during simulations made for the late 1980's. Therefore, Tassone had also modified the cross-sectional areas at these locations in his version of the model.

Once the new calibration coefficients were generated by the model, they were introduced in the input file to ONE-D-SED. The full 1968 year was simulated once more in the normal mode. It was noted that there were areas of very minor aggradation and degradation at the end of a year's simulation. These computed changes in bed- elevations were therefore retained and used as initial conditions, and once again the model was run for the baseline 1968 conditions. No further changes in bed elevations were observed. This meant that a model having a dynamic equilibrium for 1968 baseline conditions had been established.

Having completed the ONE-D-SED model building process, the historically observed 1968 water surface elevations at Port Mann were lowered in 0.1 m steps by 0.305 m over a period of 3 years. As noted beforehand, the same discharge computed for base conditions was used to prescribe conditions at Mission and Port Coquitlam. Regarding the river-bed boundary condition, both 'fixed' and 'free' boundary conditions were used at Mission. The presumption of a fixed-bed condition is based on the presence of a gravel-bed upstream of the study reach. In describing this condition, it was sufficient to specify that there were to be no changes in bed elevation with time at this location.

In prismatic channel reaches, a modified form of de Vries' numerical scheme is used (Vreugdenhil 1982) to describe the 'free' boundary condition. However, it was found that when this condition was used for the detailed representation of the Lower Fraser, due to channel non-uniformities, there was a bed-elevation stability problem in the vicinity of Mission. Therefore, in order to represent the 'free' condition for the detailed simulation exercise, the computed changes for Mission computed above (based on the simple representation of the river) were used to describe the changes in bed elevation for this case.

Each scenario (fixed- and free-boundary) was developed separately. The procedure consisted of running the model with the modified water surface elevations at Port Mann for a 1-year time interval. At the end of the year, changes in bed elevations were noted and were re-introduced as initial conditions for the subsequent year's simulation. Using these new bed elevations as the initial condition and the same (1968) hydrometric values to describe the boundary conditions, ONE-D-SED was then re-run for a total of 18 consecutive years.

The simulated changes in bed profiles along the main channel of the study reach, based on a 'fixed-bed' boundary condition at Mission, are displayed in figure 9.7. As was the case in screening-level application No. 1, degradation in the minor channels was slightly less than that in the major channels. Also consistent with the first application was the resistance to degradation in the narrower, deeper sections of the river (eg. km-15 to km-24, figure 9.7). The second effect of channel non-uniformities was seen in the simulation of the river reach near Port Mann. In this area (km-0 to km-4), during the first three years, channel aggradation (due to a progressive channel narrowing downstream of Douglas Island) is predicted. Then, after a time, as in the non-uniform case above, the model revealed an accelerated degradation process in this area. In the case presented above (screening No. 1 of the non-uniform channel), it took 4 years to reach the final degradation profile whereas in this case, due to the fact that channel non-uniformities are not as severe as in the former scenario, it took 9 to 12 years to reach the new equilibrium bed profile.

When the free-boundary condition scenario was run, the same overall degradation pattern was observed (figure 9.8). In other words the same resistance to degradation was noted for section km-15 to km-24 and the initial aggradation was followed by an accelerated degradation process between km-0 and km-4. Implicit in this scenario is that predicted bed degradation is greater than in the fixed-boundary simulation, particularly in the vicinity of Mission. It is also noted that the bed continued to degrade after 12 years because the boundary condition at Mission forces the bed throughout the study reach to degrade by the same amount as that prescribed at Mission. However, as in the fixed-bed scenario, the majority of degradation had occurred within 12 years and therefore, any additional degradation in the study reach is the same as is specified by the Mission boundary condition.

9.4 Discussion

Using two levels of screening models, certain predictions could be made regarding the bed degradation process along the Lower Fraser River. Some of the key findings of these applications are:

1. The river bed's resistance to erosion upstream of Mission plays an important role in the magnitude and time-frame of degradation in the study reach. The degradation occurs as a result of generally lower water levels at Port Mann (induced by river works in the downstream portions of the river).

2. When the system is represented by a single prismatic reach, due to the imposition of a fixed-bed condition at Mission, bed degradation is predicted to stop after 9 to 12 years (and only two-thirds of the ultimate theoretical change is achieved).

3. When a free-boundary condition is assumed, bed-degradation is rapid in the first 9 years but slows thereafter and the theoretical value is only reached asymptotically.

4. Given the assumed compatibility of changes in bed elevation of reaches joined at a node in ONE-D-SED, the presence of islands, in themselves, do not significantly effect the degradation pattern. In reality, minor channels around an island can act as sediment traps for the wash load, however the wash load component was not modelled in this simulation exercise.

5. Channel non-uniformities result in a significant change in the predicted degradation pattern. In deep (constricted) sections, the bed is resistant to degradation. Conversely, other areas can show very rapid channel degradation after a time of reduced degradation activity. In the simple network representation where it was assumed that the channel constricted to half its standard width, full degradation was predicted to occur within 4 years.

6. When the study reach was represented using actual field data, due to channel non-uniformities, full (i.e. equilibrium) degradation was predicted to occur in about 9 to 12 years. For the fixed-bed upstream condition case, degradation was arrested after 12 years. However when a free-boundary condition was imposed at Mission, after 12 years the entire reach continued to degrade by the same amount as specified at Mission.

7. In general, the predicted magnitude of degradation at Port Mann, corresponded to the imposed change in water level at that location, namely approximately 0.3m.

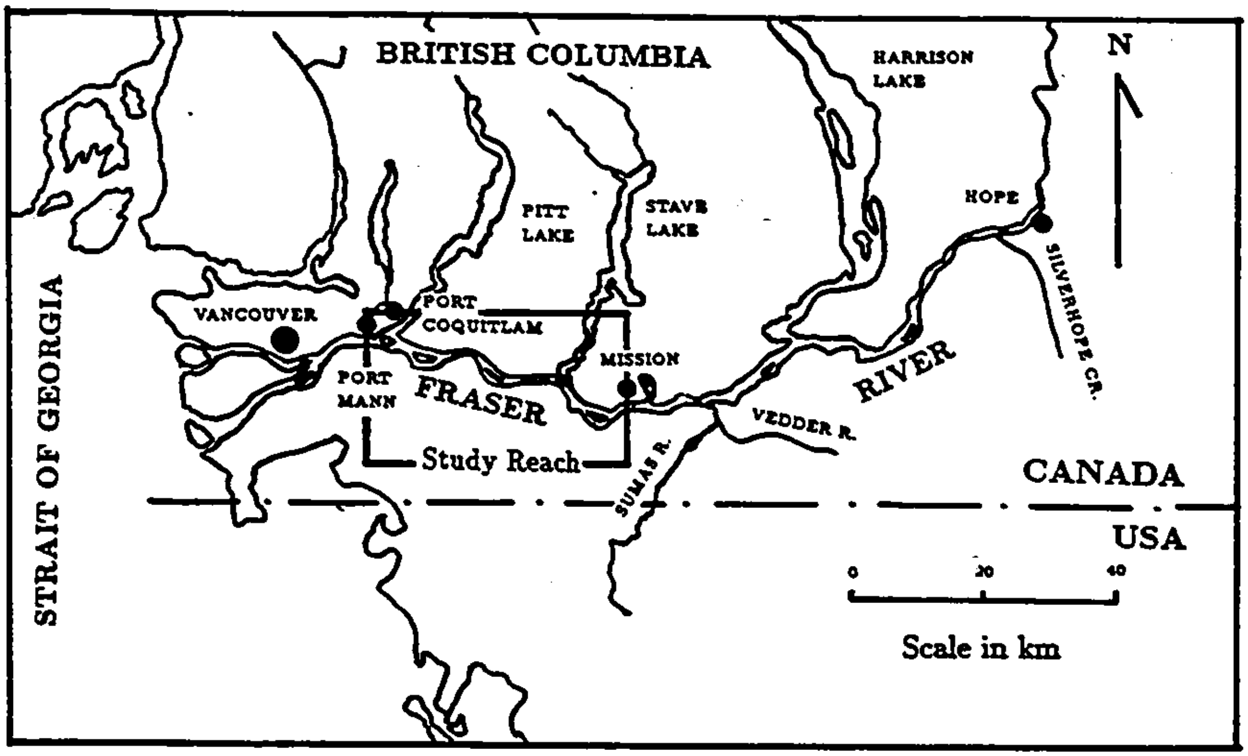

Figure 9.1: The Lower Fraser River

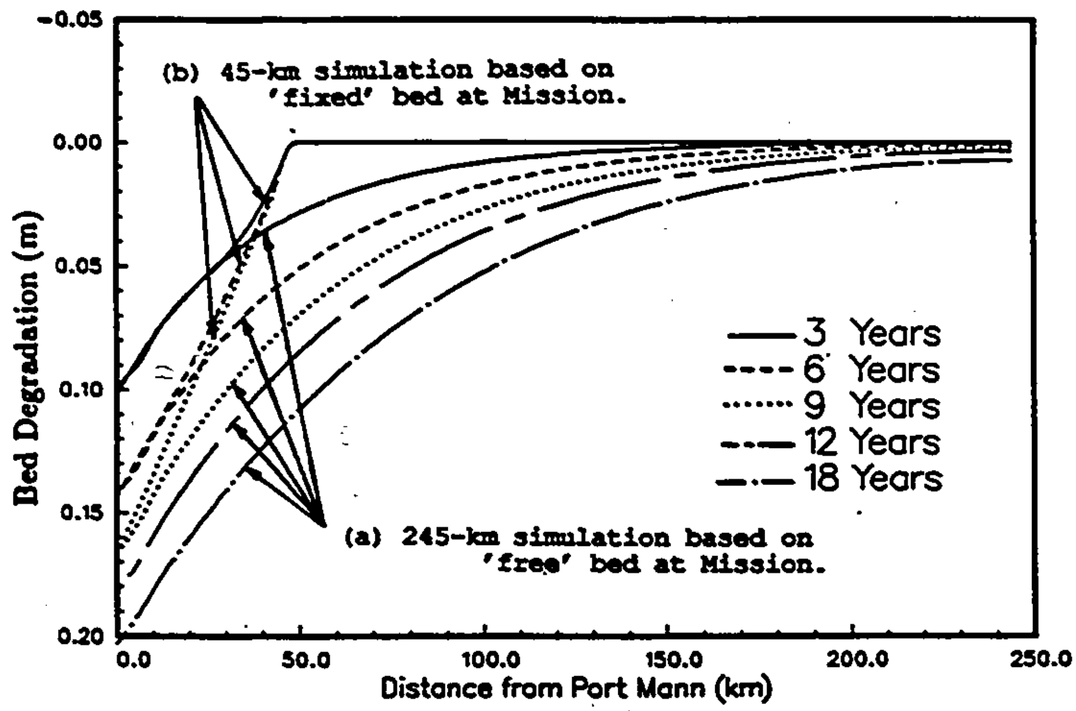

Figure 9.2: Bed Degradation Profiles for the 45 and 245-km Reaches

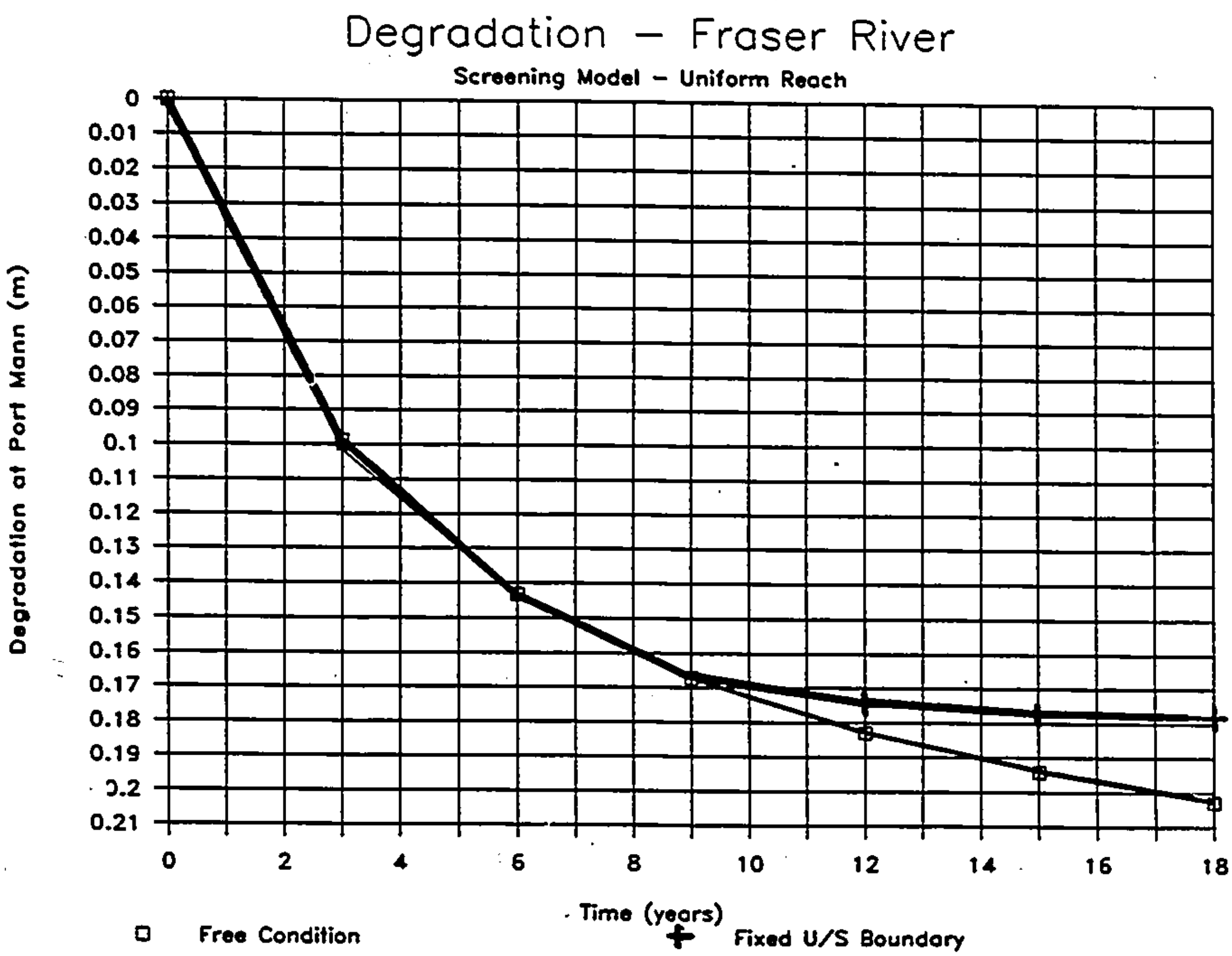

Figure 9.3: Bed Degradation at Port Mann, Function of Time

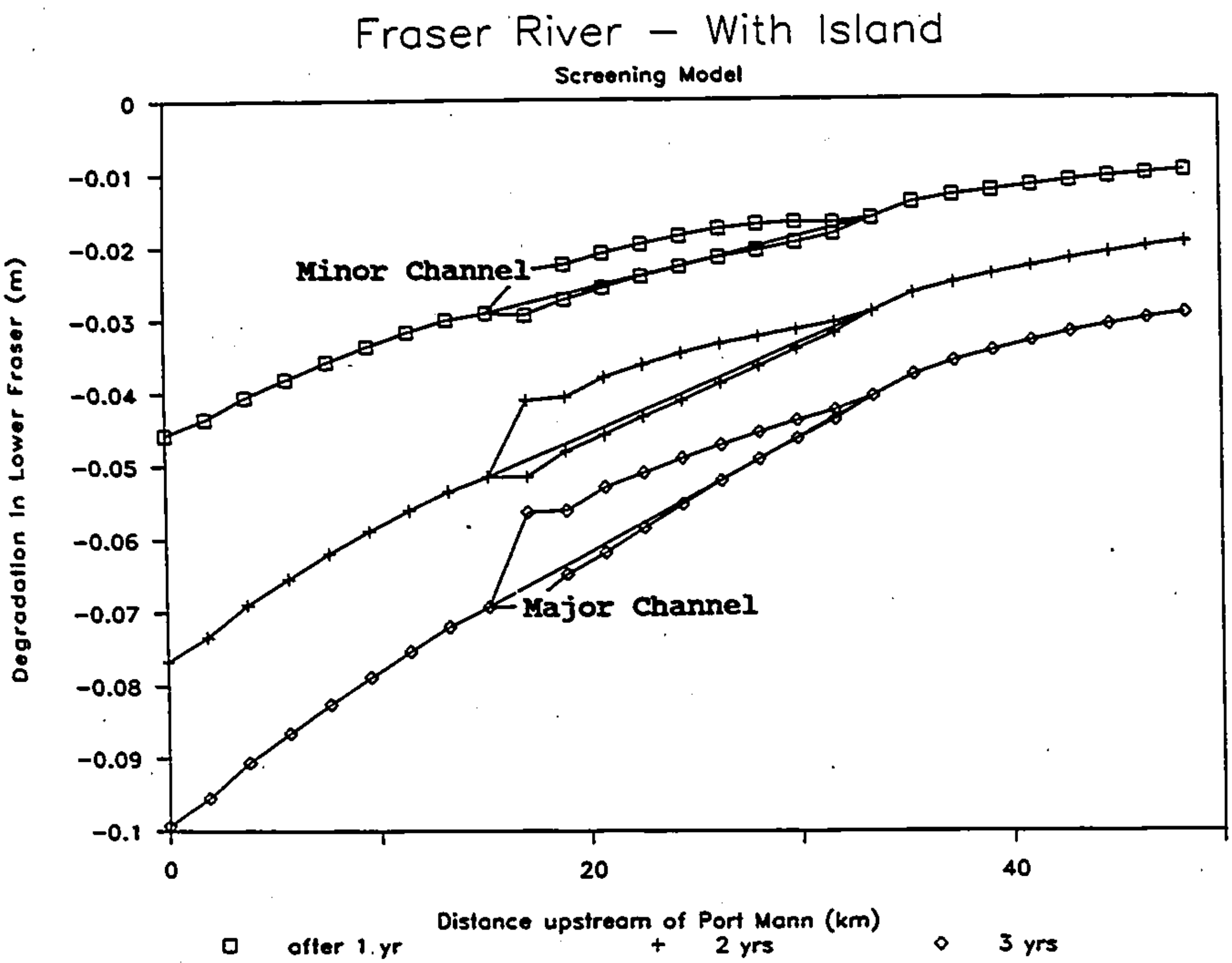

Figure 9.4: Bed Degradation Profiles for the Study Reach with an Island

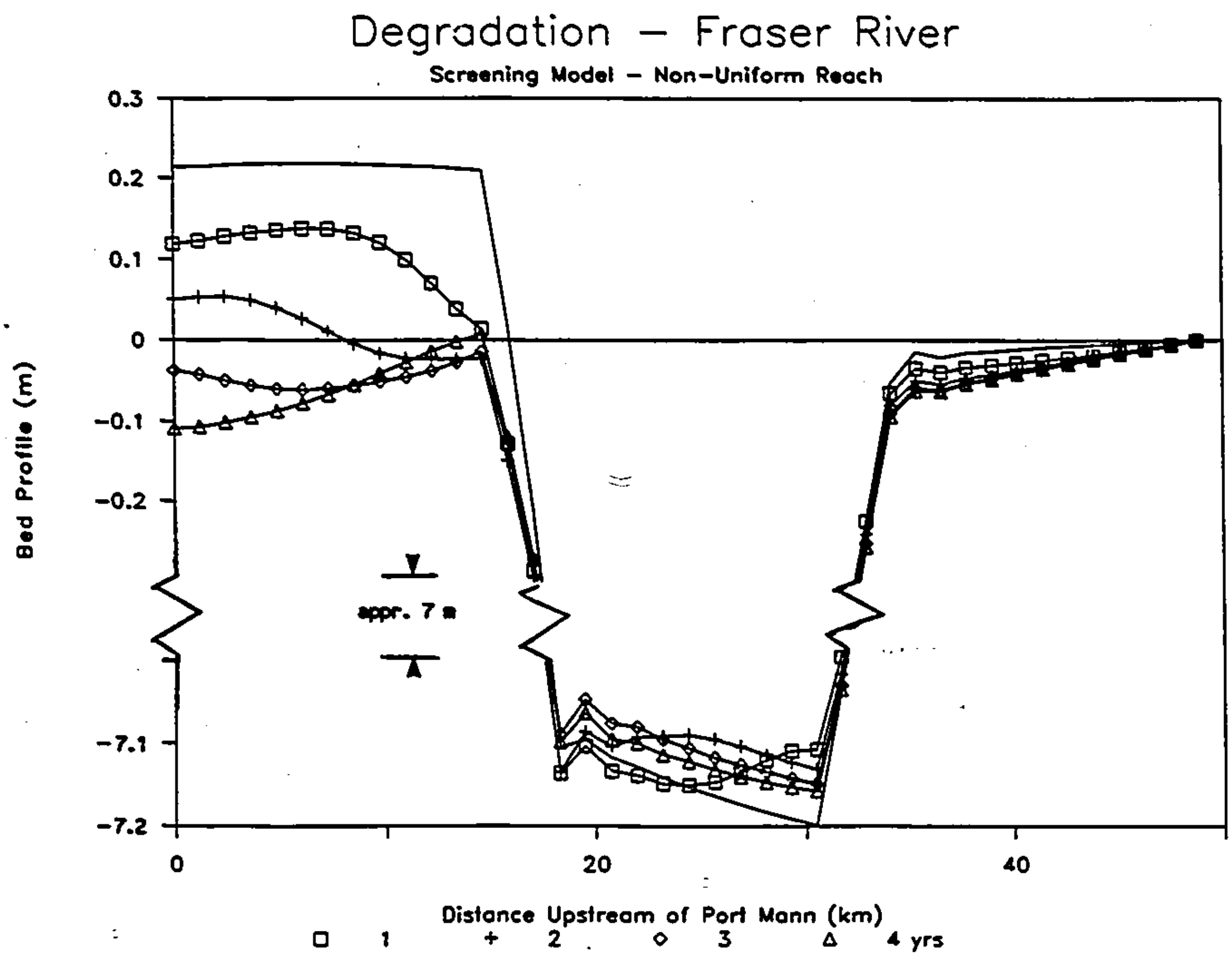

Figure 9.5: Bed Degradation Profiles for a Non-Uniform Reach

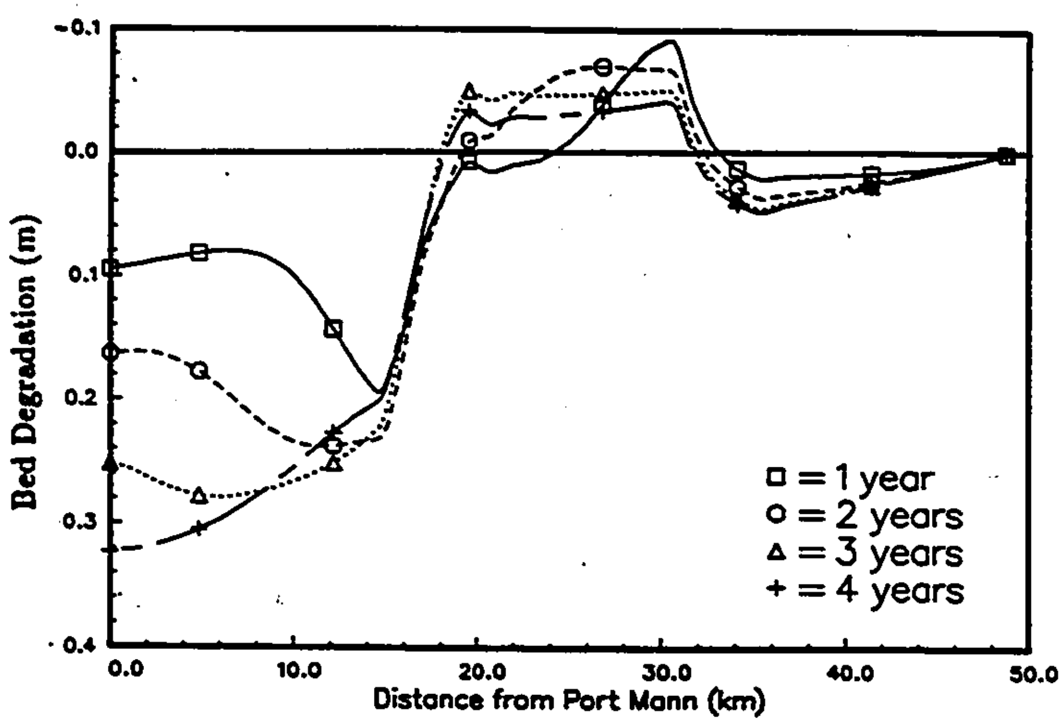

Figure 9.6: Changes in Bed Degradation Profiles for a Non-Uniform Reach

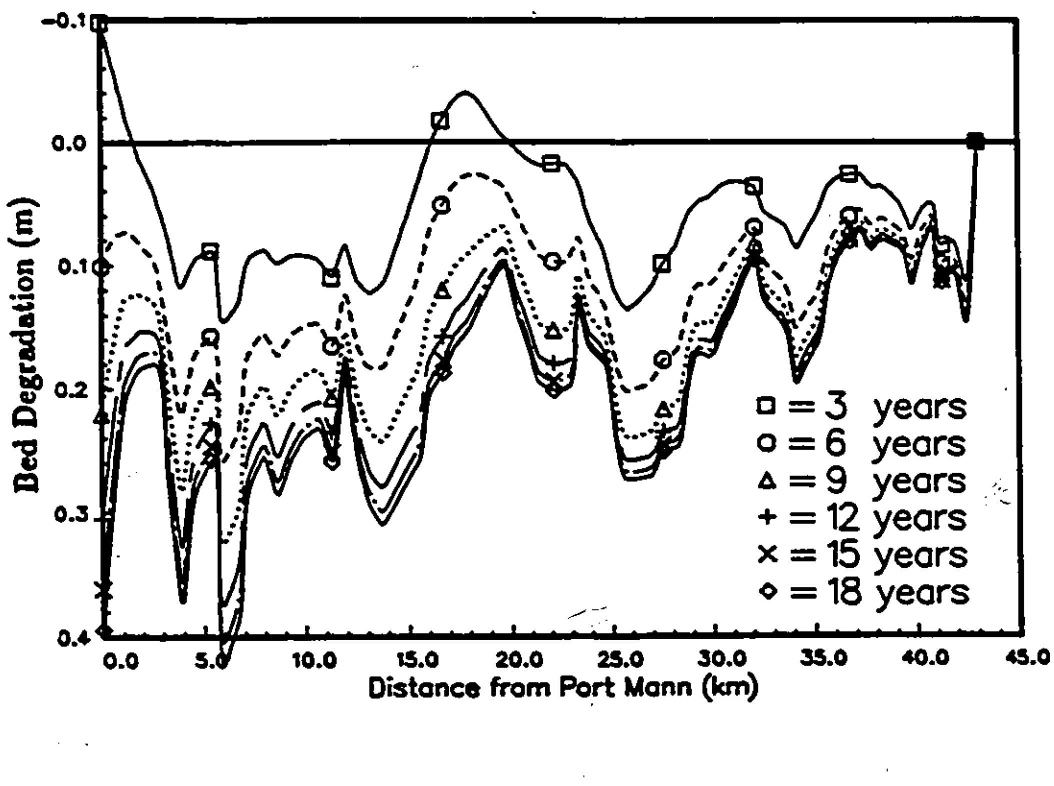

Figure 9.7: Bed Degradation Profiles in the Study Reach - Fixed-Bed at Mission

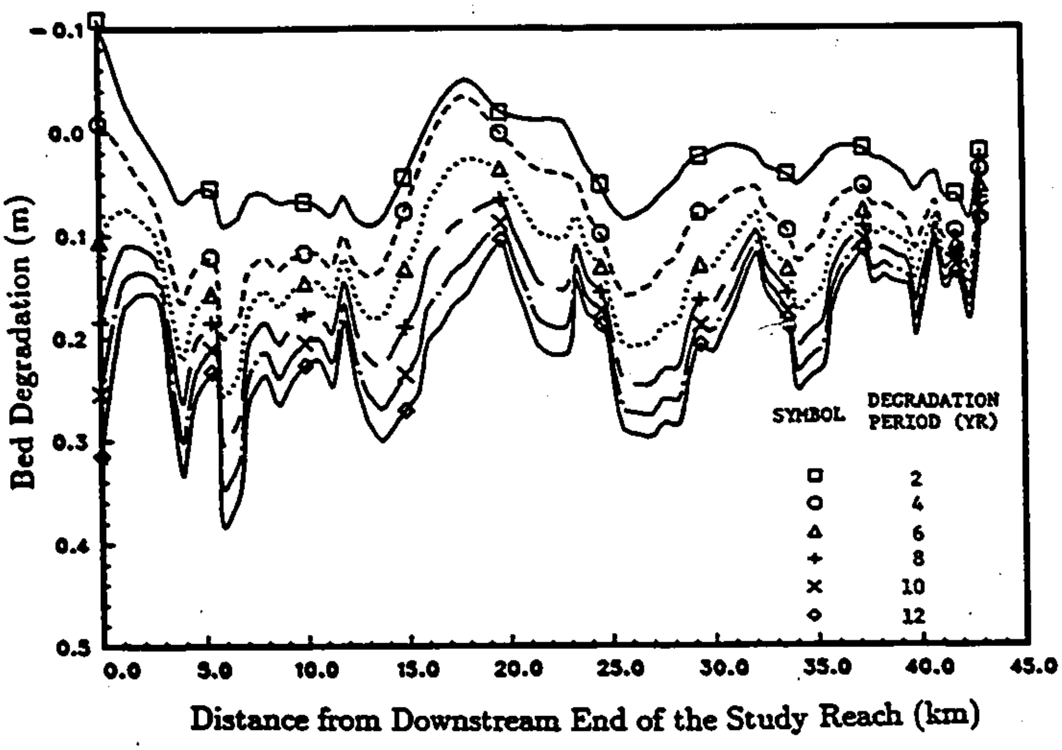

Figure 9.8: Bed Degradation Profiles in the Study Reach - Free-Bed at Mission

Chapter 10

Detailed Simulation of the Lower Fraser

In the previous chapter the predicted changes in bed elevations were obtained based on the reported finding that water levels at Port Mann are now lower than their historical mean value. In this chapter, the objective is to validate the use of ONE-D-SED for a tidally-dominated multi-channel network using field data. The Lower Fraser River was once more used as a test case for this objective. To validate the model, it was important that historically observed data be used as boundary conditions and that simulated changes in bed elevations are shown to correspond to those observed.

10.1 Basis for Model Validation

To satisfy these requirements, it was necessary to select an appropriate simulation period. Water surface elevations have been recorded at various locations within the study area since 1965. However, there are a number of data gaps (caused by failure and down-time of gauges), and in the winter months there are problems with freezing temperatures fouling almost all the gauges. Since, to run the model, the water surface elevation is required at all model boundary locations, it is only necessary for the data to be lost at one station to cause an inability to simulate that time frame. In order to maximize the period simulated, non-linear interpolation techniques were used to estimate levels where the data gaps were less than 3 days. Even so, because of larger gaps in the data, there were still some months of each year that could not be simulated (table 10.1)

Table 10.1: Study Reach Simulation Period

Year	Simulation Period
1968	January 1 - December 31
1979	July 4 - October 25
1980	April 4 - September 30
1981	March 1 - December 10
1982	February 12 - November 30
1983	February 2 - December 17
1984	March 3 - December 24

In addition to the need for hydrometric data, information on the amount of dredging which took place in the study period should be included to obtain a more accurate simulation. Virtually no dredging records exist for the study area prior to 1974. Since 1974, some records were kept by the Department of Public Works, but some of these were lost, while the remainder are incomplete and often inaccurate. Most dredging done within the study reach is site and/or project specific and is usually carried out by the private sector. Since Public Works' main concern is dredging in the downstream reaches, activity in the Mission to Port Mann reach is often overlooked. Table 10.2 provides an estimate of the dredging which has taken place in the study reach since 1974.

Table 10.2: Mission-Port Mann Dredging (m^3)

	In House	Contract	Borrow	Total
1966	0	0	0	0
1967	0	0	0	0
1968	0	0	0	0
1969	145100	0	0	145100
1970	0	0	0	0
1971	0	0	0	0
1972	0	0	0	0
1973	0	0	0	0
1974	0	0	0	0
1975	116700	0	0	116700
1976	0	0	754000	754000
1977	0	0	341000	341000
1978	0	0	0	0
1979	0	0	191900	191900
1980	0	0	218100	218100
1981	0	0	0	0
1982	79700	0	0	79700
1983	0	0	220700	220700
1984	0	0	1900	1900
1985	0	0	0	0
1986	0	0	43400	43400
1987	0	0	0	0

Finally, the key to validating the ONE-D-SED simulations is to obtain a record of changes in bed elevations in the area of interest. Bathymetric surveys of the area were taken in 1961/1962, 1979 and 1984/1986. In the first and the last cases part of the study area was surveyed in the first year and the remainder done in the second year. In the last case the lower half of the study area was done in the first year (1984) while the upper half was done in the second (1986).

The 1979 survey was a special case. During the development of the ONE-D model in the late 1970's, it was known that there had been some degradation of the river bed in the downstream reaches. To incorporate the increases in channel conveyance, a special survey of the then current channel dimensions was requested at a few key locations along the lower half of the study reach. Changes in cross-sectional area between the 1961 and 1979 surveys were then noted and used to interpolate changes in bed elevations between these special survey locations. Although all the survey maps of the 1961/62 and 1984/86 have been obtained, some of the original 1979 maps have been lost and, since the precise location of the 1979 survey lines is not known, it was difficult to determine the change in bed elevation between 1979 and 1984 at those locations.

Given the extent of the data availability for the study reach, various simulation options were available. Since good bathymetric maps are available for 1961/62 and 1984/86 the first option was to model the 1961 to 1986 period. This would have been a good choice since it includes a period of relative river-bed equilibrium (1961 to 1970), followed by a period of bed degradation (i.e. after the construction of the river training works in 1969 to 1972). However, due to the lack of hydrometric data from 1961 to 1965 and the lack of dredging data from 1961 to 1973, this option was not feasible. A second alternative was to simulate the river bed development from 1966 to 1986. This option was also attractive because of the time span involved. However, it would be a difficult exercise due to the number of gaps in the hydrometric data during the 1960's and early 1970's. Finally a third option, which simulated the study area for the period 1979 to 1984, was chosen. Though this period is relatively short, the quality of the hydrometric data is reasonably good, some dredging records exist and the 1979 and 1984 surveys can be used to estimate changes in bed elevations. Since the 1979 survey is only a partial one, changes in river-bed elevations between 1961/62 and 1984/86 were also calculated to complement the former.

As stated beforehand, calculated changes in bed elevations (and their locations within the study reach) are found in Table 10.2. It should be noted that when the calculations were made, great care was taken to measure the cross-sectional area of the river at the exact same place in all instances since the maps provided for different years were drawn to different scales. In order to obtain the average change in bed elevation, the computed 1961/1962 and 1979 cross-sectional areas were subtracted from that computed for 1984/1986 and the difference was divided by 90% of the channel top- width; (90% of channel width also was used when reporting the model's simulated change in bed elevation).

10.2 Model Calibration

10.2.1 Calibration of River Hydraulics

Prior to simulating bed transients in the study reach, it was necessary to calibrate the model from both a 'hydrodynamic' and a 'sediment transport' viewpoint. As stated previously, the 1968 version of ONE-D was provided for this study. In subsequent model applications it was found that, in order to obtain superior simulations, channel resistance should be made a function of the magnitude and the direction of the river's discharge (Tassone 1990 verbal communication). These features were not included in the version supplied for this study. Tassone reported that for discharges less than 5660 m3/s or greater than 11 330 m3/s the value of Manning's n was constant. For intermediate values, n was maximum at about 8500 m3/s. If the increase in n with discharge is directly related to the freshet event (figure 10.1) then it is probably also related to the associated sediment dynamics during that event (figure 10.2). In particular, during the onslaught of the freshet, there is a great deal of dune growth activity (figure 10.3). Once the maximum freshet discharge has reached Mission, dune height is at a maximum after which time, even though the discharge remains at a high level (figure 10.1), sediment transport and dune dynamics fall off. This implies that Manning's n is probably not only discharge related by is probably also time dependent. That Manning's n is a function of flow direction (with respect to dune orientation) was also found in ONE-D's application to the St. Lawrence River (Morse 1990a) as well as being confirmed by laboratory studies (Lau 1988).

The change in resistance along the main channel needed to be built into the 1968 version, hence, it was necessary to re-calibrate the model for the 1979-1984 simulation period. In addition to changes in n along the main channel, the value of n was also known to be a function of flow direction in the Pitt river. In this case, since the dune direction is in the upstream (i.e., flood tide) direction, the value of n is greater on the flood tide than it is on the ebb tide. In the Pitt River, the dunes are primarily orientated in the upstream direction due to the shape of the velocity profile (Ashley, 1980) and the fact that the discharge during the flood tide is higher than during the ebb tide.

Recall that the following are specified when the study area is simulated: 1) the water surface elevations at Mission, Port Mann and Port Coquitlam, 2) the discharge at the Ruskin power station and 3) local lateral inflows normally estimated by pro-rating observed runoff in locally-gauged creeks (figure 10.4, Morasse 1985). Many techniques can be used to calibrate ONE-D/ONE-D-SED for hydrodynamic simulations. First, the simulated water surface elevation at two intermediate locations can be compared with those observed at Whonock and Port Hammond. Second, during the freshet period the computed discharge at Mission can be compared to that obtained using a stage-discharge relationship developed at this site for high flow periods only. Third, simulated discharges for any location in the system can be compared with those obtained using either the traditional 'velocity-area' method or the 'moving-boat' technique (Sydor, 1983). The mean discharge at Mission also may be estimated (during low flow periods) by obtaining discharges measured at upstream stations. To estimate the mean flow entering the Fraser via the Pitt Lake/River system, a comparison may be made with those flows observed at the Ruskin power station. The latter is the fourth boundary condition of the study area and is located at the downstream end of a basin similar in nature to the Pitt drainage basin.

Knowing that, in the context of this study, the hydrodynamic calibration was primarily a case of "fine-tuning" an already validated fixed-bed model, the approach used here was slightly different than previous ones which relied more heavily on matching observed instantaneous values. With respect to water levels at Whonock and Port Hammond, simulated and historical mean monthly values were compared. With regard to the discharge at Mission and Port Mann, simulated monthly values were compared with those previously simulated and published by others. Discharge in the Pitt River was also compared to previously simulated values and to observed mean values obtained for Ruskin. At Mission and Port Mann, simulated values generally agreed within a few percent with those published though occasionally, the error was as much as 8%. Dimulated discharge from the Pitt also compared well with those implicit to results from publications and, on a pro-rated basis with those observed at Ruskin. Simulated levels at Port Hammond and Port Whonock generally agreed within 0.1 ft with those observed though very occasionally, the error was as much as 0.2 ft. This results compares well with simulations dof the study reach done by others. During this exercise, it was found that the value of Manning's n could reach a maximum of 1.126 times its base value in the main stem and that it was 1.15 times its base value on the flood tide in the Pitt River.

10.2.2 Calibration of the Sediment Transport Function

Prior to simulating channel bed dynamics for the 1979-1984 period, it was necessary to obtain calibration coefficients for the A-W equation for locations other than the Mission station. As in the case of the screening-level analyses, it was hypothesised that the study reach was essentially in dynamic equilibrium prior to implementation of the major river works downstream of Port Mann. Recall that in the 1968 version, calibration of the hydrodynamics was based on changes in channel cross-sectional area (which occurred between 1961/1962 and 1979) and increasing Manning's n by 10% to counteract the increase in channel conveyance (see previous chapter). Since it is hypothesised that the majority of bed degradation which occurred between 1961/1962 and 1979 occurred in the 1970's, in this study it was assumed that the 1961/1962 cross-sectional area data should be used for the simulation of 1968. Accordingly, the increases in cross-sectional areas were removed from the '1968 version', and Manning's n was re-evaluated in order to match those discharges computed by Morasse.

Next, as in the case of the screening-level applications, the mobile-bed option was run in the 'calibration mode' to obtain sediment transport calibration coefficients. The validity of the latter were checked by using them as part of the input and running the model in the normal (bed aggradation/degradation) mode. As before, there were some very minor changes in bed levels which were re-introduced as initial conditions. When the model was re-run a second time, it essentially predicted no further changes. Therefore, it was concluded that the sediment transport function had been calibrated. The coefficients (along with the minor changes in bed elevations) were used for subsequent simulations of the new 1979-1984 version of ONE-D-SED. This completed the model calibration exercise.

10.3 Results

The first indication that simulated values were meaningful came when 1968 simulated and observed changes in bed elevation were compared at Port Mann. While this was based on a simulation during the calibration year (and hence, by definition, no net change is allowed to occur over the full year), the bed still undergoes a degradation/aggradation cycle within the year under the influence of the spring freshet event. Although the simulated cycle appears to lag that observed by a few days, the simulated and observed degradation/aggradation cycles are in relatively good agreement (figure 10.5).

For the 1979-1984 period, the bed-boundary condition inputted at Mission represented the known minor degradation which occurred over the 1979 to 1984 period. Given this prescribed boundary condition, the model was run for all months of each year which had the required hydrometric data (table 10.1). The resulting simulated changes in river-bed elevations are presented in figures 10.6 and 10.7.

To verify that simulated changes corresponded to those observed during the same period, the latter were superimposed onto these figures. To further indicate prototype degradation, changes between 1961/1962 and 1984/1986 were also included in the figures.

In general, the overall pattern of bed degradation is reasonably well simulated. In the upper portion of the study reach (km-12 to km-44), only minor changes in bed elevation are simulated. These follow the trend of minor degradation specified at Mission. Further downstream, the simulation indicates a change from degradation to aggradation. Compared to observed values, the model underestimates aggradation in the area just upstream of Barnston Island. This may be due to underestimating the amount of bed material dredged during the 1974 to 1979 period at this particular location. In the lower portion of the study reach, increasing amounts of degradation are both predicted and observed. It is noted that about 40% of the observed degradation between 1962 and 1984 occurred in the 1979 to 1984 period.

With respect to secondary channels (figure 10.4), observed data are available at the downstream end of the reach. When compared with both 1979-1984 and 1962-1984 data sets simulated degradation is consistent with that observed. However, as in the case of the major channels in this location, simulated degradation is somewhat less than that observed. In the minor channels at the upstream end of the study reach, although degradation is simulated, aggradation was in fact observed between 1961 and 1986. The observed aggradation is in contrast to the degradation observed in the main channel (figure 10.3) and is probably due to the wash load settling out in these tranquil channels. Simulated bed elevations cannot reproduce this feature because no wash load was included in the model application exercise. Besides this anomaly, the overall simulated changes in bed elevations in the minor channels are in good agreement with those observed.

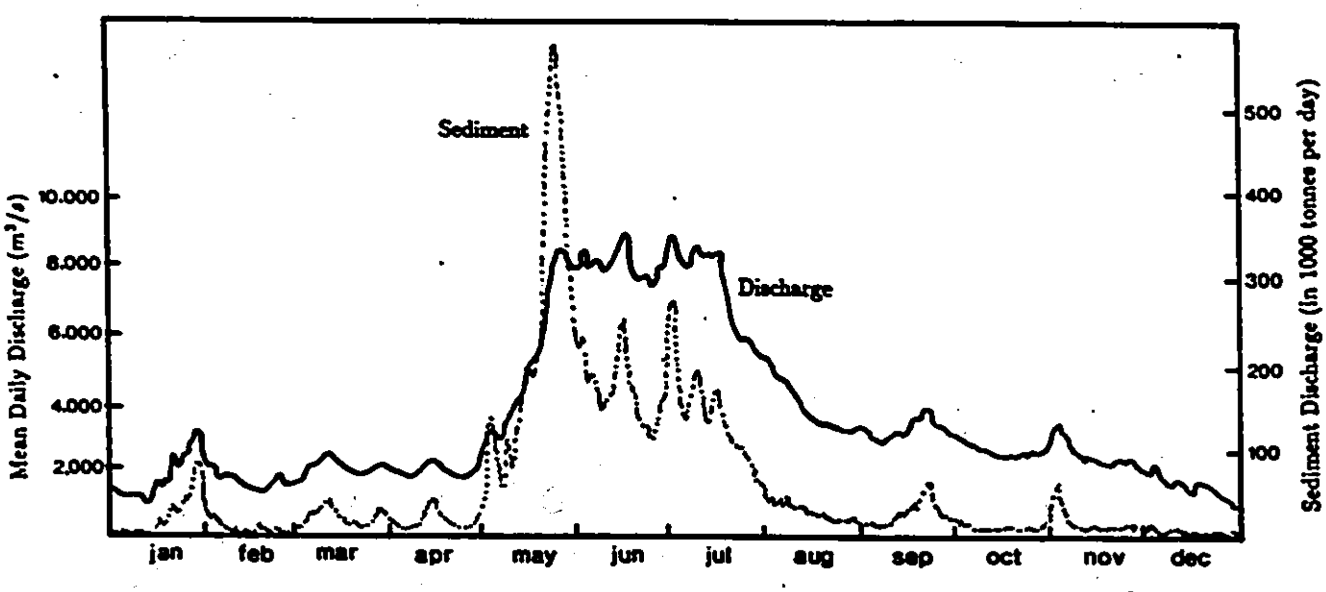

Figure 10.1: Observed Discharge and Total Sediment Discharge Hydrographs - Mission, 1968

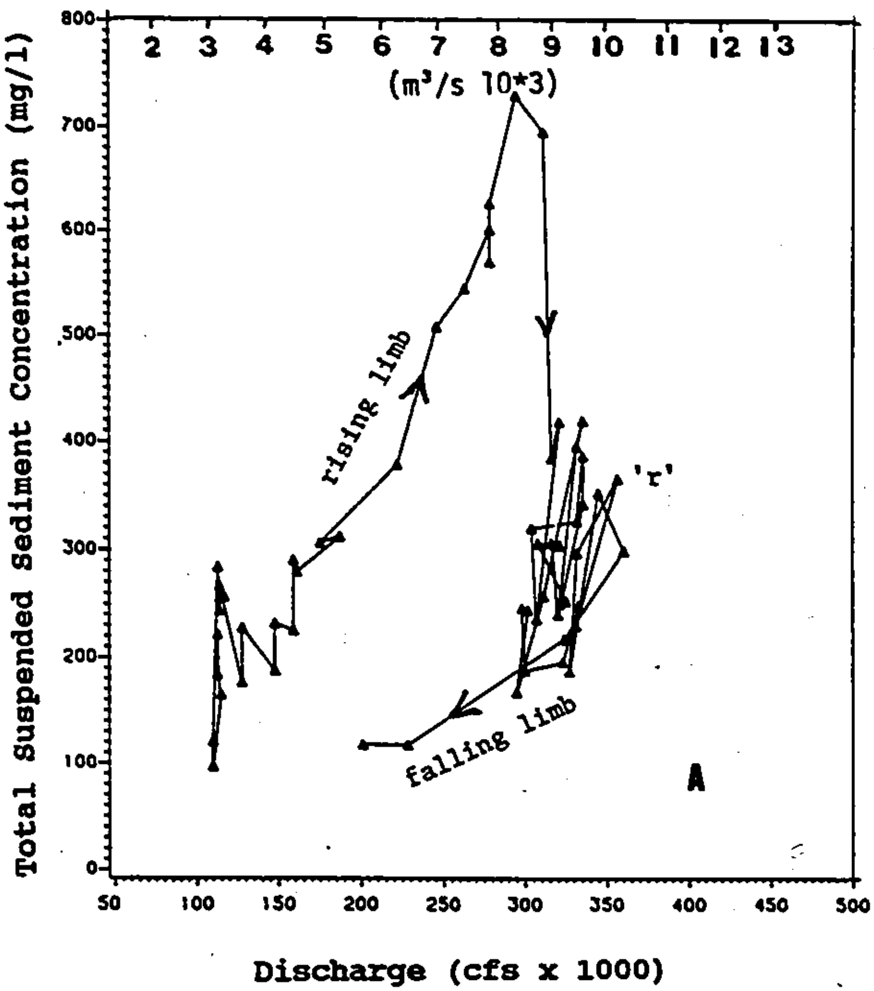

Figure 10.2: Observed Total Sediment Concentration versus Discharge - Mission, 1968

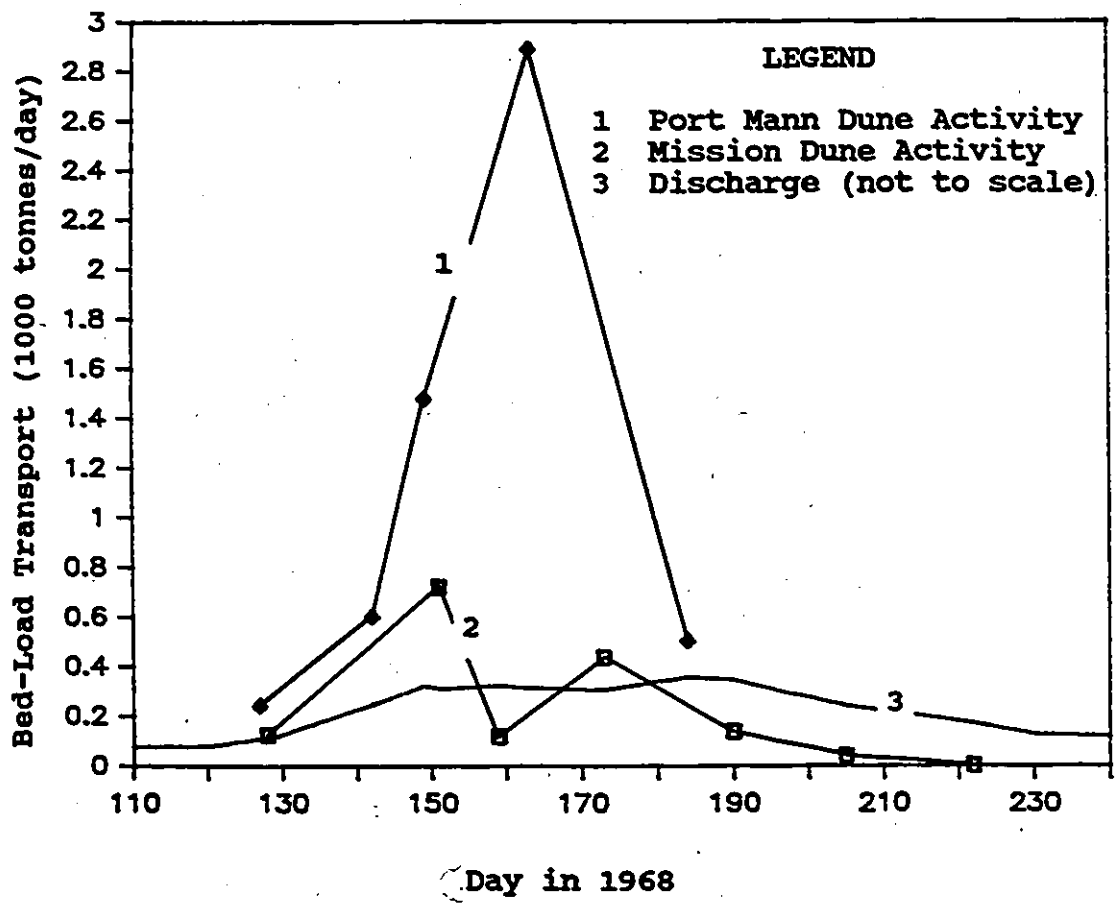

Figure 10.3: Dune Bed Load Transport versus Discharge

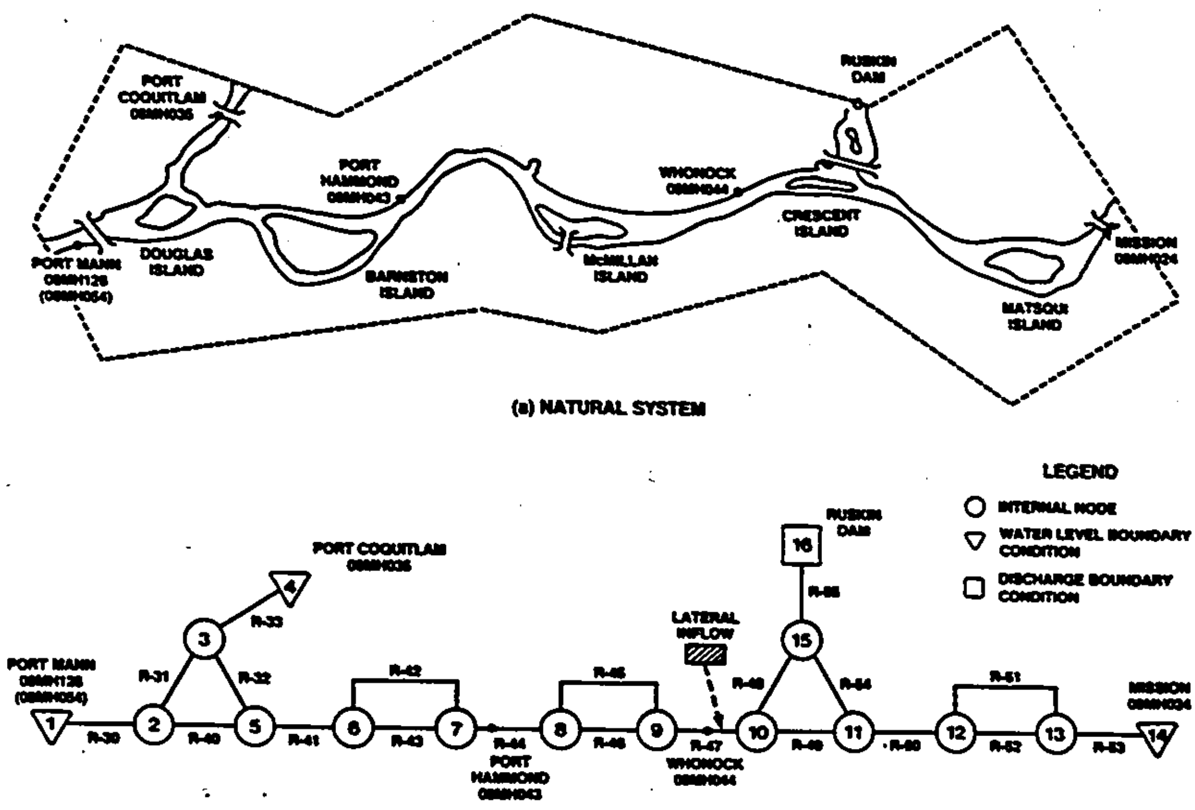

Figure 10.4: Fraser River Study Reach Natural System and Schematization

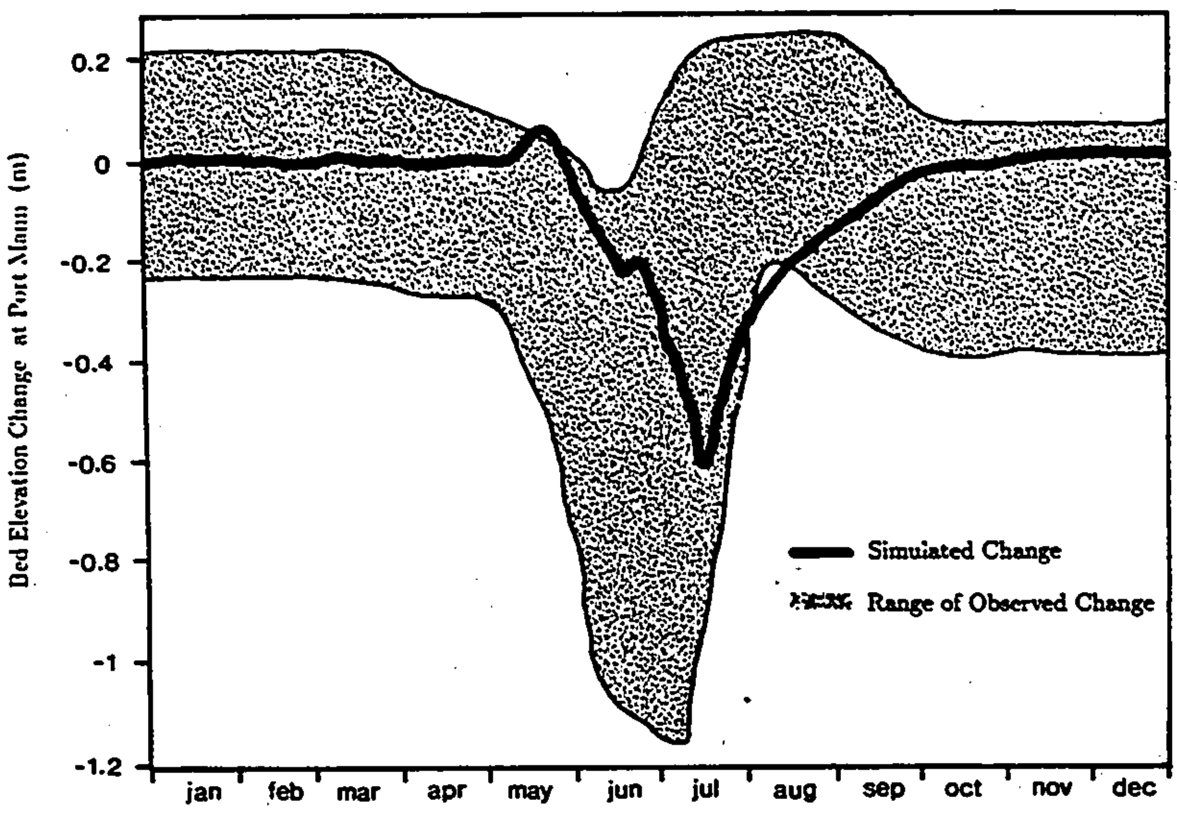

Figure 10.5: Simulated and Observed Bed Elevation Changes at Port Mann, 1968

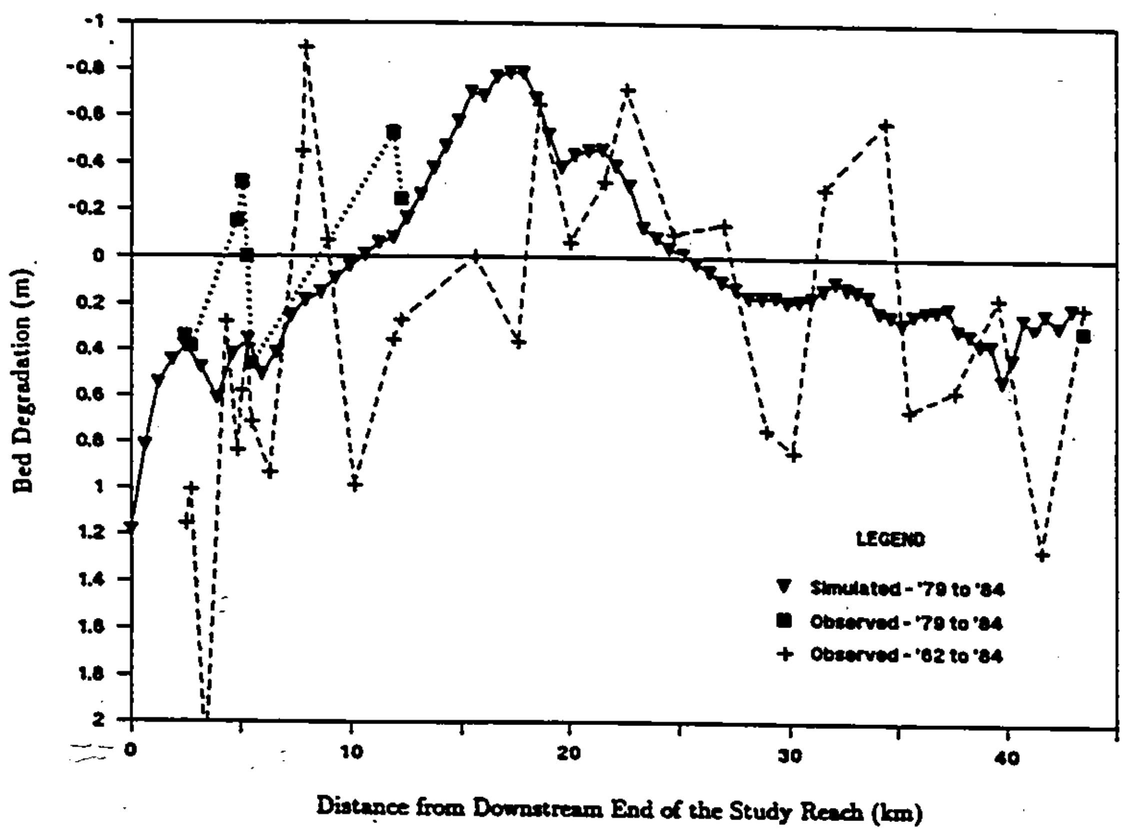

Figure 10.6: Simulated and Observed Bed Degradation Profiles - Main Channel

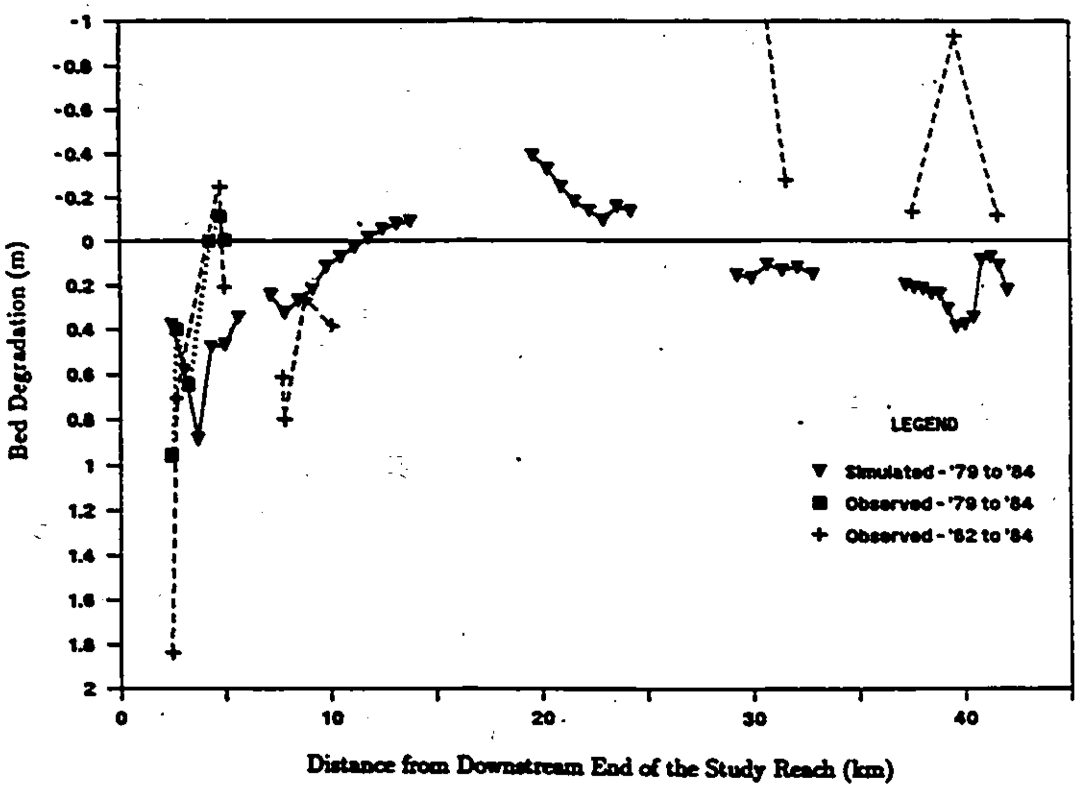

Figure 10.7: Simulated and Observed Bed Degradation Profile - Side Channels at Mission

Chapter 11

Conclusions and Recommendations

Modelling sediment transport processes is extremely challenging. At a conceptual level sediment erosion, transport and deposition are fairly easily understood. However, due to nature's complexity, quantifying these processes is another matter. In this research project significant efforts towards this end have been made. Though it is recognized that the scope of the study was necessarily limited certain conclusions, as well as recommendations for future related research, can be made. In the following text, conclusions and recommendations are grouped by topic.

11.1 Considerations in Mathematical Modelling

Based on the literature review, it is clear that many factors must be considered in regards to model selection. Some of the more important factors governing the selection of a model include: level of model sophistication, model documentation, agency support, degree of user and engineer friendliness, capacity of the model to simulate specific processes, and the numerical characteristics and order of the numerical schemes used.

It is recommended that future research endeavours should consider developing 'screening'-level models and also numerical models based on the theory of chaos.

11.2 Distribution of Suspended Sediment in the Water Column

Based on analysis of Point-Integrating data at Mission and Port Mann, it is concluded that the Rouse model is more appropriate than the constant eddy viscosity model for application to the Lower Fraser River. Though individually computed values of the Rouse Number could deviate from the median values by about 100%, the median values computed are nevertheless meaningful. It was suspected that some of the deviation may have originated from an analysis of grain fractions rather than single grain sizes. Furthermore, it is concluded that bed material transport in the near-bed zone is significant and should be added to correct Depth Integrating measurements. It is concluded that, in general, DI measurements should be increased by 7% .

It is also concluded that when comparing the results of one diffusion-dispersion model with another, it may be necessary to introduce a coefficient to account for the difference in value of the eddy viscosity model assumed. Based on a comparison of the average eddy viscosity of each model examined herein, analyses indicated that

η should be 1/6. It is concluded that the approach used to evaluate η is reasonable since the actual value found was 1/7.3.

The main recommendation coming out of the study was that research on the effect of performing analyses of grain fractions rather than unique sizes should be made. This research was undertaken in this project (see chapter 8) and the recommendations are as follows:

When two or more diffusion-dispersion models are compared, discrepancies between models should not be entirely attributed to β, as is sometimes done. Some of the discrepancies are due to the fact that the average values of the assumed eddy viscosity distributions are not necessarily the same. Therefore a coefficient such as η should be used to compare models on an equal footing; β should remain a physically-based coefficient to relate the sediment transfer coefficient to the eddy viscosity.

11.3 Modelling Mixed Sediment Fractions

The representative fall velocity (W_r) of a mixture of sediments can be significantly different than the fall velocity of the geometric mean size of the grain fraction (W_g). The ratio $\frac{W_g}{W_r}$ increases as a function of depth, fraction width, and dimensionless fall velocity ($\frac{W_g}{U_*}$) among others. When standard diffusion-dispersion models are applied to grain mixtures they should incorporate the correction coefficient γ quantified in this study.

When Depth-Integrated analyses are performed, in order to obtain a mathematically sound estimate of W_r the computed coefficient $\bar{\gamma}$ should be used. The coefficient is primarily a function of the dimensionless fall velocity and the geometric standard deviation of the grain fraction. When no correction is applied substantial errors can result in the determination of the average concentration. This is particularly true for $\frac{W_g}{U_*} \geq 0.3$, in which case errors as large as a factor of 15 can be made.

The study also indicated that a fairly large value for the reference depth (i.e., $a \simeq 0.1$) should be chosen. Otherwise calculations can be extremely sensitive to the selected value. Finally, it is suggested that much of the controversy over the value B (used in the Rouse Number) has been confused with the effect of representing a grain fraction by its geometric mean size. For example the two functions introduced by van Rijn (1984) (which are alledged to be physically-based) to modify the Rouse Number might well be replaced by γ or $\bar{\gamma}$ (which are mathematically based).

Research into the modelling of mixed suspended sediment was motivated by data analysis of the grain size distribution on the Lower Fraser River. It is recommended that the data analysis be extended to include γ and $\bar{\gamma}$ to confirm the conclusions stated herein.

11.4 Performance of de Vries' and Fromm's FD Schemes

The application of ONE-D-SED to singular sinusoidal bed transients of finite height leads to the following conclusions regarding the numerical properties of de Vries' and Fromm's finite difference schemes:

As suggested by linear analyses, the performance of de Vries' scheme was equally good using either a constant value of α or a location-specific value. It is concluded that the key to using the scheme is to select a value of β such that it is a function of the selected the bed Courant Number. When an ideal β is selected physical processes, including step wave fronts, are faithfully reproduced. This was found to be the case for any bed Courant Number ($\sigma < 1.0$) as long as the relationship of β to σ is maintained according to the relationships developed. Though the choice of β does not depend on the grid density selected, when greater than optimal values of β are used numerical effects are strongly dependent on the fineness of the computational grid (N_x) employed. For superior results, $N_x \geq 40$ should be used. When the β selected is too small, parasitical secondary waves contaminate the model's solution.

The numerical properties of Fromm's scheme were also favourable. Its use is advantageous in that it does not require the user to determine a coefficient a priori. As long as the chosen value of σ is low enough, the solution is accurate and virtually independent of N_x, for $N_x \geq 15$. On the other hand, when the system is highly non-linear, it can be difficult to choose σ small enough to avoid the introduction of parasitical waves in the simulation.

Since these findings, based on non-linear analyses, do not fully agree with the numerical properties predicted using linear analyses, it is recommended that a comparison be made and conclusions drawn regarding the findings of each method.

11.5 Sediment Transport in the Lower Fraser River

The largest sediment load in the Lower Fraser River is wash load (wl). Aside from ecological considerations, the wl introduces many difficulties for those predicting channel bed dynamics. It is difficult to quantify the bed material load (bml) when the division between the two is time- and location-dependent. For example, ONE-D-SED was unable to predict aggradation in the Lower Fraser River's minor channels due to the settling out of the wl in these reaches. In addition, the sand load upstream of the study area is wl but can be temporarily stored from August to April and then released into the study area. This means that during the onslaught of the freshet the bml in the study area can be greater than during other periods. Recognizing the inherent limitations it is however concluded that the division between wl and bml is about 0.19 mm for the study reach. When computing the bml using the A-W equation, a representative grain size of about 0.345 mm can be used. However, computed values must be increased by a factor of 2 in order to agree with observed loads.

From a detailed analysis of the cross-stream distribution of the suspended sediment concentration at Mission, it is concluded that different cross-stream distribution factors ϕ apply to different grain size classes. Whereas a factor of 0.80 should be used for the total load applications, a value of 0.60 should be used for estimating the bml.

The A-W equation was calibrated without regard to the increased bml during the dune formation period. It is recommended that the Mission "K" data set which has grain-size analysis should be compared to the A-W equation for years other than 1968. This could assist in quantifying the effect of unsteady flows on bml transport. It is also recommended that Water Survey of Canada perform full grain size analyses on data obtained at Mission's Daily vertical. This information could be used to confirm the choice of $\phi_{Db} = 0.60$.

11.6 ONE-D-SED

In this research project, ONE-D-SED was first constructed and then was validated for solutions of simple river-bed transient problems. The model's simulated velocity and attenuation of 'small' river-bed transients was the same as those suggested by analytical methods. Therefore, it is concluded that ONE-D-SED can accurately simulate the bed transient process.

From the screening-level application of ONE-D-SED to a "prismatic channel" representation of the Lower Fraser River, it is concluded that degradation, (caused by 0.305 m lower water levels at the downstream end of the study reach), proceeds rapidly at first and then continues in at an increasingly slower rate. The simulated 'half-life' of the process is about 9 years. Introducing islands in the representation of the river does not significantly effect predictions when only the bed material load is simulated. Also, the resistance of the river bed to erosion in reaches further upstream greatly affects predicted results. For example, when a fixed-bed boundary condition is assumed for Mission, bed degradation only reaches two thirds of its ultimate value at the downstream end and all degradation is arrested after 12 years.

However it is concluded that, from a numerical viewpoint, the introduction of channel non-uniformities changes the degradation pattern and the timing of events. In constricted (deep) reaches, very little degradation occurs. In other locations, simulations show an initial aggradation and then a rapid degradation process. Should the numerical results reflect nature, the amount and time-frame for the degradation event simulated is substantially affected. For example, when a central portion of the channel was reduced to half its standard width and when a fixed-bed boundary condition at Mission was adopted, predicted degradation at Port Mann increased from 0.2 m to 0.3 m and all processes were completed after only four years. On the other hand, when the entire model area was accurately represented and a fixed-bed boundary condition was used at Mission city, the full 0.3 m of degradation was predicted at Port Mann and all processes were completed after about 12 years.

From the detailed simulation of the Lower Fraser River it is concluded that, in general, ONE-D-SED satisfactorily reproduced observed 1979 to 1984 changes in the river bed. In addition, the model was able to simulate the observed 1968 Port Mann bed degradation/aggradation cycle induced by the 1968 spring freshet event. It is concluded that the model can be used to simulate channel bed dynamics occurring in tidal multi-channel networks. Given that the user can invoke a special calibration option, ONE-D-SED is particularly well suited for applications involving complex river systems. The fact that different sediment transport relationships have been incorporated into the model (and that the user has a choice of using one of two well-documented numerical schemes), the model offers a degree of flexibility.

It is recommended that ONE-D-SED be applied to other case studies to confirm model performance observed through this research. Should confirmation be forthcoming, agency support should be formalized. Also, ONE-D-SED should be further developed to include the modelling of the wash load, sediment sorting processes, and bed armouring. Finally, since ONE-D is now being used to simulate reaches downstream of Port Mann on the Lower Fraser River (and this is the area of greatest socio-economic-environmental interest), mobile-bed simulation should also be extended downstream.

11.7 Summary

In so far as ONE-D has been successfully extended to include simulation of sediment transport and channel bed transients, it is concluded that the main objectives of the project have been reached. ONE-D-SED has been validated against (i) analytical solutions of 'linear' bed-transient problems, and (ii) observed river-bed degradation in a tidal multi-channel river network. It is concluded that there are limits for which analytical solutions of bed transients of finite height apply. Associated correction factors have been quantified to adjust analytical solutions for those transients of finite height. It is also concluded that the representative fall velocity for modelling the transport of mixed suspended sediments may differ from that of the geometric mean size. Associated correction factors also have been quantified to adjust computed suspended sediment concentrations when the geometric grain size is used in lieu of the mathematically correct representative grain size.

Based on the performance of ONE-D-SED thus far it is recommended that further model testing, validation and development should be undertaken. It is also recommended that development of correction factors for bed-transients of finite height and functional relationships for these factors should continue. Developing correction factors, for characterizing sediment fractions of mixed grains, should be undertaken for diffusion-dispersion models other than those examined in the present study. Functional relationships for these factors should also be developed.

Bibliography

Abbott, M.B., Laursen, J. and Jianhua, T. (1985). Modelling Circulations in Depth-Integrated Flows Part 1: The Accumulation of the Evidence. Jour. of Hyd. Res., Vol. 23, pp. 309-326.

Ackers, P. and White, W.R. (1973). Sediment Transport: New Approach and Analysis. J. Hyd. Div. ASCE. Vol. 99/11, Nov. pp. 2041-2060.

Ackers, P. and White, W.R. (1980). Bed Material Transport: a Theory for Total Load and Its Verification. Proc. of the Int. Symp. on River Sedimentation. Mar. 24-29, Beijing, China. pp. 249-272.

Ages, A. and Woolard, A. (1976). Tides in the Fraser Estuary. Pacific Marine Science Report 76-5. Inst. of Ocean Sciences, Patricia Bay, Victoria, B.C.

Ahilan, R.V. and Sleath, J.F.A. (1987). Sediment Transport in Oscillatory Flow over Flat Beds. J. Hyd. Div., ASCE, V. 112/3. pp. 308-322.

Akiyama, J. and Fukushima, T. (1986). Entrainment of Noncohesive Bed Sediment into Suspension. River Sedimentation, Vol III. Proc. of the Third Int. Symp. of Sedimentation. Univ. of Miss., Miss., U.S.A. pp. 804-813.

Antsyferov, S.M. and Kos'yan, R.D. (1980). Sediment Suspended in Stream Flow. J. Hydr. Div., Vol. 106, No. HY2, Feb., pp. 313-330.

Appelt, V.M. (1959). Sediment Transport in the Fraser River, A Report of a Survey Conducted in 1959 by Department of Public Works, Canada.

Arai, M. and Takahashi, T. (1986). The Karman Constant of the Flow Laden with High Sediment. River Sedimentation, V. III. Proc. of the Third Int. Symp. of Sedimentation. Univ. of Miss., Miss., U.S.A. pp. 824-833.

Ariathurai, C.R. (1974). A Finite Element Model for Sediment Transport in Estuaries. Ph.D. Dissertation, Univ. of California, Davis, Cal.

Ashida, K. and Michiue, M. (1971). An Investigation of River Bed Degradation Downstream of a Dam. 14th Congress, IAHR, V. 3:247-255.

Ashley, G.M. (1980). Channel Morphology and Sediment Movement in a Tidal River, Pitt River, B.C. Earth Surface Processes, Vol. 5., pp. 347-368.

Ashley, G.M. and Moritz, L.E. (1979). Determination of Lacustrine Sedimentation Rates by Radioactive Fallout (137Cs), Pitt Lake, British Columbia. Can. J. Earth Sci., Vol. 16, pp. 965-970.

Bechteler, W. and Färber, K. (1985). Stochastic Model of Suspended Solid Dispersion. J. Hydr. Div., Vol. 111, No. 1, Jan., pp. 64-78.

Begin, Z.B. (1986). Curvature Ratio and Rate of River Bend Migration - Update. J. Hyd. Div., ASCE, V. 111/10, pp. 904-908.

Begin, Z.B., Meyer, D.F. and Schumm, S.A. (1980). Knickpoint Migration Due to Baselevel Lowering. J. Waterway, Port, Coastal and Ocean Div., ASCE., V.106/3:369-388.

Begin, Z.B., Meyer, D.F. and Schumm, S.A. (1981). Profiles of Alluvial Channels in Response to Base-Level Lowering. Earth Surface Processes and Landforms, V. 6:49-68.

Berezowsky, M. and Lara, M.A. (1986). Determination of the Friction Slope in Non-Uniform or Unsteady Flow in Rivers Considering Bedforms. River Sedimentation, Vol III. Proc. of the Third Int. Symp. of Sedimentation. Univ. of Miss., Miss., U.S.A. pp. 834-843.

Bettess, R. and White, W.R. (1983). Meandering and Braiding of Alluvial Channels. Proc. Instn Civ. Engrs, Vol. 75, Part 2, Sept., pp.525-538.

Biswas, A.N. and Chakrabarti, A.K. (1974). Sediment Transport in Tidal River. J. Hyd. Div., ASCE. V. 100/11:1677-1683.

Blench, T. (1959). River Engineering as a College Course for Civil Engineering. Engineering Journal. July. pp. 86-95.

Blench, T. (1971). Principles of River Bed Adjustment, reprint paper 1513, Joint

ASCE-ASME Transportation Eng. Meeting. July 26-30. Seattle. Wash.

Boutot. W. and Howell. G. (1985). Dissolved Oxygen Modelling of the St. Croix River -Comparison of Models. Environment Canada. Technical Bull. No. 135. Ottawa. Canada.

Bouvard. M.. Chollet. J.P. and Cunge. J.A. (1977). Progres Récents et Difficultés de Simulation Mathematiques des Rivières Alluvionaires. 17th Congress. IAHR. V. 1:165-172.

Bowen. P.T. and Harp. J.F. (1986). Cumulative Effects of Sand Mining in Inland Rivers. River Sedimentation. Vol III. Proc. of the Third Int. Symp. of Sedimentation. Univ. of Miss.. Miss.. U.S.A. pp. 1191-1199.

Bray. D.I. (1984). River Engineering. Lecture Notes. University of Moncton.

Bray, D.I. (1987). Progress Towards the Publication of a Monograph on Gravel-Bed Rivers. Proceedings 8th Canadian Hydrotechnical Conference. Montreal. Québec. May 19-22. pp.593-600.

Bray. D.I. and Davar. K.S. (1985). Resistance to Flow in Gravel-Bed Rivers. Proceedings 7th Canadian Hydrotechnical Conference. Saskaton. Sask., Vol. 1B. pp. 39-63.

Bray, D.I. and Kellerhals. R. (1979). Some Canadian Examples of the Response of Rivers to Man-Made Changes. Adjustments of the Fluvial System. Proceedings of the 10th Annual Geomorphology Sumposia Series Held at Binghamton. NY. Sept. 21-22. Edited by Rhodes. D.D. and Williams. G.P. Kendall & Hunt. Dubuque. Iowa. pp. 351-372.

Brown, B.O. and Li, R.M. (1979). Known Discharge Sediment Routing. Water Resources Publications. Fort Collins. Co.

Brownlie, W.R. (1981). Unsteady Sediment Transport Modeling. Proceedings of the Water Forum '81, ASCE. V. II:1193-1200.

Cashman. M.A. (1974). The First Sediment Computation Seminar. Jan 15 & 16. 1974. Department of the Environment. Water Resources Branch. Ottawa. Canada.

Chang, F.F.M. (1969). Computer Simulation of Riverbed Aggradation and Degradation by the Method of Characteristics. 13th Congress, IAHR, V.1:337-344.

Chang, H.H. and Hill, J.C. (1977). Minimum Stream Power for Rivers and Deltas. J. Hyd. Div. ASCE, Vol. 103/12, Dec. pp. 1375-1389.

Chang, F.F.M. and Richards, D.L. (1971). Deposition of Sediment in Transient Flow. J. Hyd. Div. ASCE., V.97/6:837-849.

Chang, H.H. (1982). Mathematical Model for Erodible Channels. Jour. Hyd. Div., ASCE, Vol. 108, HY5, May, pp. 678-689.

Chang, H.H. (1984a). Modeling General Scour at Bridge Crossings. Second Bridge Engineering Conference conducted by the Transportation Research Board, National Research Council, and the Federal Highway Administration, U.S. Department of Transportation, Sept. 24-26. Transportation Research Record 950. Washington, D.C. pp. 238-247.

Chang, H.H. (1984b). Modelling of River Channel Change. Jour. of Hyd. Div., ASCE, Vol. 110, Feb., No. HY2, pp. 157-172.

Chang, H.H. (1984c). Modeling of River Channel Change. Discussion by D.A. Beatty, T. Nakato, and closure. Jour. Hyd. Div. pp. 263-267.

Chang, H.H. (1986a). River Channel Changes: Adjustment to Equilibrium. Jour. of Hyd. Div., ASCE, Vol. 112, Jan., HY1, pp. 43-58.

Chang, H.H. (1986b). River Channel Responses during Floods. River Sedimentation, V. III. Proc. of the Third Int. Symp. of Sedimentation. Univ. of Miss., Miss., U.S.A. pp. 144-149.

Chang, H.H. and Hill, J.C. (1976). Computer Modeling of Erodible Flood Channels and Deltas. Jour. Hyd. Div., ASCE, Vol. 102, HY10, Oct., pp. 1461-1477.

Chen, Y.H., Holly, F.M., Mahmood, K. and Simons, D.B. (1975). Transport of Material by Unsteady Flow. Unsteady Flow in Open Channels, Water Res. Publ., Fort Collins, Co. V.1:313-365.

Chollet, J.P. and Cunge, J.A. (1980). Simulation of Unsteady Flow in Alluvial Streams. Proc. of the Int. Symp. on River Sedimentation. Mar. 24-29. Beijing, China. pp. 391-394.

Church, M., McLean, D.G., Kostaschuk, R. and Tassone, B. (1987). Sediment Transport in the Lower Fraser River: Summary of Results and Field Excursion Guide. Env. Can. IWD-HQ-WRB-SS-87-5.

Church, M., McLean, D.G., Mannerstrom, M. and Evans, D. (1984). Reference Materials on Sedimentation and Morphology of the Lower Fraser River. Univ. of B.C., Dept. of Geography. March.

Coleman, N.L. (1970). Flume Studies of the Sediment Transfer Coefficient. Water Resources Research, Vol. 6, No. 3, June, pp. 801-809.

Coleman, N.L. (1981). Velocity Profiles with Suspended Sediment. Jour. of Hyd. Res., Vol. 19, no.3, pp. 211-229.

Committee on Hydrodynamic Computer Models for Flood Insurance Studies (1983). An Evaluation of Flood-Level Predictions Using Alluvial River Models, Advisory Board on the Built Environment, National Research Council, National Academy Press, Washington, D.C.

Culling, W.E.H. (1960). Analytical Theory of Erosion. J. of Geology, No. 3, pp. 336-344.

Cunge, J.A. and Holly, F.M. (1986) Development Strategy for One-Dimensional Mobile-Bed Modelling System. River Sedimentation, V. III, Proc. of the Third Int. Symp. of Sedimentation, Univ. of Miss., Miss., U.S.A. pp. 83-92.

Cunge, J.A. and Perdreau, N. (1973). Mobile Bed Fluvial Mathematical Models. La Houille Blanche, No.7:561-580.

Cunge, J.A. and Simons, D.B. (1975). Mathematical Model of Unsteady Flow in Movable Bed Rivers with Alluvial Channel Resistance. 16th Congress, IAHR, V. 2:48-56.

Daily, J.E. and Harleman, R.F. (1972). Numerical Model for the Prediction of Transient Water Quality in Estuary Networks. Report No. 158, M.I.T. R72-72, Oct.

Day, T.J. (1980). A Study of the Transport of Graded Sediments. Report No. IT 190. Hydraulics Research Station Wallingford.

de Vries, M. (1959). Transients in Bed Load Transport (basic considerations). Report R3, Waterloopkunking Laboratorium, Delft.

de Vries, M. (1965). Considerations About Non-Steady Bed-Load Transport in Open Channels, 11th Congress, IAHR, V.3, paper 3.8

de Vries, M. (1969). Solving River Problems by Hydraulic and Mathematical Models. Delft Hydraulic Laboratory, Publication 76-II.

de Vries, M., (1981). Morphological Computations: Lecture Notes, f10a.I, Technische Hogeschool Delft, Afdeling der Civiele Techniek.

de Vries, M., (1982). A Sensitivity Analysis Applied to Morphological Computations, vol. D, Third Congress of the Asian and Pacific Regional Division (A.P.D.) of the IAHR, Aug. 24-26, Bandung, Indonesia, pp. 69-100.

Ditmars, J.D., Adams, E.E., Bedford, K.W. and Ford, D.E. (1987). Performance Evaluation of Surface Water Transport and Dispersion Models. J. Hyd. Div. ASCE., V.113/8:961-980.

Einstein, H.A. (1950). The Bed-Load Function for Sediment Transportation in Open Channel Flows. Tech. Bull. 1026, U.S. Dept. of Agriculture, SCS., Sept., Washington, D.C.

Engelund, F. and Fredsoe, J. (1976). A Sediment Transport Model for Straight Alluvial Channels. Nordic Hydrology, pp. 293-306.

Engelund, F. and Hansen, E. (1967). A Monograph on Sediment Transport in Alluvial Streams. Teknisk Forlag, Copenhagen.

Environment Canada (1981). Hydrometric Field Manual -Measurenent of Streamflow. Inland Water Directorate, Water Resources Branch, Ottawa.

Environment Canada (1984). Instructions for Collecting Suspended Sediment Samples. Notes for internal Use, Inland Water Directorate, Water Survey of Canada, Ottawa.

Environment Canada (1988) One-Dimensional Hydrodynamic Model - Computer Manual. Written by Water Modelling Section, Water Planning and Management Branch, Environment Canada, Feb.

Falconer, R.A., Wolanski, E. and Mardapitta-Hadjipandeli, L. (1986). Modeling Tidal Circulation in an Island's Wake. J. Waterway, Port, Coastal and Ocean Eng. V. 112/2, Mar. pp. 234-254.

Frenette, M. and Julien, P.Y. (1986). Advances in Predicting Reservoir Sedimentation. River Sedimentation, V. III. Proc. of the Third Int. Symp. of Sedimentation. Univ. of Miss., Miss., U.S.A. pp. 26-46.

Frenette, M. and Julien, Y. (1986). Advances in Predicting Reservoir Sedimentation. River Sedimentation, Vol III, Proc. of the Third Int. Symp. of Sedimentation, Univ. of Miss., Miss., U.S.A. pp. 26-46.

Frenette, M. et Julien, P.Y. (1986). LAVSED-I -Un Modele pour predire l'erosion des bassins et le Transfert de Sediments Fins dans les Cours d'Eau Nordiques. Vol. 13, No. 2, Apr., pp. 150-161.

Frenette, M. et Julien, P.Y. (1986). LAVSED-II -A Model for Predicting Suspended Load in Northern Streams. Vol. 13, No. 2, Apr., pp. 162-170.

Fromm, J.E. (1968). A Method for Reducing Dispersion in Convective Difference Schemes. J. of Computational Physics, 3(2), pp. 176-189.

Garde, R.J., Ranga Raju, K.G. and Mehta, P.J. (1981). Bed Level Variation in Aggrading Alluvial Sreams. 19th Congress, IAHR, V.3, pp. 247-253.

Gee, D.M. (1984). Role of Calibration in Application of HEC-6. Second Bridge Engineering Conference conducted by the Transportation Research Board, National Research Council, and the Federal Highway Administration, U.S. Department of Transportation, Sept. 24-26. Transportation Research Record 950, Washington, D.C. pp. 252-259.

Gessler, J. (1971). Aggradation and Degradation. River Mechanics, (ed. Shen, H.W.) V.1/8:1-24. mm

Ghosh, S.N. (1986). An Investigation on the Nature of Variation of Sediment and Momentum Transfer Coefficients in Natural River. River Sedimentation - Vol. III, Third International Symposium on River Sedimentation, The University of Mississippi, Mar. 31 - Apr. 4, pp. 187-194.

Gibbs, C.J. and Neill, C.R. (1973). Laboratory Testing of Model VUV Bed-Load Sampler. Research Council of Alberta in ass. with Dept. of Civ. Eng., Univ. of Alt. No REH/73/2, Feb.

Gill, M.A. (1980). Discussion on the paper by Soni et al. (1980). J. Hyd. Div. ASCE., V. 106/11, pp. 1955-1958.

Gill, M.A. (1983). Diffusion Model for Aggrading Channels. J. Hydr. Res., 21(5), pp. 355-365.

Golder, Brawner & Associates Ltd. (1976). Report to Reid Crowther & Partners

Ltd. on Investigation of Borrow Areas for Hydraulic Fill Materials for C.P. Rail Yards. Port Coquitlam, B.C. Mar., Vancouver, B.C.

Graf, W.H. (1971). Hydraulics of Sediment Transport. McGraw-Hill, New York.

Gunaratnam, D.J. and Perkins, P.E. (1970). Numerical Solution for Unsteady Flows in Open Channels. Hydrodynamics Laboratory. Report No. 127, Mass. Inst. of Tech. U.S.A.

Hagerty, D.J., Spoor, M.F. and Kennedy, J.F. (1986). Interactive Mechanisms of Alluvial-Stream Bank Erosion. River Sedimentation. Vol III. Proc. of the Third Int. Symp. of Sedimentation. Univ. of Miss., Miss., U.S.A. pp. 1160-1168.

Hinwood, J.B. and Wallis, I.G. (1975a). Review of Models of Tidal Waters. Jour. Hyd. Div., ASCE, Vol. 101, HY11, Nov., pp. 1405-1421.

Hinwood, J.B. and Wallis, I.G. (1975b). Classification of Models of Tidal Waters. Jour. Hyd. Div., ASCE, Vol. 101, HY10, Oct., pp. 1315-1331.

Holly, F.M. Jr. and Karim, M.F. (1986). Simulation of Missouri River Bed Degradation. Jour. Hyd. Div., ASCE, Vol. 112, HY6, Jun., pp. 497-517.

Holly, F.M. Jr., Nakato, T. and Kennedy, J.F. (1984). Computer-Based Prediction of Alluvial Riverbed Changes. Second Bridge Engineering Conference conducted by the Transportation Research Board, National Research Council, and the Federal Highway Administration, U.S. Department of Transportation, Sept. 24-26. Transportation Research Record 950. Washington, D.C. pp. 229-237.

Holly, F.M. and Rahuel, J.L. (1988). Advances in Numerical Simulation of Alluvial River Response to Disturbances. 6th IWRA World Congress on Water Resources. Ottawa, May 29 - June 3. paper W8.

Holly, F.M. Jr., Yang, J.C. and Karim, M.F. (1984). Computer-Based Prognosis of Missouri River Bed Degradation Refinement of Computational Procedures. Iowa City, Iowa Institure of Hydraulic Research.

Hwang, J.C. (1975). Degradation of Sand-Bed Channel. 16th Congress. IAHR, V.2:181-188.

Ikeda, S. and Takashi, A. (1983). Sediment Suspension with Rippled Bed. J. Hydr. Div., Vol. 109, No. 3, Mar., pp. 409-423.

Iseya, F. (1984). An Experimental Study of Dune Development and its Effect on Sediment Suspension. Environmental Research Center Papers, Ibarabi, Japan.

Isfeld, E.O., Hay, D. and Rossouw, J. (1973). Field and Model Studies on a Siltation Problem in the Fraser River. Paper for Canadian Hydraulics Conference, Univ. of Alt., Edmonton, May 10 & 11.

Itakura, T. and Kishi, T. (1980). Turbulence in Tidal Open Channel Flow with Suspended Sediments. Journal of the Hydraulics Division, Vol. 106, No. HY8, Aug., pp. 1325-1343.

Jobson, H.E. and Sayre, W.W. (1970). Predicting Concentration Profiles in Open Channels. J. Hydr. Div., Vol. 96, No. HY10, Oct., pp. 1983-1996.

Johnson, T.R. Ellis, C.R., Farrell, G.J. and Stefan, H.G. (1987). Negatively Buoyant Flow in a Diverging Channel, I: Flow Regimes. J. Hyd. Div., ASCE, V. 112/6, pp. 716-742.

Junda, C. (1980). The Viscosity of Sediment-water Mixture. Proc. of the Int. Symp. on River Sedimentation, Mar. 24-29, Beijing, China, pp. 205-212.

Karim, M.F. (1981). Computer-Based Predictors for Sediment Discharge and Friction Factor of Alluvial Streams. Ph.D. Dissertation, Univ. of Iowa, Iowa City, Iowa.

Karim, M.F. and Holly, F.M. (1986). Armouring and Sorting Simulation in Alluvial Rivers. Jour. Hyd. Div., ASCE, Vol. 112, HY8, Aug., pp. 705-715.

Karim, M.F. and Kennedy, J.F. (1982). IALLUVIAL: A Computer-Based Flow and Sediment Routing Model for Alluvial Streams and its Application to the Missouri River. IIHR Report No. 250, Iowa Institute of Hydraulic Research, The University of Iowa, Iowa City, Iowa.

Karim, B.F. and Kennedy, J.F. (1987). Velocity and Sediment- Concentration Profiles in River Flows. J. Hydr. Div., Vol. 113, No. 2, Feb., pp. 159-178.

Kawahara, M. and Umetsu, T. (1986). Two Step Explicit Finite Element Method for Sediment Transport. River Sedimentation, Vol III, Proc. of the Third Int. Symp. of Sedimentation, Univ. of Miss., Miss., U.S.A. pp. 1486-1495.

Kellerhals, R. (1984). Review of Sediment Survey Program - Lower Fraser River, British Columbia. Environment Canada, Report no. IWD-HQ-WRB-SS-84-3, 68 pp.

Kennedy, J.F. and Koh, C.Y. (1964). Sediment Transportation Mechanics: Introduction and Properties of Sediment, -Discussion, J. Hydr. Div., Vol. 90, No. HY2, Feb., pp. 171-174.

Kennedy, J.F. (1983). Reflections on Rivers, Research, and Rouse. Jour. Hyd. Div., ASCE, Vol. 109, HY10, Oct., pp. 1254-1271.

Kennedy, J.F. (1986). Keynote address. 3rd International Symposium on River Sedimentation. Univ. of Miss., Miss., U.S.A.

Kerssens, P.M.J., Prins, A. and Rijn, van L.C. (1979). Model for Suspended Sediment Transport. Jour. Hyd. Div., ASCE, Vol. 105, HY5, May, pp. 461-477.

Keulegan, G.H. and Patterson, G.W. (1943). Effects of Turbulence and Channel Slope in Translation Waves. Journal of Research, National Bureau of Standards, Vol. 30, June.

Klaassen, G.J., Klomp, R. and Zwaard, Y.J. van der. (1982). Planning and Environmental Impact Assessment of River Engineering Works via Mathematical Models. Third Congress of the Asian and Pacific Regional Division (A.P.D.) of the IAHR. Aug. 24-26, Bandung, Indonesia. Vol. A:153-176.

Komura, S. (1971). Prediction of River-Bed Degradation Below Dams. 14th Congress, IAHR, V.3:257-264.

Komura, S. and Simons, D.B. (1967). River-Bed Degradation Below Dams. J. Hyd. Div., ASCE, V.87/2:1-14.

Koutitas, c.g. (1986). Coastal Circulation and Sediment transport. River Sedimentation, Vol III. Proc. of the Third Int. Symp. of Sedimentation. Univ. of Miss., Miss., U.S.A. pp. 310-322.

Krishnappan, B.G. (1980). Field Verification of an Unsteady Non-Uniform Sediment Laden Flow Model. 19th Congress in New Delhi.

Krishnappan, B.G. (1981). Users Manual: Unsteady, Non-Uniform, Mobile Boundary Flow Model - MOBED. Hydraulics Div., National Water Research Inst., Burlington, Ontario.

Krishnappan, B.G. and Lau, Y.L. (1977). Transverse Dispersion in Meandering

Channels. Inland Waters Directorate, Canada Centre for Inland Waters, Burlington, Ontario. Scientific Series No. 75.

Krishnappan, B.C. et al. (1987). River Model. Proceedings 8th Canadian Hydrotechnical Conference, Montreal, Québec, May 19-22.

Kumar, A. and Albertson, M.L. (1986). Fall Behavior of Cylinders in Quiescent Fluids. River Sedimentation, Vol III. Proc. of the Third Int. Symp. of Sedimentation. Univ. of Miss., Miss., U.S.A. pp. 1701-1706.

Lam, C.S. (1981). A New Computation Procedure for Bottom Withdrawal Tube Particle Size Analysis. CASD Projects J292 and T861. Env. Can. Computing and Allpied Statistics Directorate.

Lane, E.W. (1955). The Importance of Fluvial Morphology in Hydraulic Engineering. J. Hyd. Div. ASCE., Vol. 81, Paper 795, pp.1-17.

Langley, H.I. (1975). BedLoad Sampling by Pumping. Public Works Canada, Pacific Region, Marine Engineering, Vancouver, B.C.

Lau, Y.L. (1988). Roughness of Reverse Flow over Dunes and its Application to the Modelling of the Pitt River. Canadian Journal of Civil Engineering, Vol. 15, Aug., pp. 547-552.

Laursen, E.M. (1980). A Sediment Concentration Distribution Based on a Revised Prandtl Mixing Theory. Proc. of the Int. Symp. on River Sedimentation. Mar. 24-29, Beijing, China. pp. 237-248.

Lewis, J.M. and Hwang, G.J. (1986). An Assessment Study of Five Sediment Transport Models. River Sedimentation, Vol III. Proc. of the Third Int. Symp. of Sedimentation. Univ. of Miss., Miss., U.S.A. pp. 766-776.

Lopez-Garcia, J. (1977). Mathematical Modelling of Alluvial Bed Transients, Thesis Presented to Colorado State University, at Fort Collins, Co., in Partial Fulfillment of the Requirements for the Degree of Master of Science.

Lu, J.Y. and Shen, H.W. (1986). Analysis and Comparisons of Degradation Models. Jour. Hyd. Div., ASCE, Vol. 112, HY4, Apr., pp. 281-299.

Lyn, D.A. (1987). Unsteady Sediment-Transport Modeling. J. Hyd. Div. ASCE., V.113, HY1, Jan., pp. 1-15.

Mahmood, K. (1975). Mathematical Modeling of Morphological Transients in Sand-Bed Canals. 16th Congress, IAHR, V.2:57-64.

Mahmood, K. and Ponce, V.M. (1976). Mathematical Modeling of Sedimentation Transients in Sand-Bed Channels. Report CER75-76-KM-VMP28, Engineering Research Center, Colorado State Univ., Fort Colins, Co.

Markofsky, M. (1984). A Technique for Reducing the Computation Time of Two-Dimensional Thermal and Water Quality Explicti Finite Difference and Finite Element Numerical Models. Proc. 4th Congr. Asian and Pacific Regional Division, IAHR, Chiang Mai, Thailand.

Markofsky, M., Lang, G. and Schubert, R. (1985). Numerical Simulation of Unsteady Suspended Solids in Open Channels, EUROMECH 192: Transport of Suspended Solids in Open Channels, Munchen, FRG, June 1985. Balkema Publishers, Netherlands.

Markofsky, M., Lang, G. and Schubert, R. (1985). Suspended Sediment Transport in Tidal Waters: Turbidity Maximum, Numerical Simulation, Physical Aspects. Proc. 21th Congress of IAHR, V.4, Melbourne, Aug. 1985.

McAnally, W.H. Jr., Letter, J.V., and Thomas, W.A. (1986). Two- and Three-Dimensional Modeling Systems for Sedimentation. River Sedimentation, V. III. Proc. of the Third Int. Symp. of Sedimentation, Univ. of Miss., Miss., U.S.A. pp. 400-411.

McLean, D.G. and Church, M.A. (1986). A Re-Examination of Sediment Transport Observations in the Lower Fraser River. Environment Canada, Report No. IWD-HQ-WRB-SS-86-6, 52 pp.

McLean, D.G. and Mannerstrom, M.C. (1985). History of Channel Instability Lower Fraser River: Hope to Mission. Univ. of B.C., Dept. of Geography.

Metigue, D.F. (1981). Mixture Theory for Suspended Sediment Transport. J. Hydr. Div., Vol. 107, No. HY6, June, pp. 659-673.

Milliman, J.D. and Meade, R.H. (1983). World-Wide Delivery of River Sediment to the Oceans. Jour. of Geology, Vol. 91, No. 1, Jan., pp. 1-20.

Miloradov, M. and Muskatirovic, D. (1971) Calculation of River Bed Deformation in Unsteady Flow. 14th Congress, IAHR, V.3:175-185.

Miloradov, M. and Radojkovic, M. (1975). Flood Routing in Natural Streams with Non-Steady Morphological Characteristics. 16th Congress, IAHR, V.2:330-337.

Morasse, B. (1985). Generation of the 1968 Hydrometric Data of the Lower Fraser River: Using the ONE-D Hydrodynamic Model. Internal Report, WPM-IWD-Environment Canada, 135pp.

Morasse, B. and Sydor, M. (1988). Generation of the 1968 Hydrometric Data of the Lower Fraser River: Using the ONE-D Hydrodynamic Model. Internal Report WPM-IWD-Environment Canada.

Morse, B. (1990a). St. Lawrence River Water-Levels Study, Application of the ONE-D Hydrodynamic Model: Report prepared for Transport Canada, Waterways Development Division, Canadian Coast Guard, 330pp.

Morse, B. (1990b). Predicting St. Lawrence River Water Levels in the Vicinity of Montreal Harbour. Report prepared for Transport Canada, Waterways Development Division, Canadian Coast Guard, 75pp.

Morse, B. and Townsend, R.D. (1987). Estimating Sediment Transport Rates for the Lower Fraser River. 8th Canadian Hydrotechnical Conf. Montreal, Quebec, May, 1987.

Morse, B. and Townsend, R.D. (1988). Some Considerations in the Numerical Modelling of Alluvial Channels. Proceedings of the 6th IWRA World Congress on Water Resources, Ottawa, May.

Morse, B. and Townsend, R.D. (1989a). Non-Linear Behaviour of Bed Transients and Convergence of de Vries' Finite Difference Scheme. 6th Int. Conference on Numerical Methods in Laminar and Turbulent Flow, Swansea, U.K. July.

Morse, B. and Townsend, R.D. (1989b). Modelling Mixed Suspended Sediment Profiles. J. Hyd. Eng., ASCE. V. 115, No. 6, June. pp. 766-780.

Morse, B. and Townsend, R.D. (1990a). Modelling Channel Bed Transients Using Explicit F-D Schemes. Journal of Hydraulic Engineering, ASCE, Vol. 116, No. 11, Nov.

Morse, B. and Townsend, R.D. (1990b). Modelling Bed Degradation in a Tidal Multi-Channel River System. Computational Methods in Surface Hydrology. Proceedings of the Eighth International Conference on Computational Methods in Water Resources, Venice, Italy, pp. 185-190.

Newton, C.T. (1951). An Experimental Investigation of Bed Degradation in an Open Channel. Trans. of Boston Soc. of Civ. Engrs., pp. 28-60.

Nicholson, J. and O'Connor, B.A. (1986). Cohesive Sediment Transport Model. Jour. Hyd. Div., ASCE, Vol. 112, Jan., pp. 621-640.

Parker, G. and Coleman, N.L. (1986). Simple Model of Sediment Laden Flows. J. Hyd. Div., ASCE, V. 111/5, pp. 356-375.

Partheniades, E. (1986). the present state of knowledge and needs for future research on Cohesive Sediment Dynamics. River Sedimentation, Vol III. Proc. of the Third Int. Symp. of Sedimentation. Univ. of Miss., Miss., U.S.A. pp. 3-25.

Petkovic, S. and Bouvard, M. (1985). Vertical Dispersion of Spherical, Heavy Particles in Turbulent Open Channel Flow. Journal of Hydraulic Research. Vol. 23, No. 1, PP. 5-20.

Ponce, V.M., Garcia, J.L. and Simons, D.B. (1979a). Modeling Alluvial Channel Bed Transients. Jour. Hyd. Div., ASCE, Vol. 105, HY3, Mar., pp. 245-256.

Ponce, V.M., Indlekofer, H. and Simons, D.B. (1979b). The Convergence of Implicit Bed Transient Models. Jour. Hyd. Div., ASCE, Vol. 105, HY4, Apr., pp. 351-363.

Public Works Canada. (1978). Proceedings of the Fraser River Shipping Channel Workshop. Dec. 2, Surrey, B.C.

Public Works Canada. (1978). Proposed Inprovements to the Fraser River Shipping Channel. Transcript - Proceedings of Public Information Meeting. May 17, Richmond, B.C.

Puls, W., Sundermann, J. and Vollmers, H. (1977). A Numerical Approach to Solid Matter Transport Computation. 17th Congress, IAHR, V.1:129-135.

Qiwei, H., MIngmin, H. (1982). Bed Load Fluctuation: Applications. J. Hyd. Div., ASCE, V. 108/2, pp. 199-210

Rathburn, R.E. and Guy, H.P. (1967). Effect on Non-Equilibrium Flow Conditions on Sediment Transport and Bed Roughness in a Laboratory Alluvial Channel. 12th Congress, IAHR, V.1:187-193.

Ribberink, J.S. and van der Sande, J.T.M. (1985). Aggradation in Rivers due to Overloading–Analytical Approaches. J. Hydr. Res., 23(3), pp. 273-283.

Richardson, E.V. and Julien, P.Y. (1986). Bedforms, Fine Sediments, Washload and Sediment Transport. pp. 854-874.

Rijn, van C.L. (1984). Sediment Transport, Part I: Bed Load Transport. J. Hyd. Div. ASCE. V.110, HY10, Oct., pp. 1431-1456.

Rijn, van C.L. (1984). Sediment Transport, Part II: Suspended Load Transport. J. Hyd. Div. ASCE. V.110, HY11, Nov., pp. 1613-1641.

Rijn, van C.L. (1984). Sediment Transport, Part III: Bed Forms and Alluvial Roughness. J. Hyd. Div. ASCE. V.110, HY12, Dec., pp. 1733-1754.

Rijn, van C.L. (1986). Mathematical Modeling of Suspended Sediment in Nonuniform Flows. J. Hyd. Div. ASCE., V.112, HY6, Jun., pp. 433-455.

Rodi, W. (1986). Use of Advanced Turbulence Models for Calculating the Flow and Pollutant Spreading in Rivers. River Sedimentation, V. III. Proc. of the Third Int. Symp. of Sedimentation. Univ. of Miss., Miss., U.S.A. pp. 1369-1382.

Rouse, H. (1937). Modern Conceptions of the Mechanics of Fluid Turbulence. Trans. ASCE., V. 102, pp. 461-543.

Samaga, B.R., Ranga Raju, K.G. and Garde, R.J. (1986). Suspended Load Transport of Sediment Mixtures. J. Hydr. Div., Vol. 112, No. 11, Nov., pp. 1019-1035.

Schiller, L. and Naumann, A. (1933). Über die grundlegenden Berechnungen bei der Schwerkraftaufbereitung. Z. VDI, Vol. 77.

Schilperoort, T., Wijbenga, A. and Zwaard, van der J.J. (1984). Mathematical Tools and their Growing Importance for River Engineering. Fourth Congress - Asian and Pacific Divsion. Int. Ass. for Hyd. Res. Chiang Mai, Thailand, Sep. 11-13, pp. 1009-1025.

Schumm, S.A. (1980). Summary of Poplar Creek Discussion. U.S. Fish and Wildlife Service Workshop on Downstream River Channel Changes from Diversions or Reservoir Construction. Aug. 27-29. Fort Collins, Co. pp. 99-101.

Sediment Survey of Canada, Inland Waters Directorate, Pacific & Yukon Region. (1976). Memorandum to E.M. Clark, Regional Director, Inland Waters Directorate re: (Purpose of) Sediment Monitoring Program (Fraser River). Apr. 7.

Sediment Survey of Canada. (1970). Hydrometric and Sediment Survey Lower

Fraser River Progress Report 1965-1968. Energy Mines and Resources. IWB.

Shen, H.W. and Hung, C.S. (1983). Remodified Einstein Procedure for Sediment Load. J. Hyd. Div. ASCE. V.109, HY4, Apr., pp. 565-578.

Shen, H.W. and Lu, J.Y. (1986). Modelling of Aggradation. River Sedimentation, V. III. Proc. of the Third Int. Symp. of Sedimentation. Univ. of Miss., Miss., U.S.A., pp. 226-234.

Shiqiang, W., White, W.R. and Bettess, R. (1986). A Rational Approach to River Regime. River Sedimentation, Vol III. Proc. of the Third Int. Symp. of Sedimentation. Univ. of Miss., Miss., U.S.A. pp. 167-178.

Shirmohammadi, A., Sheridan, J.M. and Knisel, W.G. (1987). Regional Application of an Approximate Streamflow Partitioning Mehod. Water Resources Bull. American Water Resources Association. 23/1:103-

Simons, D.B., Li, R-M. and Cottton G.K. (1984). Mathematical Model for Estimating Scour Through Bridge Crossings. Second Bridge Engineering Conference conducted by the Transportation Research Boa d, National Research Council, and the Federal Highway Administration, U.S. Department of Transportation. Sept. 24-26. Transportation Research Record 950. Washington, D.C. pp. 244-251.

Simons, D.B., Li, R.M. and Fullerton, W.T. (1980). Multiple Watershed Model for Water and Sediment Routing from Mined Areas. Simons and Li and Associates, Inc.

Snischenko, B.F. et al. (1986). The Influence of Concentration of Suspended Load and Sudden Stream Broadening on its Turbulent Characteristics. River Sedimentation, V. III. Proc. of the Third Int. Symp. of Sedimentation. Univ. of Miss., Miss., U.S.A. pp. 143-143

Soni, J.P. and Sarda, V.K. (1982). Manning's Rougness Coefficient in Degrading Alluvial Channels. Third Congress of the Asian and Pacific Regional Division (A.P.D.) of the IAHR. Aug. 24-26, Bandung, Indonesia. Vol. A, pp. 74-79.

Soni, J.P. (1981). Unsteady Sediment Transport Law and Prediction of Aggradation Parameters. Water Resources Research. American Geophysical Union, Paper No. 80W1001.

Soni, J.P., Garde, R.J. and Raju, K.G.R. (1980). Aggradation in Streams Due to Overloading. J. Hyd. Div. ASCE. Vol. 106/1, Jan. pp. 117-132.

Stichling, W. (1974). Sediment Loads in Canadian Rivers. Environment Canada. Technical Bull. No. 74. Ottawa, Canada.

Sydor, M. (1980). Fraser River One-Dimensional Model Study. Environment Canada, Water Planning and Management Branch, Ottawa.

Sydor, M. (1983). Fraser River Model Study, the Application of a ONE-Dimensional Hydrodynamic Model to the Lower Fraser River. Prepared by Water Planning and Management Branch and Water Resources Branch, Pacific & Yukon Region, 61pp.

Sydor, M. and Morasse, B. (1987). The Application of One-Dimensional Hydro-Dynamic Modelling for Flood Routing on the Red River between Emerson and Ste. Agathe. Proceedings 8th Canadian Hydrotechnical Conference, Montreal, Québec, May 19-22, pp. 353-372.

Sydor, M., Brown, G., Chang, H., Boutot, W. and Morasse, B. (1989). Getting the Best of Both Worlds - Application of Systems Analysis; from Micro to Super Computers. Conference at the University of Manitoba, Winnipeg, May, 2-5.

Task Committee on Preparation of Sedimentation Manual, Committee on Sedimentation of the Hydraulics Division (1971). Sediment Transportation Mechanics: Fundamentals of Sediment Transportation. Jour. Hyd. Div., Vol. 97, HY12, Dec., pp. 1979-2022.

Tassone, B. and McLean, D.G. (1990). Effects of Dredging on Fraser River Channel Regime. Public Works Canada, Project No. 883-578. 24pp.

Theurer, F.D. (1980). Report on the Elk River Problem Session Papers. U.S. Fish and Wildlife Service Workshop on Downstream River Channel Changes from Diversions or Reservoir Construction. Aug. 27-29. Fort Collins. Co. pp. 192-195.

Tinney, E.R. (1962). The Progress of Channel Degradation, J. Geophysical Res. V.67/4.

Torres, W.F.J. and Subhash, S.J. (1984). Aggradation and Degradation of Alluvial-Channel Beds. IIHR Report No. 274, Iowa Inst. Hydr. Res., Univ. of Iowa, Iowa City, Iowa.

Tsai, C-T and Yen, C-l. (1982). Simulation of Unsteady Flow in Movable-Bed Channels. Third Congress of the Asian and Pacific Regional Division (A.P.D.) of the IAHR. Aug. 24-26, Bandung, Indonesia. Vol. B, pp. 80-90.

Tywoniuk, N. (1973). Sediment Budget of the Lower Fraser River. Ninth Canadian Hydrology Symposium. Fluvial Processes and Sedimentation. Univ. of Alt., Edmonton, May 8 & 9.

Tywoniuk, N. and Stichling, W. (1973). Sedimentation Phenomenon of the Fraser River. IAHR International Symposium on River Mechanics. 9-12 Jan., Bangkok, Thailaind. pp. A69-1 to A69-13.

U.S. Army Corps of Engineers (1973). HEC-2: Water Surface Profiles, User's Manual; The Hydrologic Engineering Center, Davis, California.

U.S. Army Corps of Engineers (1977). HEC-6: Scour and Deposition in Rivers and Reservoirs, User's Manual; The Hydrologic Engineering Center, Davis, California.

Vanoni, V.A. (ed.), (1975). Sedimentation Engineering, ASCE-Manuals and Reports on Engineering Practice, No. 54, New York, N.Y.

Vetter, M. (1986). Velocity Distribution and Von Karman Constant in Open Channel Flows with Sediment Transport. River Sedimentation, V. III. Proc. of the Third Int. Symp. of Sedimentation. Univ. of Miss., Miss., U.S.A. pp. 814-823.

Vital, N. and Mittal, M.K. (1980). Degrdation of Ratman Torrent Downstream of Dhanami. Proc. Int. Workshop on Alluvial River Problems. IAHR. Paper No. 5, pp. 43-54.

Vreugdenhil, C.B. (1979). Fromm's Zero-Average-Phase-Error Scheme for a Non-Linear Scalar Equation. Report on Basic Research. S78 Part VII. Waterloopkundig Laboratorium, Delft Hydr. Lab., Delft, the Netherlands, May.

Vreugdenhil, C.B. (1981). Numerical Effects in Models for River Morphology. Engineering Applications of Computational Hydraulics. Vol. 1. (Ed. Abbott, M.B. and Cunge, J.A.) Pitman Advanced Pub. Program. Boston. pp. 91-108.

Wang, S.Y. (1984). The Principle and Application of Sediment Effective Power. J. Hyd. Div., ASCE, V. 109/2, pp. 97-108.

Wang, S.Y. and Adeff, S.E. (1986). Three-Dimensional Modeling of River Sedimenation Processes. River Sedimentation, Vol III. Proc. of the Third Int. Symp. of Sedimentation. Univ. of Miss., Miss., U.S.A. pp. 1496-1505.

Wang, Y.H. (1986). Deposition Behavior of Fine Sediments in an Estuarine Saline Wedge. River Sedimentation, Vol III. Proc. of the Third Int. Symp. of Sedimentation. Univ. of Miss., Miss., U.S.A. pp. 552-558.

Water Planning and Management Branch and Water Resources Branch (1983). The Application of a 1-Dimensional Hydrodynamic Model to the Lower Fraser River. Env. Can. (incl. Appendices A to E.)

Waylen, P.R. and Woo, M.-k. (1984). Regionalization and Prediction of Floods in the Fraser River Catchment, B.C. Water Resources Bull. American Water Resources Association. V. 20/6, Dec. pp. 941-949.

Wesseling, P. (1973). On the Construction of Accurate Schemes for Hyperbolic Partial Differential Equations. J. Engrg. Math., 7(1), pp. 19-31.

Western Canada Hydraulic Laboratories Ltd. (1977). Feasibility Study, Development of a Forty-Foot Draft Navigation Channel New WestMinster to SandHeads. Final Report Hydraulic Model Studies for Public Works Canada. Apr.

Western Canada Hydraulic Laboratories Ltd. (1978). Final Report, Analysis of Federal Sediment Survey Data Taken on the Lower Fraser River. Prepared for Water Survey of Canada. Oct.

White, W.R., Milli, H. and Crabbe, A.D. (1975). Sediment Transport Theory: A Review. Discussion. Proc. Instn. Civ. Engrs. Part 2, V. 59, June, pp. 265-292.

White, W.R., Paris, E. and Bettess, R. (1980). The Frictional Characteristics of Alluvial Streams: a New Approach. Proc. Instn Civ. Engrs, Vol. 69, Part 2, Sept., pp. 737-750.

Wright D.R.C., Division of Business Assistance. (1984). Market for Sand in the Lower Fraser Area. Prepared for Public Works Canada/Transport Canada. Apr., Vancouver, B.C.

Yalin, M.S. (1972). Mechanics of Sediment Transport, Pergamon Press, Braunschweig, Germany.

Yang, C.T. (1979). Unit Stream Power Equations for Total Load. J. of Hydrology. Vol. 40, pp. 123-128. Elsevier Scientific Publishing Co., Amsterdam.

Yang, C.T. and Molinas, A. (1982). Rate of Energy Dissipation and Sediment Transport. Procs of the ASCE Conference Applying Research to Hydraulic Practice, ASCE, Jackson, Miss. pp. 466-479.

Yang, C.T. and Molinas, A. (1982). Sediment Transport and Unit Stream Power Function. J. Hyd. Div., ASCE, V. 108/6, pp. 774-796

Zrymiak, P. (1987). Linking Sediment Computations to a 1-D Mathematical Model. Env. Can. IWD-HQ-WRB-SS-87-4.

Appendix A

Appendix A

There are three sections to this appendix. The first section is a description of most sediment subroutines added to ONE-D resulting in the mobile-bed version, ONE-D-SED. The reader should use this list in conjunction with figures 5.1, 5.2 and 5.3 which are flowcharts of ONE-D-SED. The next section is an explanation of the input variables used in ONE-D-SED and is given in a format consistent with the ONE-D Computer Manual (Environment Canada, 1988). Finally, dummy variables used to dimension sediment transport arrays are listed in the third section.

A.1 Description of Sediment Subroutines.

Name:	Description:
<u>SEDINI</u>	Manages calls to the following subroutines to obtain initial conditions:
SEDRDR	Reads sediment data (Card Group J).
SEDEFF	Calculates and stores active river bed width.
SEDDGR	Locates dredging activity in the river network.
SEDNSN	Moves sediment input data from specified locations to computational points internal to ONE-D.
SEDNET	Sets up reach-node connectivity to solve the Exner equation in a logical order.

SEDTR1 Calculates relevant hydraulic quantities and calls one of SEDT11 to SEDT18.

SEDT11 Calculates bml and c according to the Ackers-White equation.

SEDT12 Calculates bml and c according to Yang's equation.

SEDT13 Calculates bml and c according to the Hansen-Engelund equation.

SEDT14 Calculates bml and c according to $S = b\ u^m$, where S is the bml, b and m are constants and u is velocity.

SEDT15 Calculates bml and c according to the $S = b\ u^m\ (A/B)^d$, where, in addition to SEDT14, A is the cross-sectional area, B is the top-width and d is a constant.

SEDT16 Calculates bml and c according to $S = b\ (u - u_c)^m$, where, in addition to the above, u_c is the velocity corresponding to initiation of sediment transport.

SEDT17 Calculates bml and c according to $S = b\ (Q - Q_c)^m$, where, in addition to the above, Q is the river discharge and Q_c is the critical discharge corresponding to initiation of sediment transport.

SEDT18 Calculates bml and c according to $S = b\ (T - T_c)^m$, where, in addition to the above, T is the boundary shear stress and T_c is the shear stress corresponding to initiation of sediment transport.

SEDAD4 Book-keeping subroutine to update the values of bml and c.

SEDMXN Calculates the maximum and minimum values of bml and c.

SEDDT1 Calculates the optimal time step for the solution of the Exner equation based on de Vries scheme.

SEDDT2 Calculates the optimal time step for the solution of the Exner equation based on Fromm's scheme.

SEDZER Initializes accumulated bml and c values to zero.

SEDAD1 Updates old value of bml and c.

SEDSTO Stores current value of change in bed elevation to an output file.

<u>SEDMAN</u> Manages call to the following subroutines depending on the sediment time step in relation to the hydraulic time step:

SEDTIM Obtains present value of time-dependent sediment input parameters and calls SEDRMU to calculate water viscosity based on water temperature.

SEDTR2 Calculates pertinent hydraulic parameters and calls one of SEDT11 to SEDT18.

SEDTR3 Calculates pertinent hydraulic parameters and calls one of SEDT21 to SEDT28.

SEDT21 to SEDT28: Same as SEDT11 to SEDT18 except c is not obtained.

SEDAD2 Book-keeping subroutine for accumulated bml.

SEDAD3 Book-keeping subroutine for accumulated bml invoked at the end of a sediment time step.

SEDNOD Adjusts sediment transport calculated at nodes to ensure consistency.

SEDDVS Solves Exner equation according to short form of de Vries' scheme (eqn. IV.20).

SEDDVL Solves Exner equation according to long form of de Vries' scheme (eqn. IV.19).

SEDFRM Solves Exner equation according to Fromm's scheme (eqn. IV.21).

SEDDV2 Adjusts computed changes in bed elevations to account for sediment lateral inflows, rock outcrops and to ensure continuity of change in bed elevation at nodes.

SEDCNV Checks to see if iterative solution has converged.

SEDREW Backs up time to recalculate hydraulic and bed solution when iteration is required.

SEDSTO Writes (converged) solution of changes in bed elevation to external file.

SEDCAL Calculates calibration coefficients associated with each mesh point if a calibration run is specified.

SEDEND Re-writes solutions in more user-friendly format.

A.2 Description of Input Variables.

DESCRIPTION OF CARD GROUP J

SEDIMENT-RELATED VARIABLES

ONE-D-SED

CARD	VRBLE	COLUMN	FORMAT	DESCRIPTION
J-A	HEADS	1-72	CHR*72	Heading for mobile bed simulation.
J-B-1	ISEQN	5-10	I5	Choice of Sediment Transport Eqn. 1 = Ackers-White 2 = Yang 3 = Hansen-Engelund 4 = SCO1 * V ^ SCO2 5 = SCO1 * V ^ SCO2 * D ^ SCO3 6 = SCO1 * (V-SCOC) ^ SCO2 7 = SCO1 * (Q-SCOC) ^ SCO2 8 = SCO1 * (TAO-SCOC) ^ SCO2
J-B-1	SCO1	11-20	F10.5	Coefficient for Transport Eqn.

J-B-1	SCO2	21-30	F10.5	Exponent for Transport Eqn.
J-B-1	SCO3	31-40	F10.5	Exponent for Transport Eqn.
J-B-1	SCOC	41-50	F10.5	Value corresponding to the initiation of sediment motion.
J-B-2	PCNTCV	01-10	F10.5	Tolerance for error in the calculation of aggradation/erosion in the ITERATIVE type of model.
J-B-2	ICONVG	16-20	I5	Type of model: 1 = Normal (Un-Coupled). 2 = ITERATIVE (Coupled). 3 = No Coupling: Hydraulic Solution given by reading Tape10.
J-B-2	ISOLTP	21-25	I5	Choice of Numerical Algorithm: 1 = Calibration Run (No Solution of BZ) -1 = as 1 and print all values. 2 = de Vries' with variable alpha. -2 = de Vries' with constant alpha. 3 = Fromm's Scheme.
J-B-2	ISTS	26-30	I5	> 0 Number of hydraulic time steps before sediment computations are made. < 0 then the program calculates it at start of simulation only. = 0 then program calculates after each time sediment continuity eqn is solved.
J-B-2	RLINT	31-40	F10.4	Length of Bed Wave which is of primary interest.
J-B-3	STIME	01-10	F10.5	Day at which simulation begins.
J-B-3	SGS	11-20	F10.5	Specific Gravity of the Sediment (between 2.65 and 2.75).
J-B-3	P	21-30	F10.5	Value of the Bed Porosity (usually between 0.35 and 0.45).
J-B-4	IREADS	01-05	I5	Initial value of BZ: 1 = As user defines in cards J-D. 2 = Initialized from a previous run (Tape 26 saved as Tape 27). 3 = Program sets to 0.0
J-B-4	ISAVES	06-10	I5	Save solution of BZ: 1 = Not saved at all. 2 = Saved at every (sediment) time step (Tape20). 3 = Saved only at last time step (Tape27). 4 = Both option 2 and 3.

J-B-4	IREADW	11-15	I5	Active Bed Width: 1 = As defined by user in cards J-D. 2 = Average of Option 1 and the Topwidth at each section. 3 = 90% of Topwidth at each section. 4 = Read from Tape24.
J-B-4	ISAVEW	16-20	I5	Save input parameters for future use on Tape21: 1 = Do not save. 2 = Save CALSED, EFFW, BZMN.
J-B-4	IROCKS	21-25	I5	Are there any rock outcrops? 1 = no. 2 = program should check.
J-B-4	IARMS	26-30	I5	Is there any Bed armouring? 1 = no. 2 = program does not support this option at this time.
J-C	KID	01-05	I5	Reach ID no.
J-C	ICNTB	06-10	I5	Is a step in the bed to occur at the downstream end node of this reach? 0 = Yes (for example if there is a structure at this node). 1 = No (most internal nodes).

Other card groups are defined and available:
J-D Information related to each cross-section.
J-E Water Temperature in Network.
J-F Time dependent boundary conditions for sediment.
J-G Sediment (lateral) inflow specification.
J-H Output specifications: sedi-graphs and profiles.

A.3 Variables to Dimension Sediment Subroutines.

Since Fortran requires the dimensioning of arrays, additional variables are defined to enable the user to change the dimensions of the arrays. The variables, found in the master copy of ONE-D-SED, are replaced by a numerical value corresponding to the required dimensions. This method is consistent with the ONE-D's approach and documentation:

VX01 The number of sediment (lateral) inflows.

VX02 The number of sediment (lateral) inflow cross-section locations. This is variable >= 2***VX01** and depends on the width of all the locations.

VX03 The number of cards **J-G-3**. That is the total number of inflows given as a function of time for all locations. This variable is also >= 2***VX01**.

VX04 The number of sedi-graphs requested.

VX05 The number of sedi-profiles requested.

VX06 The number of Sediment Boundary Conditions.

VX07 As **VX03**, the total number of cards **J-F-3**. That is the total number of data given to describe the time dependence of all boundary conditions. >= 2***VX06**.

VX08 The number of water temperature entries.

Appendix B

Outline of the Ackers-White Equation

The following is a brief conceptual outline of the Ackers-White equation. For a full treatment of the matter, the reader is referred to the original paper (Ackers-White 1973). The conceptual development of the equation was presented as follows:

1. Transport of Coarse Sediment

First, a sediment mobility number for coarse grains F_{cg} is conceived as follows:

$$F_{cg}^2 = \frac{t_o'}{t_r} \tag{1}$$

where: t_o' is the grain shear stress and t_r is the resisting shear stress of the bed material.

Next, sediment transport efficiency E_{cg} is conceived as follows:

$$E_{cg} = \frac{W_e\,\bar{u}}{t_o'\,\bar{u}} \tag{2}$$

where W_e is the weight of the transported material per unit area and $\bar{u}$ is the mean velocity of the fluid.

Keeping in mind that the transport function will also be valid for transitional grain sizes, the particle Reynold s R_e number is also introduced:

$$R_e = \frac{U_* d_r}{E} \tag{3}$$

where U_* is the total shear velocity, d_r is the representative sediment size and E is the kinematic viscosity of the fluid.

For convenience, two new dimensional parameters are formed from these three as follows:

$$G_{cg} = E_{cg} F_{cg} \tag{4}$$

$$D_{gr} = R_e^{2/3} F^{-2/3} \tag{5}$$

where G_{cg} is the dimensionless sediment transport of coarse grains and D_{gr} is the dimensionless representative grain size. Finally, it is postulated that

$$G_{cg} = f(F_{cg}, D_{gr}) \tag{6}$$

2. Transport of Fine Grains

A similar analysis is used for fine grains. In this case, the sediment mobility number F_{fg} is defined as:

$$F_{fg} = \frac{U_*}{W} \tag{7}$$

where: W is the sediment fall velocity.

Next, transport efficiency E_{fg} is conceived as follows:

$$E_{fg} = \frac{W_c\, W}{U_*\, \bar{u}} \tag{8}$$

Keeping in mind that the transport function will also be valid for transitional grain sizes and that W is a function of D_{gr}, the latter is also introduced and the dimensionless sediment transport rate for fine grains is defined as:

$$G_{fg} = E_{fg}\, F_{fg}^3\, D_{gr}^3 \tag{9}$$

It is then postulated that:

$$G_{fg} = f(F_{fg}, D_{gr}) \tag{10}$$

3. Transport of All Grain Sizes

The third step of development was to combine analyses for coarse and fine grains. This was done through the introduction of the exponent nn (function of D_{gr}) such that:

$$F_{gr} = F_{fg}^{nn} \times F_{cg}^{1-nn} \tag{11}$$

$$G_{gr} = G_{fg}^{nn} \times G_{cg}^{1-nn} \tag{12}$$

The resulting dependence of G_{gr} on F_{gr} and D_{gr} was established. Therefore, to compute the bed material load (greater than 0.04 mm) the following equations should be used:

$$D_{gr} = d_r \left(\frac{g(s_s - 1)}{E^2} \right)^{1/3} \tag{13}$$

where g is the acceleration due to gravity and s_s is the mass density of sediment relative to that of fluid. The following constants are then obtained as a function of D_{gr}:

$$nn = 1 - 0.56 \log D_{gr} \tag{14}$$

subject to $0 \leq nn \leq 1$,

$$CA = \frac{0.23}{\sqrt{D_{gr}}} + 0.14 \tag{15}$$

$$mm = \frac{9.66}{D_{gr}} + 1.34 \tag{16}$$

$$\log CC = 2.86 \log D_{gr} - (\log D_{gr})^2 - 3.53 \tag{17}$$

Next, compute the sediment mobility number:

$$F_{gr} = \frac{U_*^{nn}}{\sqrt{g d_r (s_s - 1)}} \left[\frac{\bar{u}}{\sqrt{32} \log \left(\frac{10HD}{d_r} \right)} \right]^{1-nn} \tag{18}$$

where HD is the hydraulic depth defined as cross-sectional area divided by water surface width. Next, the dimensionless sediment transport rate is given by:

$$G_{gr} = CC \left(\frac{F_{gr}}{CA} - 1 \right)^{mm} \tag{19}$$

and the sediment transport (mass flux per unit mass flow rate) is given by:

$$X = s_s \frac{d_r}{HD} \left(\frac{\bar{u}}{U_*} \right)^{nn} G_{gr} \tag{20}$$

The sediment load in m^3/s can then be obtained as follows:

$$S = XQ/s_s \tag{21}$$

where Q is the fluid discharge (m^3/s).